VOLUME 102 | SUPPLEMENT 1 | MARCH 2022

LI

LABORATORY INVESTIGATION

THE BASIC AND TRANSLATIONAL PATHOLOGY RESEARCH JOURNAL

ABSTRACTS (660–799)

GYNECOLOGIC AND OBSTETRIC PATHOLOGY

2022

USCAP 111TH ANNUAL MEETING

REAL INTELLIGENCE

MARCH 19–24, 2022 LOS ANGELES, CALIFORNIA

Published by SPRINGER NATURE
www.ModernPathology.org

USCAP Creating a Better Pathologist
AN OFFICIAL JOURNAL OF THE UNITED STATES AND CANADIAN ACADEMY OF PATHOLOGY

EDUCATION COMMITTEE

Rhonda K. Yantiss
Chair

Kristin C. Jensen
Chair, CME Subcommittee

Laura C. Collins
Chair, Interactive Microscopy Subcommittee

Yuri Fedoriw
Short Course Coordinator

Ilan Weinreb
Chair, Subcommittee for Unique Live Course Offerings

Carla L. Ellis
Chair, DEI Subcommittee

Adebowale J. Adeniran
Kimberly H. Allison
Sarah M. Dry
William C. Faquin
Karen J. Fritchie
Jennifer B. Gordetsky
Levon Katsakhyan, Pathologist-in-Training
Melinda J. Lerwill
M. Beatriz S. Lopes
Julia R. Naso, Pathologist-in-Training
Liron Pantanowitz
Carlos Parra-Herran
Rajiv M. Patel
Charles "Matt" Quick
David F. Schaeffer
Lynette M. Sholl
Olga K. Weinberg
Maria Westerhoff

ABSTRACT REVIEW BOARD

Benjamin Adam
Oyedele Adeyi
Mariam Priya Alexander
Daniela Allende
Catalina Amador
Vijayalakshmi Ananthanarayanan
Tatjana Antic
Manju Aron
Roberto Barrios
Gregory R. Bean
Govind Bhagat
Luis Zabala Blanco
Michael Bonert
Alain C. Borczuk
Tamar C. Brandler
Eric Jason Burks
Kelly J. Butnor
Sarah M. Calkins
Weibiao Cao
Wenqing (Wendy) Cao
Barbara Ann Centeno
Joanna SY Chan
Kung-Chao Chang
Hao Chen
Wei Chen
Yunn-Yi Chen
Sarah Chiang
Soo-Jin Cho
Shefali Chopra
Nicole A. Cipriani
Cecilia Clement
Claudiu Cotta
Jennifer A. Cotter
Sonika M. Dahiya
Elizabeth G. Demicco
Katie Dennis
Jasreman Dhillon
Anand S. Dighe
Bojana Djordjevic
Michelle R. Downes
Charles G. Eberhart
Andrew G. Evans
Fang Fan
Julie C. Fanburg-Smith
Gelareh Farshid
Michael Feely
Susan A. Fineberg
Dennis J. Firchau
Gregory A. Fishbein
Agnes B. Fogo
Andrew L. Folpe
Danielle Fortuna
Billie Fyfe-Kirschner
Zeina Ghorab
Giovanna A. Giannico
Anthony J. Gill
Tamar A. Giorgadze
Alessio Giubellino
Carolyn Glass
Carmen R. Gomez-Fernandez
Shunyou Gong
Purva Gopal
Abha Goyal
Christopher C. Griffith
Ian S. Hagemann
Gillian Leigh Hale
Suntrea TG Hammer
Malini Harigopal
Kammi J. Henriksen
Jonas J. Heymann
Carlo Vincent Hojilla
Aaron R. Huber
Jabed Iqbal
Shilpa Jain
Vickie Y. Jo
Ivy John
Dan Jones
Ridas Juskevicius
Meghan E. Kapp
Nora Katabi
Francesca Khani
Joseph D. Khoury
Benjamin Kipp
Veronica E. Klepeis
Christian A. Kunder
Stefano La Rosa
Stephen M. Lagana
Keith K. Lai
Goo Lee
Michael Lee
Vasiliki Leventaki
Madelyn Lew
Faqian Li
Ying Li
Chieh-Yu Lin
Mikhail Lisovsky
Lesley C. Lomo
Fang-I Lu
aDeqin Ma
Varsha Manucha
Rachel Angelica Mariani
Brock Aaron Martin
David S. McClintock
Anne M. Mills
Richard N. Mitchell
Hiroshi Miyamoto
Kristen E. Muller
Priya Nagarajan
Navneet Narula
Michiya Nishino
Maura O'Neil
Scott Roland Owens
Burcin Pehlivanoglu
Deniz Peker Barclift
Avani Anil Pendse
Andre Pinto
Susan Prendeville
Carlos N. Prieto Granada
Peter Pytel
Stephen S. Raab
Emilian V. Racila
Stanley J. Radio
Santiago Ramon Y Cajal
Kaaren K Reichard
Jordan P. Reynolds
Lisa M. Rooper
Andrew Eric Rosenberg
Ozlen Saglam
Ankur R. Sangoi
Kurt B. Schaberg
Qiuying (Judy) Shi
Wonwoo Shon
Pratibha S. Shukla
Gabriel Sica
Alexa Siddon
Anthony Sisk
Kalliopi P. Siziopikou
Stephanie Lynn Skala
Maxwell L. Smith
Isaac H. Solomon
Wei Song
Simona Stolnicu
Adrian Suarez
Paul E. Swanson
Benjamin Jack Swanson
Sara Szabo
Gary H. Tozbikian
Gulisa Turashvili
Andrew T. Turk
Efsevia Vakiani
Paul VanderLaan
Hanlin L. Wang
Stephen C. Ward
Kevin M. Waters
Jaclyn C. Watkins
Shi Wei
Hannah Y. Wen
Kwun Wah Wen
Kristy Wolniak
Deyin Xing
Ya Xu
Shaofeng N. Yan
Zhaohai Yang
Yunshin Albert Yeh
Huina Zhang
Xuchen Zhang
Bihong Zhao
Lei Zhao

To cite abstracts in this publication, please use the following format: **Author A, Author B, Author C, et al. Abstract title (abs#). In "File Title."** ***Laboratory Investigation*** **2022; 102 (suppl 1): page#**

660 Fumarate Hydratase-Deficient Uterine Leiomyoma: A 5-Year Prospective Analysis of Morphology-Based Screening and Patient Outcomes at a Single Institution

Heba Abdelal[1], Natalia Buza[2], Pei Hui[3], Minhua Wang[2]
[1]Yale New Haven Hospital, Yale School of Medicine, New Haven, CT, [2]Yale School of Medicine, New Haven, CT, [3]Yale University School of Medicine, New Haven, CT

Disclosures: Heba Abdelal: None; Natalia Buza: None; Pei Hui: None; Minhua Wang: None

Background: Hereditary Leiomyomatosis and Renal Cell Carcinoma Syndrome (HLRCC) is caused by germline mutation of fumarate hydratase (FH) gene, and is characterized by early-onset multiple uterine leiomas (ULM), cutaneous leiomyomas, and an aggressive form of RCC. Morphologic features of FH-deficient ULM have been previously described and proposed as a pathology-based screening tool to identify patients at risk for HLRCC. Prospective studies in evaluating the efficacy of this approach are limited.

Design: ULM with FH-deficient histologic features – staghorn-shaped vessels, eosinophilic cytoplasmic vacuoles, macronucleoli, and perinucleolar halos – have been prospectively identified between 2016-2021 during routine work-up and subjected to FH immunohistochemistry (IHC). H&E and IHC slides were retrieved and reviewed for additional parameters: atypia, cellularity, tumor cell necrosis, and mitotic count. Clinical data were obtained from electronic medical records.

Results: FH-deficient morphology was reported in 18 of 2240 (0.8%) ULM during the study period. The median patient age was 42.5 years, 11 patients had hysterectomies and 7 had myomectomies for “symptomatic fibroids” (15/18, 83%), abnormal uterine bleeding (2/18, 11%), or *BRCA2* mutation carrier status (1/18, 6%). The median tumor size was 4 cm (range: 1.7-14.5 cm), 11 (61%) tumors showed moderate and 2 (11%) severe atypia, but none had tumor cell necrosis or increased mitotic activity. FH expression was lost in 14 tumors (78%), including in one polypoid adenomyoma (Figure 1). Genetic counseling was offered to 10 of 14 patients with FH loss, 8 of whom saw a counselor and were offered germline FH mutation analysis. Six patients elected to undergo germline testing: pathogenic FH mutation was identified in two patients, while one had a variant of unknown significance.

Figure 1 - 660

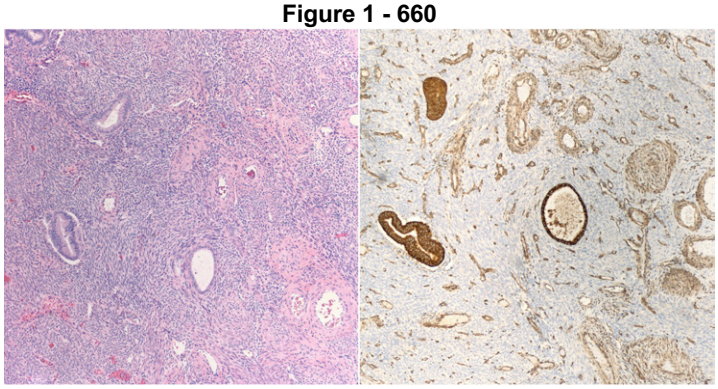

Conclusions: FH-deficient ULM is rare, representing 0.8% of our study population. Morphology and IHC-based screening of ULM can successfully identify patients at risk of HLRCC syndrome with profound implications for the patients and their families. Among our patients with FH-deficient (by both morphology and IHC) ULM 14% were found to have germline pathogenic FH mutations. Increased awareness both among pathologists and gynecologists is necessary to further improve histopathologic recognition and genetic referral rates. The morphologic spectrum of FH-deficient ULM should be expanded to include rare adenomyomas with FH-deficiency.

661 Revisiting the Necessity for Routine Appendectomies in Mucinous Neoplasms of the Ovary: An Evaluation of 460 Mucinous Ovarian Tumors

Ahlam Albloshi[1], Oluwole Fadare[2]
[1]University of California, San Diego, San Diego, CA, [2]UC San Diego School of Medicine, La Jolla, CA

Disclosures: Ahlam Albloshi: None; Oluwole Fadare: None

Background: Appendectomies are commonly performed following an intraoperative diagnosis of a mucinous ovarian neoplasm, ostensibly to identify and remove a potential source for the ovarian tumor in the event that it is found to be secondary at that

site. However, data that would justify this practice are relatively limited. Using a large single institutional cohort, we sought to identify whether there are any discernible factors that are associated with the finding of significant disease in the appendix in this setting, and whether the routine performance of appendectomies has a firm evidentiary basis.

Design: We retrieved records for 460 consecutive patients whose ovarian tumors were classified as "mucinous" on intraoperative consultation (IOC; n=246) and/or permanents (n=214). For each of the IOC-classified cases, we assessed whether or not an appendectomy was performed, as well as the presence or absence of sampled/excised peritoneal disease, bilaterality of the ovarian masses, patient age, any gross abnormality in the appendix, and the final diagnoses rendered at all sites.

Results: The distribution of IOC diagnoses on the 246 mucinous ovarian tumors were as follows: benign (114), borderline (55), carcinoma (21), mucinous neoplasm without definitive classification (53), and probable metastases (3). Appendectomies were performed on 82 (33%) of the 246 cases. In 30 (36%) of these 82 cases, the appendix was grossly normal, the ovarian tumor was unilateral, and there was no peritoneal disease. Microscopic examination of the appendices in these 30 cases showed no mucinous neoplasms therein, but one case had a 4 mm well-differentiated carcinoid. In contrast, among the remaining 52 cases (i.e. those with peritoneal disease and/or appendiceal gross abnormality and/or ovarian tumor bilaterality), 12 neoplasms (23%) were microscopically identified in the appendix (4 adenocarcinomas; 7 LAMN; 1 carcinoid) [p=0.0256]. 10 (83%) and 8 (67%) of these 12 neoplasms were associated with grossly abnormal appendices and/or peritoneal disease respectively.

Conclusions: We found no clear evidence to support the routine performance of appendectomies following frozen section diagnoses of ovarian mucinous neoplasms as a general practice. In our cohort, all identified mucinous appendiceal neoplasms were associated with gross abnormalities of the appendix, peritoneal disease, and/or ovarian tumor bilaterality. This suggests that only in patients that meet these criteria would appendectomies most likely be beneficial.

662 Prognostic Implications of Depth of Cervical Stromal Invasion in Type 1 and Type 2 Endometrial Cancers

Bassam Alkamachi[1], Simeng Zhu[1], Alexandra Sitarik[1], Mohamed Elshaikh[2], Ghassan Allo[2]
[1]Henry Ford Health System, Detroit, MI, [2]Henry Ford Hospital, Detroit, MI

Disclosures: Bassam Alkamachi: None; Simeng Zhu: *Grant or Research Support*, Varian Medical Systems; Alexandra Sitarik: None; Mohamed Elshaikh: None; Ghassan Allo: None

Background: Cervical stromal invasion (CSI) by endometrial carcinoma (EC) signifies worse prognosis needing adjuvant therapy. Prognostic implications of this invasion are unknown. We investigate in this study the prognostic significance of depth and pattern of CSI in patients with type 1 and type 2 EC.

Design: This is a retrospective study of patients with FIGO stage 2 EC, treated in 1991 -2019, grouped into type 1 and 2 ECs based on histotype. After IRB approval, we assessed microscopic depth of CSI (distance from cervical surface to deepest point of invasion in cervical stroma), and pattern of invasion (based on endocervical adenocarcinoma patterns A, B, and C). Descriptive analysis and Cox regression models were produced.

Results: Materials were available on 50 type 1 and 52 type 2 ECs. Clinical characteristics are summarized in table 1.

For type 1 EC, median (min, max) depth of CSI was 3.5(0.5-20.0) mm, with median percentage invasion of 33.3(6.7-100)%. CSI to ≥2/3 of stroma was found in 9(18%) cases, being associated with worse overall survival (OS) on univariable (HR, 4.36; p-value, 0.02) and multivariable (HR, 8.27; p-value, 0.01) analysis. CSI of 4.0 mm or more, found in 24(48%) cases, was associated with non-significant tendency for worse OS on univariable analysis, but on multivariable analysis, it correlated with worse OS (Figure 1a). The odds of recurrence was nearly 3.5 times higher with each 5-mm increase in CSI depth on univariable(OR, 3.46; 95% CI, 1.21-9.90; p-value, 0.021) and multivariable(OR, 4.11; 95% CI, 1.11-15.21; p-value, 0.034) analyses. However, the study was not powered to examine the correlation of a specific depth of invasion with recurrence rates (N=5 with recurrence). Pattern of invasion was not correlated with different OS or recurrence rate on univariable and multivariable analyses.

For type 2 ECs, median depth of CSI is 5(0.50-17.0) mm, with median percentage invasion to cervical stromal thickness of 43.7(4.6-100)%. Depth and pattern of CSI was not associated with different OS or recurrence rate after examining multiple cut points on univariable and multivariable testing (figure 2)

		Type 1 (n=50)		Type 2 (n=52)	
		n	%	n	%
Age [median(range)] years		65 (41-91)		67 (36-96)	
Race	**White**	37	74	29	55.8
	AA	11	22	21	40.4
	Other	2	4	2	3.8
Histology	**Endometrioid**	50	100	15	28.8
	serous	0	0	12	23.1
	clear cell	0	0	6	11.5
	carcinosarcoma	0	0	9	17.3
	dedifferentiated	0	0	2	3.8
	mixed	0	0	8	15.4
Grade	**1**	30	60	0	0
	2	20	40	0	0
	3	0	0	15	28.8
	(high grade)	0	0	37	71.2
Myometrial Invasion	**<50%**	23	46	25	48.1
	50% of more	27	54	27	51.9
Angiolymphatic space invasion	**Negative**	39	78	22	42
	Positive	11	22	30	58
Radiation therapy	**Yes**	42	84	41	78.8
	No	8	16	11	21.2

Figure 1 - 662

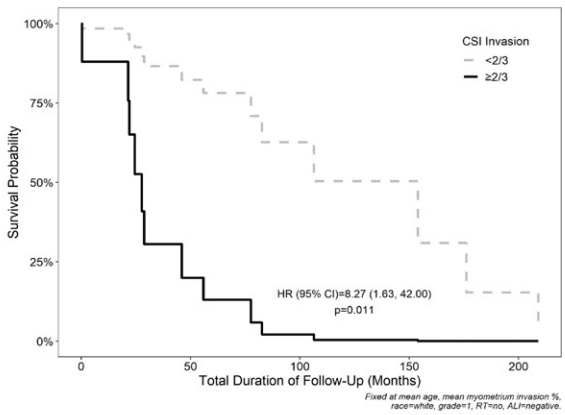

Figure 1: Fitted cox regression survival curve for the difference between CSI invasion above and below 2/3rds among type 1 patients, after adjusting for age myometrium invasion, race, grade, RT, and ALI.

Figure 2 - 662

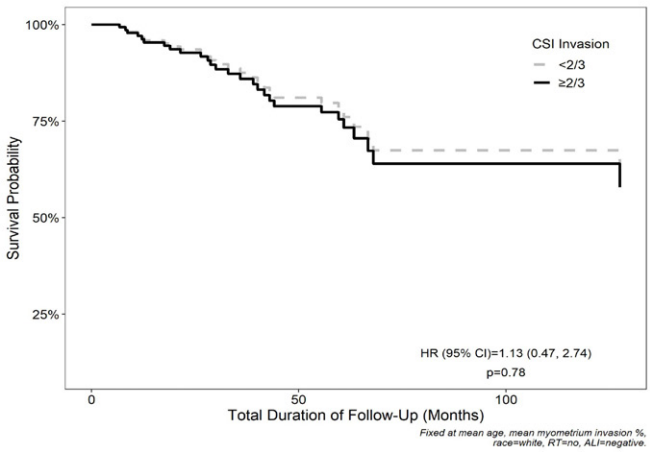

Conclusions: Higher depth of CSI, especially at 2/3 or more, is predictive of worse OS in type 1 ECs and generally correlates with higher recurrence rate. Routine reporting of CSI depth is recommended, and further prospective studies to explore adjuvant treatment adjustment are needed. In contrast, CSI characteristics are not associated with different behavior in type 2 ECs.

663 Endometrial Serous Carcinomas Lacking TP53 Mutations: How Common Are They Really?

Douglas Allison[1], Britta Weigelt[1], Lora Ellenson[1]
[1]*Memorial Sloan Kettering Cancer Center, New York, NY*

Disclosures: Douglas Allison: None; Britta Weigelt: *Advisory Board Member*, Repare Therapeutics; Lora Ellenson: None

Background: Endometrial serous carcinoma (ESC) is defined by the WHO as a carcinoma “with diffuse, marked nuclear pleomorphism, typically exhibiting papillary and/or glandular growth”. Identification of *TP53* mutations is considered “supportive”, with 88% of the ESCs in The Cancer Genome Atlas study (Nature 2013) harboring a *TP53* somatic mutation. However, with widespread adoption of p53 immunohistochemistry (IHC) and molecular testing, evidence of *TP53* mutation is increasingly becoming a de facto requirement among many pathologists for diagnosis. Here, we sought to define the prevalence of ESCs lacking *TP53* mutations in a large series of endometrial cancers subjected to clinical sequencing and explore their clinicopathologic characteristics.

Design: We identified all ESCs at our institution that underwent clinical testing with our in-house next-generation sequencing assay from 2015 to present. We reviewed patient charts and pathology reports, noting clinicopathologic findings. Cases with mixed histology (e.g. mixed endometrioid or clear cell), cases lacking in-house pathology review, and cases with low tumor purity were excluded. For patients with multiple samples, the sample with the highest tumor purity was considered.

Results: Of the 351 identified ESCs, all but three (i.e. 348, 99.1%) harbored an alteration in *TP53*. Other commonly identified alterations included mutations in *PIK3CA* (41%) and *PPP2R1A* (36%), and amplification of *ERBB2* (19%). Of the three *TP53* wild-type ESCs, one showed aberrant expression of p53 by IHC (null pattern), while another was an external case where IHC was not performed. Only one bona fide ESC had no detected *TP53* mutation and wild-type p53 expression by immunohistochemistry: a 63 year old woman who presented with postmenopausal bleeding with subsequent hysterectomy demonstrating pT1bN1 disease (Figure 1). NGS showed a *PIK3CA* in-frame deletion and a nonsense mutation in *ZFHX3,* among other alterations.

Figure 1 - 663

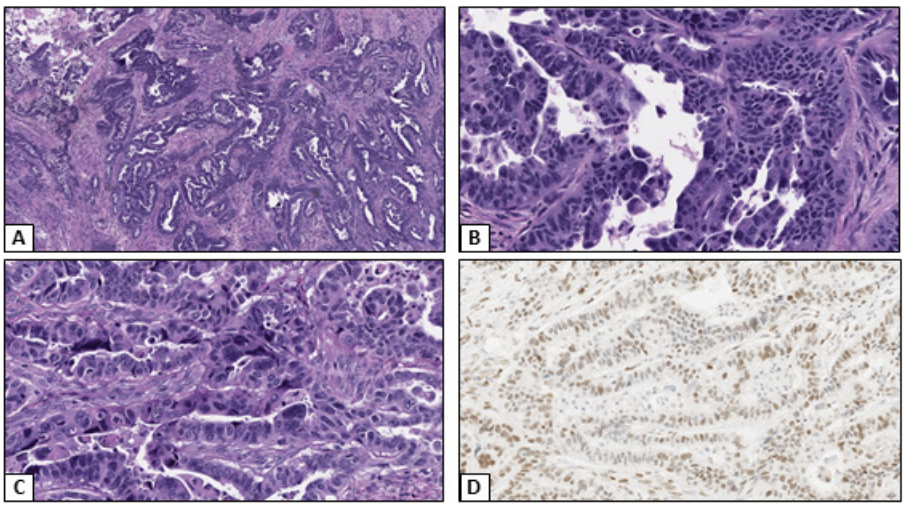

Figure 1. Endometrial serous carcinoma lacking a TP53 mutation. The tumor shows typical morphology with glandular and focal papillary architecture (A) and marked nuclear pleomorphism (B, C). Immunohistochemistry for p53 shows wild-type staining (D).

Conclusions: ESCs lacking *TP53* somatic mutations are vanishingly rare, with only one confirmed *TP53* wild-type case in this cohort of 351 patients, and one additional case where confirmatory IHC could not be performed. Our data demonstrate that *TP53* wild-type ESCs are even rarer than previously thought. However, the data may also reflect that modern pathologists are increasingly reluctant to diagnose ESC in the absence of aberrant p53 expression/*TP53* mutation.

664 Immunohistochemical Profiles Including p53, MMR, PR and CTNNB1 are Associated with Survival of Patients Diagnosed with Ovarian Endometrioid Carcinoma

Zainab Alshamma[1], Monica Rodriguez[2], Eun-Young Kang[3], Cheng-Han Lee[4], Michael Anglesio[5], Martin Koebel[6]
[1]University of Alberta, Calgary, Canada, [2]Cumming School of Medicine, University of Calgary, Calgary, Canada, [3]University of Calgary, Calgary, Canada, [4]BC Cancer, Vancouver, Canada, [5]The University of British Columbia, Vancouver, Canada, [6]Alberta Precision Laboratories, University of Calgary, Calgary, Canada

Disclosures: Zainab Alshamma: None; Monica Rodriguez: None; Eun-Young Kang: None; Cheng-Han Lee: None; Michael Anglesio: None; Martin Koebel: None

Background: We and others have recently established that ovarian endometrioid carcinomas (OEC) are comprised of the same molecular subtypes as endometrial endometrioid carcinomas, namely, abnormal p53 (p53abn), MMR deficient (MMRd), *POLE*-mutated and no specific molecular profile (PMID: 32737030). The goal of the current study was to assess whether a limited immunohistochemical profile could achieve a similar stratification in independent cohorts where *POLE* mutation testing was not available.

Design: Tissue microarrays from 3 cohorts comprised of 392 ovarian endometrioid carcinomas were stained with p53, PMS2, MSH6, PR and CTNNB1. Expression was interpreted as follows: p53: abnormal mutation-type (overexpression, complete absence,

cytoplasmic) versus normal wild-type pattern; PMS2 and MSH6: complete absence of expression in tumor cells with an internal control (loss), geographic absence (subclonal) or retained; PR: absent/loss, focal/reduced (1-50%) and diffuse/retained (>50%); CTNNB1: nuclear (any nuclear expression, i.e. as few as 1% of tumor cells) versus membranous. Unsupervised hierarchical clustering, Kaplan-Meier survival and Cox proportional-hazards regression were performed.

Results: OEC cases showed p53abn in 48/389 (12.3%), MMRd in 48/378 (12.7%), PR loss in 62/393 (15.8%), PR reduced in 54/392 (13.8%), and CTNNB1 nuclear in 150/378 (39.7%). p53abn, 3-tier PR, and nuclear CTNNB1 were associated with survival in univariable analysis (log-rank p<0.0001, p<0.0001, p=0.024) while MMRd was not. Unsupervised hierarchical clustering created 5 clusters, which were associated with survival in univariable (log-rank p<0.0001) and multivariable analysis (p=0.0009) adjusted for age, stage and cohort. The largest difference in 5-year survival rates (YSR) was observed between cluster 5 (96.3% 5-YSR) and cluster 2 (70.5% 5-YSR). Cluster 5 accounted for 31.7% of all cases and was characterized by ubiquitous nuclear CTNNB1 expression. Cluster 2 accounted for 14.6% of the cases and was characterized by ubiquitous loss of PR expression in combination with p53abn in a subset of cases.

Figure 1 - 664

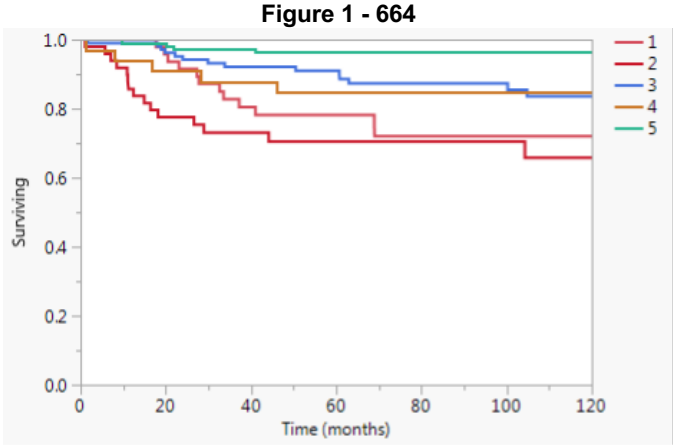

Conclusions: PR and CTNNB1 seem to have additional value in the prognostication of ovarian endometrioid carcinomas and should be integrated in molecular subtyping approaches.

665 Loss of NF1 Expression Occurs at Significant Frequency in Tubo-Ovarian High-grade Serous Carcinoma and is Associated with Other Favorable Biomarkers

Zainab Alshamma[1], Eun-Young Kang[2], Linda Cook[3], Yangxin FU[4], Cheng-Han Lee[4], David Reuss[5], Martin Koebel[6]
[1]University of Alberta, Calgary, Canada, [2]University of Calgary, Calgary, Canada, [3]University of New Mexico Health Sciences Center, Albuquerque, NM, [4]University of Alberta, Edmonton, Canada, [5]University of Heidelberg, Heidelberg, Germany, [6]Alberta Precision Laboratories, University of Calgary, Calgary, Canada

Disclosures: Zainab Alshamma: None; Eun-Young Kang: None; Linda Cook: None; Yangxin FU: None; Cheng-Han Lee: None; David Reuss: None; Martin Koebel: None

Background: PARP inhibitors are effective in treating homologous repair (HR)-deficient tubo-ovarian high-grade serous carcinomas (HGSC). No targeted therapies for HR-proficient HGSC are available. Inactivating mutations and genomic losses of NF1 are anti-correlated with BRCA1/2 mutations suggesting that NF1 could be a potential target in HR-proficient HGSC. Our objective was to determine the prevalence of loss of NF1 protein expression and its correlation with the clinicopathological parameters in HGSC.

Design: Tissue microarrays from a population-based cohort of 596 HGSC were stained with a previously validated NF1 antibody (clone NFC, PMID: 28862263). Expression was interpreted as complete absence in tumor cells with an internal control (loss), geographic absence (subclonal) or retained. Kaplan-Meier survival and Cox proportional-hazards regression were performed.

Results: Loss of NF1 expression was detected in 89/596 (14.9%) of HGSC, including 9 cases (1.5%) with subclonal loss. Patients with HGSC showing loss of NF1 expression were on average 3 years younger (p=0.022) but showed no differences in stage at

diagnosis, residual disease and chemotherapy status. Loss of NF1 expression was significantly associated with favorable biomarkers such as higher degree of PR expression (p=0.014) and loss of RB1 expression (p=0.0022), and inversely associated with the unfavorable combination of CCNE1 high-level amplification/overexpression (p=0.012). No associations with WT1, TP53, or proliferation surrogates such as CDKN2A, MCM3 or Ki-67 were seen. Within HGSC, loss of NF1 expression was not associated with disease specific survival in univariable analysis (log-rank p=0.47). There was, however, a suggestive trend for favorable short-term survival at 2 years when comparing tumors with NF1 loss to no alteration (HR=0.52, 95% CI 0.20-1.10, p=0.091), which disappeared at 10 years (HR=1.04, 95% CI 0.74-1.43, p=0.82). As previously shown, tumors with combined CCNE1 alterations had a significantly shorter survival compared to both groups (Figure).

Figure 1 - 665

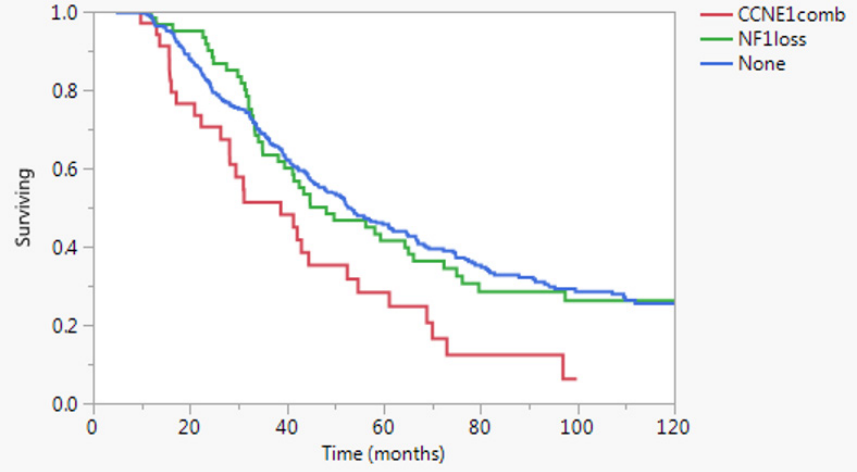

Conclusions: NF1 loss is present in a significant proportion of HGSC and associated with longer survival compared to cases with combined CCNE1 alterations suggesting that the HR-proficient subgroup of HGSC is molecularly heterogeneous. The suggestive short-term survival benefit diminishes over time suggesting that NF1 may be implicated in treatment resistance. Preclinical models are required to determine whether NF1 is a valid target in HGSC.

666 Paraneoplastic Anti-N-Methyl-D-Aspartate (NMDAR) Receptor Encephalitis Associated with Ovarian Germ Cell Tumors. A Clinicopathologic Study of 25 Cases

Isabel Alvarado-Cabrero[1], Ana Elena Martin-Aguilar[2], Rafael Estevez-Castro[3], Raquel Valencia-Cedillo[4]
[1]Mexican Oncology Hospital SXXI, IMSS, Mexico City, Mexico, [2]Hospital de Oncologia, CMN Siglo XXI IMSS, [3]Santiago, Dominican Republic, [4]Mexican Oncology Hospital IMSS, Mexico City, Mexico

Disclosures: Isabel Alvarado-Cabrero: None; Ana Elena Martin-Aguilar: None; Rafael Estevez-Castro: None; Raquel Valencia-Cedillo: None

Background: Anti-NMDAR encephalitis is a subcategory of auto-immune encephalitis. It is known for its aggressive presenting symptoms and rapid deterioration, yet, it is treatment responsive. It is associated in 50% to ovarian teratoma. The goal of this study was to examine the morphologic features of a set of germ cell ovarian tumors that were resected for usual/surgical indications.

Design: Our population consisted of 25 patients diagnosed with anti-NMDAR encephalitis associated with ovarian tumor from 1999-2010, Medical records were reviewed to determine clinical features and pathologic tumor characteristics.

Results: Twenty-five women (16-41 years) developed seizures, amnesia and psychiatric symptoms. Extensive workup was pursued in all patients before ovarian tumor resection. Cerebrospinal fluid antibodies revealed Anti-NMDA receptors in all patients. Brain Magnetic Resonance Imaging was normal in 19 cases and 6 patients showed fluid-attenuated inversion recovery and T2 hyperintensities over the left cerebral cortex and cerebellum. Associated tumors. Tumors ranged from 2.5 to 12cm diameter. Thirteen patients had mature teratoma and seven immature teratoma. In addition, five patients had a malignant mixed germ cell tumor (MMGCT) of the ovary. Histopathologic combination was: mature teratoma and yolk sac tumor (n:2), teratoma and dysgerminoma (n:2). One patient had a very rare case of MMGCT, tumor consisted of yolk sac tumor, embryonal carcinoma,

dysgerminoma and teratoma. Tumor resection and immunotherapy resulted in improvement or full recovery of sixteen of 25 patients. Although 9 cases had weight gain (n:4), sleep disturbances (n:3) and fatigue (n:2).

Conclusions: 1. Our findings indicate that a young woman with acute psychiatric symptoms, seizures and central hypoventilation physicians should suspect a paraneoplastic disorder. The tumor search should focus in the ovaries. 2. We report here for the first time a patient with anti-NMDAR encephalitis in association with malignant mixed germ cell tumors of the ovary.

667 Benign Stratified Intraepithelial Mucinous Proliferation of the Uterine Cervix, a Previously Unreported Potential Mimic of SMILE: Review of 702 Samples

Elizabeth Arslanian[1], Kamaljeet Singh[1], Katrine Hansen[2], C. James Sung[3], M. Ruhul Quddus[3]
[1]Women and Infants Hospital, Providence, RI, [2]Brown University Pathology, Providence, RI, [3]Women & Infants Hospital/Alpert Medical School of Brown University, Providence, RI

Disclosures: Elizabeth Arslanian: None; Kamaljeet Singh: None; Katrine Hansen: None; C. James Sung: None; M. Ruhul Quddus: None

Background: Stratified mucin-producing intraepithelial lesion (SMILE) is a histologic subtype of HPV-associated cervical adenocarcinoma in situ (AIS). At our academic center, we have observed benign changes similar to SMILE in endocervical specimens. We aim to establish histologic characteristics and prevalence of this morphologic pattern by retrospectively reviewing cervical samples at our academic hospital center.

Design: We retrospectively retrieved 296 consecutive cases accessioned as endocervical biopsies at our academic hospital center during a two-and-a-half-month period in 2021. Some included multiple specimens, totaling 483 biopsies and 219 endocervical curettages (ECC), n=702. We included cases showing at least focal endocervical epithelial stratification with pencillate nuclei. We rejected specimens in which layering represented tangential sectioning, tubal metaplasia, immature squamous metaplasia, microglandular hyperplasia, AIS, HSIL or SMILE.

Results: We identified stratified intraepithelial mucinous proliferation in 51 patients (hyperplastic (multilayered) n=27; non-hyperplastic (bilayered) n=24). We found hyperplastic proliferation in 6% of biopsies (29/483) and in 0.9% of ECC (2/219). Histologic findings included epithelial stratification, intracytoplasmic apical mucin visible on low-power, paler cytoplasm, low nuclear to cytoplasmic ratio, pencillate nuclei, rare mitoses and absence of apoptotic bodies. Luminal infoldings were present in a few cases. Changes ranged from focal (59%) to multifocal (41%) and were limited to glandular clefts in 65% of cases. IHC studies (n=12) showed negative p16 and low Ki-67, suggesting absence of underlying high-risk HPV infection. A p53 stain (n=1) revealed wild-type expression. HSIL was concomitant in 29.6% (8/27) of patients with hyperplastic proliferation. None of the cases showed gastric-type differentiation. In 87% of cases with available levels, changes persisted on deeper sections, excluding tangential sectioning artifact.

Table 1. Clinicopathologic characteristics of the 51 patients with stratified intraepithelial mucinous proliferation.

Stratified Intraepithelial Mucinous Proliferation		**n=51 (%)**
Extent of involvement		
Focal (1 gland)		30 (59)
Multifocal (> 1 gland)		21 (41)
Variant		
Hyperplastic		27 (53)
Non-Hyperplastic		24 (47)
Type of glandular involvement		
Cleft only		33 (65)
Surface only		3 (6)
Both cleft & surface		6 (12)
Mitoses, present		3 (6)
Levels		15
Persistent changes on levels		13
Regression of changes on levels		2
Immunohistochemistry		
p16 (n=11)	Positive block-like	0
	Negative or patchy	11
Ki-67 (n=11)	Negative or low	9

	Increased, slightly	2
p53 (n=1)	Wild-type pattern	1
	Mutated pattern	0
Inflammation around / into involved glands		27 (53)
Mild		15 (29)
Moderate		10 (20)
Severe		2 (4)
Concomitant lesion on biopsy / ECC		
HSIL		16 (31)
AIS		2 (4)
SMILE		0
High-risk HPV infection		
HPV 16		8 (16)
HPV 18		3 (6)
Other		31 (61)
Pap smear		
NIL		12 (24)
ASC-US		15 (29)
LSIL		15 (29)
ASC-H and HSIL		8 (16)
AGC		0

Figure 1 - 667

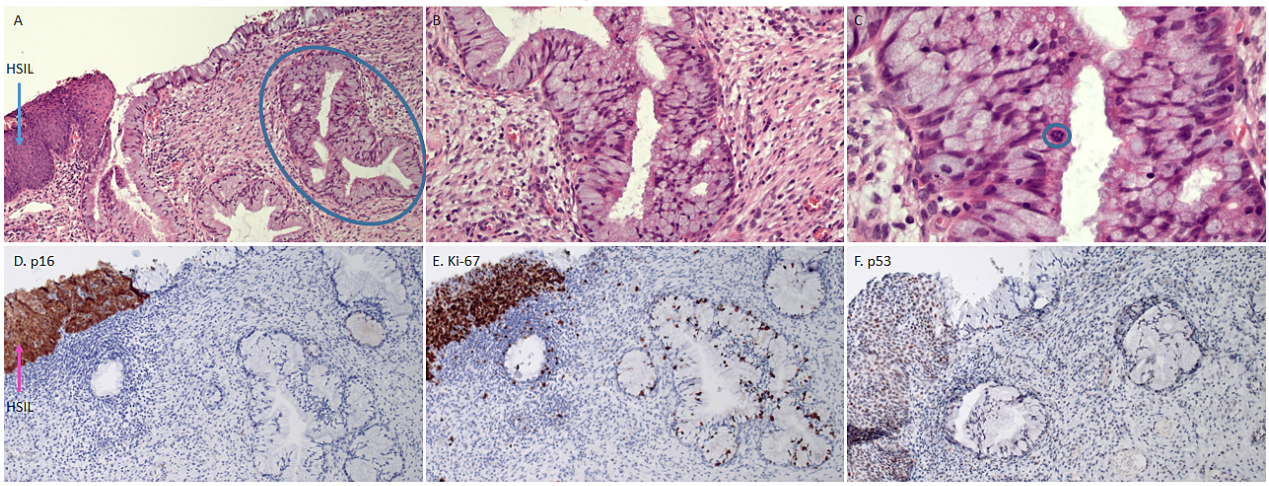

Figure 1. Mimicker of SMILE and its Immunohistochemical Findings. A. HE, 10X. Hyperplastic variant (right), with adjacent HSIL (left). B. HE, 20X. Hyperplastic variant, stratified mucinous cells with small bland nuclei. C. HE, 40X. Hyperplastic variant, mitotic figure. D. p16, 10X. Negative (right); internal control: block-positive HSIL (left). E. KI-67, 10X: Slightly increased mitotic activity (right); increased full-thickness staining in HSIL (left). F. p53, 10X: Wild-type pattern.

Figure 2 - 667

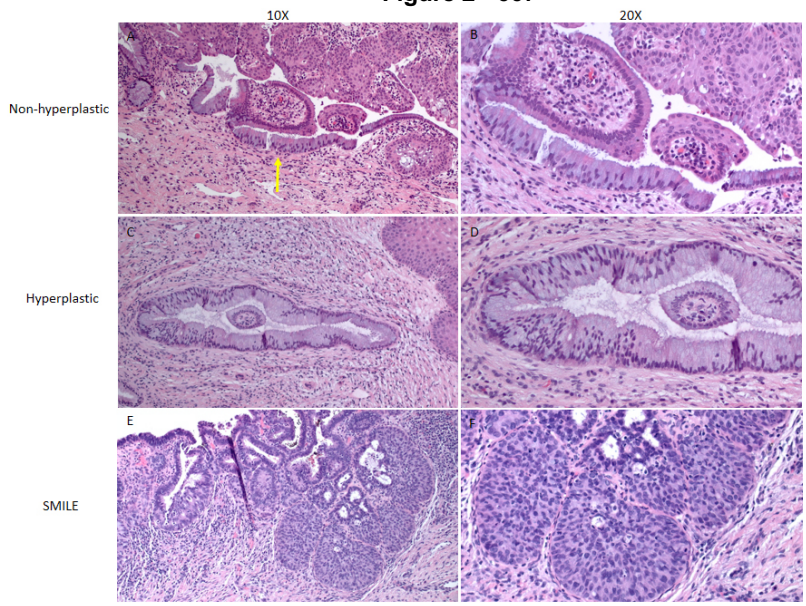

Figure 2. Non-hyperplastic and Hyperplastic Variants of Previously Undescribed Mimicker of SMILE. A-B. Non-hyperplastic variant. Abrupt bilayering of mucin-producing cells with pale cytoplasm and small bland pencillate to round nuclei. C-D. Hyperplastic variant. Abrupt multilayering of mucin-producing cells with pale cytoplasm and small bland pencillate to round nuclei. E-F. SMILE. Multilayered atypical mucin-producing cells with mitoses and apoptotic figures.

Conclusions: We describe benign stratified intraepithelial mucinous proliferation of the uterine cervix, which shares morphologic features with SMILE. We believe the hyperplastic variant of these changes represent a previously unreported diagnostic pitfall. Because of the often coexistent HSIL, we propose that this finding be considered a potential marker for further scrutiny to rule out bona fide dysplasia. Follow-up studies and molecular HPV testing are needed to further characterize our findings.

668 Collagen IV and Laminin Immunostaining to Adjudicate Silva Classification of HPV-Associated Endocervical Adenocarcinoma

Elizabeth Arslanian[1], M. Ruhul Quddus[2], Katrine Hansen[3], C. James Sung[2], Kamaljeet Singh[1]
[1]Women and Infants Hospital, Providence, RI, [2]Women & Infants Hospital/Alpert Medical School of Brown University, Providence, RI, [3]Brown University Pathology, Providence, RI

Disclosures: Elizabeth Arslanian: None; M. Ruhul Quddus: None; Katrine Hansen: None; C. James Sung: None; Kamaljeet Singh: None

Background: HPV-associated cervical adenocarcinoma (CXCA) Silva classification stratifies risk of nodal metastases, recurrence and survival. Extent of destructive invasion defines Silva patterns (A: none; B: focal; C: diffuse). Collagen IV and laminin immunohistochemistry (IHC) have been shown to identify basement membrane defects in CXCA. No study has assessed these defects in the 3 Silva patterns. We hypothesize that basement membrane defects progressively worsen from AIS to type C. We investigate using collagen IV and laminin IHC to assess invasion as an adjunct to Silva classification.

Design: We retrospectively retrieved 32 CXCA (hysterectomy or cone) from our academic center database with their clinical and histological details. We reviewed H&E slides to confirm the diagnosis and to select a tissue block with the highest Silva pattern of invasion for IHC. We performed collagen IV (C1V22, CellMarque) IHC in all cases. We used two polyclonal laminin antibodies: Thermofisher (Ab1), n=5 and Neomarkers (Ab2), n=27. Basement membrane IHC staining around neoplastic glands was scored as: 0=intact strong; 1=decreased but circumferential; 2=non-circumferential with breaks; 3=absent.

Results: There were 5 (16%) type A, 15 (47%) type B and 12 (38%) type C pattern CXCA. Mean age was 46 years old (26-76), with mean tumor size of 10 mm (2-35) and mean depth of invasion of 5 mm (2-15). The FIGO stage was 1A1 in 4 (13%), 1A2 in 6 (19%), 1B1 in 8 (25%), 1B2 in 2 (6%) and IIA in a 1 (3%) cases. Collagen IV staining was abnormal in CXCA foci in 31 (97%) cases (Table 1). Only one pattern A CXCA showed intact collagen IV. Score 3 was noted in 20/28 cases (71%) with destructive invasion (Silva B or C). Concurrent AIS was identified in 11 (55%) cases, with intact collagen IV staining being most common (p=0.001). This pattern was 97% specific for AIS and was not observed in pattern A invasive carcinoma. Laminin Ab1 (n=5) showed

incomplete staining in areas of destructive invasion. Tumor cells expressed laminin Ab2 in 7 CXCA, but it was not sensitive for epithelial basement membrane.

Table 1. Collagen IV Staining Score in 32 Invasive Endocervical Adenocarcinomas and in 5 AIS

	Score 0	Score 1	Score 2	Score 3
AIS	6 (54%)*	1 (10%)	3 (26%)	1 (10%)
Silva A	0	0	3 (60%)	2 (40%)
Silva B or C	1 (4%)	2 (7%)	4 (15%)	20 (74%)*

Legend: Each case is scored according to the highest score observed, as follows: 0 = intact strong; 1 = decreased but circumferential; 2 = non-circumferential with breaks; 3 = absent.

*p-value=.001 (Fisher's Exact test)

Figure 1 - 668

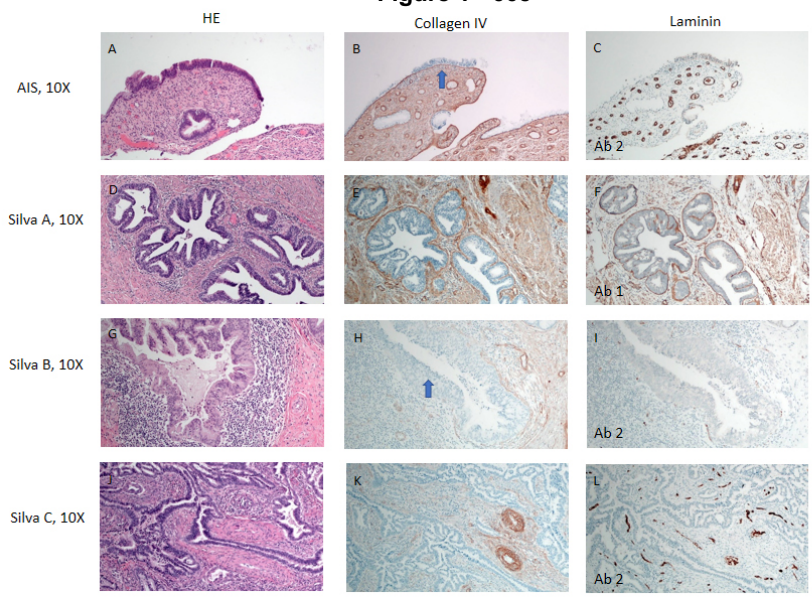

Figure 1. Collagen IV and Laminin Basement Membrane Immunostaining in HPV-Associated Endocervical Adenocarcinoma. A. AIS. B. Intact staining (score 0). C. Antibody failing to highlight basement membrane surrounding benign and malignant endocervical glands (not scored). D. Invasive adenocarcinoma. E. Circumferential staining of reduced intensity (score 1) F. Circumferential staining of reduced intensity (score 1). G. Focal desmoplastic reaction (destructive invasion). H. Incomplete staining (score 2) associated with desmoplasia. I. Antibody failing to highlight basement membrane surrounding benign and malignant endocervical glands (not scored). J. Diffuse destructive invasion. K. Absent staining (score 3) L. Antibody failing to highlight basement membrane surrounding benign and malignant endocervical glands (not scored).

Figure 2 - 668

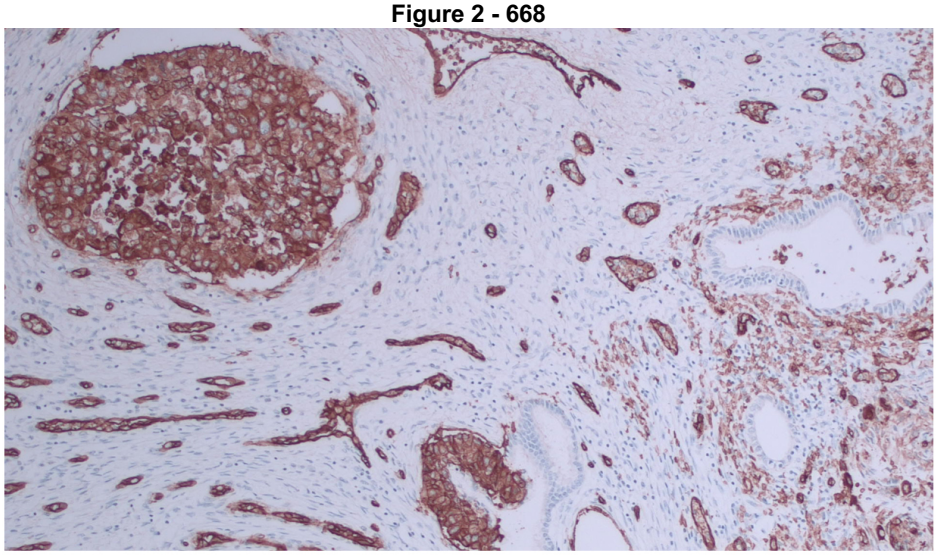

Figure 2. 10X, Laminin Cytoplasmic Immunostaining in In Situ and Invasive Endocervical Adenocarcinoma Tumor Cells.

Conclusions: Abnormal collagen IV expression is observed in 97% of invasive CXCA. Silva patterns B and C frequently show complete loss of collagen IV expression whereas AIS foci retain intact collagen IV staining. Laminin expression in the endocervix is antibody dependent. We propose collagen IV and laminin IHC as an additional tool to assess destructive invasion in CXCA, which can be used to adjudicate AIS and Silva pattern classification.

669 Stratified Mucinous Intraepithelial Lesion (SMILE) and Its Association with "Benign" Stratified Intraepithelial Mucinous Proliferation: Report of a Series

Elizabeth Arslanian[1], Kamaljeet Singh[1], Katrine Hansen[2], C. James Sung[3], M. Ruhul Quddus[3]
[1]Women and Infants Hospital, Providence, RI, [2]Brown University Pathology, Providence, RI, [3]Women & Infants Hospital/Alpert Medical School of Brown University, Providence, RI

Disclosures: Elizabeth Arslanian: None; Kamaljeet Singh: None; Katrine Hansen: None; C. James Sung: None; M. Ruhul Quddus: None

Background: HPV-associated cervical squamous intraepithelial lesions and adenocarcinoma in situ (AIS) including its subtype SMILE (stratified mucinous intraepithelial lesion) are known precursors to squamous cell carcinoma and invasive adenocarcinoma, respectively. Our group recently described benign stratified intraepithelial mucinous proliferation, a morphologic pattern potentially mimicking SMILE. As noted, a significant proportion of concurrent high-grade squamous intraepithelial lesion (HSIL) is associated with this pattern. As the same risk factors underlie HSIL and SMILE, we hypothesize that benign stratified intraepithelial mucinous proliferation is associated with both SMILE and HSIL.

Design: We retrospectively searched for SMILE in our academic hospital's database using the keyword "SMILE" from 2010 to 2021 (n=19). Six (6) cases were eliminated for various reasons. The H&E and immunohistochemistry slides were reviewed to confirm SMILE diagnosis and record concurrent HSIL, AIS and benign stratified intraepithelial mucinous proliferation using the following criteria for the diagnosis of the latter: multilayering of mucin-producing endocervical cells, pencillate nuclei, absence or paucity of mitoses, no apoptotic bodies and no cytologic atypia. We used comparative data from the cohort in which we had described benign stratified intraepithelial mucinous proliferation (retrospective review of 702 cervical samples).

Results: Concurrent benign stratified intraepithelial mucinous proliferation (figure 1) is identified in 54% of SMILE cases (figure 2, table 1), and HSIL and AIS in 11 (85%) and in 4 (31%) cases of SMILE respectively. In most instances, SMILE and benign proliferation were detected in separate glands. However, bona fide SMILE and benign proliferation were noted even within the same gland, involving distinct areas.

Table 1. Clinical and pathological characteristics of 13 cases of SMILE

SMILE	**13 (%)**
Age	
Mean	38
Median	32
HPV infection	
HPV 16	5 (38)
HPV 18	1 (8)
High-risk HPV, unknown subtype	3 (23)
Unknown infection status	4 (31)
Negative	0
Pap smear	
HSIL	1 (8)
ASC-H	3 (23)
LSIL	1 (8)
ASC-US	3 (23)
NIL	2 (15)
Unavailable	3 (23)
Concurrent intraepithelial lesion	
HSIL	11 (85)
Benign stratified intraepithelial mucinous proliferation	7 (54)
AIS	4 (31)

Figure 1 - 669

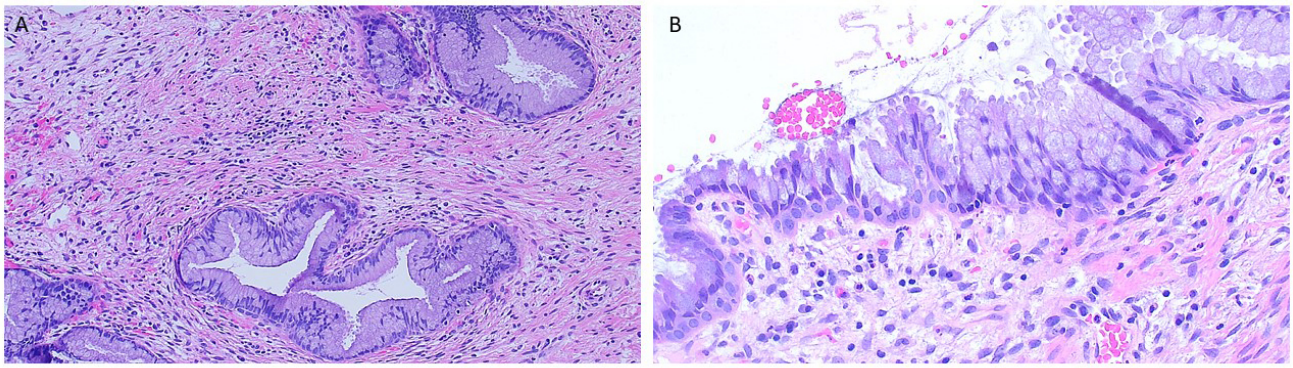

Figure 1. Benign stratified intraepithelial mucinous proliferation of the uterine cervix, H&E. A. Endocervical clefts showing focal stratification of benign mucinous cells with pencillate nuclei, low magnification. B. Endocervical surface showing focal stratification of benign mucinous cells with pencillate nuclei, high magnification.

Figure 2 – 669

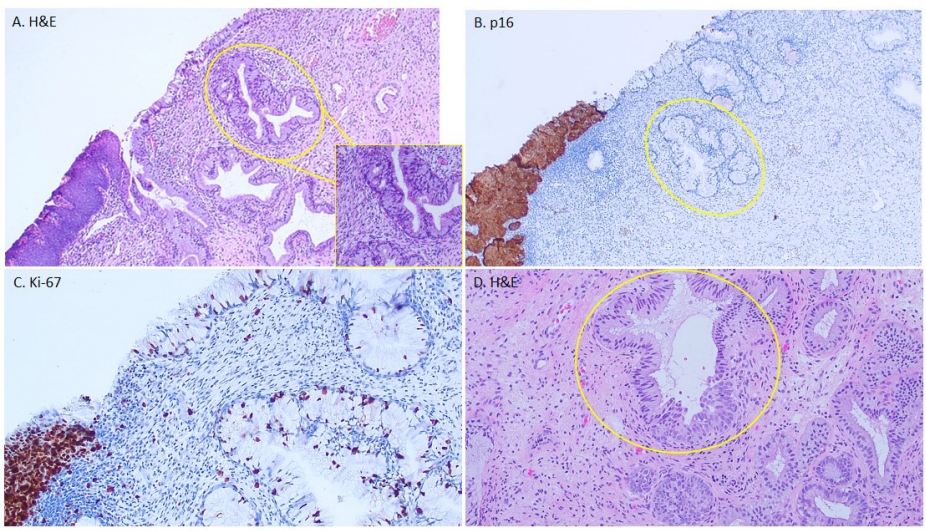

Figure 2. Concurrent benign stratified intraepithelial mucinous proliferation and squamous and glandular intraepithelial lesions. A. Benign stratified intraepithelial mucinous proliferation (right and inset) and HSIL (left), low magnification. B. p16 block positivity in HSIL and negative benign stratified intraepithelial mucinous proliferation (circled), low magnification. C. Ki-67 full-thickness positivity in HSIL and low staining in benign stratified intraepithelial mucinous proliferation, medium magnification. D. Gland (circled) partially involved by benign stratified intraepithelial mucinous proliferation (bottom left) and SMILE (bottom), medium magnification.

Conclusions: Fifty-four (54%) of SMILE cases had concurrent benign stratified intraepithelial mucinous proliferation, raising the question of a possible causal relationship. We recommend examination of additional deeper levels into the block to exclude true dysplasia on biopsies. It appears prudent to document "benign proliferation" on the surgical pathology report so that the clinician can take precautionary measures if indicated. Exploring larger cohorts and molecular characterization of benign stratified intraepithelial mucinous proliferation could provide further insight into its potential association with cervical intraepithelial neoplasia.

670 Immunohistochemical Analysis of Leiomyosarcoma-Associated Genetic Abnormalities in Leiomyomas with Bizarre Nuclei

Ridin Balakrishnan[1], Amir Momeni Boroujeni[2], Lora Ellenson[1], Sarah Chiang[1]
[1]Memorial Sloan Kettering Cancer Center, New York, NY, [2]Brigham and Women's Hospital, Harvard Medical School, Boston, MA

Disclosures: Ridin Balakrishnan: None; Amir Momeni Boroujeni: None; Lora Ellenson: None; Sarah Chiang: None

Background: Leiomyoma with bizarre nuclei (LMBN) is a benign leiomyoma variant that frequently harbors somatic *FH* mutations. Distinction from uterine leiomyosarcoma (LMS) is difficult due to significant morphologic overlap and limited role of

immunohistochemistry in this differential diagnosis. Soft tissue and uterine LMS frequently harbor genetic alterations in *TP53*, *ATRX*, *RB1, PTEN*, *DAXX*, *MDM2* and *CDKN2A* which are detectable by immunohistochemical methods. In this study, we evaluate the immunohistochemical expression of p53, ATRX, RB1, PTEN, DAXX, MDM2, and MTAP in LMBN and uterine LMS to determine their utility as potential diagnostic tools.

Design: Formalin-fixed paraffin-embedded tissue was obtained from LMBN (n=9) and uterine LMS (n=7) diagnosed from 2016-2020. FH immunostaining was previously performed on all LMBN as part of the clinical diagnostic work up, and all tumors were FH-deficient. A panel of immunohistochemical stains targeting ATRX, RB1, P53, PTEN, DAXX, MTAP and MDM2 was performed on LMBN and uterine LMS. Stains were interpreted as wildtype or mutant patterns (Table 1).

Results: Six of nine (66.6%) FH-deficient LMBN showed wild-type ATRX, RB1, P53, PTEN, DAXX, MTAP and MDM2 expression. Three (33.4%) remaining LMBN had either equivocal or mutant staining patterns for at least one marker: mutant RB1 and equivocal P53 (n=1); mutant P53 (null, n=1); equivocal RB1 and P53 (n=1). Six of seven (85.7%) uterine LMS showed mutant expression patterns in at least one marker, and five of seven (71.4%) tumors showed mutant staining in at least two markers. Frequency of mutant ATRX, RB1, P53, PTEN, DAXX, MTAP and MDM2 staining among LMS was 28.5%, 57.1%, 42.9%, 0, 28.5%, 14.3% and 28.5%, respectively. Only one of seven (14.3 %) LMS demonstrated wild-type expression of all markers.

Table 1: Immunohistochemical expression patterns

Antibody	Wild-Type	Mutant
ATRX	Any nuclear staining	Absent nuclear staining
RB1	Any nuclear staining	Absent nuclear staining
P53	Heterogeneous nuclear staining	Strong, diffuse (overexpression) or absent nuclear staining (null)
PTEN	Diffuse nuclear and cytoplasmic staining	Absent nuclear and cytoplasmic staining
DAXX	Any nuclear staining	Absent nuclear staining
MTAP	Diffuse nuclear and cytoplasmic staining	Absent nuclear and cytoplasmic staining
MDM2	Absent nuclear staining	Diffuse nuclear staining

Conclusions: Our study demonstrates that mutant immunohistochemical expression patterns of p53, ATRX, RB1, PTEN, DAXX, MDM2 and/or MTAP are frequent among uterine LMS with most tumors demonstrating abnormal staining of at least two markers. Mutant patterns are rare among LMBN and only involve one marker when present. A panel of these markers may be helpful in the distinction between LMS and LMBN.

671 Endometrial Endometrioid Carcinoma with a Prominent Component of Giant Cells Are Frequently p53 Aberrant and Associated with Poor Clinical Outcomes

Elisha Barbato[1], Karuna Garg[1], Amy Joehlin-Price[1]
[1]Cleveland Clinic, Cleveland, OH

Disclosures: Elisha Barbato: None; Karuna Garg: None; Amy Joehlin-Price: None

Background: Giant cell carcinoma (GCC) is rare and diagnostically challenging. Reported cases in the literature are typically mixed with high grade endometrial carcinoma (EC), often endometrioid EC (EEC), with the giant cell (GC) component arbitrarily comprising at least 10% of tumor volume. The clinical significance, if any, of <10% GC component is not known. Our aim was to perform a detailed analysis of EEC with any amount of GCs, summarizing clinicopathologic variables including their immunohistochemical (IHC) profile. A secondary aim was to determine if extent of the GC component influences clinical outcome.

Design: A search for EEC (with or without GCs) was performed and slides were reviewed. Cases with an easily identifiable component of GCs visible from 4x were included. Percentage of GCC and morphologic details were recorded. Clinical data was obtained from electronic medical records. IHC for p53, p16, ER, PAX-8, mismatch repair (MMR) proteins, beta-catenin, beta-hCG, GATA3, AE1/3, and EMA was performed.

Results: Twenty cases were included. The GC component comprised 1-50% of total tumor volume (median 10%). All cases demonstrated anaplastic and haphazardly-arranged GC nuclei. In 6 cases, GCs also demonstrated abundant eosinophilic cytoplasm. In 3 cases, nuclei were eccentrically-placed, forming ring shapes in one and Reed Sternberg-appearing cells in another.

Fifteen patients had material available for IHC (Table 1). Notable findings include a high proportion of p53 mutational patterns (73%) and 1 (7%) MMR deficient case. Three cases demonstrated rare beta-hCG expression, but none were sufficient to diagnose trophoblastic differentiation.

Median age was 64 years (range 47-88). All patients had FIGO grade 3 EEC. 11 (55%), 2 (10%), 4 (20%), and 3 (15%) patients presented with FIGO clinical stage I, II, III, and IV disease, respectively. Nineteen patients had clinical outcome data available. Six patients (32%) died of disease between 10 and 31 months after diagnosis (median 15 mos). Three (16%) died of unknown or other causes, and the remaining 10 showed no evidence of disease at last follow up (median 21.5 months, range 2-129 mos). Patients who died of disease demonstrated 5, 5, 10, 10, 15, and 40% GCC; no trends relating GC amount to outcome emerged.

Table 1.

	EEC	GCs
	n/15 (%)	
	(combined if no differences)	
p53		
Wild type	4/15 (27%)	
Diffuse	8/15 (53%)	
Null	3/15 (20%)	
MLH1/PMS2 retained	14/15 (93%)	
MSH2/MSH6 retained	15/15 (100%)	
ER		
Positive	10/15 (67%)	5/15 (33%)
Negative	5/15 (33%)	10/15 (67%)
PAX-8		
Diffuse	13/15 (87%)	11/15 (73%)
Focal or patchy	1/15 (7%)	1/15 (7%)
Negative	1/15 (7%)	3/15 (20%)
Beta-catenin		
Cytoplasmic	13/15 (87%)	
Scattered nuclear + cytoplasmic	2/15 (13%)	
Beta-hCG positive	0/15 (0%)*	
Focal GATA3 positive	5/15 (33%)	3/15 (20%)
p16		
Diffuse, block positive	6/15 (40%)	
Negative or patchy	9/15 (60%)	
AE1/3		
Diffuse	9/15 (60%)	6/15 (40%)
Focal or patchy	6/15 (40%)	6/15 (40%)
Negative	0/15 (0%)	3/15 (20%)
EMA		
Diffuse	6/15 (40%)	4/15 (27%)
Focal or patchy	9/15 (60%)	10/15 (67%)
Negative	0/15 (0%)	1/15 (7%)
*Three cases showed a rare cell(s) positive but expression was too rare to interpret cases as having trophoblastic differentiation.		

Conclusions: EEC with GCs frequently show aberrant p53. A significant subset of the patients died of disease soon after diagnosis. There was no correlation between the amount of GC component and clinical outcome. Data regarding their molecular/TCGA classification is forthcoming.

672 Progression-Free Survival in High Stage Endometrial Carcinoma Differs By Site of Extra-Uterine Spread

Roshan Bhattarai[1], Roberto Vargas[2], Karuna Garg[2], Amy Joehlin-Price[2]
[1]Cleveland Clinic Foundation, Cleveland, OH, [2]Cleveland Clinic, Cleveland, OH

Disclosures: Roshan Bhattarai: None; Roberto Vargas: None; Karuna Garg: None; Amy Joehlin-Price: None

Background: High stage endometrial carcinoma (EC) is plagued by variable treatment strategies and poor outcomes. Staging in EC cases with extra-uterine disease is often difficult for the pathologist, as clinical data to support our current FIGO staging are

limited. In this study, we aim to compare clinical outcomes between groups of patients with advanced-stage EC and varying degrees of extra-Müllerian involvement.

Design: A search of departmental archives was performed identifying patients with FIGO stage III and IV EC diagnosed between 2000 and 2020. Clinicopathologic variables were recorded from electronic medical records. Cases were separated into whether their extrauterine disease was confined to the Müllerian tract (serosa, adnexa), confined to the pelvis (peritoneal spread and invasion of other organs in the pelvis), or spread to the abdominal cavity (omentum, liver, pancreas, or spleen, among other sites). Overall survival (OS) and progression-free survival (PFS) data were compared using log-rank tests. Kaplan-Meier graphs were constructed.

Results: Outcome data was available for 202 patients, with a median age of 65 years (range 33-93 years). Lymph node involvement was identified in 113 patients (56%) and 103 (51%) demonstrated involvement of the serosa and/or adnexa. Pelvic extension to the peritoneum or pelvic organs was identified in 32 (16%). Abdominal extension (spread to the omentum or extrapelvic abdominal organs) was identified in 11 (5%). Many patients demonstrated multiple sites of spread. At the time of analysis, 81 patients (40%) were without evidence of disease (NED), 5 (2%) were alive with disease (AWD), 65 (32%) died of disease (DOD), 27 (13%) died of other causes, and 24 (12%) died of unknown causes. Patients with disease confined to the Müllerian tract had significantly better PFS (p = 0.007), but not OS (p = 0.092), compared to those with pelvic or abdominal spread (Figure 1). Multivariable analysis was precluded by the number of patients available for analysis.

Figure 1 - 672

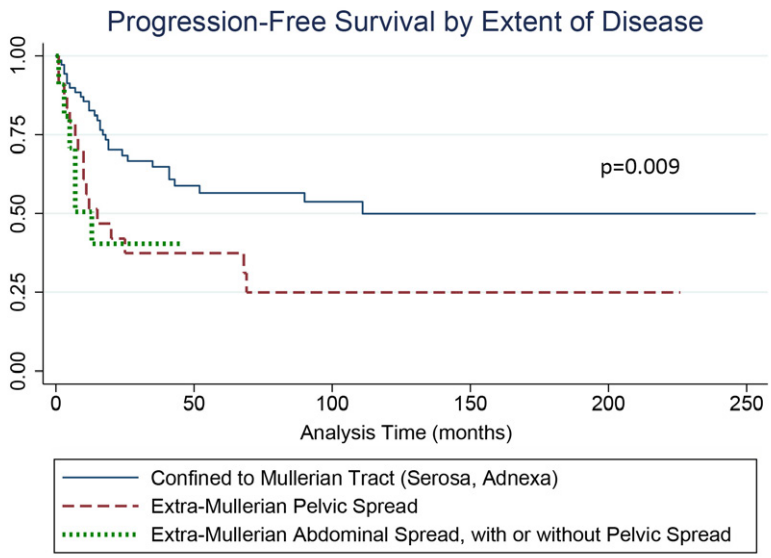

Conclusions: Progression-free survival in EC differs by site of extra-uterine spread. Larger studies are necessary to determine whether OS is similarly impacted by site of spread and if other variables potentially impact outcomes.

673 Heterogeneous Loss of Mismatch Repair (MMR) Protein Expression in Endometrial Carcinomas: An Unusual and Unknown Pattern With Distinct Molecular Characteristics

Graziele Bovolim[1], Sara da silva[1], Rodrigo Abreu[1], Bruna Gonçalves[1], Giovana Torrezan[1], Dirce Carraro[1], Marcelo Corassa[1], Glauco Baiocchi[1], Louise De Brot[1]
[1]A.C.Camargo Cancer Center, Sao Paulo, Brazil

Disclosures: Graziele Bovolim: None; Sara da silva: None; Rodrigo Abreu: None; Bruna Gonçalves: None; Giovana Torrezan: None; Dirce Carraro: None; Marcelo Corassa: None; Glauco Baiocchi: None; Louise De Brot: None

Background: Immunohistochemistry (IHC) for repair gene proteins is used to identify mismatch repair (MMR) deficiency associated with microsatellite instability (MSI). Positive nuclear staining represents retained expression of MMR proteins and complete loss of staining MMR deficiency. Heterogeneous expression pattern (HEP) (mixed positive and totally negative areas) is

observed in endometrial carcinomas (EC) and guidelines recommend interpretation of HEP as retained expression, but there is no consensus regarding classification and interpretation of HEP, nor knowledge of the impact of classifying HEP as a different molecular subtype regarding clinical and prognostic features.

Design: From January/2007 to December/2017 354 cases with EC were identified,13 with HEP. Molecular classification was made based on the PROMISE protocol for EC. Each area (retained and lost expression) was macrodissected and molecular status was evaluated separately regarding MSI status (Idylla), MLH1 promoter methylation (NGS - cutoff for positivity ≥ 15%), POLE status (NGS) and p53 status (IHC). Clinical and pathologic variables were also evaluated and correlated with each case.

Results: Findings are presented in table 1. Endometrioid histology was predominant (12 cases), as absent lymphovascular invasion (10 cases), absence of MELF pattern (9 cases), FIGO Grade 1 (9 cases), <50% of myometrial invasion (11 cases) and T1 stage (12 cases). All patients were alive and disease-free at the last follow-up. Three cases that would be described as retained by IHC presented in the molecular analysis as MSI-H (case 1) or MLH1 methylated (cases 1, 2 and 9). In HEP cases MSH6 was more frequent (7 cases, 6 isolated). MLH1 was altered in 5 cases, and was the only protein associated with co-alterations (with MSH6 and PMS2). Three cases were MLH1 methylated, found both in lost and retained areas. As POLE status, there were 5 mutated cases, 2 of those with mutations both in lost and retained areas, and 3 only the lost area. One case had p53 aberrant pattern (MSH6 altered), that was seen both in the retained and in the lost areas and only 1 case was MSI-H (PMS2 altered).

CASE	MMR PATTERN BY AREA	MMR PROTEIN ALTERED	MSI STATUS (IDYLLA)	MLH METHYLATION (%)	POLE STATUS (FREQUENCY)	P53 STATUS
1	Positive	MSH2	MSI-H	44,8%	NOT MUTATED	WT
	Negative			31,5%	NOT MUTATED	WT
2	Positive	PMS2	MSS	31,3%	NOT MUTATED	WT
	Negative			39,7%	NOT MUTATED	WT
3	Positive	MLH1	MSS	5,7%	c.857C>G; p.P286R (27%)	WT
	Negative			11,4%	c.857C>G; p.P286R (25%)	WT
4	Positive	MSH6	MSS	0,5%	NOT MUTATED	ABERRANT
	Negative			1,0%	NOT MUTATED	ABERRANT
5	Positive	MSH6	MSS	5,1%	NOT MUTATED	WT
	Negative			1,2%	NOT MUTATED	WT
6	Positive	MSH6	MSS	5,5%	NOT MUTATED	WT
	Negative			4,2%	NOT MUTATED	WT
7	Positive	MSH6	MSS	2,2%	NOT MUTATED	WT
	Negative			0,4%	NOT MUTATED	WT
8	Positive	MSH6	MSS	5,0%	NOT MUTATED	WT
	Negative			2,2%	NOT MUTATED	WT
9	Positive	PMS2 + MLH1	MSS	88,8%	c.857C>G; p.P286R (39%)	WT
	Negative			88,1%	c.857C>G; p.P286R (36%)	WT
10	Positive	MLH1	MSS	0,8%	NOT MUTATED	WT
	Negative			1,6%	c.856C>T; p.P286S (59%); c.890C>T; p.S297F (59%)	WT
11	Positive	MSH6	MSS	1,2%	NOT MUTATED	WT
	Negative			4,0%	NOT MUTATED	WT
12	Positive	MLH1	MSS	1,2%	NOT MUTATED	WT
	Negative			2,1%	c.890C>T; p.S297F (7%)	WT
13	Positive	MSH6 + MLH1	MSS	2,2%	NOT MUTATED	WT
	Negative			2,1%	c.856C>T; p.P286S (5%)	WT

Figure 1 - 673

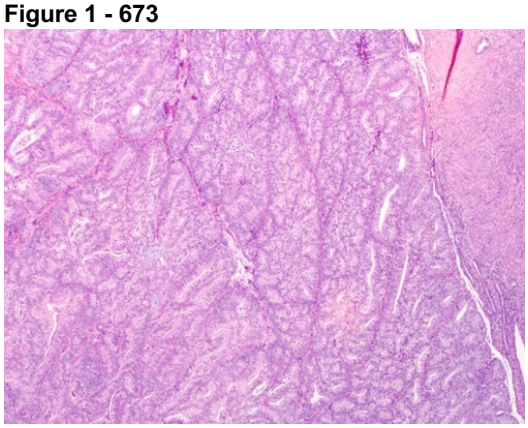

Figure 2 - 673

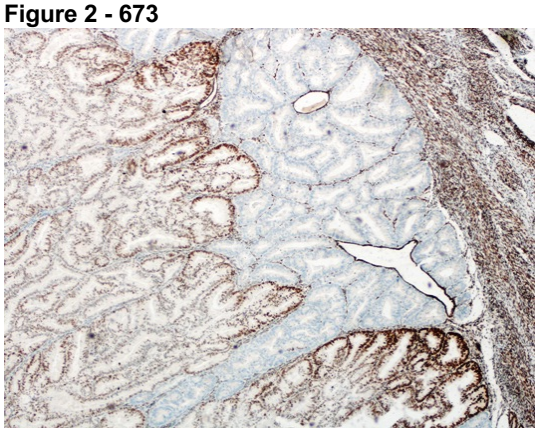

Conclusions: Correlation between IHC and molecular findings is heterogeneous, and determination between retained or lost expression of MMR proteins by IHC when HEP occurs, however feasible, does not represent the actual molecular alterations. Thus, molecular analysis should be performed every case to adequately determine the intrinsic features of each tumor. Due to the rarity of this finding, this is financially viable and has the potential to change clinical practice in a subset of patients. HEP should be reported as a distinct pattern, and not considered as a synonym expression of retained expression of MMR proteins in EC.

674 MTG-CYP2E1 Fusions Molecularly Define Most Vulvar Angiomyofibroblastomas

Baris Boyraz[1], Ryosuke Tajiri[2], Rofieda Alwaqfi[3], Esther Oliva[4], Robert Young[5], Masanori Hisaoka[2], Jaclyn Watkins[4]
[1]Massachusetts General Hospital, Boston, MA, [2]University of Occupational and Environmental Health, Kitakyushu, Japan, [3]University of Iowa Hospitals & Clinics, Iowa City, IA, [4]Massachusetts General Hospital, Harvard Medical School, Boston, MA, [5]Harvard Medical School, Boston, MA

Disclosures: Baris Boyraz: None; Ryosuke Tajiri: None; Rofieda Alwaqfi: None; Esther Oliva: None; Robert Young: None; Masanori Hisaoka: None; Jaclyn Watkins: None

Background: Angiomyofibroblastomas (AMFB), rare benign vulvovaginal mesenchymal tumors, cause significant diagnostic difficulty due to histologic overlap with other mesenchymal tumors in the region and lack of specific immunoprofile. Until the recent discovery of *MTG-CYP2E1* fusion in a cohort of 5 AMFBs, no recurrent genetic alteration had been discovered.

Design: Seven AMFBs were identified from our departmental and consultation files. An average of 5 H&E slides were reviewed (range 2-8). Three tumors were selected for next-generation sequencing (104 genes) and sarcoma fusion assay (28 genes). All tumors were submitted for RT-PCR for *MTG-CYP2E1* fusion.

Results: Patients ranged from 28 to 50 years (mean 41.7, median 42). Tumors were typically tan-gray and ranged from 2 to 23 cm (mean 8.7, median 3.4). Microscopically, they demonstrated classic morphologic features including alternating hypo/hypercellular areas, capillary channels surrounded by epithelioid tumor cells, and variable amount of adipose tissue. None of the three tumors tested by NGS/sarcoma fusion assay showed a reportable variant, copy number alteration or fusion transcript. RT-PCR for *MTG-CYP2E1* was successful in six of seven tumors, and four of them (4/6, 66.7%) showed the fusion transcript.

Conclusions: Most AMFBs demonstrate *MTG-CYP2E1* fusion. In circumstances where the diagnosis proves elusive on morphology alone, identification of this transcript aides in the correct diagnosis. For the small subset of AMFBs that do not demonstrate the fusion, our methods failed to demonstrate other pathognomonic copy number alterations, single nucleotide variants, or previously defined fusion transcripts.

675 Uterine Tumors Resembling Ovarian Sex Cord Tumors (UTROSCTs): A Detailed Clinicopathological Study of 70 Cases

Baris Boyraz[1], Jaclyn Watkins[2], Robert Young[3], Esther Oliva[2]
[1]Massachusetts General Hospital, Boston, MA, [2]Massachusetts General Hospital, Harvard Medical School, Boston, MA, [3]Harvard Medical School, Boston, MA

Disclosures: Baris Boyraz: None; Jaclyn Watkins: None; Robert Young: None; Esther Oliva: None

Background: UTROSCTs are rare neoplasms showing clinical, morphologic and immunohistochemical overlap with other mesenchymal tumors. Most tumors are benign and morphologic features predictive of aggressive behavior are not well established. We report a large series of UTROSCTs focusing on pathologic features and their potential predictive role for clinical behavior.

Design: 70 tumors (66 hysterectomy, 4 resection) were identified from the departmental pathology files and our consultation files. An average of 5 H&E slides were reviewed (range 1-32).

Results: Patients ranged from 21 to 84 years (mean 52.4, median 53). Tumors were typically tan-yellow (38 submucosal; 32 intramyometrial) and ranged from 0.6 to 20 cm (mean 4.9, median 3.5). Microscopically, 62 were well-circumscribed and 8 infiltrative (6 only minimally). In 22 tumors, a prominent smooth muscle component was intimately admixed throughout

('pseudoinvasion'). Architectural patterns included cords (n=53), diffuse (n=50), trabeculae (n=37), nests (n=35), hollow tubules (n=34), retiform (n=22), solid tubules (n=18), pseudoangiomatoid (n=10), whorled (n=5) and pseudopapillary (n=3). Cells were epithelioid (n= 67, predominant in 64; 15 with minor foamy cytoplasm), spindled (n=14; predominant in 6) and/or rhabdoid (n=18; extensive in 2). Cytologic atypia was absent to mild in 54, moderate in 15 and severe in 1. Mitoses were ≤2/10 HPF in 53, 3-5/10 HPF in 11 and >5/10 HPF in 6 (greatest: 9/10HPF). Necrosis was present in 3 and lymphovascular invasion in 2. Follow-up was available for 48 patients (22-192 months; mean 76.2, median 72). 5 patients had recurrence/metastases; lung in 1 at time of initial diagnosis; brain and femur in 1, pelvis in 3 from 30 to 144 months (mean 73.5, median 60) in the remainder, and 2 died of disease. All malignant tumors showed >3 of following 5 features (4 features in 4, 5 in 1) compared to benign tumors (0 in 26, 1 in 7, 2 in 8, 3 in 2): size >5cm, at least moderate cytologic atypia, mitotic rate ≥3/10HPF, infiltrative borders and necrosis (Table 1). Tumors with 'pseudoinvasion' were typically small (0.7-8.0 cm; mean 2.6, median 2.2); only 3 showed up to 1 feature and they were all benign.

	Malignant UTROSCTs (n=5)	Benign UTROSCTs (n=43)
Follow-up duration (months)	48-144; Mean: 88.8, Median: 96	22-192; Mean: 83.3, Median: 72
Age (years)	32-73; Mean: 55.6, Median: 58	22-84; Mean: 51, Median: 51
Size (cm)	6-13; Mean: 10, Median: 11	0.6-12; Mean: 4.1, Median: 2.75
Borders	WC: 1, MI: 2, EI: 1, ES: 1	WC: 41, MI: 2
Necrosis	2/5	1/43
Mitotic rate (/10HPF)	3-5: 1, >5: 4	≤2: 35, 3-5: 6, >5: 2
Cytologic atypia	4 moderate, 1 severe	36 mild, 7 moderate

MI: minimally infiltrative, WC: well-circumscribed; EI: extensively infiltrative; ES: extended to serosa

Conclusions: UTROSCTs are rare showing wide morphologic spectrum and low malignant potential typically associated with late recurrences. A combination of at least 4 of 5 features as described above predicted aggressive behavior.

676 Clinicopathological Review of Gynecologic Tract Metastases from Breast Cancer

Ankica Braun[1], Sindhuja Sivanandham[1], Vijaya Reddy[1], Indu Agarwal[1], Paolo Gattuso[1], Lei Yan[1]
[1]Rush University Medical Center, Chicago, IL

Disclosures: Ankica Braun: None; Sindhuja Sivanandham: None; Vijaya Reddy: None; Indu Agarwal: None; Paolo Gattuso: None; Lei Yan: None

Background: Breast cancer is the most common cancer in women, affecting one in eight females. Breast carcinoma most frequently metastasizes to bone, lung, and liver. However, metastases to gynecologic tract are rarely seen in clinical practice. We undertook a retrospective study to assess location, histologic subtype, relationship with BRCA mutations, and survival in breast cancer patients with metastases to gynecologic tract.

Design: The surgical pathology specimens were identified from our institution's database from 2000 to 2021 for breast cancer that metastasized to gynecologic tract. The clinicopathologic characteristics were reviewed in detail.

Results: A total of 28 cases metastatic breast carcinoma to the gynecologic tract were identified. The mean age of patients was 48, ranging from 25 to 83 years. The sites of metastasis were as follows: twenty cases (71%) ovary - four (20%) unilateral, nine (45%) bilateral, and seven (35%) as part of synchronous multiple gynecologic sites; three cases (11%) endometrium - two involved only endometrium and one as part of multiple gynecologic sites; two cases (7%) - vagina - one involved only vagina, and one as part of multiple gynecologic sites and vulva one (4%). Eighteen cases (64%) were metastatic lobular carcinoma and ten (36%) metastatic ductal carcinoma. ER was positive in 27 cases (96%). PR was positive in 16 cases (57%). HER-2/neu was positive in four cases (14%). BRCA1/2 mutation was detected in three (17%) and negative in 15 cases (83%). Regarding the primary breast carcinoma diagnosis, eight cases (29%) were synchronous, and 20 cases (71%) metachronous, diagnosed 8 to 324 months prior (mean 71 months). Interestingly, in one case the first presentation was vaginal bleeding and the curettage revealed metastatic breast cancer. Fifteen cases (54%) had extra-gynecologic tract metastases. Of these, four (27%) were synchronous, eight (53%) occurred before the gynecologic tract metastases (mean 25 months), and three (20%) after (mean 28 months). On follow-up five (18%) patients were alive (0-5 years from gynecologic tract metastasis), 11 (39%) deceased from the disease, and 12 (43%) lost to follow-up.

Conclusions: The ovaries are the most common site of gynecologic tract for breast cancer metastasis, followed by endometrium and vagina. Invasive lobular carcinoma, although rarer, more commonly spreads to gynecologic tract. ER expression (96%) in conjunction with the histopathologic features were strong parameters to detect metastatic breast carcinoma.

677 HER2 Expression in Ovarian Endometrioid Carcinoma

Chau Bui[1], Bonnie Balzer[1], Horacio Maluf[1], Fabiola Medeiros[1]
[1]Cedars-Sinai Medical Center, Los Angeles, CA

Disclosures: Chau Bui: None; Bonnie Balzer: *Consultant*, Core Diagnostics, Castle Biosciences, PathologyWatch; Horacio Maluf: None; Fabiola Medeiros: None

Background: HER2 overexpression has become increasingly helpful to predict response to anti-HER2 agents in gynecologic cancer. Recently, several phase II clinical trials evaluating the efficacy of HER2 antagonists in the treatment of ovarian carcinoma have shown promising results. *HER2* amplification has been reported in a small percentage of ovarian serous carcinomas. We recently encountered in clinical practice a metastatic primary ovarian endometrioid carcinoma (OEC) metastatic to pelvic lymph nodes in which NGS revealed *HER2* amplification. Publications on the expression of HER2 in ovarian OEC are lacking to date. This study aims to characterize HER2 expression in OEC.

Design: A total of 48 primary OECs were identified over a 15-year span. Archival slide review and HER2 immunohistochemistry (4B5 Rabbit Monoclonal Antibody, laboratory-developed test) was performed in all cases. HER2 expression was evaluated by image analysis using standard breast cancer criteria. PAX8, WT1, and p53 immunohistochemistry, and *HER2* FISH were performed on the two cases with equivocal HER2 scores.

Results: The study consisted of 48 OECs from patients aged 35 to 82 years with 38 grade FIGO 1 (79.17%), 6 FIGO 2 (12.50%), and 4 FIGO 3 (8.33%). 46 cases were negative for HER2 overexpression - score 0 (95.83%), and 2 cases were equivocal - score 2+ (4.17%). Of these 2 cases, *HER2* amplification by FISH was positive in one case (FIGO 3) and negative in one case (FIGO 1). Both cases were positive for PAX8, negative for WT1, and showed wild type p53 immunostaining pattern.

Conclusions: In this cohort, no primary OEC showed HER2 overexpression, but two cases had scored 2+, one of which harboring *HER2* amplification, indicating that OECs with equivocal HER2 expression by immunohistochemistry warrant testing for amplification by FISH as other tumor types. Our findings contribute to the growing evidence that *HER2* is amplified in a small percentage of OECs and thus may serve as an attractive therapeutic target in patients with recurrent or metastatic disease, for which currently options for targeted therapy are limited.

678 Digital Imaging Analysis of HER2 Immunohistochemistry in Endometrial Serous Carcinoma

Bindu Challa[1], Saba Shafi[1], Anil Parwani[2], Zaibo Li[1]
[1]The Ohio State University Wexner Medical Center, Columbus, OH, [2]The Ohio State University, Columbus, OH

Disclosures: Bindu Challa: None; Saba Shafi: None; Anil Parwani: None; Zaibo Li: None

Background: The Visiopharm HER2 digital imaging analysis (DIA) algorithm assesses digitized HER2 immunohistochemistry (IHC) by measuring cell membrane connectivity. We aimed to utilize this algorithm to score HER2 IHCs in endometrial serous carcinoma and compare with pathologists' reads.

Design: The study cohort consisted of 59 consecutive endometrial serous carcinoma resection specimens. HER2 IHC slides were scanned using Philips IntelliSite Scanners and the digital images were analyzed using Visiopharm HER2-CONNECT App to obtain the connectivity values (0-1) and scores (0: connectivity = 0; 1+: 0 < connectivity ≤ 0.12; 2+: 0.12 < connectivity ≤ 0.49; 3+: connectivity > 0.49). (Figure 1)

HER2 IHC and the connectivity analyzed by Visiopharm HER2 IHC algorithm. A, B) one case with HER2 IHC 1+; C, D) one case with HER2 IHC 2+; E, F) one case with HER2 IHC 3+. A, C, E) HER2 IHCs; B, D, F) HER2 connectivity (green color line) detected by Visiopharm.

HER2 DIA scores were compared with pathologists' manual scores. (Table 1)

Results: The concordance between HER2 DIA scores and pathologists' scores was 88.1% (52/59). All discordant cases (n=7) were only one-step discordant with 6 from equivocal to negative and 1 from equivocal to positive. HER2 fluorescence in situ hybridization (FISH) performed in those 6 equivocal cases changed to negative showed not-amplified results and HER2 FISH performed in equivocal case changed to positive showed amplified result.

Table 1. The correlation between HER2 DIA scores and pathologist' scores.

		Visiopharm			
		negative (0/1+)	equivocal (2+)	positive (3+)	total
Pathologists	negative (0/1+)	27	6	0	33
	equivocal (2+)	0	13	0	13
	positive (3+)	0	1	12	13
	total	27	20	12	59

Figure 1 - 678

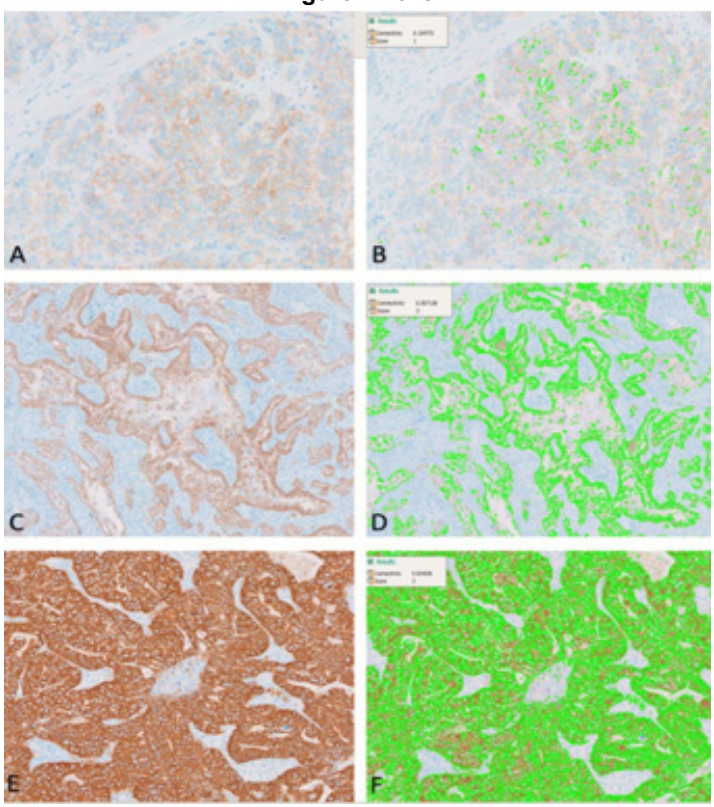

Conclusions: HER2 IHC DIA demonstrates excellent concordance with pathologists' scores. Furthermore, HER2IHC DIA is able to decrease the number of equivocal cases (35%, 7/20) and accurately discriminates between HER2 positive and negative cases.

679 PD-L1 (22C3) Expression and Molecular Alterations in Ovarian Carcinomas

Jeffrey Chang[1], Shuko Harada[1], Rebecca Arend[1], Sameer Al Diffalha[1], Andrea Kahn[1], Alexander Mackinnon[1], Christine Pesoli[1], Xiao Huang[1]
[1]*The University of Alabama at Birmingham, Birmingham, AL*

Disclosures: Jeffrey Chang: None; Shuko Harada: None; Rebecca Arend: None; Sameer Al Diffalha: None; Andrea Kahn: None; Alexander Mackinnon: None; Christine Pesoli: None; Xiao Huang: None

Background: Programmed death ligand 1 (PD-L1) expression in ovarian carcinomas continues to be an area under exploration. The correlation of PD-L1 and other biomarkers such as tumor mutation burden (TMB) and homologous recombination deficiency (HRD) to anti-PD-L1 immunotherapy also remains unclear. Several studies have reported a lower response compared to other tumors; however, when response is achieved, it is often more durable. Recent studies suggest PD-L1 expression is highest in mucinous, high grade serous and endometrioid tumors. For more targeted therapy, it is important to further investigate PD-L1 expression and the molecular profile of ovarian cancers.

Design: PD-L1 IHC and Next-generation sequencing was performed at the request of the treating oncologists. 138 patients diagnosed and treated for ovarian carcinomas between 2013 and 2021 were identified. The ovarian carcinomas are classified according to the 2020 WHO classification. The 22C3 PD-L1 tumor proportion score (TPS), TMB, loss of heterozygosity (LOH), and the genomic sequencing were obtained from reports. A PD-L1 score of a ³ 1% was used as the cutoff for positivity and ³ 16% for LOH. Fisher's exact test was used to analyze the correlation between PD-L1 and the various parameters.

Results: Of the 138 ovarian carcinomas identified, 45 (33%) were PD-L1 positive and 93 (67%) were PD-L1 negative. Endometrioid carcinoma showed the highest percentage of PD-L1 positivity (Figure 1A). There was not a significant difference in TMB among the subtypes (Figure 1B). Also, TMB and LOH of PD-L1 positive and PD-L1 negative tumors did not differ. Comparison of genomic alterations between PD-L1 positive and PD-L1 negative tumors is demonstrated in figure 2. Genomic alteration arranged by targetable pathways is shown in table 1. PD-L1 positive tumors showed higher PTEN mutation (5/45, 11%) than PD-L1 negative ones (1/93, 1%) (p-value=0.0142). BRAF, CHEK2, PIM1, PPP2R1A, MUTYH, CCND3, MET and MLH1 were identified in only PD-L1 negative tumors.

Pathway	Alteration	Total (n=138)	PD-L1 Pos (n=45)	PD-L1 Neg (n=93)
Cell Cycle Control	TP53	79%	78%	82%
	CCNE1	14%	18%	13%
	CDKN2A	9%	4%	11%
	CDKN2B	6%	2%	8%
	RB1	5%	2%	6%
	CCND2	3%	4%	2%
	MDM2	2%	2%	2%
	CCND3	1%	0%	2%
MAPK Pathway	KRAS	12%	11%	13%
	NF1	10%	13%	9%
	BRAF	2%	0%	3%
	NRAS	1%	2%	1%
DNA Repair	BRCA1	9%	7%	11%
	BRCA2	6%	9%	5%
	RAD21	5%	4%	5%
	ATM	4%	4%	3%
	CHEK2	2%	0%	3%
	MUTYH	1%	0%	2%
	BRIP1	1%	4%	0%
	MLH1	1%	0%	1%
Transcription Regulation/Factors	ARID1A	9%	9%	10%
	MYC	7%	4%	9%
	ZNF703	3%	2%	3%
PI3K/AKT/mTor Pathway	PIK3CA	8%	9%	8%
Receptor signaling	PRKCI	6%	7%	6%
	ERBB2	6%	2%	9%
	FGFR1	5%	2%	6%
	PTEN*	4%	11%	1%
	NOTCH3	4%	2%	4%
	FGFR2	2%	2%	2%
	GNAS	2%	2%	2%
	PIM1	2%	0%	3%
	PPP2R1A	2%	0%	3%
	MET	1%	0%	1%
	NOTCH1	1%	2%	0%
Telomerase Activity	TERC	6%	7%	6%
Chromatin Modification	NSD3	4%	2%	5%
	MLL2	2%	2%	2%
Wnt Pathway	CTNNB1	2%	2%	2%

Figure 1 - 679

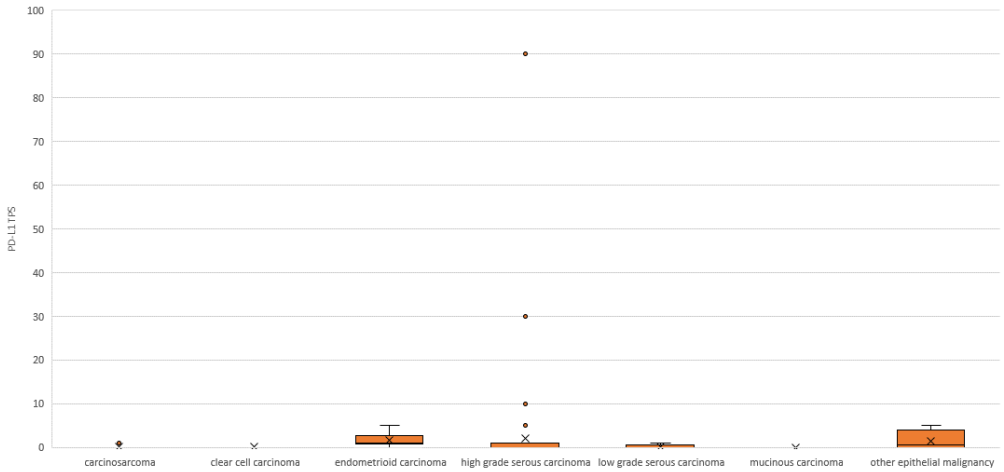

PD-L1 Pos.	Carcinosarcoma n=10	Clear cell carcinoma n=7	Endometrioid carcinoma n=6	High grade serous carcinoma n=92	Low grade serous carcinoma n=13	Mucinous carcinoma n=2	Other epithelial malignancy n=8
n(%)	1(10%)	1(14%)	5(83%)	31(34%)	3(23%)	0(0%)	4(50%)

Figure 1A

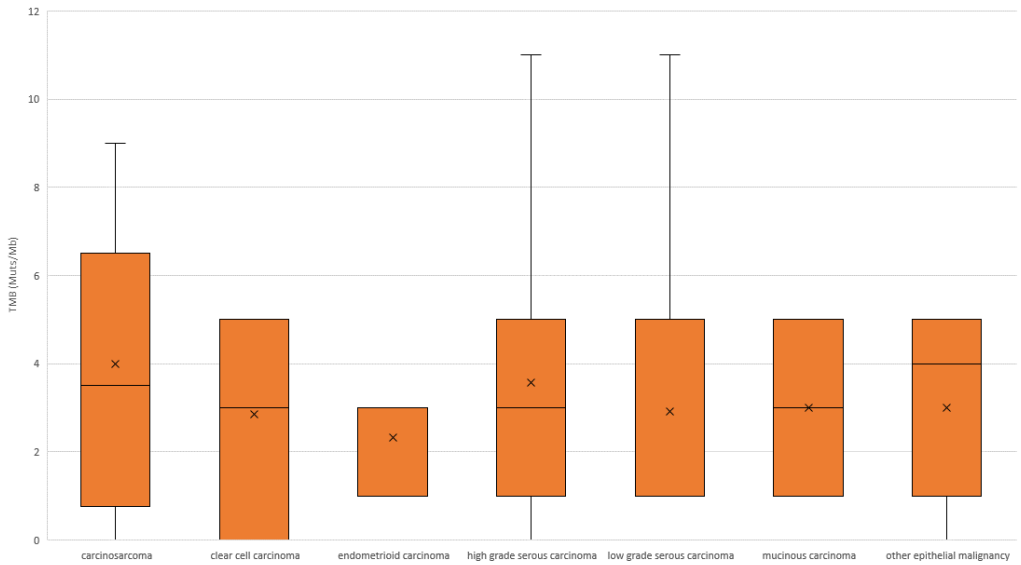

Figure 1B

Figure 2 – 679

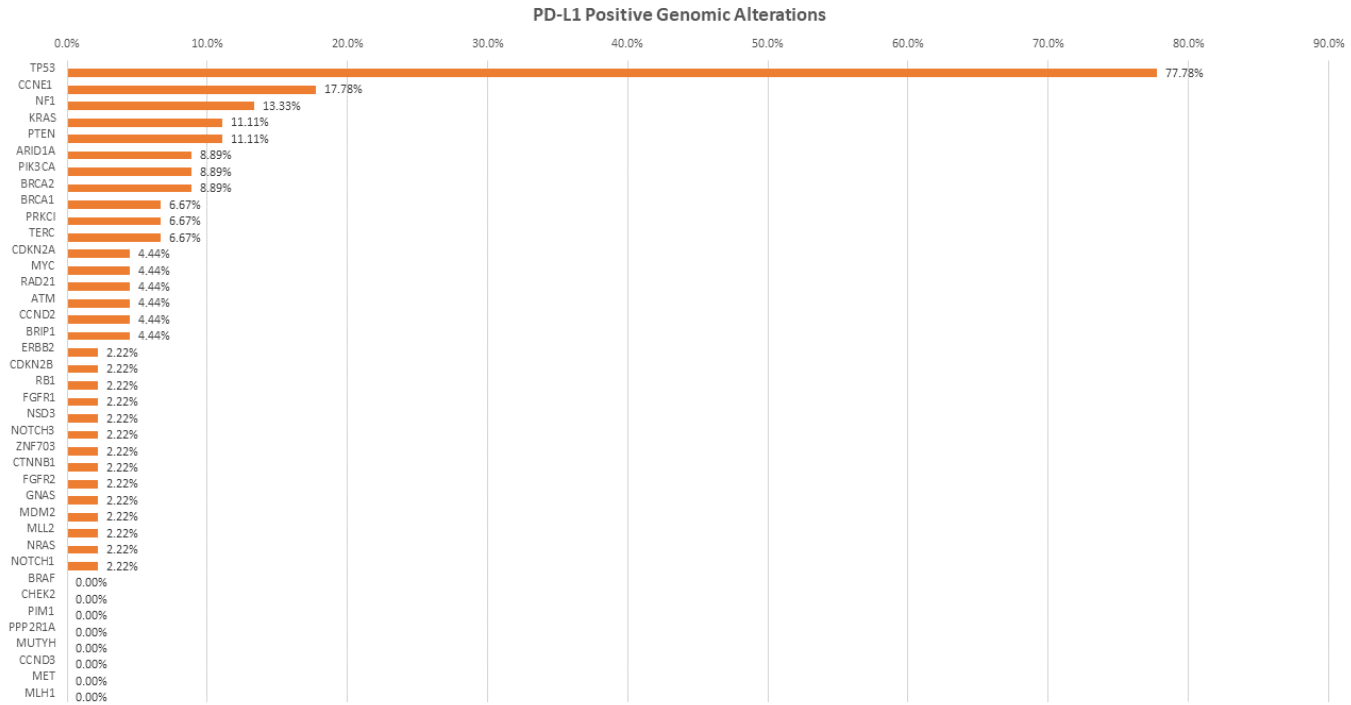

Figure 2A

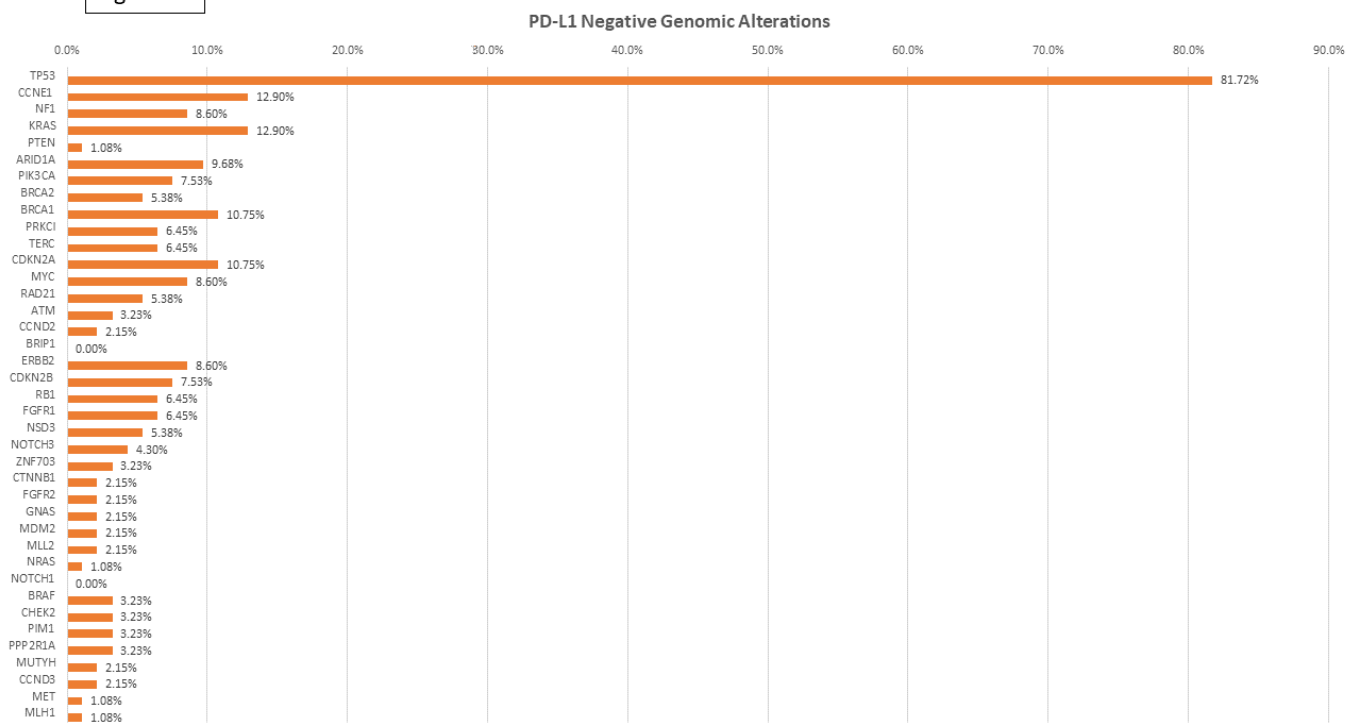

Figure 2B

Conclusions: Our study did not reveal a difference in TMB and LOH between PD-L1 positive and PD-L1 negative ovarian carcinomas. Correlation between PD-L1 expression and PTEN mutation is demonstrated. The significance of this correlation likely warrants further investigation.

680 Intraoperative Frozen Section Evaluation of Ovarian Sex Cord-Stromal Tumors and Its Mimics - A Series of 127 Cases With Emphasis on Potential Diagnostic Pitfalls

Jason Chng[1], Shing Lih Wong[1], Ruoyu Shi[1]
[1]*Singapore General Hospital, Singapore, Singapore*

Disclosures: Jason Chng: None; Shing Lih Wong: None; Ruoyu Shi: None

Background: Ovarian sex cord-stromal tumors are infrequently encountered in the frozen section consultation setting. The related diagnostic difficulties specific to frozen section evaluation and diagnosis are seldom discussed.

Design: We analyzed the clinicopathological features of 127 frozen sections of ovarian sex cord-stromal tumours and their mimics to determine the accuracy of intraoperative interpretation, reasons for deferrals and causes of discrepant results.

Results: 79.5% patients (median age, 56) presented with a unilateral ovarian mass. In 96 of cases (75%), the frozen section diagnosis concurred with the permanent section diagnosis. The diagnosis was deferred in 26 cases (20.3%), with the commonest cause of deferral being the presence of a hypercellular epithelioid or spindled appearance indistinguishable from other poorly differentiated malignant tumors. Six major discrepancies (4.6%) are due to the presence of sex cord differentiation in endometrioid carcinoma, overinterpretation of non-neoplastic stromal cells, misinterpretation of solitary fibrous tumor as a fibroma, overlooked subtle metastatic carcinoma cells and sampling error of a cystic adult granulosa cell tumor.

Table 1. Details of cases with discrepancies in frozen section of ovarian sex cord stromal tumors

Frozen section diagnosis	Permanent section diagnosis	Problematic pathologic features	Diagnostic problems in frozen section
Adult granulosa cell tumor	Endometrioid carcinoma with sex-cord stromal tumor like areas	Cellular epithelioid	Relatively monotonous cytology with Call-Exner body like appearance
Fibroma	Metastatic carcinoma with signet ring cell features	Cellular spindle and necrosis	The signet ring cell morphology is subtle and overlooked partially due to striking cellular spindle appearance of the ovarian stroma.
Fibroma	Solitary fibrous tumor	Cellular spindle	The low grade nuclei atypia among the cellular spindle cells. The typical stag-horn vessel architecture is not well demonstrated.
Sclerosing stromal tumor	Endometriosis	Edematous and cellular spindle stromal cells	Solid whitish macroscopic appearance. Endometriotic glands and stroma are under sampled during frozen section.
Adult granulosa cell tumor	Endometrioid carcinoma with Sertoli-form like feature	Cellular epithelioid and spindle cytology with trabeculae and nests architecture	Trabeculae and nests architecture, cellular monotonous cytology and Call-Exner body like appearance. Lack of necrosis and glandular formation.
Benign epithelial lined cyst	Adult granulosa cell tumor	Cellular spindle	A dominant cystic macroscopic appearance with limited tumor sampled.

Figure 1 – 680

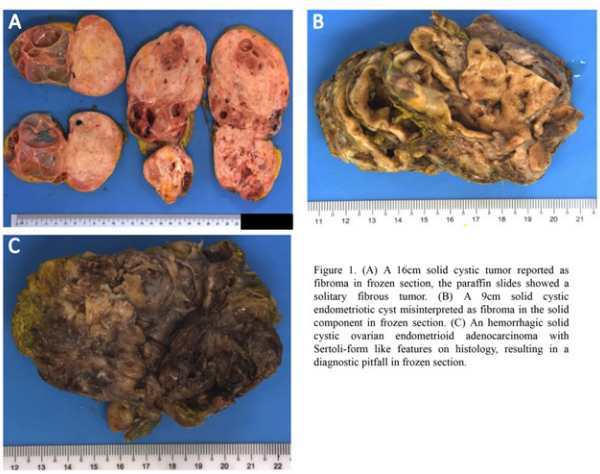

Figure 1. (A) A 16cm solid cystic tumor reported as fibroma in frozen section, the paraffin slides showed a solitary fibrous tumor. (B) A 9cm solid cystic endometriotic cyst misinterpreted as fibroma in the solid component in frozen section. (C) An hemorrhagic solid cystic ovarian endometrioid adenocarcinoma with Sertoli-form like features on histology, resulting in a diagnostic pitfall in frozen section.

Figure 2 - 680

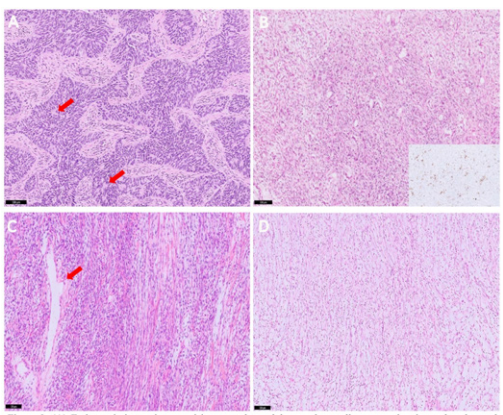

Figure 2. (A) Endometriotic carcinoma misinterpreted as adult granulosa cell tumour, showing trabeculae and nests architecture, cellular monotonous cytology and Call-Exner body like appearance(Arrows). (B) The signet ring cell morphology is subtle on frozen section(Highlighted by cytokeratin on immunohistochemistry, Inlet). (C) Solitary fibrous tumor interpreted as fibroma, stag-horn vessel architecture is difficult to appreciate(Arrow). (D) Edematous ovarian stroma resembles spindle cells in fibroma.

Conclusions: Most ovarian sex cord-stromal tumors can be accurately diagnosed in the frozen section setting. The presence of a hypercellular epithelioid or spindled appearance may cause difficulty in differentiation from other neoplasms. Due to the limitation of sampling in the frozen section setting, it is important to be aware that some epithelial and endometrioid stromal neoplasms may show foci of sex cord-like differentiation, and that sex cord-stromal tumours may masquerade as mesenchymal lesions and vice versa.

681 Proteomics Shows Upregulation of Lymphatic System Associated Proteins in Cancer-associated Stroma of the High Grade Serous Ovarian Carcinoma

Anna-Lee Clarke-Brodber[1], Chen Wang[1], Cristine Charlesworth[1], Ruifeng (Ray) Guo[1], Yajue Huang[1]
[1]Mayo Clinic, Rochester, MN

Disclosures: Anna-Lee Clarke-Brodber: None; Chen Wang: None; Cristine Charlesworth: None; Ruifeng (Ray) Guo: None; Yajue Huang: None

Background: High-grade serous ovarian carcinoma (HSGC) is the most common ovarian carcinoma (70%) and often presents with extensive extraovarian (peritoneal) involvement. The invasiveness of this tumor type is in stark contrast to its low-grade counterparts in low grade serous carcinoma, serous borderline tumors (SBT) and cystadenomas which are predominantly confined to the ovary. This brings into question the proteomic landscape of the HGSC stroma which encourages carcinomatosis. This study seeks to understand the nature of the neoplastic stroma by investigating the protein expression profile of the carcinoma adjacent stroma and distant stroma of HGSC and SBT.

Design: A search of the Mayo Clinic pathologic accession system was used to identify patients with a diagnosis of HGSC and SBT. A total of 10 cases were selected, 5 from each group, with each case re-reviewed to verify the diagnosis. The cancer stroma and normal stroma were identified. Nano-scale liquid chromatography mass spectrometry data of trypsin-digested samples was collected and the peptides were separated by reversed phase chromatography. The MaxQuant workflow was used to process mass spec data into relative protein abundances. Patient and tissue groups were compared using t-tests. The function and organ expression of the statistically significant proteins were characterized using the NCBI Gene database.

Results: In assessing HGSC cancer stroma (CS) to normal stroma (NS) there were 2483 proteins identified, 179 of which were statistically significant ($p < 0.05$) with 19 having a $p < 0.01$. 8 of 14 (57%) upregulated proteins show high expression in the lymphatic system (LS) which includes the lymph node, bone marrow and/or spleen. These 8 proteins can be grouped into 3 functional groups: 1. apoptosis/gene expression regulation 2. complement activation and 3. actin binding proteins. SBT showed 2/8 (25%) of the upregulated proteins were LS related. TGFB1 was the only common upregulated protein in the HGSC and SBT cancer stroma. In comparing SBT and HGSC cancer stromas, 3/5 (60%) of the upregulated proteins in the HGSC were LS related whereas none (0/3) in the SBT cancer stromas showed no LS relation. Figure 1 shows the heat map protein expression profile for HGSC and SBT cancer to normal stroma.

Figure 1 - 681

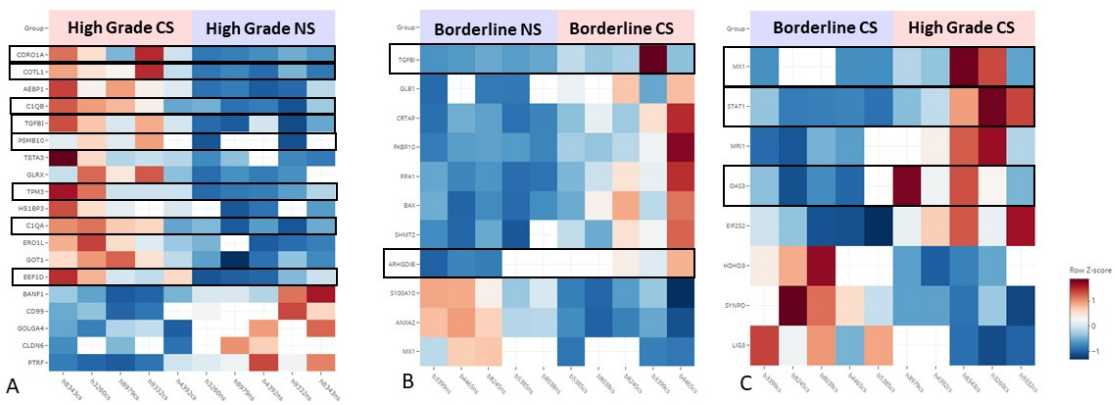

Figure 1 shows heat maps of statically significant proteins ($p < 0.01$): a) high-grade serous cancer stroma to normal stroma, with 8/14 (57%) related to the LS system b) serous borderline cancer stroma to normal stroma, with 2/8 (25%) related to the LS system and c) serous borderline and high-grade serous carcinoma cancer stroma, with 3/5 (60%) related to the LS system in the high-grade serous cancer stroma, and 0/3 (0%) related to the LS system in the borderline serous cancer stroma.

Conclusions: In the cancer stroma of HGSC of the ovary, there appears to be upregulation of LS associated proteins when compared the SBT and normal stroma. Future studies are necessary to further elucidate the significance of these proteins.

682 Low Grade Fibromyxoid Sarcoma of the Gynecologic Tract: Clinical, Pathologic and Molecular Characterization of an Institutional Series

Danielle Costigan[1], David Chapel[2], Christopher Fletcher[3], Marisa Nucci[4], Carlos Parra-Herran[4]
[1]The University of North Carolina at Chapel Hill, Chapel Hill, NC, [2]Michigan Medicine, University of Michigan, Ann Arbor, MI, [3]Brigham and Women's Hospital, Boston, MA, [4]Brigham and Women's Hospital, Harvard Medical School, Boston, MA

Disclosures: Danielle Costigan: None; David Chapel: None; Christopher Fletcher: None; Marisa Nucci: None; Carlos Parra-Herran: None

Background: Low Grade Fibromyxoid Sarcoma (LGFMS), a malignant fibroblastic neoplasm characterized by *FUS-CREB3L2* fusions (less often *FUS-CREB3L1* or *EWSR1-CREB3L1*), is exceedingly rare in the gynecologic tract. Thus, it can be confused with other myxoid lesions such as superficial or deep angiomyxoma and myxoid smooth muscle tumors. We describe an institutional cohort of 7 female genital LGFMS.

Design: Patients with female genital LGFMS were identified in our in-house and consultation files. Clinical and pathologic information was recorded. When available, archival material was used for immunohistochemistry and detection of fusions by fluorescence in-situ hybridization (FISH).

Results: Mean age at presentation was 43 years (range 34-59). Lesion was located in the vulva (5 cases, always superficial and lateral involving labia), vagina (1 case, posterior fornix) and pelvis (1 case). Gross appearance, available in 5 cases, described a well-circumscribed lesion, 4 cm in average size (range 2-8.7 cm). Microscopically, however, the tumors often had blurred/infiltrative edges (5/7). All cases showed a mixture of myxoid and fibrous areas with varying lobulation. Cell arrangement was swirling in 5 cases and patternless in two. Cells were fusiform and cytologically bland with inconspicuous cytoplasm. There were no mitoses, necrosis or hemorrhage. The vasculature was uniform and composed of small arterioles in an “arcade” pattern. Four cases had scattered lymphocytes. Margins were positive in 3 lesions, of which 2 underwent re-excision (with one having residual LGFMS). EMA was positive in 4/6 cases and MUC4 in 5/6 cases. FISH detected *FUS* rearrangement in 5/7 lesions. The two remaining tumors also lacked *EWSR1* rearrangement. Follow-up, available in 5 patients, ranged from 10 to 150 months (mean 75); all were alive free of disease.

Conclusions: In the gynecologic tract, LGFMS affects young adult women and predominantly presents in the vulva. Thus, it is important to entertain LGFMS when encountering a bland myxoid spindle cell neoplasm in this location. Tumor lobulation, small vasculature and positive EMA & MUC4 are helpful in distinguishing LGMFS from mimickers such as superficial and deep angiomyxoma and prompting molecular testing. Despite being often infiltrative, most lesions can be safely excised or re-excised if margins are positive. Our series shows a relative indolent behaviour with no recurrences, however long-term surveillance is required given the well-recognized potential for late relapse.

683 Clear Cell Carcinoma of the Cervix, A Clinicopathologic Study of 33 Cases in the Post-Diethylstilbestrol (DES) Era

Hecca Cox[1], Elizabeth Euscher[2], Preetha Ramalingam[2], Mario Marques-Piubelli[2], Barrett Lawson[2], Anais Malpica[2]
[1]Baylor College of Medicine, Houston, TX, [2]The University of Texas MD Anderson Cancer Center, Houston, TX

Disclosures: Hecca Cox: None; Elizabeth Euscher: None; Preetha Ramalingam: None; Mario Marques-Piubelli: None; Barrett Lawson: None; Anais Malpica: None

Background: Cervical clear cell carcinoma (CxCCCa) is an HPV-independent, uncommon tumor (Tu) with an alleged bimodal age distribution in the post-diethylstilbestrol (DES) era. Limited information about its pathogenesis, clinical/pathologic/immunohistochemical features and molecular landscape is available. In this study, we present our experience with 33 of such cases.

Design: 33 CxCCCas were retrieved from our files (1992-2020). Clinical features recorded were: patient's (pt's) age, presentation, history (Hx) of DES exposure, personal or family Hx of Tus, FIGO stage, treatment (Tx) and follow-up (f/u). H&E slides were reviewed in all cases and pathology features were documented. Immunohistochemical (IHC) stains, HRHPV in situ hybridization (ISH), and molecular studies were obtained in selected cases. Kaplan-Meier curves were used assess overall survival (OS) using SPSS (Statistics for Windows, Version 24.0. Armonk, NY: IBM Corp.).

Results: Clinicopathologic findings are summarized in Table 1. One pt had DES exposure. Tumors were positive for PAX-8 (20/20), napsin A (23/25), HNF1β (22/24), AMACR (11/20), glypican-3 (6 /19), CEA (10/24), CK5/6 (8/21), ER (21/25) while negative for p63 (5/5), p40 (19/19), and PR (7/7). p53 showed wild type staining in 20/25 cases, 2/25 had diffuse (aberrant) staining and 3/25 with a null-phenotype. Loss of MMR proteins was seen in 2/8 cases (both with MSH2 and MSH6 lost). HRHPV ISH was negative in 18/19 cases, the only positive Tu was a pt with Hx of genital warts. Molecular studies (9) showed the following mutations (mu): *TP53* and *PTEN* (1), *BRCA2* and *NFE2L2* (1), *BRCA2* (1), indeterminate *GNAS* (1), and no mu (5). Median OS was 154 months, (95CI, 74.5 -233.4).

Table 1. Clinicopathologic Features of 33 Cases of CxCCCa

Characteristics	Results
Patient's age (yrs), median (range)	57 (20 – 82)
Presentation (n=26)	
Abnormal or Postmenopausal bleeding	16
Abnormal Pap smear	7
Abnormal Pelvic Exam	2
Asymptomatic	1
Personal History of Other Tumors (n=23)	5/23
Solitary Fibrous Tumor (lung)	1
Ductal Carcinoma in Situ	1
Basal Cell Carcinoma	1
Colon Carcinoma	1
Squamous cell carcinoma of cervix	1
Family History of Other Tumors (n=31)	19/31
Breast Cancer	15
Lung Cancer	6
Colon Cancer	4
Prostate	2
Others	19
Tumor size (largest dimension) (cm), median (range)	4.3 (5.5 – 7.9)
Predominant Histologic pattern*	
Tubuloglandular	14
Solid	13
Papillary	5
Cystic	5
Intracytoplasmic mucin	18/33
Inflammatory Infiltrate (n=33)**	
Lymphoplasmacytic	26
Neutrophilic	15
Eosinophilic	3
Mitotic index/10HPFs, median (range)	6 (1 – 62)
FIGO Stage (n=32)	
Stage I	21
Stage II	6
Stage III	0
Stage IV	5
Treatment	
Surgery	10
Adjuvant chemotherapy and or radiotherapy	7
Only chemotherapy and or radiotherapy	15
Outcomes	
Follow-up in months, median (range)	43 (2-297)
Alive with no Evidence of Disease (ANED)	17/33
Alive with Disease (AWD)	2/33
Dead of Disease (DOD)	13/33
Dead of Other Causes (DOC)	1/33

*All cases had a combination of patterns
**More than 1 type in certain cases

Conclusions: CxCCa had no bimodal age distribution in our study. A familial or personal Hx of Ca suggests that either somatic or germline mutations play a role in its pathogenesis. MSH2 and MSH6 loss is seen in a subset of pts. The frequent association of breast cancer in CxCCCa merits further investigation into the genetic landscape of these tumors. Most pts present with low stage disease and an overall favorable prognosis.

684 Molecular Classification of Endometrial Carcinoma and Immune Phenotypes: an Integrated Approach to Improve Risk Stratification

Antonio De Leo[1], Dario de Biase[1], Martina Ruscelli[2], Marco Grillini[3], Angelo Corradini[3], Francesca Rosini[4], Thais Maloberti[2], Giovanni Tallini[5], Donatella Santini[3], Claudio Ceccarelli[3]
[1]University of Bologna, Bologna, Italy, [2]Alma Mater Studiorum-University of Bologna, Bologna, Italy, [3]S.Orsola-Malpighi Hospital, University of Bologna, Bologna, Italy, [4]IRCCS Azienda Ospedaliero-Universitaria di Bologna, Bologna, Italy, [5]University of Bologna School of Medicine, Bologna, Italy

Disclosures: Antonio De Leo: None; Dario de Biase: None; Martina Ruscelli: None; Marco Grillini: None; Angelo Corradini: None; Francesca Rosini: None; Thais Maloberti: None; Giovanni Tallini: None; Donatella Santini: None; Claudio Ceccarelli: None

Background: Compartmentation of the immune response into three main phenotypes - inflamed, immune-excluded, and immune-deserted phenotypes - has been proposed as the main predictor of response to immune receptor inhibitory blocks. The objective of the study is to define and characterize the immune phenotypes of a consecutive series of endometrial carcinoma (EC) by correlating them with TCGA molecular subtypes, clinicopathologic features, and prognosis.

Design: Immunohistochemistry (IHC) and Next-Generation Sequencing (NGS) were used to assign TCGA molecular EC subgroups: *POLE* mutant (POLE), mismatch repair deficient (MMRd), p53 mutant (p53abn), and no specific molecular profile (NSMP). Immune markers (CD20, CD3, CD8, PD-1, PD-L1, CD68) were assessed by IHC and quantified by digital image analysis on whole tumor tissue sections to define the three immune phenotypes.

Results: 129 ECs were stratified into 4 molecular subtypes: 6 *POLE* (4.6%), 44 MMRd (34.1%), 27 p53abn (20.9%), and 52 NSMP (40.3%). Immune phenotypes were statistically associated with different TCGA molecular subtypes ($p<0.0001$, see table). The inflamed phenotype was commonly identified in MMRd and *POLE* subtypes; however, 50% of NSMP and 18% of p53abn tumors were characterized by an intense immune response. The immune-desert phenotype was prevalent in NSMP (40.4%) and p53abn (29.6%) tumors, whereas the immune-excluded phenotype was frequently seen in *POLE*, p53bn, and MMRd groups. TCGA molecular subtypes were statically associated with different clinical outcomes, whereas the immune phenotypes alone showed a trend in discriminating prognosis. A profound variation in immune response was seen in the NSMP group. Interestingly, in the latter, the diverse immune phenotypes were associated with different prognosis: recurrent events (6/52, 11.5%) were identified in the immune-desert (4) and immune-excluded (2) tumors, whereas the inflamed ECs were characterized by the most favorable outcome (log-rank test $p=0.009$).

Molecular subgroups and immune phenotypes				
	POLE	**MMRd**	**p53abn**	**NMSP**
Immune- desert	0 (0.0%)	3 (6.8%)	8 (29.6%)	21 (40.4%)
Immune- excluded	3 (50.0%)	11 (25.0%)	14 (51.9%)	5 (9.6%)
Inflamed	3 (50.0%)	30 (68.2%)	5 (18.5%)	26 (50.0%)
Total	6	44	27	52

Conclusions: TCGA molecular classification is essential in EC risk assessment. Molecular subgroups are associated with different patterns of immune response that could constitute an additional parameter to guide the therapeutic approach. Particularly in the NSMP subgroup, characterization of the immune phenotype has shown a relevant impact in predicting different outcomes. The integration of TCGA molecular subgroups and immune phenotypes could represent a promising and attractive opportunity to improve the predictive-prognostic stratification of patients.

685 Long Term Tumor Dormancy in a BRCA1 Heterozygote

Nadine Demko[1], Setor Amuzu[1], Lili Fu[2], Barbara Riverapolo[1], Celine Domecq[3], Leanne de Kock[1], Nancy Hamel[4], Lucy Gilbert[1], Paz Polak[5], Jiannis Ragoussis[1], William Foulkes[6]

[1]McGill University, Montréal, Canada, [2]McGill University Health Centre, Montreal, Canada, [3]McGill University Health Centre, Montréal, Canada, [4]McGill University, Research Institute of the McGill University Health Network, Montréal, Canada, [5]Icahn School of Medicine at Mount Sinai, New York, NY, [6]McGill University, Montreal, Canada

Disclosures: Nadine Demko: None; Setor Amuzu: None; Lili Fu: None; Barbara Riverapolo: None; Celine Domecq: None; Leanne de Kock: None; Nancy Hamel: None; Lucy Gilbert: *Primary Investigator*, Pfizer, Astra Zeneca, Merck Sharp & Dohme, Karyopharm, Tesaro, IMV, Alkermes, Clovis, ImmunoGen Inc, Roche, Mersana, Espersas, Novocure GmbH, Oncoquest Pharmaceuticals; *Advisory Board Member*, AstraZeneca, GSK, Eisai, Eisai-Merck; *Consultant*, Alkermes; Paz Polak: None; Jiannis Ragoussis: None; William Foulkes: *Grant or Research Support*, AstraZeneca

Background: Ovarian high grade serous carcinoma (HGSC) is currently thought to mainly arise from the Fallopian tubes from a precursor lesion referred to as serous tubal intraepithelial carcinoma (STIC). Germline pathogenic variants (GPVs) in *BRCA1/2* are the most important causes of HGSC and risk reducing salpingo-oophorectomy (RRSO) is offered to *BRCA1/2* heterozygotes. We report a case of pelvic HGSC developing 15 years post-RRSO, following an occult Fallopian tube HGSC that was missed on initial pathologic examination.

Design: Given the long interval, it was debated whether the second tumor was a recurrence or an independent primary lesion, hence molecular studies were undertaken to address this question. Whole exome sequencing (WES) of blood, normal tissue, the Fallopian tube carcinoma (FTC) and the pelvic carcinoma (PC) DNA samples were performed using the Illumina HiSeq 4000.

Results: On pathologic examination, the pelvic tumour showed typical morphology of HGSC and abnormal (diffuse aberrant) staining for P53 on immunohistochemistry (IHC; Figure 1A and 1B). The patient's previous pathology material from the RRSO with hysterectomy was reviewed and a tiny focus (0.8 mm) of HGSC with adjacent STIC was identified showing high grade nuclear atypia with abnormal (diffuse aberrant) staining for P53 (Figure 1C and 1D).

Analysis of copy number variation (CNV) profiles (Figure 2A) derived from WES shows loss of heterozygosity (LOH) of chromosome 17 in both the FTC and the PC, consistent with the presence of the *BRCA1* GPV in both normal and tumor tissues (Figure 2B). There is whole genome duplication in the PC (ploidy 4.3) compared to the FTC (ploidy 2.1) and a higher frequency of amplifications. We found greater genomic instability in the PC than the FTC, shown by greater number of CNV segments in the PC versus the FTC (Figure 2A). Further supporting a common origin for these tumors, we found an identical *TP53* mutation (NM_000546.6:c.701A>G, p.Tyr234Cys mutations in the FTC and PC; Figure 2C).

Study	Pt	BRCA status	Age at RRSO	Pre-RRSO findings	Primary tumour at RRSO				Recurrence			
					Year of diagnosis	Type and stage	IHC staining pattern	TP53 mutation and method	Year of diagnosis	Type and extent	IHC staining pattern	P53 mutation and method
Our present case	1	BRCA1	45	NED	2003	Occult HGSC and STIC, IA	Diffuse aberrant	c.701A>G (p.Y234C) WES	2018	HGSC, peritoneal, right lower quadrant	Diffuse aberrant	c.701A>G (p.Y234C) WES
Blok et al, 2019	1	BRCA1	46	NED	~2005	STIC, IA	Diffuse aberrant	c.817C>T (p.R273C)	2015	HGSC, peritoneal	Diffuse aberrant	c.817C>T (p.R273C)
	2	BRCA1	53	NED, previous breast cancer	~2005	STIC, IA	Null pattern	c.249_250delGG NGS-targeted	2012	HGSC, peritoneal	Null pattern	c.249_250delGG NGS-targeted
Anglesio et al, 2017	1	N/A	53	N/R	1988	TO HGSC, IA	Diffuse aberrant	c.785G>T (p.G262V), COSM11198 NGS (full gene)	2015	HGSC, diffuse peritoneal HGSC	Diffuse aberrant	c.785G>T (p.G262V), COSM11198 Sanger (single- amplicon)
	2	N/A	45	N/R	2009	TO HGSC, IIIC	Null pattern	c.780delC (p.S261 fs*84), COSM45668 Sanger (full gene)	2016	HGSC, left inguinal node HGSC	Null pattern	c.780delC (p.S261 fs*84), COSM45668 Sanger (full gene)
	3	N/A	54	N/R	1997	TO HGSC, IIIC	Null pattern	c.574C>T (p.Q192*), COSM10733 Sanger (single-amplicon)	2016	HGSC, pelvic lymph node left obturator fossa	Null pattern	c.574C>T (p.Q192*), COSM10733 Sanger (full gene)

Figure 1 - 685

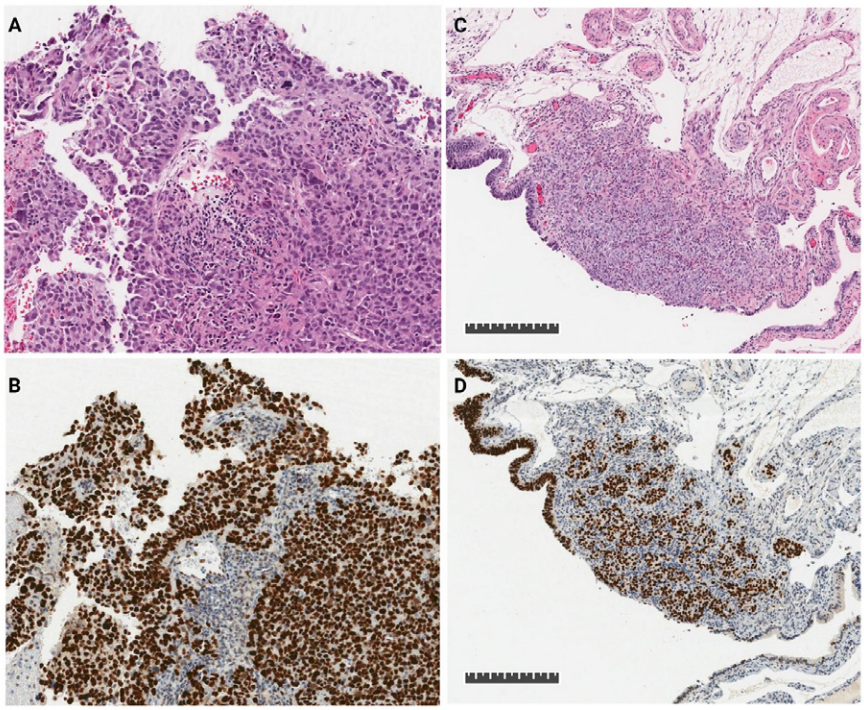

Figure 2 - 685

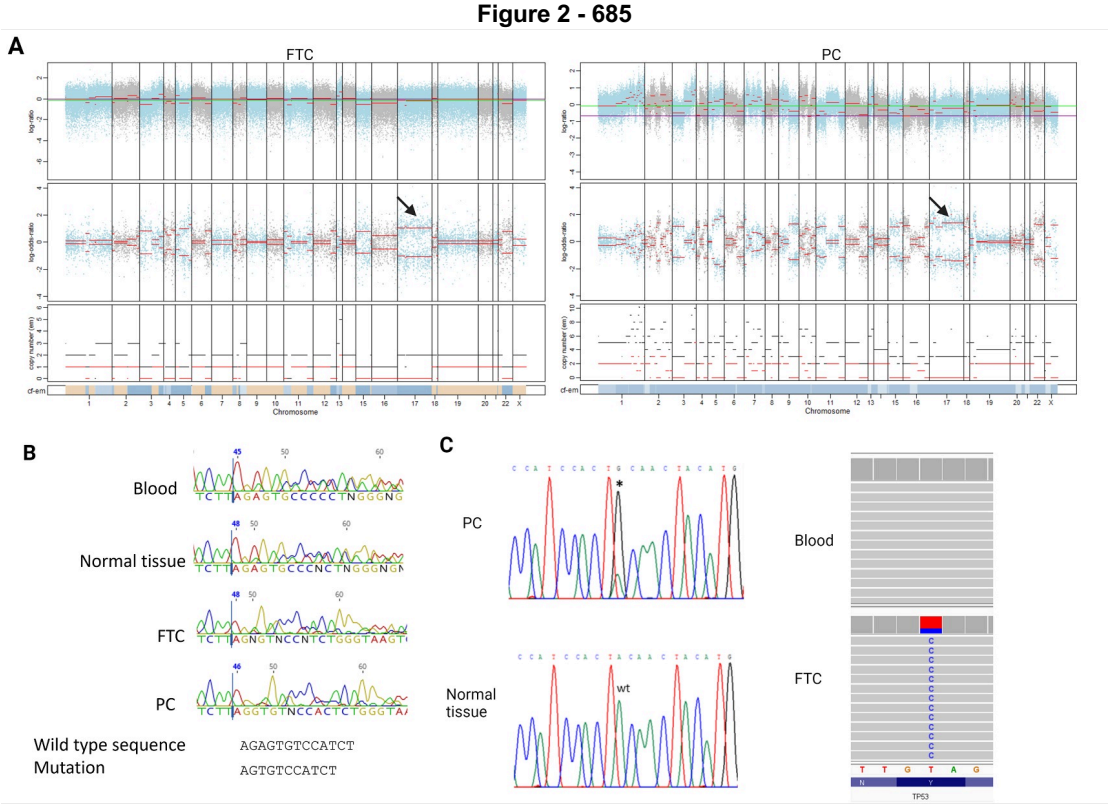

Conclusions: Exome sequencing of DNA derived from normal and tumor tissues showed that the pelvic tumor is a recurrence from the original Fallopian tube tumor. Occult HGSC or STIC in the RRSO specimen followed by peritoneal HGSC is uncommon but has been identified in previous studies (Table 1). Nonetheless, our case is the first to use WES to validate the finding that pelvic or peritoneal HGSCs developing after a significant time interval after the RRSO originate from a common precursor.

686 Embryonal Rhabdomyosarcoma of the Uterine Cervix: A Clinicopathologic Study of 94 Cases

Kyle Devins[1], Robert Young[2], Jennifer Bennett[3], Mariacristina Ghioni, Esther Oliva[5]
[1]Massachusetts General Hospital, Boston, MA, [2]Harvard Medical School, Boston, MA, [3]University of Chicago, Chicago, IL, [4]Institute of Oncology - IRCCS, Milan, Italy, [5]Massachusetts General Hospital, Harvard Medical School, Boston, MA

Disclosures: Kyle Devins: None; Robert Young: None; Jennifer Bennett: None; Mariacristina Ghioni: None; Esther Oliva: None

Background: Cervical embryonal rhabdomyosarcoma (cERMS) typically occurs in young women, frequently with *DICER1* mutations. A better prognosis than at other sites has been suggested. We report 94 cERMS highlighting the clinical background, pathologic spectrum, and correlation with outcome.

Design: The tumors were studied focusing on clinical history, pathologic findings, and follow-up.

Results: Patients ranged from 7–59 (mean=28) yrs; 22 were >40. Eight had DICER1 syndrome (Sertoli-Leydig cell tumor=7, pleuropulmonary blastoma=2, multinodular goiter=2, pineal blastoma=1). Presentations included vaginal bleeding (n=70), protruding vaginal mass (n=20), or tumor passed per vagina (n=4). All patients underwent polypectomy or biopsy, and 39 had slides from subsequent resections reviewed (conization=4, trachelectomy=4, hysterectomy=31). Tumors ranged from 2 – 24 (mean=5.7) cm. Most formed a single polypoid mass, but 7 were multiple. 33 showed invasion of the cervical wall. Trapped endocervical glands were present in 84 tumors. The usual appearance was aggregates of hyperchromatic rounded to spindled cells with scant cytoplasm set in a background that was edematous to myxoid. 37 tumors had conspicuous foci devoid of overtly malignant cells. The cellular foci occasionally became confluent (n=24) or sheet-like (n=5). A cambium layer was seen in all tumors. Hyperchromatic cells with scant cytoplasm typically predominated (n=81), but 13 tumors were mostly composed of cells with variable amounts of eosinophilic cytoplasm. “Strap cells” were present in 79, rhabdomyoblasts in 26, and cross striations in 44. Forty tumors contained fetal-type cartilage. Focal anaplasia was seen in 15 tumors and multinucleated cells in 12. Mitoses and apoptosis were frequent. All 38 tumors tested were positive for desmin, myogenin, and myoD1. Follow-up, available for 74 patients (mean=145 months), disclosed recurrences in 19, 9 locally after conservative resection. Two with DICER1 syndrome developed second primary cERMS 7 and 14 yrs following conservative resection; in one patient the tumors were proven to be independent based on molecular studies. Nine patients, all with deep cervical stromal invasion (hysterectomy=8, conization=1), died of disease.

Conclusions: cERMS is often a subtle diagnosis and may be mistaken for a polyp. Most have a good prognosis, all those in this series experiencing disease progression and death exhibiting deep cervical invasion. Germline DICER1 testing should be considered, particularly in young patients.

687 PD-L1 and MHC I Expression in Uterine Carcinosarcomas

Megan Dibbern[1], Anne Mills[2], Leigh Cantrell[1], Mark Stoler[1], Taylor Jenkins[1]
[1]University of Virginia Health System, Charlottesville, VA, [2]University of Virginia, Charlottesville, VA

Disclosures: Megan Dibbern: None; Anne Mills: None; Leigh Cantrell: None; Mark Stoler: None; Taylor Jenkins: None

Background: Uterine carcinosarcomas (UCS) are aggressive malignancies with minimal adjuvant treatment options. Recent literature demonstrates PD-L1 expression in a majority of UCS, suggesting possible vulnerability to anti-PD-1/PD-L1 checkpoint inhibitor therapy in these tumors. However, alterations in major histocompatibility complex class I (MHC I) expression may represent a mechanism of immunotherapeutic resistance in PD-L1-positive malignancies. We herein assess the relationship between PD-L1 and MHC I expression in UCS.

Design: 37 UCS were immunohistochemically stained for PD-L1 and MHC I on representative whole sections from treatment naive-tumors. PD-L1 was assessed using the combined positive score (CPS) with a threshold of ≥1 required for positivity. MHC I was classified as present, subclonally lost, or absent. Statistical analysis was performed using a two-tailed Fisher Exact test.

Results: 78% of UCS were PD-L1-positive (29/37) and 65% (24/37) showed subclonal or complete loss of MHC I expression, including over half of PD-L1-positive cases (19/37, 51%). Both carcinomatous and sarcomatous components were present on the representative section in 31 of 37 cases, including 16 cases with subclonal loss and 5 cases with absent MHC I expression. Of these, 48% (10/21) showed loss of MHC I expression in both components and 52% (11/21) showed loss in only the sarcomatous component. No case showed loss of MHC I expression solely in the carcinomatous component. In the cases with absent MHC I

expression, 3 showed loss in both components: 2 cases with subclonal loss in the carcinomatous component and complete loss in the sarcomatous component and 1 case with absent MHC I expression in both components. Overall, the sarcomatous component was more likely than the carcinomatous component to have any MHC I loss (p=0.015).

Conclusions: Although the majority of UCS are PD-L1-positive, two-thirds also show some loss of MHC I expression, with one-third showing loss in only the sarcomatous portion and one-third with loss in both tumoral components. This suggests possible resistance to immunotherapy targeting the PD-1/PD-L1 axis in a large subset of UCS, particularly in cases with a more pronounced sarcomatous component. However, as the carcinomatous component is frequently the driver of recurrent disease, a subset of UCS with intact MHC I expression may be more likely to respond to checkpoint inhibitor therapy.

688 Progressive Microsatellite Instability in Recurrent MSI-H Endometrial Adenocarcinomas Coincides with ARID1A Frameshift and CTNNB1 Mutations

Darin Dolezal[1], Minhua Wang[1], Natalia Buza[1], Pei Hui[2]
[1]Yale School of Medicine, New Haven, CT, [2]Yale University School of Medicine, New Haven, CT

Disclosures: Darin Dolezal: None; Minhua Wang: None; Natalia Buza: None; Pei Hui: None

Background: The majority of patients with microsatellite instability-high endometrial carcinoma (MSI-H EC) have early-stage, low-grade endometrioid tumors. The mutation status of MSI-H EC in the setting of relapse has yet to be investigated. We used PCR-based microsatellite marker analysis and NGS to evaluate accumulation of insertions/deletions and single nucleotide variants in recurrent MSI-H ECs.

Design: A pathology database search revealed 12 cases of local recurrence (avg. time to relapse: 34 months, range: 5 to 55) in 10 patients with sporadic MSI-H EC, endometrioid type; two patients had re-recurrence of disease. Recurrent tumor, matched endometrial primary, and patient normal tissue were subjected to MSI PCR testing targeting 8 microsatellite markers (5 mono- and 3 dinucleotide repeats). FoundationOne CDx was performed on recurrent (n=12) and primary (n=8) tumors.

Results: MSI testing revealed that a significant number of stable microsatellite (MSS) markers in the primary tumor converted to MSI in the recurrences: 58% (46/80) in primary tumors vs. 81% (64/79) in recurrent tumors (p=.001), and 94% (15/16) in re-recurrences. The average number of MSI markers seen per tumor significantly increased from primary (4.6) to recurrence (6.6, p=0.01). Furthermore, many unstable MSI markers in the primary tumor became more unstable (i.e., accumulated additional insertion/deletions): 67% (36/46) at recurrence and 60% (9/15) at re-recurrence (Figure 1). NGS revealed an elevated tumor mutational burden in recurrent tumors (25.5 mutations/Mb) in comparison with their primary tumors (20.1 mutations/Mb, p=0.16). Notably, at least one damaging frameshift mutation in *ARID1A* was present across all primary and recurrent tumors, and two damaging mutations in *ARID1A* were detected in 7/8 primary and 9/12 recurrent tumors. Activating mutations in *PIK3CA* and/or damaging mutations in *PTEN* or *PIK3R1* were also seen in all cases. Moreover, activating mutations in *CTNNB1* were seen in the majority of recurrent tumors (7/12) whereas none were found in the primary tumors (0/8, p=0.01), suggesting a role for Wnt/β-catenin signaling in development of the tumor recurrence.

Figure 1 - 688

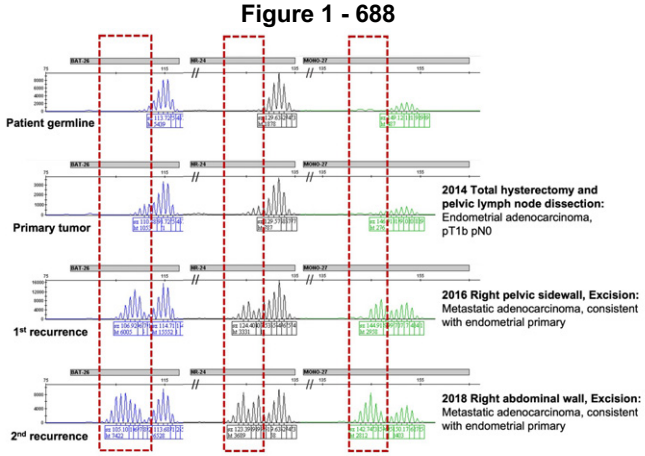

Figure 1. PCR-CE MSI testing performed on recurrent MSI-H EC from a single patient. Three representative microsatellite markers (blue, black, green) are shown above to illustrate the progressive accumulation of new microdeletions (1 nucleotide-shifted peaks shown within red boxes) from primary tumor (2nd row) to first recurrence (3rd row) and second recurrence (4th row). All tumor samples showed similar tumor cellularity and are compared to the patient's benign tissue (top row).

Conclusions: In summary, progressive microsatellite instability develops in recurrent tumors of MSI-H endometrial endometrioid carcinomas. Damaging *ARID1A* mutations were strongly associated with MSI-H endometrial carcinomas and activating *CTNNB1* mutations may play an important role in the development of tumor recurrence.

689 Endometrial Tumors with POLE Mutation: A Clinicopathologic Characterization of a Single Institution Series

Elizabeth Euscher[1], Richard Yang[1], Anais Malpica[1], Barrett Lawson[1], Preetha Ramalingam[1]
[1]The University of Texas MD Anderson Cancer Center, Houston, TX

Disclosures: Elizabeth Euscher: None; Richard Yang: None; Anais Malpica: None; Barrett Lawson: None; Preetha Ramalingam: None

Background: In The Cancer Genome Atlas (TCGA) integrated molecular classification of endometrial carcinoma, tumors in the *POLE* (ultramutated) group showed an excellent clinical outcome. Since then, multiple studies have shown a favorable prognosis for *POLE* ultramutated tumors across multiple histotypes. This study characterizes the clinicopathologic features of endometrial tumors with *POLE* mutation detected at a single institution.

Design: The molecular database was searched (2018-2021) for endometrial tumors with *POLE* mutation. We obtained the following clinicopathologic features from the medical records: patient age, tumor histology, FIGO stage, sites of recurrent disease, treatment, mismatch repair status (MMR) and follow up.

Results: Results are summarized in Table 1. Although endometrioid carcinoma, FIGO grade 3 and undifferentiated/dedifferentiated carcinoma represented a plurality of the cases (6/15, 40%), the study group also included an unexpected number of low grade endometrioid carcinomas (5/12, 42%). MMR testing was performed in fourteen cases with results indicating microsatellite instability in 5 (36%). 12/15 patients had genomic testing at the time of tumor recurrence or progression. 3 patients with early genomic testing showing *POLE* mutation had treatment related to tumor grade or stage. Three patients who had early stage tumors and no therapy experienced recurrence.

Clinicopathologic Features of Endometrial Tumors with POLE Mutation

Case	Age	FIGO Stage	Histology	Recurrence	Microsatellite Stability	Primary Treatment	Follow Up
1	89	IIIc	High-grade, favor serous	Never achieved remission	Stable	Chemotherapy	AWD (24 mo)
2	72	IIIc	Endometrioid, FIGO grade 2	Unkn	High	Unkn	LTF
3	63	Ia	Endometrioid, FIGO grade 2	Lung	High (MLH1 methylation)	XRT	DOD (113 mo)
4	35	Ia	Possible Dedifferentiated CA	Bone, retroperitoneum	High	None	DOD (270 mo)
5	66	Ib	Somatic Yolk Sac Tumor	Abdomen	Stable	Chemotherapy	DOD (27 mo)
6	61	IIIc	Possible Dedifferentiated CA	Never achieved remission	Not done	Chemotherapy	DOD (4 mo)
7	68	IIIa	Carcinosarcoma	None	Stable	Chemotherapy	NED (18 mo)
8	57	IIIc	Endometrioid, FIGO grade 2	None	Stable	Neo-adjuvant chemotherapy	NED (31 mo)
9	68	IIIa	Possible Dedifferentiated CA	Pelvis	Stable	Chemotherapy	AWD (15 mo)
10	61	II	Possible Dedifferentiated CA	None	High	Pelvic XRT	NED (10 mo)
11	55	IIIc	Endometrioid, FIGO grade 2	Liver	High; MLH-1 methylation	Chemotherapy	NED (33 mo)
12	59	Ia	Endometrioid, FIGO grade 2	Pelvis	High	None	AWD (70 mo)
13	41	Ia	Endometrioid, FIGO grade 3	None	Stable	Chemotherapy	NED (5 mo)
14	56	IIIc	Undifferentiated CA	Lung	Not done	Chemotherapy/XRT	NED (45 mo)
15	66	Ia	Endometrioid, FIGO grade 3	Lung	Stable	None	AWD (57 mo)

Conclusions: The tumors in this study are heterogeneous, but enriched for high grade carcinoma. The finding of *POLE* mutation in a somatic yolk sac tumor is a novel finding. Just over a third of cases had MMR testing indicative of an MSI high tumor suggesting that sole reliance upon MMR immunohistochemistry could miss a subset of endometrial tumors (including low grade endometrioid carcinoma) with *POLE* mutation. Knowledge of *POLE* mutational status was not integrated into treatment decisions

since *POLE* mutation was detected at the time of recurrence or disease progression in 80% of cases. While many tumors in this study had better than predicted outcome for tumor grade or stage, 3 patients with low grade or stage carcinoma who did not receive treatment at diagnosis recurred or died of disease. This suggests that the survival benefit for *POLE* ultramutated tumors could be related to therapeutic response for some patients rather than a de novo improved outcome.

690 Extra-Uterine Mesonephric-Like Carcinoma Is Associated with Endometriosis and May Behave Aggressively

Elizabeth Euscher[1], Mario Marques-Piubelli[1], Preetha Ramalingam[1], Barrett Lawson[1], Anais Malpica[1]
[1]*The University of Texas MD Anderson Cancer Center, Houston, TX*

Disclosures: Elizabeth Euscher: None; Mario Marques-Piubelli: None; Preetha Ramalingam: None; Barrett Lawson: None; Anais Malpica: None

Background: Extra-uterine mesonephric-like carcinoma (eMLC) is under-recognized due to its rarity and histologic overlap with more common types of upper gynecologic tract carcinoma (CA). Studies have shown endometrial MLC to behave aggressively compared to low grade endometrioid carcinoma (LGEC) and serous carcinoma (SC). Recent reports suggest eMLC to show a similar aggressive pattern when compared to ovarian LGEC and clear cell CA (CCC). This study compares the clinicopathologic features of eMLC to LGEC, CCC and high grade SC (HGSC).

Design: 21 ovarian eMLC, 36 LGEC, 27 CCC and 41 HGSC (2002-2021) were compared with respect to patient (pt) age, FIGO stage, presence of endometriosis, presence of additional histologic components, treatment, recurrence, and disease status at last follow up. Where applicable, the original pathology diagnosis (dx) for the eMLC cases was noted. The unpaired t-test, Chi-square, uni- and multivariate (Cox regression) analysis were performed using SPSS (Statistics for Windows, Version 24.0. Armonk, NY: IBM Corp.). A p value < 0.05 was considered significant.

Results: Table 1 summarizes the clinicopathologic features of our cohort. 17/21(81%) eMLC were originally misclassified as LGEC (5); adenoCA NOS (3); mixed CA (2); high grade EC (1); seromucinous CA (1); HGSC (1); low grade SC (1); transitional CA (1); mullerian carcinosarcoma (1); female adnexal tumor of probable Wolffian origin (1). Compared to other subtypes, eMLC more frequently had additional components (12/21): borderline (4); LGEC (3); CCC (2); low grade SC (1); mixed LGE/CCC (1); malignant cartilage (1). EMLC and CCC were more likely to be associated with endometriosis (p<0.0001) while HGSC was more likely to present at advanced stage (p=0.0003). EMLC, HGSC and CCC were more frequently associated with distant recurrences compared to LGEC (p<0.00001). Considering overall and progression free survival (OS, PFS) for all subtypes, presentation at lower FIGO stage (I/II) was associated with improved OS (p=0.006) and PFS (p<0.001). Pts with metastases (MTs) had improved OS and PFS (p<0.001) when MTs were confined to the pelvis vs omentum/liver/lung. Although pts without recurrence had better OS and PFS (p<0.001), those who recurred had improved OS and PFS when MTs were confined to the pelvis or abdominal peritoneum vs lung/liver (p<0.001). Histologic subtype was associated with longer PFS for LGEC/CCC vs HGSC/eMLC (p=0.006). Multivariate models examining age, histotype, FIGO stage, MT and recurrence sites showed only age as a significant predictor of OS and no variable was associated with improved PFS.

Clinicopathologic Features for the Study Cohort

	eMLC (n=21)	LGEC (n=36)	CCC (n=27)	HGSC (n=41)
Age (mean, years)	57	58	56	59
Stage I/II	12	28	19	12
Stage III/IV	8	8	8	29
Endometriosis	12 (57%)	14 (39%)	18 (67%)	3 (7%)
Additional histologic component	12 (57%)	13 (36%)	1 (4%)	1 (2%)
Chemotherapy	15 (71%)	30 (83%)	26 (4%)	40 (2%)
Recurrence/never cleared	12 (57%)	3 (8%)	8 (30%)	22 (54%)
No evidence of disease at last follow up	7 (33%)	30 (83%)	19 (70%)	19 (46%)

Conclusions: EMLC is often misclassified and in contrast to endometrial MLC, is frequently admixed with either borderline tumor or a mullerian type CA. The presence of additional histotypes in over half of eMLC in this study may explain the overlapping clinical features between eMLC and the other subtypes in the study cohort. When considering PFS and OS, stage at presentation and MT location are predictive of adverse outcome. Although eMLC did not segregate into a more aggressive pattern when the

other histotypes were considered, it is associated with stage at presentation and recurrences in the lung/liver pointing to more aggressive behavior compared to LGEC.

691 Extra-Uterine Mesonephric-Like Carcinoma: A Single Institution Clinicopathologic Study of 21 Cases

Elizabeth Euscher[1], Preetha Ramalingam[1], Barrett Lawson[1], Anais Malpica[1]
[1]The University of Texas MD Anderson Cancer Center, Houston, TX

Disclosures: Elizabeth Euscher: None; Preetha Ramalingam: None; Barrett Lawson: None; Anais Malpica: None

Background: Extra-uterine mesonephric-like carcinoma (eMLCA) is uncommon and shares histologic, immunohistochemical (IHC) and molecular (MOL) features with endometrial MLCA. Despite increased awareness, challenges diagnosing eMLCA persist due to histologic overlap with more common types of upper gynecologic CA. This largest single institution series describes the clinicopathologic, IHC, and MOL features of eMLCA.

Design: In 21 eMLCA (2002 to present) we recorded the following: patient (pt) age, tumor stage, primary site, pt outcome, presence of endometriosis, presence of synchronous endometrial CA, presence of additional histotypes, architectural patterns and nuclear characteristics, presence/absence of eosinophilic secretions, and IHC and MOL results.

Results: Table 1 shows selected results. One pt had an occult synchronous low grade endometrial CA (LGECA). 12 (57%) cases had premalignant/other histotypes present. ONe pt with low grade serous CA(LGSCA) had MLCA in a recurrence. H&E slides showed intraluminal eosinophilic secretions (focal to prominent) in all cases and varying proportions of architectural patterns: glandular 21/21; papillary 15/21; slit-like 10/21; trabecular 8/21; solid 7/21; and spindle cell 6/21. One case had sarcomatous differentiation (heterologous cartilage). All cases had at least focally vesicular nuclei with nuclear grooves. IHC facilitated diagnosis in all cases: PAX8 15/16; GATA3 18/21; TTF1 16/21; CD10 10/10; calretinin 7/10; ER 7/20; PR 5/17; AR 0/1; WT1 0/17.
MOL testing in 11 cases identified mutations (MUT) in *KRAS* (8), *NRAS* (2) and *TP53* (1). 7 pts w *KRAS* MUT had additional MUTs: *PTEN* (2), *PIK3CA* (2), *SPOP* (2), *ARID1A* (1), *TP53* (1). Four (19%) eMLCA were correctly classified. Misclassified eMLCA had the following dx: LGECA(5); adenoCA NOS (3); mixed CA (2); high grade ECA (1); seromucinous CA (1); high gradeSCA (1); LGSCA (1); transitional CA (1); carcinosarcoma (1); and female adnexal tumor of probable Wolffian origin (1).

Clinicopathologic Features of eMLCA

Case	Age	FIGO stage	Original Dx	Primary Site	Endometriosis	Other histology	Recurrence site	Pt Outcome
1	51	III	LGECA	Peritoneum	Yes	None	Lung	AWD (220 mo)
2	61	I	MLCA	Ovary	Yes	None	Unkn	LTF
3	74	III	LGECA	Ovary	No	None	Liver, Lung	DOD (32 mo)
4	69	IV	LGECA	Peritoneum	No	None	Lung Mt at presentation	DOD (45 mo)
5	66	IV	High grade SCA	Peritoneum	No	None	Liver, Lung	AWD (77 mo)
6	61	III	LGECA + high grade SCA	Ovary	Yes	None	Lung	AWD (34 mo)
7	66	III	Transitional cell CA	Ovary	No	LG serous CA	Lung	AWD (31 mo)
8	74	II	Clear cell + LGECA	Ovary	No	Clear Cell CA	Liver	AWD (36 mo)
9	68	I	High grade ECA	Ovary	No	None	Abd peritoneum	AWD (18 mo)
10	48	III	LGSCA	Ovary	No	Borderline	Pelvis	AWD (74 mo)
11	53	II	MLCa	Ovary	Yes	Borderline	Unkn	LTF
12	64	I	AdenoCA NOS	Ovary	Yes	Borderline	None	NED (8 mo)
13	60	I	MLCA	Ovary	Yes	Endometrioid CA	Recent Case	Recent Case
14	52	I	MLCA	Ovary	Yes	EndometrioidCA	Recent Case	Recent Case
15	44	I	Carcinosarcoma	Ovary	Yes	None	Recent Case	Recent Case
16	50	I	SeromucinousCA	Ovary	Yes	Endometrioid	Recent Case	Recent Case
17	54	unkn	AdenoCA NOS	Ovary	Yes	Endometrioid + Clear Cell CA	Recent Case	Recent Case
18	37	I	LGECA	Ovary	No	Borderline	Liver	AWD (37 mo)
19	54	III	LGECA	Ovary	Yes	None	Lung	DOD (18 mo)
20	51	II	High grade CA, NOS	Ovary	Yes	Clear Cell CA	Recent Case	Recent Case
21	63	I	FATWO	Ovary	No	None	Abd Peritoneum	AWD(45 mo)

Conclusions: ELMCA is often misclassified due to its rarity and association with more common upper GYN histotypes. Lost or diminished ER/PR expression and positive GATA3, TTF1, CD10 and/or calretinin facilitate diagnosis. An association with endometriosis and the presence in some cases of additional MUT frequently associated with endometrioid CA support a similar

pathogenesis to endometrial MLCA. EMLCA's propensity for lung and liver recurrence/metastasis suggests the potential for aggressive behavior similar to its endometrial counterpart.

692 Distinguishing Differentiated Vulvar Intraepithelial Neoplasia from its Mimic Lichen Sclerosus Using Immunohistochemical Evaluation of CK13, CK17, GATA3, and p53

Saleh Fadel[1], Sarah Strickland[2], Aleksandra Paliga[3]
[1]The Ottawa Hospital, University of Ottawa, Ottawa, Canada, [2]University of Ottawa, Ottawa, Canada, [3]The Ottawa Hospital, Ottawa, Canada

Disclosures: Saleh Fadel: None; Sarah Strickland: None; Aleksandra Paliga: None

Background: Differentiated vulvar intraepithelial neoplasia (dVIN) is a Human Papilloma Virus (HPV)-independent squamous intraepithelial lesion and is a precursor to vulvar invasive squamous cell carcinoma. Morphologic features of dVIN may be subtle and can show overlap with lichen sclerosus (LS). Building on previous studies we present the first series to characterize the staining patterns of dVIN and LS with CK13, CK17, GATA3, and p53 in order to determine if one or a combination of these markers may be used to distinguish between these two entities.

Design: 22 cases of dVIN and 22 cases of LS diagnosed between 2015-2020 at The Ottawa Hospital, ON, Canada were retrieved. The diagnosis of dVIN was based on morphologic features and required basal atypia as well as a negative p16 stain. Immunohistochemistry for p53, CK13, CK17 and GATA3 was performed on whole tissue sections. The localization of expression (basal, parabasal, and superficial), percentage of cells staining and staining intensity was scored independently by two co-authors. A third author was consulted regarding discrepant cases. P53 was assessed as mutant if there was >80% basal staining, parabasal/diffuse overexpression, or cytoplasmic staining.

Results: Most cases of both dVIN (91%) and LS (81%) showed mutant pattern of p53 expression. All 18 cases of LS with mutant pattern showed basal overexpression whereas only 6 of the dVIN cases (30%) had this pattern, with the remainder showed parabasal/diffuse overexpression (46%) and cytoplasmic (18%). 8 dVIN cases (36%) had absent basal CK13 staining with > 25% superficial staining compared to only 1 LS case (5%). This pattern had a specificity of 95% and a positive predictive value of 89% for the diagnosis of dVIN. 9 dVIN cases (41%) had absent basal/parabasal CK17 staining with > 50% superficial staining compared to 0 LS cases. This pattern was 100% specific and 40% sensitive. Absent basal/parabasal expression of GATA3 was more often seen in dVIN but was also seen in a small subset of LS cases (59% versus 14%).

Conclusions: Mutant pattern of p53 expression was seen in the majority of cases of both dVIN and LS; however LS cases showed only basal overexpression and did not show other mutant patterns (parabasal/diffuse and cytoplasmic staining). Although the other markers tested showed poor sensitivity for the diagnosis of dVIN, absent basal CK13 with >25% superficial staining and absent basal/parabasal CK17 with >50% superficial staining were highly specific for the diagnosis of dVIN.

693 AIRMEC - an Artificial Intelligence Model to Predict the Molecular Endometrial Cancer Classification from H&E Images

Sarah Fremond[1], Sonali Andani[2], Jurriaan Barkey Wolf[1], Jouke Dijkstra[1], Jan Jobsen[3], Mariel Brinkhuis[4], Suzan Roothaan[4], Ina Jürgenliemk-Schulz[5], Ludy Lutgens[6], Remi Nout[7], Elzbieta van der Steen-Banasik[8], Stephanie de Boer[1], Melanie Powell[9], Naveena Singh[10], Linda Mileshkin[11], Helen Mackay[12], Alexandra Leary[13], Hans Nijman[14], Vincent Smit[1], Carien Creutzberg[1], Nanda Horeweg[1], Viktor Kölzer[2], Tjalling Bosse[1]

[1]Leiden University Medical Center, Leiden, Netherlands, [2]University Hospital Zurich, Zurich, Switzerland, [3]Medisch Spectrum Twente, Enschede, Netherlands, [4]LabPON, Hengelo, Netherlands, [5]University Medical Center Utrecht, Utrecht, Netherlands, [6]Maastricht UMC+, Maastricht, Netherlands, [7]Erasmus University Medical Center, Rotterdam, Netherlands, [8]Radiotherapiegroep, Arnhem, Netherlands, [9]Barts Health NHS Trust, London, United Kingdom, [10]Vancouver General Hospital, Vancouver, Canada, [11]Peter MacCallum Cancer Centre, Mt Stuart, Australia, [12]Sunnybrook Health Sciences Centre, Odette Cancer Centre, Toronto, Canada, [13]Gustave Roussy, Villejuif, France, [14]University Medical Center Groningen, University of Groningen, Groningen, Netherlands

Disclosures: Sarah Fremond: None; Sonali Andani: None; Jurriaan Barkey Wolf: None; Jouke Dijkstra: None; Jan Jobsen: None; Mariel Brinkhuis: None; Suzan Roothaan: None; Ina Jürgenliemk-Schulz: None; Ludy Lutgens: None; Remi Nout: None; Elzbieta van der Steen-Banasik: None; Stephanie de Boer: None; Melanie Powell: None; Naveena Singh: None; Linda Mileshkin: None; Helen Mackay: None; Alexandra Leary: None; Hans Nijman: None; Vincent Smit: None; Carien Creutzberg: None; Nanda Horeweg: None; Viktor Kölzer: None; Tjalling Bosse: None

Background: Endometrial Carcinomas (ECs) are molecularly classified into polymerase-ε mutated (*POLE*mut), mismatch-repair deficient (MMRd), p53 abnormal (p53abn) and no specific molecular profile (NSMP). Utilising Artificial Intelligence (AI) to identify molecular alterations from H&E-stained whole slide images (WSIs) of tumors has shown promise to be a cost-effective alternative to ancillary tests and to reveal morpho-molecular correlates. Here, we developed and tested an AI model that can predict the molecular EC classes from H&E-WSIs.

Design: Digital H&E-WSIs from 2,001 molecularly classified ECs of the *trans*PORTEC repository were split into a training-validation cohort (N=1,608) and an independent test cohort (PORTEC-3, N=393). First, a self-supervised model was trained on randomly sampled tiles (360-micron image patches extracted from WSIs) to derive robust EC-specific features. Next, a weakly-supervised model was trained by assigning an attention score to each feature tile to predict slide-level molecular EC class. The accuracy of the final pipeline (AIRMEC) was analysed by calculating the area under the receiver operating characteristic curve (AUC) on PORTEC-3. AIRMEC was first built to predict the 4 molecular classes. A 3-class model was subsequently developed excluding the MMRd class since MMR-IHC is routinely performed for Lynch Syndrome screening. Most informative tiles were visualized for pathologist review. Correlations with clinical outcomes were investigated using Kaplan-Meier's methodology and univariate Cox' proportional hazards models.

Results: On PORTEC-3, the 4-class and 3-class AIRMEC models achieved a macro-averaged AUC of 0.856 and 0.916 respectively (Table 1). Attention maps of correctly classified H&E-WSIs showed high attention towards the invasive border for *POLE*mut ECs whereas towards the tumor center for other molecular classes. The highest discriminative tiles confirmed known morpho-molecular features (Figure 1). Risk of recurrence by AIRMEC predictions were (HR 2.64, 95%CI 1.66-4.20) for p53abn ECs and (HR 0.50, 95%CI 0.21-1.18) for *POLE*mut ECs as compared to the NSMP reference (Figure 2).

	4-class AIRMEC model				3-class AIRMEC model			
	AUC	PPV	Sensitivity	Specificity	**AUC**	PPV	Sensitivity	Specificity
Macro average (N=393)	**0.856**	0.578	0.610	0.881	**0.916**	0.739	0.763	0.888
*POLE*mut (N=51)	**0.817**	0.137	0.380	0.883	**0.911**	0.608	0.674	0.906
MMRd (N=134)	**0.806**	0.784	0.580	0.863	-	-	-	-
NSMP (N=120)	**0.889**	0.675	0.771	0.865	**0.918**	0.892	0.775	0.893
p53abn (N=88)	**0.911**	0.716	0.708	0.912	**0.917**	0.716	0.840	0.864

Table 1: Performance of the 4-class and 3-class AIRMEC models on PORTEC-3 (N=393). AUC refers to the area under the receiver operating characteristic curve and PPV to the positive predictive value. AUCs per class are computed as binary labels (one-vs-rest AUC). Metrics for the 4-class or 3-class are unweighted averaged values (macro average).

Figure 1 - 693

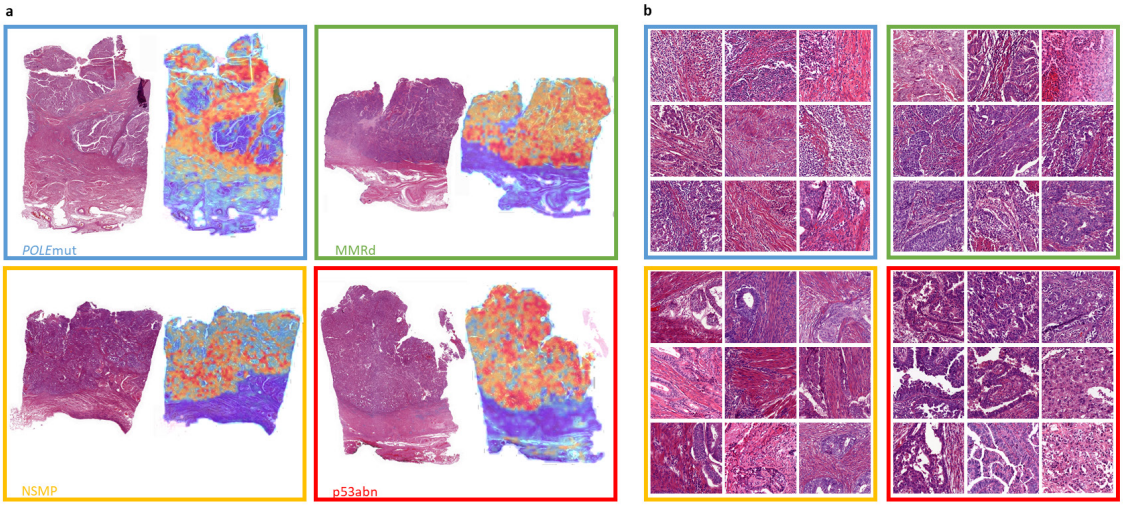

Figure 1: AIRMEC predictions interpretability on PORTEC-3. a. AI-based attention scores are displayed as heatmaps for one representative case of each EC molecular subgroup *POLE*mut, MMRd, NSMP, p53abn. Red regions show high attention evidence whereas blue low importance toward the molecular prediction. b. Galleria of the most attended tile for 9 correctly classified cases within each class. Highly discriminative tiles confirmed known morpho-molecular correlates: tumor-infiltrating and peritumor lymphocytes, tertiary lymphoid structures, solid tumor growth, endometrioid morphology in *POLE*mut EC; similar features but less pronounced within MMRd EC; glandular architecture with smooth luminal borders, absence of lymphocytes and squamous differentiation within NSMP EC; pleiomorphic nuclei, desmoplastic stromal reaction, ragged luminal surface with hobnailing cells within p53abn EC.

Figure 2 - 693

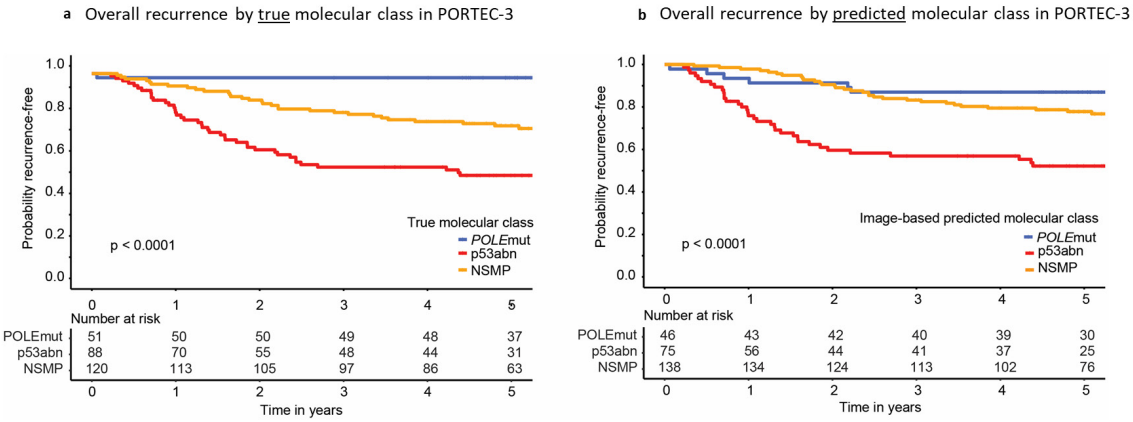

Figure 2: Overall recurrence in PORTEC-3 as stratified by the true and predicted molecular EC classification. a. Time overall recurrence by true molecular class assessed according to WHO-2020. b: Time to overall recurrence by molecular class predicted by the 3-class AIRMEC model.

Conclusions: AIRMEC has promising predictive performance for molecularly classifying EC from H&E-WSI. AIRMEC predictions are interpretable and allow for deeper investigation of morpho-molecular correlations in EC. *POLE*mut EC is the most challenging class to predict correctly. We foresee clinical utility of reliable AI-based classification by AIRMEC, especially combined with MMR IHC.

694 Early Complete Hydatidiform Mole with Placental Mesenchymal Dysplasia

Masaharu Fukunaga[1], Natsu Fukunaga[2]
[1]Shin-Yurigaoka General Hospital, Kawasaki, Japan, [2]Showa University Northern Yokohama Hospital, Yokohama, Japan

Disclosures: Masaharu Fukunaga: None; Natsu Fukunaga: None

Background: Early complete moles (CM) with placental mesenchymal dysplasia (PMD) component may pose a diagnostic challenge because it is very rare and resembles a twin placenta with CM or partial mole, and early PMD histology is not well-known. In such cases, the differential diagnosis is very important for patient management.

Design: This was a study 18 cases of CM with PMD in the first trimester, which were retrieved from 955 cases of hydropic placental tissue. They were histopathologically reviewed and an immunohistochemical study of p57 (Kip2) (p57) and TSSC3, both of which are products of paternally imprinted, maternally expressed genes, was also conducted.

Results: Four cases of twins with CM and PMD and 14 cases of mosaic CM with PMD component were identified. All cases of twins with CM and PMD exhibited two populations of villi, each with CM and early PMD histology. The PMD component in all cases was histologically characterized by moderate swelling of stem villi with cistern formation, mild stromal cell and vascular proliferations, and the absence of trophoblastic hyperplasia. In cases of mosaic CM with a PMD component, many villi showed mixed CM and PMD morphologies, and fetal parts were observed in 4 cases. There was a discordant pattern of p57 expression in the PMD component, with positive staining in villous cytotrophoblasts and negative stromal cells, indicating a mixture of androgenetic and biparental cells. There was negative staining of cytotrophoblasts and stromal cells in the CM component. TSSC3 was positive for cytotrophoblasts and negative for stromal cells in the PMD component. TSSC3 was negative for cytotrophoblasts in the CM component. A patient with twins with CM and PMD developed persistent trophoblastic disease.

Conclusions: Early CM with PMD has a very complicated histology. Immunohistochemical examinations of p57 and TSSC3 are useful for the differential diagnosis of early CM with PMD and can be screening tools for cytogenetic analyses. Twins with CM and PMD were composed of two populations of villi, each with CM and early PMD histology. A discordant pattern of p57 expression indicates androgenetic/biparental mosaic conceptions in PMD. Mosaic conception cases comprised a p57-discordant PMD component and a p57-negative androgenetic CM component in individual villi. It is important to identify CM with PMD at an early stage to reduce the risk of persistent trophoblastic disease. These patients should be followed-up with human chorionic gonadotropin monitoring.

695 Somatically Derived Germ Cell Tumors of the Female Genital Tract

Masaharu Fukunaga[1], Natsu Fukunaga[2]
[1]Shin-Yurigaoka General Hospital, Kawasaki, Japan, [2]Showa University Northern Yokohama Hospital, Yokohama, Japan

Disclosures: Masaharu Fukunaga: None; Natsu Fukunaga: None

Background: Female genital tract carcinomas with germ cell tumors (GCTs) are very rare and pose diagnostic and therapeutic challenges. GCTs generally arise in the ovary and occur in young women. They are rare in those over the age 40. The histogenesis is controversial.

Design: A total 18 cases of female genital tract carcinomas with GCTs in patients aged 40 years or over, except one of 31 years, were clinicopathologically and immunohistochemically studied.

Results: The age of the patients ranged from 31 to 79 years (mean:59.3). Regarding anatomic sites, eight were in the endometrium, 6 in the ovary, 2 in the tube, and one each in the cervix or peritoneum. Eleven patients had yolk sac tumors (YSTs)(Fig. 1 and 2), 5 had choriocarcinoma, 2 had immature teratoma. There were carcinomas (including three cases of carcinosarcoma) comprising high-grade serous carcinoma (n=7), endometrioid carcinoma (n=3), large cell neuroendocrine carcinoma (n=3), clear cell carcinoma (n=3), and gastric type mucinous carcinoma (n=2). Five of YSTs were hepatoid variant(Fig. 2). Glandular morphologies including enteroblastic differentiation were observed in YSTs. There was some immunophenotypic overlap with carcinomas and YSTs. They shared EMA and CK7 positivity. One YST developed after chemotherapy for peritoneal high-grade serous carcinoma, indicating morphologic and genetic alterations induced by chemotherapy. Follow-up data were available in 11 cases. The stages were FIGO stage IA (3 cases), IB (1), IIA (1), IIb (4), IIIA (2), IIIB (1), IIIC (2), and IVB (4). Six patients died of the disease within 12 months (mean:8.5) after surgery.

Figure 1 - 695

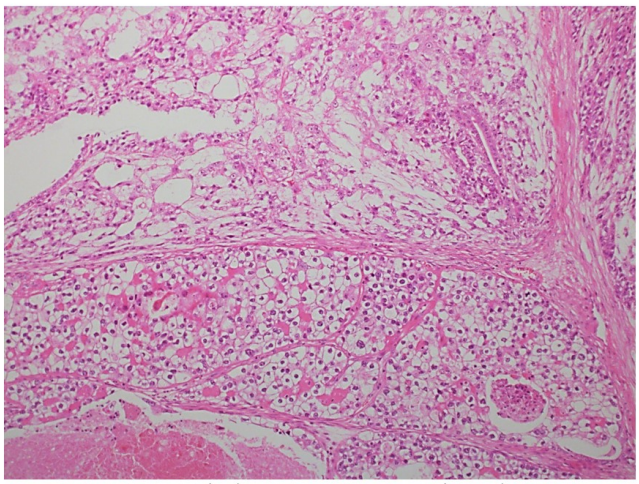

Figure 1. Yolk sac tumor (top) and clear cell carcinoma (bottom) of the ovary.

Figure 2 - 695

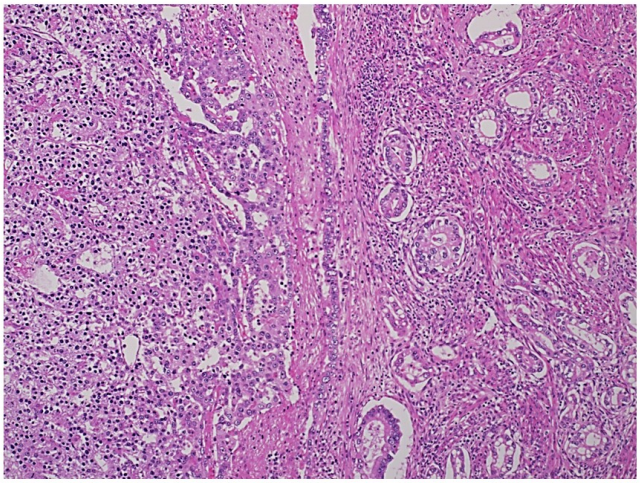

Figure 2. Hepatoid variant yolk sac tumor (left) and gastric type mucinous carcinoma (right) of the endometrium.

Conclusions: The findings suggest the association between GCT and carcinoma, with the former probably arising from the latter through a process of neometaplasia or retrodifferentiation in various sites of the female genital track. Somatic epithelial neoplasm can be of various histologic types. Glandular morphology in YST mimics that of clear cell, mucinous, or other carcinomas. Comprehensive pathologic diagnoses are necessary. This type of tumor can occur also in young patients. Its recognition is necessary in view of its unusually aggressive behavior and associated poor prognosis. Adjuvant chemotherapy regimens should include platinum-based chemotherapy, aiming at the treatment of both carcinoma and GCT.

696 Ovarian Steroid Cell Tumors Lack Uniform Peri-Cellular Reticulin Staining: A Potential Pitfall with Luteinized Adult Granulosa Cell Tumor that is Resolved by FOXL2 Immunostaining

Cynthia Gasper[1], Nicholas Ladwig[2], Rebecca Wolsky[3], Joseph Rabban[2]
[1]UCSF Pathology, San Francisco, CA, [2]University of California, San Francisco, San Francisco, CA, [3]University of Colorado, Denver, CO

Disclosures: Cynthia Gasper: None; Nicholas Ladwig: None; Rebecca Wolsky: None; Joseph Rabban: None

Background: Ovarian steroid cell neoplasms and non-neoplastic proliferations may morphologically mimic luteinized adult granulosa cell tumors (AGCT), a diagnostic challenge compounded by a similar sex cord-stromal immunophenotype (positive inhibin, calretinin, and SF1). Although FOXL2 immunoexpression distinguishes ovarian steroid cell lesions (FOXL2 negative) from all other ovarian sex cord-stromal lesions (FOXL2 positive), this stain is not widely available. Reticulin staining pattern reliably distinguishes classical AGCT (absence of uniform peri-cellular staining) from cellular fibroma (presence of uniform peri-cellular staining) but reticulin staining patterns in ovarian steroid cell tumors and non-neoplastic proliferations are not well studied.

Design: Reticulin staining and FOXL2 immunostaining were performed on whole slide sections of a large spectrum of ovarian steroid cell neoplasms and non-neoplastic proliferations, luteinized AGCT, and luteinized proliferations. Reticulin staining of the individual steroid cells or AGCT tumor cells were evaluated for uniformly intact peri-cellular staining and, if absent, further classified as complete absence of peri-cellular staining or heterogenous areas of absent versus intact peri-cellular staining. FOXL2 was interpreted as positive if any nuclear staining of the steroid cells or AGCT tumor cells was present.

Results: Absence of uniform peri-cellular reticulin staining was observed in 8/8 steroid cell tumors NOS, 1/1 Leydig cell tumor, 1/1 nodular stromal hyperthecosis, 6/6 pregnancy luteoma, 11/11 luteinized AGCT and 8/8 corpus luteum. FOXL2 staining was negative in all of the steroid cell neoplasms and non-neoplastic proliferations with patchy weak staining in 5/5 pregnancy luteomas and positive in all luteinized AGCT and corpus luteums.

Figure 1 - 696

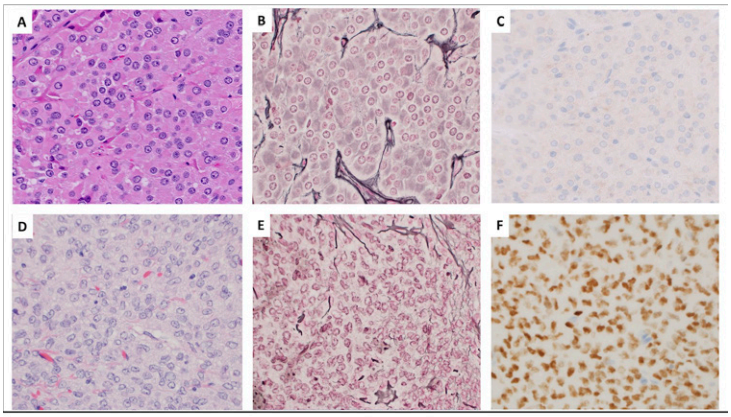

Figure
Steroid cell tumor. H&E (A); reticulin (B); FOXL2 (C).
Luteinized granulosa cell tumor. H&E (D); reticulin (E); FOXL2 (F)

Conclusions: Reticulin staining patterns do not distinguish ovarian steroid cell neoplasms or non-neoplastic proliferations from luteinized AGCT as uniform peri-cellular staining is absent in all lesions. This may potentially result in misclassification of steroid cell lesions as luteinized GCT. FOXL2 immunostaining resolves this differential diagnosis. This study provides further rationale for pathology practices to convert to using FOXL2 immunostaining as the primary first-line marker for ovarian sex cord-stromal pathology instead of calretinin and inhibin.

697 Preferentially Expressed Antigen in Melanoma (PRAME) Expression is More Common in HPV-Independent Vulvar Squamous Neoplasia than in HPV-Associated Vulvar Squamous Neoplasia

Sarah Gradecki[1], Landon Hobbs[2], William Kane[1], Anne Mills[1], Shyam Raghavan[2], Taylor Jenkins[3]
[1]University of Virginia, Charlottesville, VA, [2]University of Virginia School of Medicine, Charlottesville, VA, [3]University of Virginia Health System, Charlottesville, VA

Disclosures: Sarah Gradecki: None; Landon Hobbs: None; William Kane: None; Anne Mills: None; Shyam Raghavan: None; Taylor Jenkins: None

Background: Preferentially expressed antigen in melanoma (PRAME) immunohistochemistry (IHC) was initially put to diagnostic use in melanoma, but is now being evaluated in many different malignancies. Because the PRAME protein acts a dominant repressor of retinoic acid signaling, topical retinoid therapies could potentially be used to treat PRAME$^+$ lesions with minimal side effects. Vulvar squamous intraepithelial neoplasia (VIN) is an ideal target for PRAME evaluation as VIN is often multifocal or extensive, and current treatment involves surgical excision, which can be disfiguring and negatively impacts quality of life. The current project aims to evaluate PRAME expression in HPV-associated and HPV-independent squamous lesions of the vulva; namely, high-grade squamous intraepithelial lesions (HSIL), HSIL-associated vulvar squamous cell carcinoma (VSCC), differentiated vulvar intraepithelial neoplasia (dVIN), and dVIN-associated VSCC.

Design: Full tissue sections of 109 cases of squamous vulvar neoplasia (31 HSIL, 29 HSIL-associated VSCC, 22 dVIN, and 27 dVIN-associated VSCC) were stained with PRAME antibody (Abcam, Cat #Ab219650). Expression was scored by the percent of tumor cells showing positive staining. Strength of expression (0, 1+, 2+, 3+) and cellular location of staining (nuclear, nucleolar, cytoplasmic) was documented. Groups were compared using Wilcoxon rank-sum or Kruskal-Wallis tests.

Results: HPV-independent lesions (dVIN and dVIN-associated VSCC) were more likely to show tumoral PRAME expression (p = 0.003). Subgroup analysis demonstrated that the highest rates of PRAME expression were in dVIN-associated VSCC, while HSIL had the lowest rates of PRAME expression ($p < 0.001$) (Figure 1). The PRAME$^+$ lesions demonstrated a nuclear or nucleolar staining pattern and there was no significant difference in strength of expression between any groups.

Figure 1 - 697

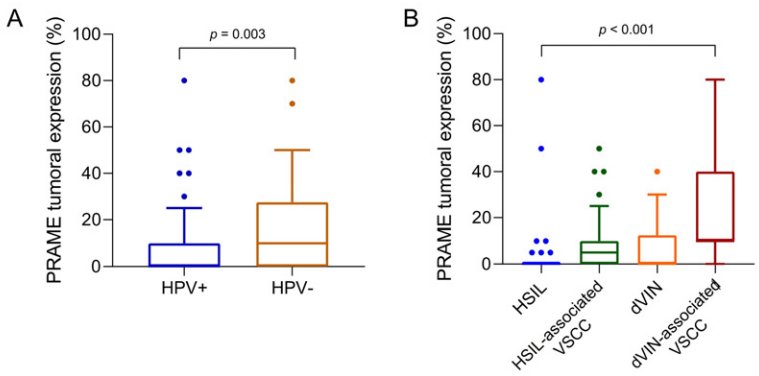

Figure 1: HPV-independent lesions (dVIN and dVIN-associated VSCC) were significantly more likely to show tumoral PRAME expression than HPV-associated lesions (HSIL and HSIL-associated VSCC) (A). Invasive carcinoma associated with dVIN showed the highest levels of PRAME expression, while HSIL showed the lowest (B).

Figure 2 - 697

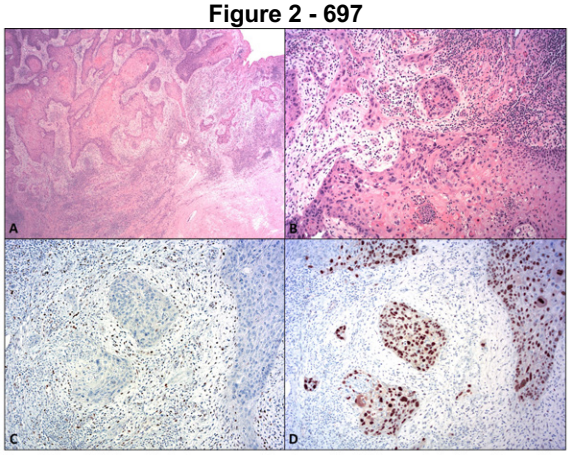

Figure 2: A case of dVIN-associated vulvar squamous cell carcinoma with null p53 expression that showed strong, diffuse (80%) nuclear expression of PRAME (A: H&E, 20x, B: H&E, 100x, C: p53, 100x, D: PRAME, 100x).

Conclusions: The higher rates of PRAME expression in HPV-independent vulvar lesions suggests the different biological drivers of HPV-independent and HPV-associated vulvar neoplasia result in differential PRAME expression. The highest rates of expression were seen in dVIN-associated VSCC (Figure 2), indicating a possible correlation between aggressive tumor behavior and PRAME expression. These findings also suggest that HPV-independent lesions may be more likely to respond to PRAME-targeted therapy, which offers the possibility of new treatment options for tumors that often have poor clinical outcomes.

698 PD-L1 and MHC Class I Expression in Ovarian Cancers Treated with Checkpoint Inhibitor Therapy

Laurie Griesinger[1], Akua Nyarko-Odoom[2], Santos Acosta Martinez[2], Nancy Shen[2], Kari Ring[2], Elizabeth Gaughan[1], Anne Mills[2]

[1]University of Virginia Health System, Charlottesville, VA, [2]University of Virginia, Charlottesville, VA

Disclosures: Laurie Griesinger: None; Akua Nyarko-Odoom: None; Santos Acosta Martinez: None; Nancy Shen: None; Kari Ring: None; Elizabeth Gaughan: None; Anne Mills: None

Background: There is evidence that biomarkers such as PD-L1 and MHC class I help identify candidates for anti-PD-1/PD-L1 checkpoint inhibition, but this has not been studied in ovarian malignancies.

Design: PD-L1 and MHC Class I immunostaining was performed on pre-treatment whole tissue sections from ovarian carcinoma patients who received anti-PD-1/PD-L1 immunotherapy either alone or in conjunction with conventional chemotherapy, histone deacetylase inhibitors, or angiogenesis inhibitors. The PD-L1 Combined Positive Score (CPS) was calculated, and a score of ≥ 1 considered positive. MHC class I status was categorized as intact or subclonal loss. Drug response was assessed using RECIST criteria, and both best response and final response status at the time of last follow-up were recorded.

Results: The tumors consisted of high-grade serous (23), clear cell (2), small cell hypercalcemic-type (1), endometrioid (1), and undifferentiated carcinomas (1) and carcinosarcomas (2). PD-L1 was positive in 26 of 30 cases (87%), with CPS ranging from 1-100. No patients with therapeutic response data available (n=18) attained complete response. 6 achieved partial response (PR; 33%), 3 had stable disease (SD; 17%), and 9 demonstrated progressive disease (PD; 50%) as best response. By final follow-up, 12 of 18 patients had progressed (67%). All 6 patients without progression had PD-L1+ tumors, however, 10 of 12 progressive tumors were also PD-L1+. Although overall PD-L1 status was not significantly tied to progression, on average the PD-L1 CPS was higher among patients with PR or SD vs. PD (CPS 15 versus CPS 5). 7 of 30 (23%) patients showed subclonal loss of MHC class I, only 3 of whom had response data; all 3 had a best response of PD, with no PR or SD. 9 of 15 patients with intact MHC class I and response data had a best response of SD or PR.

Conclusions: A subset of ovarian carcinoma patients benefit from anti-PD-1/PD-L1 checkpoint inhibition either alone or in conjunction with other approaches. While a PD-L1 CPS ≥1 captured all responders, it also identified many cases that failed to benefit. Notably, there was a trend towards higher CPS absolute values among responders. Additionally, response rates were higher in patients with intact MHC class I. Larger studies are required to determine whether quantitative PD-L1 scores and MHC

class I status show statistically significant value as biomarkers for response to anti-PD-1/PD-L1 checkpoint inhibition in ovarian carcinomas.

699 Clinical Characteristics of HPV-Independent Vulvar Intraepithelial Neoplasia (VIN) with Morphologic Features Resembling HPV-Associated Lesions

Geoffrey Halling[1], Stephanie Skala[1]
[1]*University of Michigan, Ann Arbor, MI*

Disclosures: Geoffrey Halling: None; Stephanie Skala: None

Background: Vulvar squamous cell carcinoma (SCC) may arise by HPV-associated or HPV-independent pathways; the respective precursor lesions are high-grade squamous intraepithelial lesion (HSIL/uVIN) and HPV-independent vulvar intraepithelial neoplasia (including differentiated vulvar intraepithelial neoplasia [dVIN]). Although classic morphologic features can be helpful in distinguishing these precursors, HPV-independent VIN with morphologic features mimicking HSIL have been reported. Here, we aim to describe the clinical context of these lesions, as this information may be diagnostically or prognostically useful.

Design: The surgical pathology archives of a large academic institution were queried for patients with dVIN; 37 patients had 3+ specimens available for review. Material from each patient was reviewed for lesions that morphologically resembled or were originally diagnosed as HSIL. The electronic medical records were reviewed for age at diagnosis, history of lichen sclerosus (LS), history of invasive carcinoma, time from VIN diagnosis to invasion, history of HPV infection, and HPV-associated lesions at other sites.

Results: Review of multiple cases from each patient revealed 10 cases of VIN resembling HSIL (confirmed by p16 and/or p53 immunohistochemistry +/- high-risk HPV in situ hybridization). The age at time of first VIN diagnosis in our system ranged from 55-86 years (mean 73.7). 8 patients (80%) had history of LS. 9 (90%) had prior or subsequent invasive carcinoma; the remaining patient had a specimen with a focus suspicious for invasion. 6 patients had invasive carcinoma prior to VIN at our institution, 1 had a reported history of vulvar cancer prior to VIN, 1 had invasive carcinoma develop 25 months following VIN. None had history of HPV infection (5 negative testing, 5 no testing). No patients had HPV-associated lesions at other sites.

Patient	Age at VIN diagnosis	History of LS	Invasive SCC	Time from VIN to Invasion	High-risk HPV Result	HPV-associated lesions at other sites
1	58	Yes	Yes	Reported outside history of invasive SCC prior to VIN	Negative	No
2	72	Yes	Yes	Invasive SCC prior to VIN	Not tested	No
3	68	No	Yes	Invasive SCC prior to VIN	Negative	No
4	71	Yes	Yes	Invasive SCC prior to VIN	Not tested	No
5	86	No	Suspicious focus in one case	N/A	Negative	No
6	86	Yes	Yes	Invasive SCC prior to VIN	Not tested	No
7	80	Yes	Yes	Invasive SCC prior to VIN	Negative	No
8	81	Yes	Yes	Invasive SCC prior to VIN	Not tested	No
9	80	Yes	Yes	Invasive SCC prior to VIN	Not tested	No
10	55	Yes	Yes	25 months	Negative	No

Figure 1 - 699

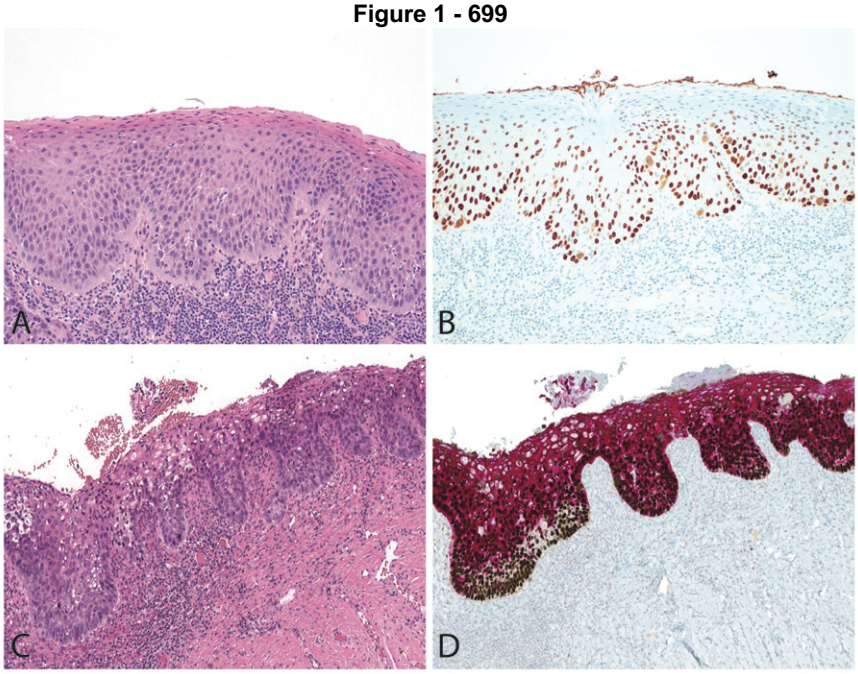

Figure 1. HPV-independent vulvar intraepithelial neoplasia (VIN) with high-grade atypia mimicking HPV-associated VIN (HSIL) (A, H&E), aberrant p53 expression on IHC confirming HPV-independent VIN (B). High grade nuclear atypia mimicking HSIL (C, H&E), aberrant p53 and full thickness CK17 expression on IHC confirming dVIN (D).

Conclusions: HPV-independent VIN with morphologic features of HPV-associated lesions are in keeping with those of dVIN, including older age (mean 73.7 years), association with LS (80%) and invasive carcinoma (90%), and absence of HPV infection or HPV-associated lesions at other sites. These findings highlight the importance of clinical features when classifying VIN and illustrate the value of maintaining a low threshold for ordering p16 and p53 immunostains regardless of morphologic features.

700 Histologic Features of Ovarian Background Tissue in Primary Mucinous Ovarian Tumors Versus that of Metastasis

Nadia Hameed[1], Preetha Ramalingam[1], Mario Marques-Piubelli[1], Elizabeth Euscher[1], Anais Malpica[1]
[1]The University of Texas MD Anderson Cancer Center, Houston, TX

Disclosures: Nadia Hameed: None; Preetha Ramalingam: None; Mario Marques-Piubelli: None; Elizabeth Euscher: None; Anais Malpica: None

Background: Recently, it has been proposed that the absence of background hypercellular ovarian cortex and the paucity of primordial follicles (PF) in ovarian mucinous borderline tumors (MBT) and mucinous carcinomas (MCa) can be used in the distinction from metastatic carcinomas (MET). The aim of our study is to evaluate the practical validity of this theory.

Design: 145 cases of primary ovarian mucinous neoplasms (POvMNs): n=70 and MET: n=75 were retrieved from our files (1986-present). The following parameters were recorded: patient (pt) age, laterality, primary site of tumor in MET, histotype, patterns of invasion (expansible vs. infiltrative), thickness of cellular cortex (CCx) categorized as absent, <0.3 mm and ≥ 0.3 mm, presence and number (№) of oocytes/5mm (4x objective) and cystic follicles (CF), and appearance of the albugenia. Pathology reports and all H&E slides were reviewed (1-79 slides per case). The Mann-Whitney, chi-square and Fisher's exact tests were performed.

Results: Table 1. summarizes selected results. Histotypes were: MCa (n=52), Anaplastic Ca (n=1), MBT (n=10), MBTMI (n=1), MBT/MI/IEC (n=3), MBT/IEC/anaplastic Ca (n=1), MBT/anaplastic Ca (n=1), and MBT (n=1). FIGO stage: I (n=62), IIA (n=2), IIIA (n=5). MET were as follows: 46 colorectal Ca, 15 endocervical Ca, 8 appendiceal MCa, 2 pancreatic Ca, 2 breast Ca, and one each of urachal Ca and uterine serous Ca. CCx thickness of ≥ 0.3 mm (*p.<0001*) and infiltrative pattern correlated with MET (*p.0016*). Oocytes were identified in 36/75 (48%) cases of POvMNs (range 1-17) and in 27/75 (36%) cases of MET (range 1-30). Thickened albuginea was significantly associated with POvMNs (p.*<0001*). Presence or absence of CFs was not significant

(*p*.4256). Other parameters that were significantly associated with POvMNs were young age (p<0.01), unilaterality (*p.<0001)* and expansile pattern of invasion (*p.<0001*).

Parameters	Primary ovarian neoplasms (n=70)	Metastatic ovarian carcinoma (n=75)	***p*-value**
Age (range; median in years)	15-86; 35	24-81; 48	**<0.001**
Laterality	Bilateral (n=2) Unilateral (n=67) Unknown (n=1)	Bilateral (n=45) Unilateral (n=30)	**<0.001**
Expansile pattern	Yes (n=43) No (n=10) N/A (n=17)*	Yes (n=30) No (n=45)	**<0.001**
Infiltrative pattern	Yes (n=24) No (n=30) N/A (n=16)*	Yes (n=52) No (n=23)	**0.0016**
Albuginea	Thickened (n=70) Normal (n=0)	Thickened (n=48) Normal (n=27)	**<0.001**
Cellular cortex	**Present** (n=35) < 0.3 mm (n=19) ≥ 0.3 mm (n=16) **Absent** (n=35)	**Present** (n=59) < 0.3 mm (n=9) ≥ 0.3 mm (n=50) **Absent** (n=16)	**<0.001**
Cystic follicles	Present (n=13) Absent (n=57)	Present (n=18) Absent (n=57)	0.4256

*Mucinous borderline tumors

Conclusions: This study supports the theory that absence of hypercellular CCx correlates with POvMNs. However, quantification of oocytes/PF was not reliable due to patient age, lack of CCx when tumor replaces the entire ovary, and prior therapy. The higher № of oocytes in POvMNs is likely biased by the young age of these patients. For clinical practical use it is critical to sample the Ov cortex and uninvolved Ov, if present. The above findings can be used in conjunction with other well-established parameters in distinguishing POvMNs from METs in challenging cases.

701 Reporting Lymph Node Metastasis Size and Extracapsular Extension for Ovarian, Fallopian Tube and Peritoneal Carcinoma Is Not Clinically Relevant

Nadia Hameed[1], Elizabeth Euscher[1], Preetha Ramalingam[1], Mario Marques-Piubelli[1], Barrett Lawson[1], Anais Malpica[1]
[1]The University of Texas MD Anderson Cancer Center, Houston, TX

Disclosures: Nadia Hameed: None; Elizabeth Euscher: None; Preetha Ramalingam: None; Mario Marques-Piubelli: None; Barrett Lawson: None; Anais Malpica: None

Background: The 2013 FIGO Staging for ovarian (Ov), fallopian tube (FT) and peritoneal carcinoma (Per Ca) requires categorizing pN1 into N1a (≤10 mm) and N1b (>10 mm). Recording this non-evidence-based parameter adds extra time to pathology examination in order to meet the specifications of the current synoptic reporting. This study evaluates the impact of lymph node metastasis size (LN MS) and extracapsular extension (ECE), among other factors, on progression-free survival (PFS) and overall survival (OS) for these cases.

Design: 124 cases of Ov/FT/Per Ca with LN and omental (Om) resection were retrieved from our files (2006 to 2011). Recorded parameters were: patient's (pt's) age, clinical presentation, primary tumor site, histotype, FIGO stage, site and total number (Nº) of LNs, (Nº) of (+) LNs along with MS [isolated tumor cells (ITC) and ≤ 10mm or >10 mm], presence of ECE, Om status [negative (-) or (+)], therapy (Tx), and follow-up (f/u). All pathology reports and H&E slides were reviewed (1-46 per case). Univariate analysis (UVA) and multivariate (Cox regression) analysis (MVA) were performed using SPSS (Statistics for Windows, Version 24.0. Armonk, NY: IBM Corp.).

Results: Results are summarized in Table 1. Histotypes included: 72 high-grade serous, 32 mixed, 11 endometrioid, 4 clear cell, and 4 mucinous Cas, and 1 carcinosarcoma. At last f/u (median 64 months) pts were: no evidence of disease (n=48), died of disease (n=57), alive with disease (n=5), died of other causes (n=8), and unknown (n=6). Nº of (+) LNs was the only parameter significantly associated with OS and PFS by both UVA (*p.008*, and *p.001)*, and MVA (*p.048, p.010*). Histotype, and FIGO stage were significant only by UVA. Om (+) pts had worse OS and PFS compared with Om (-) by UVA. ECE, ITC, LN MS size, and site of LN did not correlate with OS or PFS.

Characteristics	Univariate analysis			Multivariate analysis	
	OS	PFS		OS	PFS
	p value	p value		p value	p value
Age (33 to 80 yrs, median 56)	0.215	0.054			
Primary site	0.392	0.151			
Ovary (n=91)					
FT (n=9)					
Peritoneum (n=6)					
Tubo-ovarian (n=18)					
Histology	<0.001	<0.001		0.240	0.483
High-grade serous (n=72)					
Non-serous (n=52)					
FIGO stage	<0.001	<0.001		0.349	0.143
I (n=25)					
II (n=12)					
III (n=56)					
IV (n=31)					
Treatment (n=123)	<0.001	0.002		0.598	0.117
Adjuvant (n=81)					
Neoadjuvant (n=21)					
Both (n=14)					
Neoadjuvant and radiation (n=1)					
Radiation (n=1)					
None (n=5)					
LN status	<0.001	<0.001			
LN (+) (n=63)					
LN (-) (n=61)					
Total number of (+) LN	0.008	0.001		0.048*	0.010**
LN met category***	0.913				
ITC	0.167	0.108			
Met ≤ 10 mm	0.073	0.256			
Met > 10 mm	0.462	0.291			
ECE (n=22)	0.502	0.305			
Omentum status					
(+) vs (-) (n=59, n=65)	<0.001	<0.001		0.693	0.309
*HR: 1.13					
** HR: 1.1					
*** Largest LN MS was utilized					

Conclusions: This study confirms that high grade serous histotype, FIGO stage, and Om involvement correlate with OS and PFS by UVA. In contrast to the reported significance of ECE in endometrial Ca, this parameter was not found to have an impact on either OS or PFS in our cases of Ov/FT/Per Ca. MVA showed that the only significant prognostic parameter was Nº of (+) LNs. LN MS did not correlate with either OS or PFS, indicating its lack of clinical relevance. Therefore, while inclusion of LN status in the synoptic report for Ov/FT/Per Ca is needed, reporting ECE and granular measurement of LN MS should not be required.

702 A Subset of SMARCB1 (INI-1) Deficient Vulvar Neoplasms are Positive for Germ Cell Markers

Phoebe Hammer[1], W. Glenn McCluggage[2], David Kolin[3], Brooke Howitt[1]
[1]Stanford Medicine/Stanford University, Stanford, CA, [2]The Royal Hospitals/Queen's University of Belfast, Birmingham, United Kingdom, [3]Brigham and Women's Hospital, Boston, MA

Disclosures: Phoebe Hammer: None; W. Glenn McCluggage: None; David Kolin: None; Brooke Howitt: None

Background: SMARCB1 (INI-1) deficient vulvar neoplasms are a rare group of aggressive tumors that include proximal-type epithelioid sarcoma, myoepithelial carcinoma and sarcomas which are difficult to classify. A recent report has suggested that so-called vulvar yolk sac tumors may represent morphologic variants of SMARCB1-deficient tumors rather than true germ cell neoplasia. The immunoreactivity of germ cell markers in typical appearing SMARCB1-deficient vulvar neoplasms has not been established.

Design: Ten SMARCB1 (INI-1) deficient vulvar neoplasms were retrospectively identified in the pathology databases of three institutions. All available H&E and immunohistochemical slides were reviewed and additional germ cell tumor markers (SALL4, glypican-3, OCT3/4, and AFP) were performed when material was available. These tumors were compared to three SMARCB1-deficient vulvar neoplasms with pure yolk sac tumor morphology recently reported in the literature.

Results: The clinical and immunohistochemical features are summarized in Table 1. The 10 vulvar tumors occurred in adult women (median age 41 years, range 20 to 69 years) and measured 2.0 to 18.0 cm (median 4.6 cm). Seven tumors were classified as epithelioid sarcoma, and three were diagnosed as myoepithelial carcinoma or favor myoepithelial carcinoma. Nine cases showed complete loss of INI-1 by immunohistochemistry, while one showed focal retention of INI-1 with complete loss of SMARCA4. Three of nine stained cases (33%) were focally positive for SALL4 and all tested cases were negative for glypican-3 (n = 9). Of the three SALL4 positive cases, one also showed focal staining for OCT3/4 (Figure), but all tested cases were negative for AFP (n=7). The three SMARCB1-deficient vulvar tumors with pure yolk sac tumor morphology exhibited diffuse SALL4 and glypican-3 expression in all cases while AFP was focally positive in 2 of 3 cases.

Table 1. Summary of the clinical and immunohistochemical features of 10 SMARCB1 (INI-1) deficient vulvar neoplasms.

Case	Diagnosis	Age	Size (cm)	SMARCB1/ INI1	SMARCA4/ BRG1	SALL4	Glipican-3	OCT 3/4
1	Epithelioid sarcoma	31	3.0	Lost	Retained	Negative	Negative	Negative
2	Epithelioid sarcoma	56	2.7	Lost	Retained	Focally positive	Negative	Focally positive
3	Epithelioid sarcoma	46	18.0	Lost	Retained	Negative	Negative	Negative
4	Epithelioid sarcoma	69	12.5	Lost	NP	Negative	Negative	Negative
5	Myoepithelial Carcinoma	28	N/A	Lost	NP	Negative	Negative	Negative
6	Myoepithelial Carcinoma	31	1.8	Lost	NP	Negative	Negative	Negative
7	Favor Myoepithelial Carcinoma	69	5.8	Lost	NP	Negative	Negative	Negative
8	Epithelioid sarcoma	36	2.0	Lost	NP	NP	NP	NP
9	Epithelioid sarcoma	58	6.5	Focal retention	Lost	Focally positive	Negative	Pending
10	Epithelioid sarcoma	20	4.5	Lost	Retained	Focally positive	Negative	Pending

Figure 1 - 702

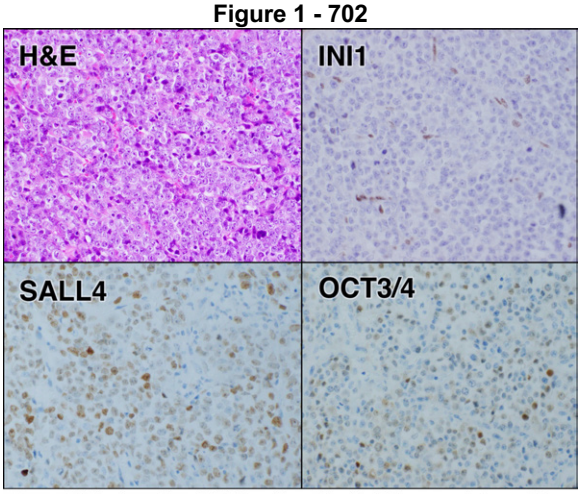

Figure. Histologic sections (400X) from Case 2 (epithelioid sarcoma) show a diffuse proliferation of malignant epithelioid cells with large nuclei and prominent nucleoli. By immunohistochemistry, the tumor shows complete loss of INI1 and is focally positive for SALL4 and OCT3/4.

Conclusions: SALL4 and OCT3/4 are positive in a subset of SMARCB1 deficient vulvar neoplasms and may pose a diagnostic pitfall resulting in consideration of the possibility of a germ cell tumor. In the absence of yolk sac tumor-like morphology, no yolk sac tumor markers (glypican-3/AFP) appear to be expressed in SMARCB1 deficient vulvar neoplasms with typical morphology of epithelioid sarcoma or myoepithelial carcinoma.

703 HER2/neu Status Assessment in Endometrial Serous Carcinoma: Comparison of a Proposed Testing and Interpretation Algorithm to 2018 ASCO/CAP Guidelines for Breast Cancer, Using an Institutional Cohort of Cases Dually Tested by Immunohistochemistry and Fluorescence In situ Hybridization

Sherin Hashem[1], Somaye Zare[1], Oluwole Fadare[2]
[1]University of California, San Diego, La Jolla, CA, [2]UC San Diego School of Medicine, La Jolla, CA

Disclosures: Sherin Hashem: None; Somaye Zare: None; Oluwole Fadare: None

Background: Human epidermal growth factor receptor 2 (HER2) status is now routinely assessed in endometrial serous carcinoma (ESC) due to its reported predictive value. Recently, an algorithm for assessing HER2 status has been proposed, inclusive of interpretation guidelines for HER2 immunohistochemistry (IHC) and fluorescence In situ Hybridization (FISH) (PMID: 33536574). In this study, we assessed the performance of this proposed HER2 testing algorithm by comparing it with the established system for breast cancers (2018 ASCO/CAP guidelines) using a cohort of cases that were dually tested (by IHC and FISH).

Design: 27 consecutive cases of ESC that had been assessed for HER2 status by both IHC and FISH, as is routine practice at our institution, formed our study cohort. Slides were reviewed, and IHC scores were assigned according to the proposed criteria (PMID: 33536574; Fig 1) as well as by 2018 ASCO/CAP criteria for breast cancers. FISH interpretations were assigned per applicable criteria for each system.

Results: By proposed criteria, 3.7% (n=1), 22.2% (n=6), 51.9% (n=14) and 22.2% (n=6) had IHC scores of 0, 1+, 2+ and 3+ respectively, whereas comparable proportions using breast criteria were 11.1% (n=3), 22.2% (n=6), 37% (n=10) and 29.6% (n=8) respectively (kappa 0.47, 1.0, 0.7, 0.8, respectively; table 1). The proposed criteria resulted in a slightly higher proportion (x 1.4-fold) of 2+ (equivocal) cases. The HER2 amplification rates amongst the cases classified as 2+ (equivocal) by IHC in the proposed and breast systems were 33.3% and 11.1% respectively ($p>0.05$). In both systems, there were no cases that were assigned a 3+ IHC score and were found to be non-amplified by FISH. Additionally, there were no IHC score 0 or 1+ cases that were found to be amplified using either system. Overall, the same 9 (33%) of 27 cases were classified as HER2-abnormal (3+ IHC and/or FISH amplified) using both systems. Intra-tumoral heterogeneity of HER2 protein expression was present in 13 (48%) of the 27 cases, 30.8% of which showed HER2 amplification by FISH.

Table 1: HER2/neu status determination by IHC and FISH in endometrial serous carcinoma: a comparison of proposed criteria and 2018 ASCO/CAP breast cancer criteria.

	Proposed criteria (n=27)			**2018 ASCO/CAP breast criteria (n=27)**		
Score	# of cases (%)	FISH positive	FISH negative	# of cases (%)	FISH positive	FISH negative
0	1 (3.7%)	0	1	3 (11.1%)	0	3
1+	6 (22.2%)	0	6	6 (22.2%)	0	6
2+	14 (51.8%)	3	11	10 (37%)	1	9
3+	6 (22.2%)	6	0	8 (29.6%)	8	0

Figure 1 - 703

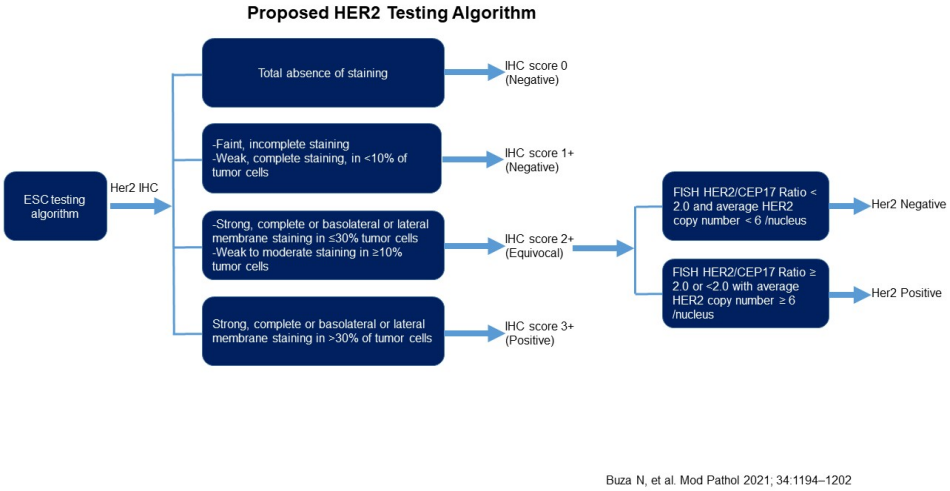

Buza N, et al. Mod Pathol 2021; 34:1194–1202

Conclusions: The proposed and breast systems each captured identical proportions of HER2 abnormal cases (33%). Both systems displayed a 100% concordance between IHC and FISH for IHC scores 0, 1+ and 3+ cases, which supports performing FISH only on IHC 2+ cases. The interpretation issues specifically associated with ESC, including heterogeneous and frequent basolateral/lateral staining, make the proposed system more suited for this histotype.

704 Circulating Tumor TP53 is Associated with Necrosis in Both Leiomyoma and Leiomyosarcoma and is a Potential Biomarker for Pre-operative Identification of Uterine Leiomyosarcoma

Saleh Heneidi[1], Jean Lopategui[2], Bonnie Balzer[1], Yizhou Wang[1], Chintda Santiskulvong[1], Carissa Huynh[1], Farin Amersi[1], Allan Silberman[3]

[1]Cedars-Sinai Medical Center, Los Angeles, CA, [2]Cedars-Sinai Medical Center, West Hollywood, CA, [3]Cedars-Sinai, Los Angeles, CA

Disclosures: Saleh Heneidi: None; Jean Lopategui: None; Bonnie Balzer: *Consultant*, Core Diagnostics, Castle Biosciences, PathologyWatch; Yizhou Wang: None; Chintda Santiskulvong: None; Carissa Huynh: None; Farin Amersi: None; Allan Silberman: None

Background: Uterine leiomyosarcoma (LMS) is highly aggressive, with a dismal prognosis and nearly always unsuspected prior to resection for presumed leiomyoma (LM). Occult LMS is reported in 0.2% (1 in 500) of women undergoing surgery for fibroids. The major problem is that there is no reliable preoperative method to distinguish LMS from a LM or STUMP (smooth muscle tumor of uncertain malignant potential), and patient prognosis for LMS is even poorer if the tumor is transected, which occurs in procedures performed for LM. Thus, there is considerable need for a reliable preoperative test to assess the proper surgical procedure for LMS. *TP53* alterations are reportedly associated with uterine LMS in 60% of cases.

Design: We screened plasma for *TP53* variants in patients with pathologically confirmed LMS. We evaluated *TP53* circulating tumor DNA (ctDNA) by next-generation sequencing (NGS) in a cohort of 11 LMS, 1 STUMP, 11 LM, and 2 atypical LM, reviewing clinical data to assess disease burden, ranging from no evidence to extensive metastatic disease. DNA extraction used QIAamp Kits. NGS libraries targeting the entire exonic region of *TP53* were prepared using a QIASeq Targeted DNA Custom Panel, sequenced on MiSeq with 150bp paired end sequencing and a read depth of 2x0.5M (plasma) and 2x1M (formalin-fixed paraffin embedded tissue).

Results: Pathogenic *TP53* variants were seen in 7/10 LMS tissue and 5/6 LMS plasma samples. Atypical LM and STUMP had wild-type (WT) *TP53*. In the 8 plasma samples with TP53 mutated LMS, patients had extensive metastatic disease, and 3/4 WT TP53 LMS patients had no evidence of disease, with the discordant WT LMS being a TP53 deep deletion that is not detected by this assay. Of note, necrosis was closely associated with detectable pathogenic *TP53* variants, with all cases occurring in the

setting of necrosis (11/11), and no case without necrosis having pathogenic TP53. Interestingly, only 2/12 LM had necrosis, and both were found to harbor pathogenic *TP53* variants.

Patient	Age/ Ethnicity	Tumor/Size/Necrosis/Features	Tissue *TP53* mutation/VAF	Plasma *TP53* mutation/VAF	Clinical Status
1	49 White (W)	LMS, 12 cm, mitosis (15/10hpf), necrosis, **only focal atypia**	Wild-type (WT)	NA	NED, 7 years
2	46 W	HGLMS, 14 cm aggr, necrosis,	p.R248Q, 4%	p.R248Q , 2.4%	Deceased, 48 mo
3	60 W	HG LMS, 24 cm, 90% necrosis/cystic degeneration	WT	p.E258V, 2%	MD
4	69 Asian (A)	LMS, 15 cm, necrosis	p.E221*, 16%	p.E221*, 86% p.V173M, 20%	Deceased,6 mo
5	63 W	HGLMS, 8 cm, necrosis	p.R337C, 22%	p.R337C, 31%	Massive MD, 20y
6	60 W	HGLMS, 17 cm, necrosis	p.R174_R175delinsWC 77%	p.R174_R175delinsWC 0.8%	Deceased, 24 mo
7	33 A	Atypical LM, 11cm (POST THERAPY) /(Hx of HGLMS, myomectomy)	WT	WT	NED
8	49 W	Atypical cellular LM, 13 cm, <5 mitosis, (STUMP), focal necrosis	WT	WT	NED
9	83 W	Atypical LM, 15 cm, mitosis 5-10/10hpf	WT	N/A	NED
10	41, other	LM, 16.8 cm Infarcted	p.V31I, 50% polymorphism	p.V31I, 47% polymorphism	
11	35 A	LM, 15 cm	WT	WT	
12	37 Black (B)	LM, 17 cm aggr	WT	WT	
13	48W	LM, 7 cm	WT	NA	
14	38W	LM, 3-9 cm, 11 cm aggr **Hyalinizing necrosis**	**p.Y234C, 20% (pathogenic)**	NA	
15	47	LM, 8cm	WT	NA	
16	44 A	LM, 5.5 cm aggr	WT	NA	
17	57 B	Undiff LMS, necrosis	c.559+1G>T splice, 19% p.I162S, 57%	NA	Deceased, 7 mo
18	35 B	LM, 9.7 cm	WT	NA	
19	58 W	LMS, 8cm, Mit>10/10hpf, necrosis	p.Y234C, 70%	NA	Hospice, 3years
20A	62 W	HG LMS, Mit>10/10hpf, necrosis	p.Y234C, 91%	NA	Hospice, 3years
20B	63 W	HG LMS, 20cm, necrosis	WT, 99% **(CNV not detected)**	NA	NED
21	52 W	HG LMS, 15 cm, no necrosis noted	NA	WT (no TP53 241 detected)	Deceased, 17 mo
22	41 B	LM (morcellated), 11cm **focal infarct-type necrosis**	**p.Y236D, 2.4% (pathogenic)**	NA	NED
23	62 W	LM 1.4 cm	WT	NA	NED
24	45 W	LM, 11cm, ischemic/degen changes	WT	NA	NED
25	33 W	LM, 5.7cm	WT	NA	NED

Conclusions: This study is the first to identify pathogenic *TP53* ctDNA in patients with necrotic LM and LMS, illustrating a potential mechanism of necrosis/inflammation driving the generation of pathogenic mutations and possibly offering the earliest predictive marker for *TP53* inactivation. Further study is needed to determine the preoperative utility of NGS ctDNA *TP53* mutational status as a useful molecular biomarker to help guide surgery and avoid unwarranted manipulation and pelvic contamination of undetected LMS.

705 Molecular Therapeutic Target Profiles of High-Grade Ovarian Carcinomas: An Institutional Experience

Sachie Ikegami[1], Paul Lee[2]
[1]*University of Cincinnati Medical Center, Cincinnati, OH,* [2]*University of Cincinnati, Cincinnati, OH*

Disclosures: Sachie Ikegami: None; Paul Lee: None

Background: High-grade ovarian carcinomas (HGOC) are characterized by the presence of mutations in different pathways including RB, PI3K/RAS and homologous recombination. The importance in identifying HGOC molecular subtypes is increasingly crucial to targeting treatment strategies such as Poly-ADP Ribose Polymerase (PARP) inhibitors or immunotherapy. The aim of this study is to report the genetic/proteomic profile of HGOC in a single institution cohort.

Design: Clinical files were searched for all tubo-ovarian HGOC that were sequenced between January 2017 and August 2021, which yielded 32 total cases. We restricted this set to "non-endometrioid type" ovarian carcinomas, which included high-grade serous carcinoma (90.6%), carcinosarcomas (6.3%), and clear cell carcinoma (3.1%). The specimen site was agnostic which ranged from adnexa to metastatic sites. Demographic information, pathologic diagnosis, mismatch protein expression, microsatellite instability status, tumor mutational burden (TMB), panel next generation sequencing variant data, and protein expression (PDL-1, ER, and PR) are reported in this study.

Results: The median age of the cohort was 64 (range 49-83) years. *TP53* mutations were the most commonly identified in 81.3% cases. Homologous recombination deficiency (HRD) was found in 21.9% cases including 2 *BRCA1* and *FANCM* mutations each, and 1 *RAD50* mutations in addition to a *BRCA2* and *ATM* mutation variant with unknown significance. Other commonly altered pathway was PI3K/RAS (34.3%) consisted of 4 *NF1* mutations (12.5%) and 3 *PIK3CA* mutations (9.4%), 1 *KRAS* mutation (3.1%) and 4 *AKT* amplification (12.5%). The RB pathway alteration was found in 9.4% cases. Most cases had low TMB (average 5 ± 2.1 Mutations/Mb). PDL-1 IHC revealed positive in 11 cases (34.3%) including 3 co-existences with HRD. Proficient mismatch protein expressions were concordant with microsatellite stable sequencing results in all cases. ER and PR expressions were observed in 50% and 28.1%, respectively.

Figure 1 - 705

Table 1. Homologous Recombination Deficient Case List

	Age	Diagnosis	HR gene mutation	TMB (Mutations/Mb)	*TP53* mutation	PD-L1 (CPS)	ER	PR	MSI
1	56	HGSC	*BRCA1* Exon 10|D1162fs	Low (6)	Exon 6|S215R	Negative (0)	(+)	(+)	Stable
2	60	HGSC	*BRCA1* Exon 13|p.E1470*	Intermediate (9)	Exon 5|p.Q165fs	Positive (1)	(-)	(-)	Stable
3	56	HGSC	*FANCM* Exon 10|p.E288X	Low (4)	Exon 8|p.E285K	Negative (0)	(-)	(-)	Stable
4	67	HGSC	*FANCM* Exon 10|c.1582-1G>T	Low (1)	Exon 8|p.R273H	Positive (1)	(+)	(-)	Stable
5	52	HGSC	*RAD50* Exon 6|p.R278*	Low (2)	Not detected	Positive (1)	(+)	(-)	Stable
6	62	HGSC	*BRCA2* (VUS) Exon 11|E1382del	Low (4)	Exon 7|R248Q	Negative (0)	(+)	(+)	Stable
7	74	HGSC	*ATM* (VUS) Exon 18|p.L927F	Low (2)	Exon 5|c.559+1G>T	Negative (0)	(+)	(-)	Stable

HR: Homologous recombination, HGSC: High-grade serous carcinoma, TMB: Tumor Mutation Burden, PD-L1: Programmed Death-Ligand, CPS: Combined Positive Score, ER: Estrogen Receptor, PR: Estrogen Receptor, MSI: Microsatellite Instability (MLH1, MSH2, MSH6, PM2), VUS: variant of uncertain significance

Conclusions: The HRD prevalence in our cohort was relatively low compared with literature. The variants identified in the HGOC demonstrate at least one potentially targetable gene or protein expressions that were susceptible for hormone/immune therapies. This result suggests molecular characterization for HGOC offers potential to guide precision therapeutics.

706 Biomarker Expression in Ovarian Mucinous Carcinoma: Correlation with Tumor Grading and Patient Outcome

Lina Irshaid[1], Amir Momeni Boroujeni[1], Marisa Nucci[1], Carlos Parra-Herran[1]
[1]Brigham and Women's Hospital, Harvard Medical School, Boston, MA

Disclosures: Lina Irshaid: None; Amir Momeni Boroujeni: None; Marisa Nucci: None; Carlos Parra-Herran: None

Background: Ovarian Mucinous Carcinoma (OMC) is a distinct subtype of epithelial ovarian cancer with prevalent *KRAS*, *TP53* and *ERBB2* alterations. While there is yet to be consensus on the role of histologic grading, the Silverberg system and grading based on the invasive growth pattern (Growth-Based Grading, GBG) have both been recently shown to correlate with survival and are now included as non-core reporting elements by the International Collaboration on Cancer Reporting (ICCR). We aimed to evaluate the correlation between expression of biomarkers prevalent in OMC with these grading schemes, as well as patient outcome.

Design: Primary OMC were retrospectively identified from our archives and reviewed by three pathologists to confirm diagnosis and determine grading (Silverberg and GBG). Cases with uncertain primary site, associated with teratoma or including only intraepithelial carcinoma were excluded. p53, p16 and Her2 immunohistochemistry (IHC) were performed on the area with the worst histologic grade. A subset of tumors underwent tumor-only next generation sequencing using a comprehensive gene panel. Clinical outcome parameters were collected from medical records.

Results: A total of thirty-six OMCs were identified, 14 of which underwent sequencing. The average patient age was 49 (19-80) years. Compared to Silverberg 1 (Silv low grade) tumors, OMCs with Silverberg 2-3 (Silv high grade) more often showed mutant p53 IHC expression (P=0.0001). When each component of the Silverberg scoring system was individually analyzed, only mitotic score correlated with p53 expression (high score correlating with mutant p53). 7/33 cases showed Her2 3+ IHC; among those, 4 tumors were sequenced and all showed *ERBB2* amplification. There was no association between Silverberg and p16 or Her2 IHC. High grade OMCs, either by Silverberg or GBG, had an increased risk of recurrence after remission (P=0.02 & 0.03, respectively). There was no association between mutant p53 IHC, *TP53* mutations, Her2 IHC or *ERBB2* amplification and patient outcome.

Figure 1 - 706

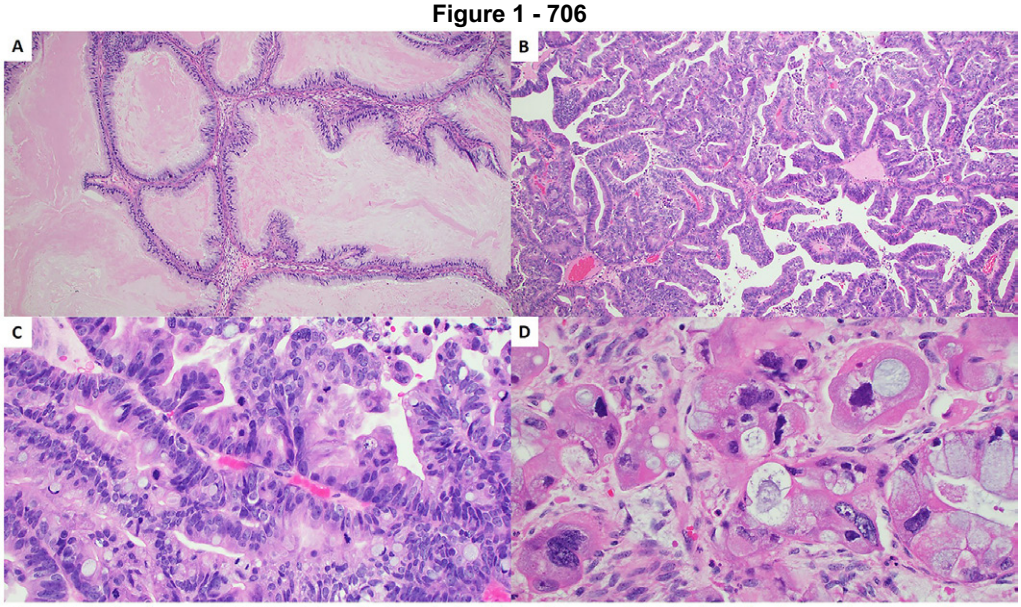

Figure 1. A) Silverberg grade 1 OMC with predominantly glandular architecture (H&E, 10x). B) Silverberg grade 2 OMC with papillary architecture (H&E, 10x). C) Grade 3 mitotic score (H&E, 40x). D) Grade 3 nuclear score (H&E, 40x).

Conclusions: p53, p16 and Her2 expression does not correlate with tumor recurrence in OMC. Likewise, growth pattern (expansile or infiltrative) does not correlate with expression of these biomarkers. On the other hand, mutant p53 expression is associated with high Silverberg grade. This association is most likely related to cell proliferation. Lastly, Silverberg and GBG grading are associated with risk of recurrence after remission, further supporting recent ICCR recommendations.

707 Molecular Landscape of Mullerian Clear Cell Carcinomas Reveals Prognostic Subgroups: A Study of 98 Cases

Lina Irshaid[1], Danielle Costigan[2], Fei Dong[3], Marisa Nucci[1], David Kolin[3]
[1]Brigham and Women's Hospital, Harvard Medical School, Boston, MA, [2]The University of North Carolina at Chapel Hill, Chapel Hill, NC, [3]Brigham and Women's Hospital, Boston, MA

Disclosures: Lina Irshaid: None; Danielle Costigan: None; Fei Dong: None; Marisa Nucci: None; David Kolin: None

Background: Mullerian clear cell carcinomas (CCC) are often aggressive, chemoresistant tumors. The prognostic significance of molecular subclassification of endometrioid carcinomas is well-established. However, less is known about the molecular landscape of CCC. The aim of this study was to better characterize the genetic landscape of a large cohort of CCC and correlate these findings with clinicopathologic features.

Design: Ninety eight CCC (70 ovary, 23 endometrium, 5 peritoneal/abdominal wall) were retrospectively identified from the archives of one institution. Tumors had undergone tumor-only targeted sequencing using a hybrid capture next generation sequencing panel, which detects single nucleotide variants (SNV), insertions and deletions, and copy number changes in over 275 genes. ER, PR and ARID1A immunohistochemistry were performed if material was available. Clinicopathologic parameters were collected from medical records.

Results: Clinicopathologic and molecular data are summarized in Table 1 and Figure 1, respectively. Fifty eight cases (59%) were stage 2 or higher at diagnosis. Only 63% achieved remission following standard therapy (55/87) and of those 40% recurred within a year. Median tumor mutational burden was 7.3 mutations/megabase (range 1.3-185). The most common SNV involved *ARID1A* (41/98; 41%), *PIK3CA* (39/98; 39%), *TP53* (20/98; 20%) and *PTEN* (10/98; 10%). Copy number loss of *ARID1A* was in 9/98 (9%) and *ERBB2* amplification was present in 4/98 (4%). *ARID1A* mutations were associated with a better disease-free survival (DFS) than wild-type tumors. When classified according to the TCGA/ProMisE endometrial carcinoma molecular subgroups, 3 (3%) were POLE ultramutated, 5 (5%) were microsatellite unstable (MSI-H), 17 (17%) were *TP53*-mutant type and 73 (74%) were no specific molecular profile (NSMP). *POLE* and MSI-H tumors were characterized by an excellent prognosis, and the *TP53*-mutant group had a worse disease-free survival than NSMP (Figure 2, log-rank p = 0.03). This prognostic stratification was also significant for the subgroup of stage I tumors.

Table 1. Clinical and pathologic characteristics of patients with Mullerian clear cell carcinoma, stratified by site of disease.

Site	**Ovary (n = 70)**	**Endometrium (n = 23)**	**Peritoneum/abdominal wall (n = 5)**
Age in years, mean (range)	53.1 (35-78)	61.9 (44-76)	55.6 (42-72)
Tumor size in cm, mean (SD)	11.8 (5.7)	4.5 (1.9)	7.6 (3.9)
FIGO stage, n (%) I II III IV	32/70 (46%) 16/70 (23%) 18/70 (26%) 4/70 (6%)	9/23 (39%) 4/23 (17%) 6/23 (26%) 4/23 (17%)	0/5 (0%) 3/5 (60%) 0/5 (0%) 2/5 (40%)
Lymph node involvement, n (%)	12/46 (26%)	4/16 (25%)	2/3 (67%
Endometriosis, n (%)	43/70 (61%)	1/23 (4.3%)	3/5 (60%)
IHC ER (≥1%), n (%)	7/45 (16%)	5/15 (33%)	1/5 (20%)
PR (≥1%), n (%)	8/36 (22%)	3/15 (20%)	1/5 (20%)
ARID1A (retained), n (%)	20/36 (56%)	7/10 (70%)	4/4 (100%)
DFS in months, median (SD)	35.3 (40.9)	21.8 (26.4)	49.9 (51.6)
OS in months, median (SD)	47.6 (39.3)	22.0 (28.7)	28.8 (33.5)
Died of disease, n (%)	15/67 (22%)	8/22 (36%)	2/5 (40%)

SD: standard deviation; FIGO: International Federation of Gynecology and Obstetrics; IHC: immunohistochemistry; DFS: disease free survival; OS: overall survival.

Figure 1 - 707

Figure 1. Oncoprint of molecular features of Mullerian clear cell carcinoma.

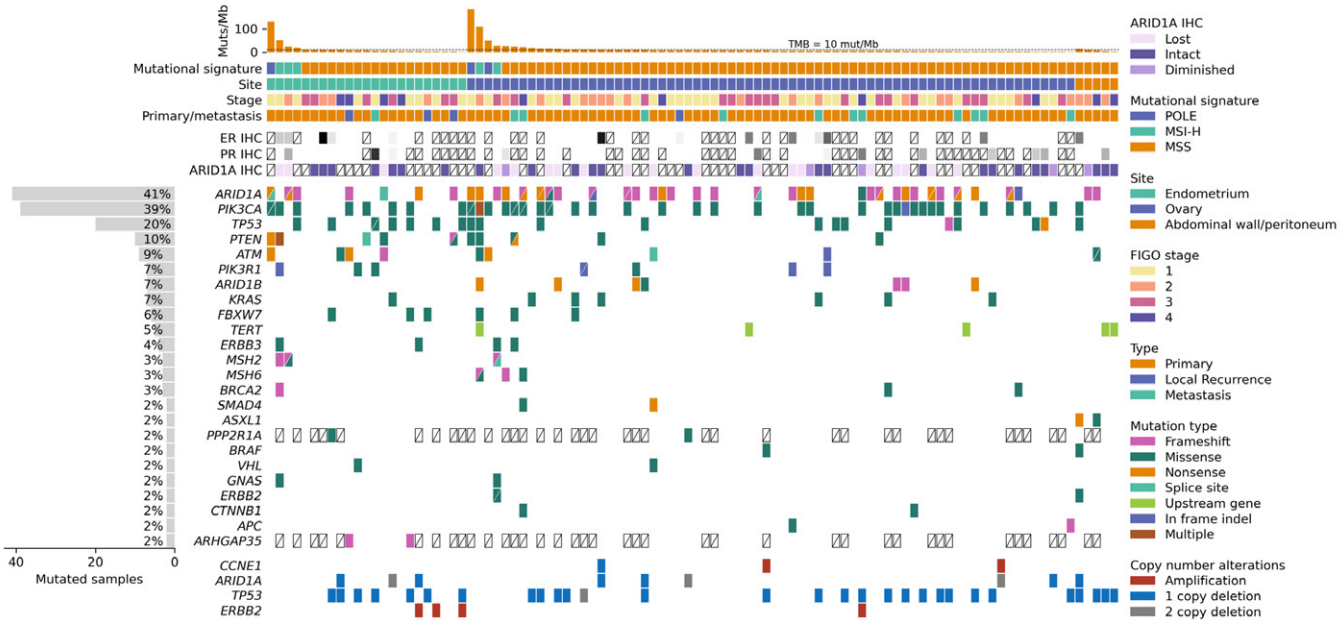

Figure 2 - 707

Figure 2. Disease-free survival of Mullerian clear cell carcinomas as a function of molecular subgroup.

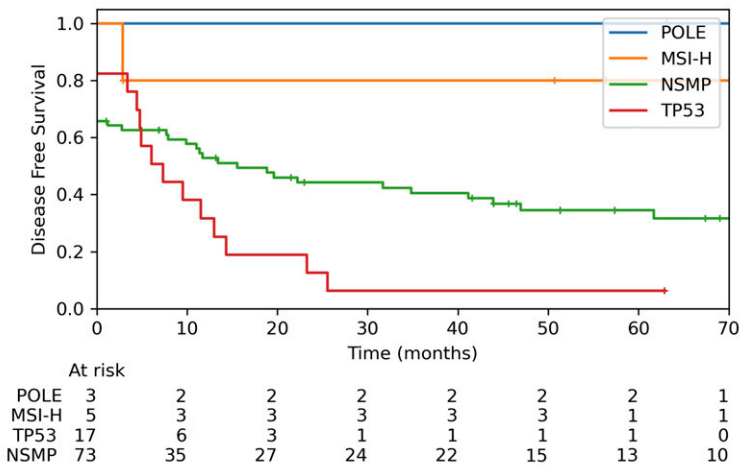

Conclusions: This large cohort of genetically characterized Mullerian CCC demonstrates that hypermutated (*POLE* and MSI-H) tumors are associated with an excellent prognosis, while the remaining tumors can be stratified based on *TP53* mutations. These findings suggest that routine molecular profiling of Mullerian CCC may be warranted for both prognosis and identification of potential targeted treatment such as immunotherapy and anti-HER2 agents.

708 Walthard Cell Nests/transitional Cell Metaplasia at the Distal Fallopian Tubes and Pelvic Mesothelium are Derived from Reserve Cells Beneath the Tubal Epithelium or the Mesothelial Cells

Uiree Jo[1], Chang Ohk Sung[1], Kyu-Rae Kim[2]
[1]Asan Medical Center, University of Ulsan College of Medicine, Seoul, South Korea, [2]Asan Medical Center, South Korea

Disclosures: Uiree Jo: None; Chang Ohk Sung: None; Kyu-Rae Kim: None

Background: Walthard cell nest or transitional cell metaplasia (TCM) is a benign cluster of urothelial/transitional-type epithelium most commonly found at the distal fallopian tube and/or mesothelial surface of the female genital organs, but histogenetic process is largely unknown. Investigation for the cell of origin of TCM might have the key to unveil the pathogenetic mechanism of ovarian Brenner tumor. Recently, we identified a distinct layer of keratin 17 (reserve cell marker)-expressing cells beneath the tubal epithelium and the mesothelium at the TCM foci, thereby hypothesized that TCM could be derived from reserve cells as in cases of cervical squamous metaplasia.

Design: To elucidate the histogenetic process of TCM, histologic features and immunohistochemical staining patterns for keratin 17, p63, GATA-3, estrogen receptor (ER), and androgen receptor (AR) were analyzed at the 29 TCM foci occurring in 23 fallopian tubes and 6 mesothelial surfaces.

Results: Histologically, an additional reserve layer was identified beneath the tubal epithelium (17/23, 73.9%) and the mesothelium (4/6, 66.7%) in the vicinity of TCM foci, and it gradually formed multilayers of reserve cells, and the cells showing urothelial characteristics having grooved nuclei and clear cytoplasm. GATA-3, p63, and AR were uniformly and strongly expressed in all TCM foci (29/29) from the single or multilayered reserve cells to the mature urothelium-like nests. The AR expression was significantly stronger than the ER expression during the entire cellular changes of reserve cells, and the AR expression was reciprocal to the ER expression, although there were overlap of ER and AR expression in the same foci in 5 cases (5/29, 17.2%). Keratin 17 was expressed in the reserve cells in an early single-layered stage, but it rapidly disappeared as they formed a multilayered structure, whereas p63 and GATA-3 expressions were maintained during the entire process of reserve cell change but negative in the overlying tubal epithelium.

Conclusions: Based on these results, we propose that TCM has a similar histogenetic step to those of cervical squamous metaplasia, in which a single layer of reserve cells emerged by "top-down differentiation" beneath the tubal epithelium or the mesothelial cells, they proliferated to form a multilayered structure and then differentiated to have urothelial characteristics. Androgen might have a role in the proliferation and differentiation of reserve cells in the histogenesis of TCM.

709 Clinicopathologic Analysis of a Cohort of FIGO grade 2 Uterine Endometrioid Carcinoma: Presence of Extensive Lymphovascular Invasion and Destructive Myometrial Invasion Correlate with Clinical Outcome but Amount of Solid Growth does not Affect Prognosis

Amy Joehlin-Price[1], Michelle Kuznicki[1], Johanna Kelley[1], Natalie Banet[1], Karuna Garg[1]
[1]Cleveland Clinic, Cleveland, OH

Disclosures: Amy Joehlin-Price: None; Michelle Kuznicki: None; Johanna Kelley: None; Natalie Banet: None; Karuna Garg: None

Background: FIGO grade 2 endometrial endometrioid carcinoma (EEC) is defined by the presence of solid growth involving 6-50% of the tumor. The clinical outcome of this group is heterogeneous, but closer to FIGO grade 1 EEC such that combining FIGO grade 1 and 2 EEC into a low-grade category has been proposed. With this in mind, our aim was to evaluate a large cohort of FIGO grade 2 EEC for percentage of solid growth, lymphovascular invasion (LVI) and pattern of myometrial invasion, and to correlate these features with clinical outcome.

Design: After obtaining IRB approval, the pathology database was searched for FIGO 2 EEC. All available H&E slides were reviewed. The extent of solid growth was divided into 6-10%, >10-25% and >25-50%. LVI was classified as extensive if >3 foci were present. Myometrial invasion pattern was recorded and included pushing, infiltrating without desmoplasia, MELF, destructive with a broad invasive front associated with extensive desmoplasia, and adenoma malignum-like.

Results: 177 cases were identified with (age range 22 to 91, median 64) at FIGO stage I (141, 80%), II (9, 5%), III (22, 12%) and IV (5, 3%). At last follow up, 148 patients (84%) showed no evidence of disease, 8 (5%) were alive with disease, 13 (17%) were

dead of disease, 8 (5%) were dead of other causes. Recurrences occurred in 28 (16%) patients. Review of slides showed variable solid growth (6-50%, median 20%). Forty cases (23%) showed extensive LVI, 21 (12%) showed focal LVI, and 116 (66%) showed no LVI. Patterns of invasion, some of which were present concurrently with others, included 30 (17%) destructive, 59 (33%) MELF, 38 (21%) infiltrative, 4 (2%) adenoma malignum-like, and 10 (6%) pushing. In univariable analyses, the % solid growth, destructive invasion, and extensive LVI did not impact overall survival (p=0.828, 0.423, and 0.189, respectively), but both destructive myometrial invasion and extensive LVI were associated with significantly worse recurrence free survival (figure 1A and B, p<0.001 and p=0.002, respectively). In a multivariable analysis accounting for FIGO clinical stage, destructive invasion, and extensive LVSI, only low vs. high stage (p=0.002) and the presence of destructive myometrial invasion (p=0.003) remained significant.

Figure 1 - 709

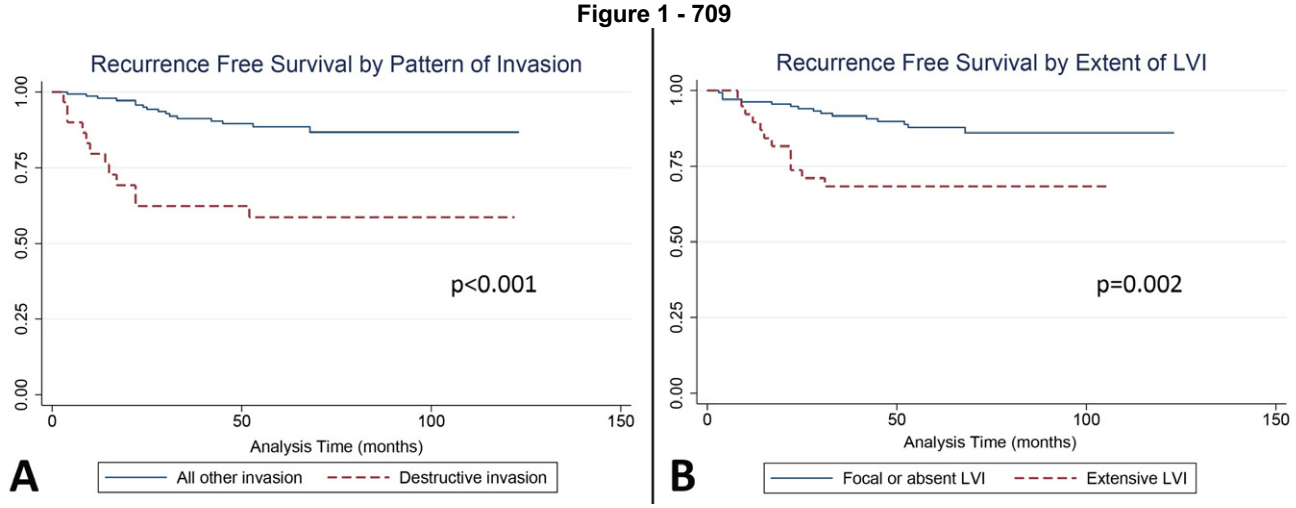

Conclusions: In our analysis of a large cohort of FIGO grade 2 EEC, tumor stage, presence of extensive LVI and destructive myometrial invasion correlated with clinical outcome. The amount of solid growth was not associated with any prognostic significance.

710 Comparison of HER2 Expression Between p53-Aberrant Endometrioid Carcinoma and Serous Carcinoma of the Uterus

Amy Joehlin-Price[1], Nicholas Ladwig[2], Carrie Hoyle[1], Lauren McCoy[1], Cathy Sprague[1], Yunn-Yi Chen[2], Walter Devine[2], Raza Hoda[1], Miglena Komforti[1], Karuna Garg[1]
[1]Cleveland Clinic, Cleveland, OH, [2]University of California, San Francisco, San Francisco, CA

Disclosures: Amy Joehlin-Price: None; Nicholas Ladwig: None; Carrie Hoyle: None; Lauren McCoy: None; Cathy Sprague: None; Yunn-Yi Chen: None; Walter Devine: None; Raza Hoda: None; Miglena Komforti: None; Karuna Garg: None

Background: The addition of trastuzumab has improved survival in *Her2* amplified uterine serous carcinoma (USC). Given some genetic overlap, we previously reported HER2 overexpression in a small cohort of p53-aberrant (p53-ab) high grade endometrial endometrioid carcinoma (EEC). The aim of this study was to evaluate HER2 expression in a larger cohort of p53-ab EEC and to compare the staining pattern with USC.

Design: We expanded on a previous cohort of 18 HER2-tested p53-aberrant EEC, performing HER2 IHC with limited FISH confirmation in 46 additional cases of high grade p53-ab EEC for a total of 64 p53-ab EEC. Thirteen USC with 3+ IHC (n=9) or 2+ IHC with FISH amplification (n=4) were included for comparison.

Results: Four of 64 (6%) p53-ab EEC showed 3+ HER2 expression, a rate significantly lower than the published rates in USC. Of these, three EEC underwent successful FISH testing and were *Her2* amplified (one case had technical issues). Of the four 3+ cases, 3 showed strong, complete membranous staining in 100% of tumor cells while the final case expressed HER2 in 40% of cells, notable for an abrupt transition between completely positive and negative areas. No cases of EEC demonstrated basolateral staining, even in the glandular areas. Ten additional p53-ab EEC cases with high 1+ to 2+ HER2 expression and one with 5% of cells showing 2 to 3+ HER2 expression were all negative for amplification by FISH. Amongst the 13 USC, HER2 staining was seen

in 10-95% of cells (median 70%) with predominantly strong intensity staining, but with 6 cases showing moderate staining intensity. 11 cases (85%) had at least focal basolateral staining, and 5 cases (38%) were notable for a markedly abrupt transition from strongly positive to entirely negative.

HER2 IHC	Number of cases (%)	HER2 FISH*
0	23 (36%)	0/10 amplified
1+	27 (42%)	0/7 amplified
2+	10 (16%)	0/9 amplified
3+	4 (6%)	3/3 amplified

*Remaining cases pending testing.

Conclusions: We found 3+ HER-2 expression in 6% of our p53-ab EEC with a high concordance of 3+ IHC with FISH amplification (3/3 tested). Compared to USC, p53-ab EEC appear to show lower frequency of HER2 amplification, less heterogeneity in the staining and basolateral staining pattern appears to be uncommon. These results have clinical and therapeutic implications and should be confirmed in larger studies.

711 Endometrial Carcinoma Lymph Node Metastasis Size, Pattern and Tumor Histology Vary Based on Lymph Node Sampling Procedure Performed: Clinicopathologic Analysis of 244 Lymph Node Metastases

Amy Joehlin-Price[1], Matthew Thomas[1], Karuna Garg[1]
[1]Cleveland Clinic, Cleveland, OH

Disclosures: Amy Joehlin-Price: None; Matthew Thomas: None; Karuna Garg: None

Background: With the adoption of sentinel lymph node (SLN) biopsies for both low and high grade endometrial carcinoma (EC), our methods for evaluation have shifted and we have noticed an increased detection of smaller-sized metastases. Although this shift is somewhat intuitive given our SLN ultrastaging protocols, no standardized evaluation of lymph node (LN) metastases sizes and patterns has been reported in the literature since this shift. We aimed to evaluate institutional EC LN metastases and compare the sizes and patterns of metastases to procedures performed, histology, and grade.

Design: The institutional database was searched for EC with positive LNs, to include isolated tumor cells (ITCs). Slides were reviewed, and information including size and pattern of metastasis were recorded. Grade, histology, procedure performed, and other clinicopathologic variables were obtained from the electronic medical record.

Results: LNs from 244 patients were included and included 92 low grade endometrioid EC, 60 high grade endometrioid EC, 45 serous, 11 clear cell, 19 carcinosarcoma, 9 dedifferentiated EC, and 4 mixed EC. SLN biopsies alone were performed in 23 patients; LN dissections alone were performed in 217 patients; and the remaining 4 patients underwent SLN biopsies followed by full LN dissections. A higher proportion of SLN biopsies were performed in cases of low grade EC compared to LN dissections (see Table 1). Median LN metastasis size in SLN biopsies and LN dissections was 1.25 mm (range 0.1-9) and 9 mm (range 0.13-70), respectively. A greater proportion of cases with ITCs only were noted in SLN biopsies. Review of LN slides demonstrated five predominant patterns of LN metastases: sinus histiocyte-like, glandular, cystic, papillary, and solid. Additionally, many cases were notable for surrounding fibrosis or desmoplasia. The distribution of metastasis patterns are detailed in Table 1, notable for an increased proportion of sinus histiocyte-like metastases and absence of desmoplasia in SLN biopsies. When examining low grade EC alone, findings were similar, with smaller metastases, increased ITCs, more sinus histiocyte-like metastases, and absent desmoplasia in SLN biopsies.

	All EC		Low Grade EC Only	
	SLN biopsies	LN dissections	SLN biopsies	LN dissections
	(n=23)	(n=217)	(n=17)	(n=75)
Age, median (range)	60 (36-80)	64 (38-83)	60 (36-80)	61 (38-81)
Histology				
Low grade endometrioid	17 (74%)	75 (35%)	----	----
High grade endometrioid	3 (13%)	57 (26%)	----	----
Serous	2 (9%)	43 (20%)	----	----
Clear cell	0 (0%)	11 (5%)	----	----
Carcinosarcoma	0 (0%)	19 (9%)	----	----
Dedifferentiated	1 (4%)	8 (4%)	----	----
Mixed	0 (0%)	4 (2%)	----	----
Size of metastasis, median (range)*	1.25 mm (0.15-9)	9 mm (0.13-70)	1 mm (0.15-1.5)	6 mm (0.25-60)
ITCs only	8 (35%)	12 (6%)	8 (47%)	6 (8%)
Pattern of metastasis				
Sinus histiocyte-like	19 (83%)	62 (29%)	16 (94%)	27 (36%)
Glandular	5 (22%)	161 (74%)	2 (12%)	56 (75%)
Cystic	1 (4%)	28 (13%)	0 (0%)	16 (21%)
Papillary	2 (9%)	37 (17%)	1 (6%)	5 (7%)
Solid	6 (26%)	83 (38%)	1 (6%)	14 (19%)
With desmoplasia	0 (0%)	59 (27%)	0 (0%)	22 (29%)

*ITCs are omitted from reported measurements.

Conclusions: Size of metastases are smaller in SLN biopsies, and LN metastasis patterns differ between SLN biopsies and LN dissections. Awareness of these patterns maximizes our clinical recognition and ease of LN metastasis diagnosis in EC.

712 5-hmC in Uterine Smooth Muscle Tumors: Potentially Useful as a Diagnostic Marker but Does Not Correlate with Tumor Aggressiveness

Terri Jones[1], Rohit Bhargava[2], Esther Elishaev[2], Thing Rinda Soong[3], Mirka Jones[3]
[1]University of Pittsburgh Medical Center, Pittsburgh, PA, [2]UPMC Magee-Womens Hospital, Pittsburgh, PA, [3]University of Pittsburgh, Pittsburgh, PA

Disclosures: Terri Jones: None; Rohit Bhargava: None; Esther Elishaev: None; Thing Rinda Soong: None; Mirka Jones: None

Background: The prediction of early recurrences and metastasis is crucial in the therapeutic approach to treatment of uterine smooth muscle tumors (uSMT). Various gross, microscopic and immunohistochemical features have been previously indicated as prognostic factors. The loss of 5-hydroxymethylcytosine (5-hmC), an epigenetic modification which promotes DNA demethylation, has been associated with disease progression in several malignancies, including gastrointestinal SMT. Thus far, 5-hmC expression has not been investigated in uSMT.

Design: Nuclear expression of 5-hmC by immunohistochemistry was evaluated by H-score in 103 uSMT, including 58 leiomyosarcomas (LMS), 11 smooth muscle tumors of uncertain malignant potential (STUMP), 12 leiomyomas with bizarre nuclei (LBN), and 22 leiomyomas (LM). Results were correlated with clinicopathologic data and statistical analysis was performed using Chi-square tests and Cox proportional hazard regressions.

Results: The mean 5-hmC H-score was 117 in LMS (median 120), 152 in STUMPs (median 150), 218 in LBN (median 240) and 244 in LM (median 260), respectively. There were significant differences in 5-hmC expression between uSMT tumor types ($p < .001$), with LMS having a significantly lower H-score than STUMPs ($p = 0.001$) and LM ($p = 0.04$). There was also a significant decrease in overall and cumulative survival of all uSMT with low and intermediate 5-hmC expression compared to high expression ($p < 0.001$), but significance was not present for LMS cases only.

Conclusions: 5-hmC levels differ significantly between benign and malignant uSMT, with LMS being more likely to show 5-hmC loss than benign tumors. Even though 5-hmC does not appear to be marker of aggressiveness as it is for GI SMT, it may play a role in tumorigenesis of uSMT. Given the significantly lower expression of 5-hmC in LMS compared with STUMPs, it may prove diagnostically useful in cases in which distinguishing between these two tumors types is challenging.

713 The Potential Therapeutic Implications of TIM-3, Gal-9, MHC class I, and PD-L1 Expression in Uterine Leiomyosarcomas

Terri Jones[1], Rohit Bhargava[2], Esther Elishaev[2], Thing Rinda Soong[3], Mirka Jones[3]
[1]University of Pittsburgh Medical Center, Pittsburgh, PA, [2]UPMC Magee-Womens Hospital, Pittsburgh, PA, [3]University of Pittsburgh, Pittsburgh, PA

Disclosures: Terri Jones: None; Rohit Bhargava: None; Esther Elishaev: None; Thing Rinda Soong: None; Mirka Jones: None

Background: Although uterine leiomyosarcomas (uLMS) have been shown to exhibit PD-L1 positivity, trials with PD-1 inhibitors have proved ineffective as treatment. We compared the expression of PD-L1 with related immune targets, T cell immunoglobulin and mucin-domain containing-3 (TIM-3) and galectin-9 (Gal-9), as well as factors that may mediate immune evasion, such as MHC class I (MHC), in uLMS.

Design: Membranous TIM-3, Gal-9, and MHC expression was assessed by IHC in 58 uLMS, including 53 primary tumors and 5 recurrent/metastatic tumors. Tumors with known stage included 37 low stage and 12 high stage. TIM-3 and Gal-9 were calculated as H-score for tumor cells and tumor infiltrating immune cells (TIICs), combined positive score (CPS), and tumor proportion score (TPS). MHC was scored as intact (>90% positive), subclonal loss (10-90% positive) or diffuse loss (<10% positive) in tumor cells. PD-L1 positivity was reported as a TPS. Results were correlated with clinicopathologic data.

Results: 90% of uLMS showed co-expression of TIM-3 and GAL-9 in either tumor cells, immune cells or both. TIM-3 was predominantly expressed in TIIC (52/58) and positive in a minority of tumors (3/58). Gal-9 was positive in the majority of cases in both TIIC (53/58) and tumor cells (42/58). PD-L1 expression was found in 35 TIM-3 positive and 54 Gal-9 positive uLMS, respectively. Loss of MHC expression (either subclonal or diffuse) was seen 46/58 of tumors, 50% of which were PD-L1 positive. There were significant associations on multivariable Cox regression analysis for low stage ($p = 0.002$) and negative tumoral PD-L1 result ($p = 0.039$) with improved disease-specific survival. In tumor cells, the PD-L1 status was significantly associated with Gal-9 expression ($p = 0.021$, Chi square).

Conclusions: While clinical trials of anti-PD-1 therapy have not shown promise in uLMS, the significant co-expression of Gal-9 in PD-L1-positive cases indicates that the TIM-3/Gal-9 axis may be involved in immune evasion in these tumors. Thus, it may be worth investigating the action of anti-TIM-3 agents in uLMS. The loss of MHC expression was identified in a majority of cases, indicating that this may be a pathway of immune escape in uLMS.

714 Tumor Immune Checkpoint and Histone Methylation Predictors of Prognosis in Vulvar Squamous Cell Carcinoma (SCCA)

Terri Jones[1], Lauren Skvarca[1], Alison Garrett[2], Emily O'Brien[3], Emily MacArthur[3], Esther Elishaev[2], Chengquan Zhao[3], Rohit Bhargava[2], Mirka Jones[4], Thing Rinda Soong[4]
[1]University of Pittsburgh Medical Center, Pittsburgh, PA, [2]UPMC Magee-Womens Hospital, Pittsburgh, PA, [3]Magee-Womens Hospital, University of Pittsburgh Medical Center, Pittsburgh, PA, [4]University of Pittsburgh, Pittsburgh, PA

Disclosures: Terri Jones: None; Lauren Skvarca: None; Alison Garrett: None; Emily O'Brien: None; Emily MacArthur: None; Esther Elishaev: None; Chengquan Zhao: None; Rohit Bhargava: None; Mirka Jones: None; Thing Rinda Soong: None

Background: Therapies targeting the PD-1/PD-L1 pathway and other immune checkpoint molecules are useful anticancer treatments. H3K27me3 is a histone methylation and modification marker involved in tumorigenesis. Little is known about its relationship with immune checkpoint molecules in vulvar cancers. We investigated the expression of a combined immune checkpoint and histone methylation biomarker panel in vulvar SCCA.

Design: Immunohistochemical expression of PD-L1, TIM-3, Gal-9, H3K27me3, MHC class I (MHCI), and extent of CD8+ tumor infiltrating lymphocytes (TILs) were examined in 169 vulvectomy specimens. PD-L1, TIM-3 and Gal-9 expression was measured via Tumor Proportion Score (TPS) and Combined Positive Score (CPS). Cross-sectional analyses were done with Fisher's exact tests. Overall survival (OS) and recurrence-free survival (RFS) were assessed via log-rank tests and Cox proportional regression models with adjusted hazard ratios (aHRs) and 95% confidence intervals (CIs) as measures.

Results: Median age was 71 years. Most were of pT1a (11%) or pT1b (86%) stage, with 17% being high-grade, 22% having lymph node metastases (LN+), and 51% being p16+. High (>50%) tumoral H3K27me3 expression ($H3K27me3^{High}$) was noted in 34% of

SCCA, and was associated with p16+ status (Table 1). PD-L1 TPS+, TIM-3 TPS+ and Gal-9 TPS+ status was seen in 61%, 57% and 48% of cases. Positive PD-L1 TPS was associated with LN+ and p53+ status. Similar observations were seen with positive TIM-3 TPS and high (>50%) PD-L1 CPS. High (>50%) tumoral MHC1 expression was associated with increased CD8+ TILs, TIM-3 TPS+ as well as PD-L1 TPS+ status. Median follow-up time was 21 months (range: 1-152 months). High CD8+ TILs, TIM-3 TPS+, H3K27me3^{High} (Figure 1A-C) and p16+ status were indicators for improved OS. Statistically significant OS predictors included high CD8+ TILs (aHR: 0.4; CI: 0.2-0.7) and TIM-3 TPS+ status (aHR: 0.5; CI: 0.2-0.9) after controlling for other tumor features. H3K27me3^{High}, TIM-3 TPS+ and p16+ status predicted longer RFS (Figure 1D-F), with TIM-3 TPS+ and p16+ status being statistically significant RFS predictors (aHR: 0.5; CI: 0.3-0.9); (aHR: 0.4; CI: 0.2-0.7) after confounding adjustment.

Table 1. Correlation of clinicopathologic features with immune checkpoint and histone methylation biomarker expression in vulvar SCCA (N=169)

Select clinicopathologic features			H3K27me3			CD8+ TILs			TIM-3 TPS			GAL-9 TPS			PD-L1 TPS			PD-L1 CPS		
			Low n=112	High (>50%) n=57		Low n=52	High (>50%) n=117		Negative n=73	Positive n=96		Negative n=88	Positive n=81		Negative n=65	Positive n=104		Negative n=73	Positive n=96	
		N	column %		P	column %		P	column %		P	column %		P	column %		P	column %		P
Age (yrs)	<60	39	20	28	0.5	23	23	0.76	20	25	0.52	23	22	0.69	28	20	0.53	25	15	0.02
	60-79	84	52	46		46	51		48	51		47	53		46	52		45	71	
	≥80	46	28	26		31	26		32	24		30	25		26	28		30	14	
Tumor characteristics																				
Grade	Low/Intermediate	141	83	84	0.85	73	88	0.02	84	83	0.97	84	83	0.81	86	82	0.45	84	80	0.54
	High	28	17	16		27	12		16	17		16	17		14	18		16	20	
p16	Negative/focal	83	54	39	0.05	42	52	0.24	45	54	0.13	44	54	0.19	35	58	0.005	42	77	<0.001
	Strong and diffuse	86	45	61		58	48		55	46		56	46		65	42		58	23	
p53	Negative/focal	87	54	47	0.45	54	50	0.68	68	39	<0.001	55	48	0.41	62	45	0.04	56	34	0.02
	Strong and diffuse	82	46	53		46	50		32	61		45	52		38	55		44	66	
MHCI expression	Low	85	49	53	0.67	73	40	<0.001	70	35	<0.001	61	38	0.003	74	35	<0.001	59	17	<0.001
	High (>50%)	84	51	47		27	60		30	65		39	62		26	65		41	83	
Lymphovascular invasion	Negative	139	84	79	0.42	85	81	0.6	82	82	0.99	84	80	0.51	83	82	0.82	84	77	0.38
	Positive	30	16	21		15	19		18	18		16	20		17	18		16	23	
Positive lymph nodes	No	131	82	68	0.04	77	78	0.9	85	72	0.04	82	73	0.16	91	69	0.001	84	54	<0.001
	Yes	38	19	32		23	22		15	28		18	27		9	31		16	46	
pT stage	1a	19	9	8		10	9	0.95	10	9	0.9	12	6	0.47	17	4	0.01	12	0	0.11
	1b	146	89	88		88	89		87	89		86	91		81	93		86	97	
	≥2	4	2	4		2	2		3	2		2	3		2	3		2	3	

Figure 1 - 714

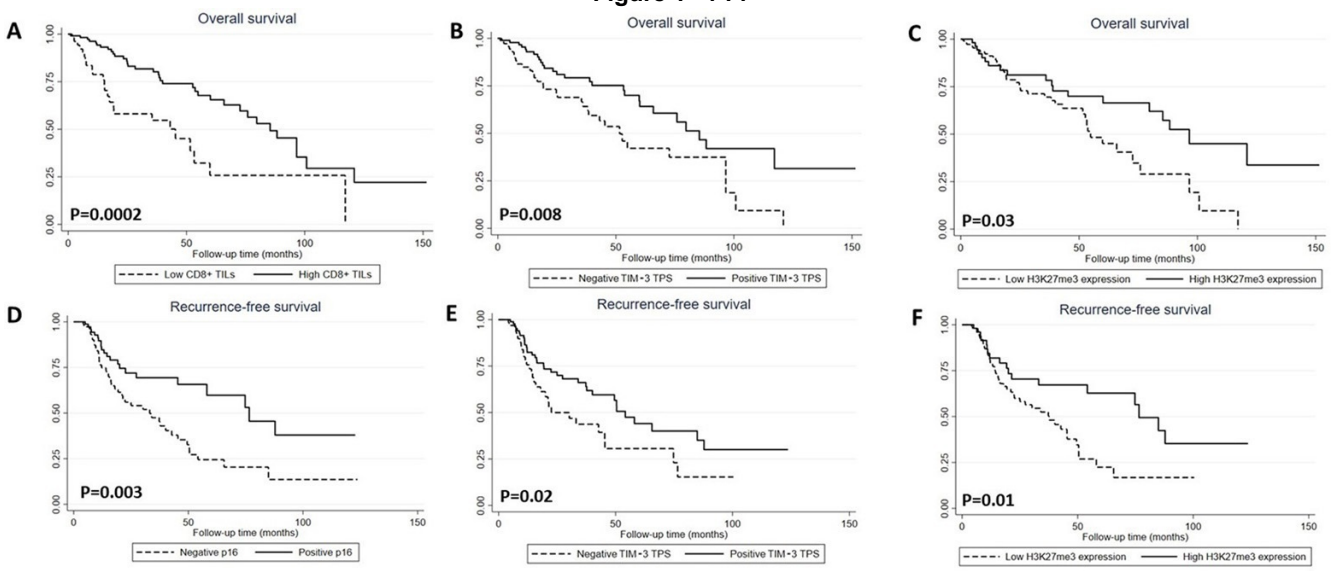

Conclusions: Our study suggests that vulvar SCCA with a combined profile of positive p16 status, high CD8+ TILs, TIM-3 TPS+ and H3K27me3^{High} status are associated with improved prognosis. The findings will be instructive in developing a comprehensive stratification system that better predicts the prognosis of vulvar SCCA.

715 Abnormal Nuclear Membrane Staining Pattern by MLH1 Immunohistochemistry in Endometrioid Adenocarcinoma: A Diagnostic Pitfall

David Jou[1], Grace Malvar[1], Katharine Germansky[2], Jonathan Hecht[2], Monika Vyas[1]
[1]Beth Israel Deaconess Medical Center, Harvard Medical School, Boston, MA, [2]Beth Israel Deaconess Medical Center, Boston, MA

Disclosures: David Jou: None; Grace Malvar: None; Katharine Germansky: None; Jonathan Hecht: None; Monika Vyas: None

Background: Immunohistochemistry (IHC) for mismatch repair (MMR) proteins is now a part of routine diagnostic work-up of endometrial adenocarcinoma. Loss of nuclear staining for MLH1/PMS2 triggers reflex testing for MLH1 promoter methylation while loss of MSH2/MSH6 or isolated loss of MSH6 and PMS2 are followed by germline testing for detection of Lynch syndrome. However, directing reflex work-up can be challenging if the IHC results deviate from the usually described patterns. We noticed an unusual nuclear membranous staining pattern of MLH1. The goal of the study is to determine the significance of this staining pattern and highlight this pitfall in IHC interpretation.

Design: The pathology database was reviewed for any cases of endometrioid adenocarcinoma with any abnormal MMR protein expression. The H&E and MMR [MLH1 (G168-15), PMS2 (A16-4), MSH2 (FE11), MSH6 (44/MSH6)] stained slides were retrieved and evaluated. Histologic features (FIGO grade, solid, mucinous, secretory, papillary morphology) were noted. The MMR IHC was reviewed for loss of nuclear expression and abnormal staining patterns (such as cytoplasmic, dot like nuclear, nuclear membranous). Results of MLH1 promoter methylation and/or germline testing were recorded.

Results: 52 cases of endometrioid adenocarcinomas with abnormal IHC staining patterns were identified from 2017-2020. In this cohort, 41 cases were MLH1/PMS2 deficient and 11 were MSH2/MSH6 deficient. 6/41 (14.6%) cases showed nuclear membranous expression of MLH1 (focal in 1 and diffuse in 5 cases). All cases were accompanied by loss of PMS2 (Fig. 1D) in the same foci and the cases were accompanied by at least some areas showing complete loss of MLH1. On review of histology, in 3 cases foci of abnormal MLH1 expression showed mucinous morphology with squamous/morular metaplasia whereas typical glandular areas showed complete loss of expression. 2 (33%) were FIGO grade 1 while 4 (66%) were FIGO grade 2-3. MLH1 promoter hypermethylation was detected in 5/6 cases while further work-up was not available for the remaining case.

Figure 1 - 715

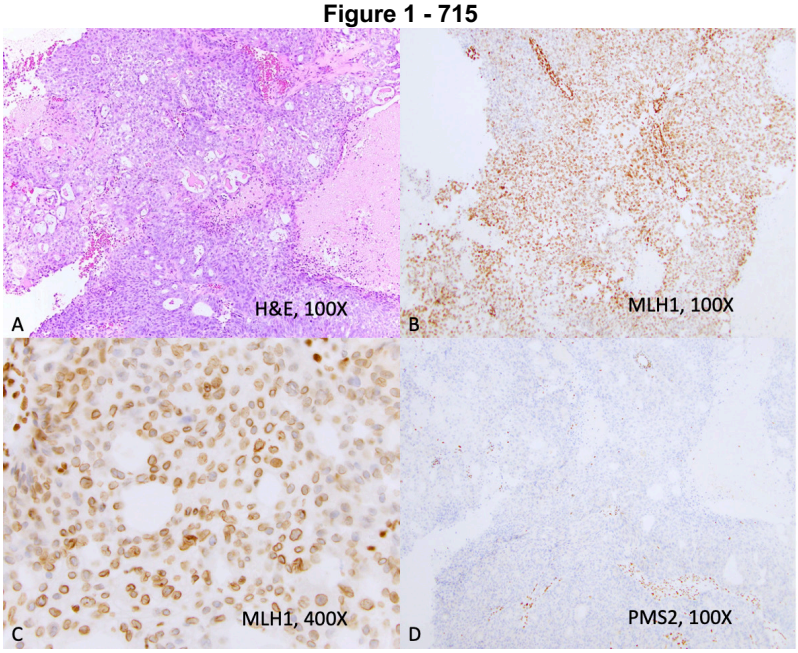

Conclusions: Nuclear membranous expression of MLH1 represents an aberrant staining pattern which is seen with complete loss of PMS2 and frequently associated with MLH1 promoter hypermethylation. This pattern may be related to a specific antibody clone. Failure to recognize this pattern of MLH1 expression as aberrant can lead to erroneous interpretation of isolated PMS2 loss which can trigger unnecessary germline testing.

716 The Clinical Utility and Impact of Next Generation Sequencing in Gynecologic Cancers

Vijaya Kadam Maruthi[1], Mahyar Khazaeli[2], Mohamed Desouki[3]
[1]University at Buffalo, Buffalo, NY, [2]University at Buffalo, SUNY, Buffalo, NY, [3]Roswell Park Comprehensive Cancer Center, Buffalo, NY

Disclosures: Vijaya Kadam Maruthi: None; Mahyar Khazaeli: None; Mohamed Desouki: None

Background: In this era of personalized medicine, next generation sequencing (NGS) has increasingly facilitated in the identification of molecularly targeted therapies for cancer treatment. However, clinical utility is an emerging challenge. Our objective was to identify the clinical utility and impact of NGS testing in the gynecologic (gyn) cancers in our tertiary cancer center.

Design: We conducted a retrospective review of clinico-pathologic data of 299 gynecological cancers who had NGS testing performed between 2014 and 2020 to identify 1) if NGS recognized actionable targets for which therapy is available, 2) whether the patient's treatment course was changed based on the actionable targets and 3) whether there was improved survival after the treatment change.

Results: Most common gyn tumors were high grade serous carcinomas (52.5%), endometrioid carcinomas (17.0 %), squamous cell carcinomas (5.7%) and carcinosarcomas (5.3%). Tumor grades were high, intermediate, and low in 73.6%, 6% and 14.7%, respectively. 61% of the patients had advanced stage disease (III or IV) at the time of diagnosis. The number of genetic alterations ranged from 0-25 with a mean of 2.8/case. Most frequently altered genes are demonstrated in Fig 1. Among 299 patients, 100 (33.4%) had actionable alterations. Subsequently 79 (79%) received a targeted treatment (group 1) and 21 (21%) had no change in treatment (group 2) based on NGS results. The NGS results didn't show any actionable alterations in 199 patients (group 3). The death rate in group 1, 2 and 3 was 54.4%, 42.8% and 50.2% with an average survival of 18.6, 6.6 and 10.8 months respectively with statistically significant difference (P-0.002) [Fig2].

Figure 1 - 716

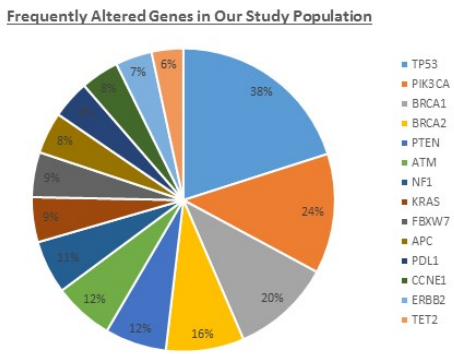

Figure 2 - 716

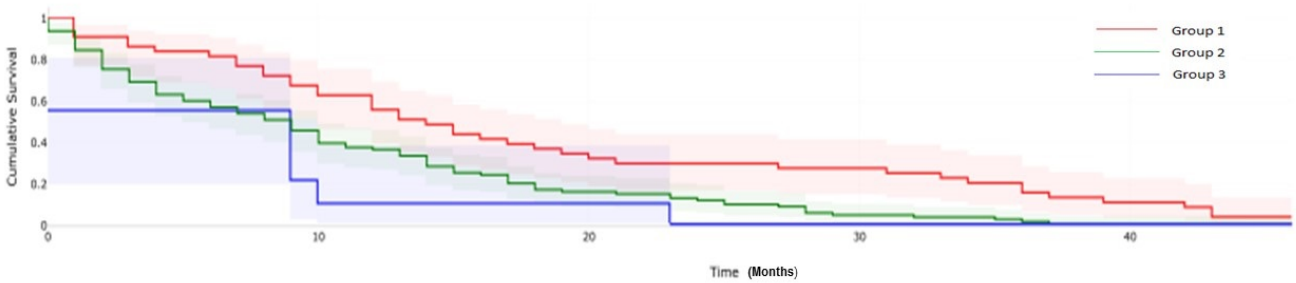

Conclusions: NGS testing for gyn cancers detected a 33.4 % of actionable alterations with a high clinical action rate of 79%. Along with a high clinical utility of NGS it also seemed to improve the survival of the gyn cancer patients who received targeted treatment.

717 SHH and IHH Protein Expression in High-Grade Serous Ovarian Carcinomas

Valentina Karin-Kujundzic[1], Anita Skrtic[1], Semir Vranic[2], Ljiljana Serman[1]
[1]School of Medicine, University of Zagreb, Zagreb, Croatia, [2]College of Medicine, Qatar University, Doha, Qatar

Disclosures: Valentina Karin-Kujundzic: None; Anita Skrtic: None; Semir Vranic: None; Ljiljana Serman: None

Background: High-grade serous ovarian carcinomas (HGSCs) are the most common and lethal type of all epithelial ovarian cancers. The aberrant activation of several signaling pathways, including the Hedgehog (HH) signaling pathway, has been observed in ovarian cancer. HH signaling is activated by HH ligands, Sonic Hedgehog (SHH), Indian Hedgehog (IHH), and Desert Hedgehog (DHH), which inhibit the transmembrane protein PTCH. The role of the Hh signaling pathway in ovarian cancer has not been sufficiently investigated. In the current study, we explored the expression of SHH and IHH proteins in a cohort of serous ovarian carcinomas and cell lines.

Design: Formalin-fixed paraffin-embedded (FFPE) samples of 37 HGSCs were used for this study, while normal ovarian (n=20) and fallopian tube tissue samples (n=10) served as controls. HGSC cell lines, OVCAR5, OVCAR8, and OVSHAO, and control cell line, normal fallopian tube non-ciliated epithelium cell line FNE1, were also used in the study. SHH and IHH expression were analyzed using immunohistochemistry in tissue samples and by immunofluorescence in cell lines.

Results: SHH and IHH protein expression were significantly higher in HGSCs compared with both healthy ovarian surface epithelium ($p<0.001$ and $p<0.001$, respectively) and healthy fallopian tube epithelium ($p=0.04$ and $p<0.001$, respectively). Similarly, SHH and IHH protein expression was significantly higher in HGSC cell lines, OVCAR5, OVCAR8, and OVSAHO compared with normal fallopian tube non-ciliated epithelium cell line, FNE1.

Conclusions: Our data indicate that HH ligands SHH and IHH may play an active role in the molecular pathogenesis of high-grade serous ovarian carcinomas. Increased SHH and IHH protein expression in HGSC samples and cell lines indicate that the tumor promoter role of these ligands can potentially be achieved through autocrine SHH and IHH signaling. Therefore, these HH ligands might serve as potential therapeutic targets for HGSCs. Further studies should confirm these findings and their clinical relevance.

718 Comprehensive Molecular Characterization of Recurrent Low Grade / Low Stage Endometrial Endometrioid Carcinomas

Neslihan Kayraklioglu[1], Walter Devine[1], Nicholas Ladwig[1], Karuna Garg[2], Jocelyn Chapman[1], Joseph Rabban[1]
[1]University of California, San Francisco, San Francisco, CA, [2]Cleveland Clinic, Cleveland, OH

Disclosures: Neslihan Kayraklioglu: None; Walter Devine: None; Nicholas Ladwig: None; Karuna Garg: None; Jocelyn Chapman: None; Joseph Rabban: None

Background: Although most low grade/low stage endometrial endometrioid cancers (EEC) have a favorable prognosis, the 5-10% that do recur tend to be chemoresistant. Predicting recurrence remains enigmatic though early literature suggests *CTNNB1* mutation may be prognostic. This study employed next generation sequencing to characterize molecular alterations, including those of The Cancer Genome Atlas (TCGA) molecular classification system, in recurrent low grade, low stage EEC from a single institution, with comparison to reported alterations in non-recurrent EECs from the publicly available TCGA database.

Design: 32 recurrent FIGO grade 1 or 2, FIGO stage I or II EEC from a single institution were analyzed using a clinically validated targeted DNA sequencing panel that includes 529 cancer-related genes, quantitation of tumor mutational burden (TMB), analysis of genome-wide copy number alterations and MSI Sensor evaluation for microsatellite instability. A comparison group of non-recurrent low grade/low stage EEC with at least 24 months of follow-up time was identified from the TCGA database (n=63, sequencing data available from 52).

Results: Patient age, tumor stage and grade were not significantly different between recurrent and non-recurrent EEC (Table 1). TCGA categories of recurrent EEC were 68.7% copy number-low (CN-low), 21.8% hypermutated (MSI), 6.2% CN-high, and 3.1% ultramutated (*POLE* mutated); this distribution was not significantly different from the non-recurrent EEC. Of the most commonly altered genes (Figure 1 and Table 1), *ARID1A* mutation was more common in the recurrent EEC while *PIK3CA* mutation was more common in non-recurrent EEC. No difference in *CTNNB1* mutation was detected between the two groups. Recurrent EEC harbored gains in chromosome 1q (50%), 10p (25%), 10q (31.2%) and loss in 16q (25%) but this was not statistically different

than in the non-recurrent EEC. TMB was high (≥10 mutation/Mb) in 17/32 recurrent EEC. Median time to recurrence was 19 (range 2-114) months and 14/31 died of disease (8 CN-low; 4 MSI; 2 CN-high). Incidence of death was highest in CN-high (2/2) and MSI (4/7) versus CN-low (8/22).

	Recurrent (n=32)	Non-recurrent (n=63)	p value
Average Age	63	62.7	0.9
Median Follow up (m)	71 (9-330)	46 (24-112)	
Median Time to Recurrence (m)	19 (2-114)	N/A	
Tumor stage & Grade			
Stage I	27 (84.3%)	59 (93.6%)	0.1
Grade 1	9 (28.1%)	30 (47.6%)	0.08
Grade 2	18 (56.2%)	29 (46%)	0.3
Stage II	5 (15.6%)	4 (6.3%)	0.1
Grade 1	1 (3.1%)	1 (1.5%)	1
Grade 2	4 (12.5%)	3 (4.7%)	0.2
TCGA category		(n=53 available data)	
CN-Low	22 (68.7%)	29 (54.7%)	0.2
MSI	7 (21.8%)	18 (33.9%)	0.3
CN-High	2 (6.2%)	2 (3.7%)	0.6
POLE mutated	1 (3.1%)	4 (7.5%)	0.6
Single nucleotide variants		(n=52 available data)	
PTEN	25 (78.1%)	46 (88.5%)	0.2
ARID1A	22 (68.7%)	23 (44.2%)	*0.04
PIK3R1	14 (43.7%)	18 (34.6%)	0.4
PIK3CA	12 (37.5%)	35 (67.3%)	*0.01
CTNNB1	10 (31.2%)	20 (38.5%)	0.6
KRAS	6 (18.7%)	15 (28.8%)	0.4
FGFR2	6 (18.7%)	9 (17.3%)	1
TP53	5 (15.6%)	3 (5.8%)	0.2
Copy number alterations		(n=61 available data)	
1q gain	16 (50%)	21 (34.4%)	0.1
10p gain	8 (25%)	17 (27.8%)	0.8
10q gain	10 (31.2%)	18 (29.5%)	1
16q loss	8 (25%)	7 (11.4%)	0.1
8p gain	6 (18.7%)	9 (14.7%)	0.7
8q gain	6 (18.7%)	8 (13.1%)	0.5

Figure 1 - 718

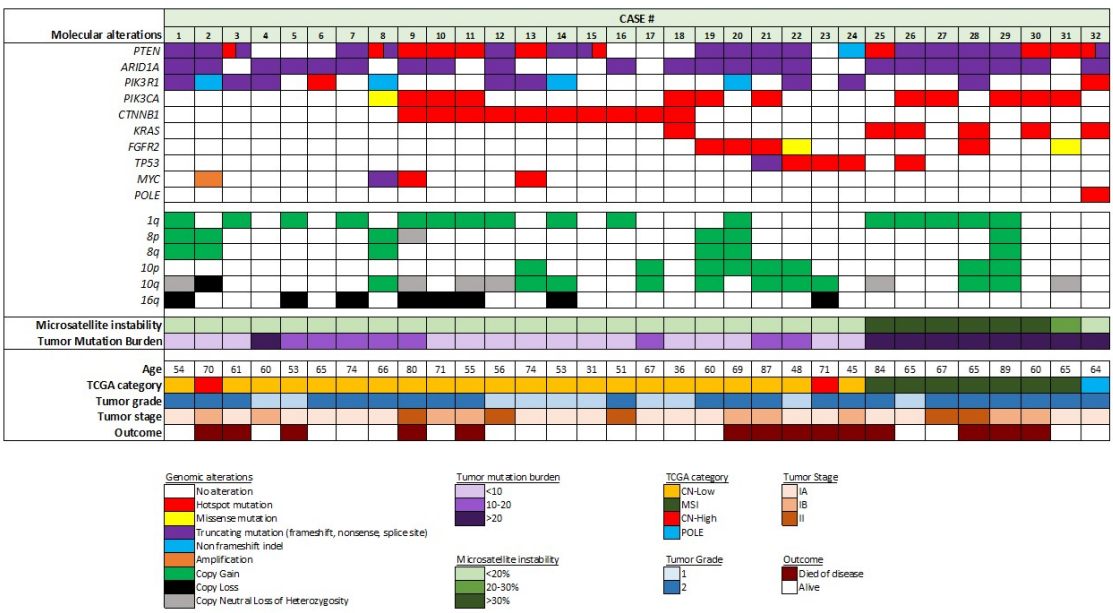

Conclusions: TCGA molecular category, *CTNNB1* mutation and 1q/10q alteration did not distinguish recurrent versus non-recurrent low grade low stage EEC though CN-high and MSI status may predict adverse outcome among those with recurrent disease. High TMB merits further study as a potential prognostic variable in this cohort of EEC.

719 Selection of Endometrial Carcinomas For POLE Testing: Specificity Analysis of Morphologic Features

Kianoosh Keyhanian[1], Lucy Han[2], Brooke Howitt[3], Teri Longacre[4]
[1]The Ottawa Hospital, University of Ottawa, Ottawa, Canada, [2]Stanford Pathology, Stanford, CA, [3]Stanford Medicine/Stanford University, Stanford, CA, [4]Stanford University, Stanford, CA

Disclosures: Kianoosh Keyhanian: None; Lucy Han: None; Brooke Howitt: None; Teri Longacre: None

Background: Ultramutated/*POLE*-mutant endometrial carcinoma (P^M EC) is one of the four TCGA defined molecular groups of EC. Identification of this phenotype is clinically relevant given its association with the best prognosis amongst the EC molecular classes despite frequent high nuclear grade. However, *POLE* mutation testing is not widely available. Recognizing the most high-yield pathological features of P^M EC is key in maximizing testing efficiency. At our institution, *POLE* mutation testing is performed on EC consult cases when morphologic features are suspicious for an ultramutated phenotype. Our objective was to compare the morphological and immunohistochemical (IHC) features between consult ECs with verified *POLE* mutations and the ones that were tested but negative.

Design: Consult cases of EC that had undergone *POLE* hotspot mutation testing over the past 2.5 years were enrolled. Cases with pathogenic or likely pathogenic mutations were assigned to the P^M group. Tumor histology was reviewed including histotype, peritumoral lymphocytes (PTL), tumor infiltrating lymphocytes, bizarre nuclei (markedly enlarged nuclei with smudged chromatin), eosinophilic cytoplasm and tumor heterogeneity. Biomarker (mismatch repair proteins, p53, beta-catenin, ER, PR) expression was also reviewed. Z score was used to compare the ratios.

Results: Out of 24 consult cases, 12 were found to harbor *POLE* mutation (50%) and 12 were wild-type (P^{WT}) (50%). Average age: 51 in P^M and 70.5 in P^{WT} (P: 0.01). Histologic features (Figure 1) of both groups are listed in Table 1A and B. Briefly, ambiguous histomorphology (6/12 vs. 1/12; P: 0.02) and presence of more than rare bizarre nuclei (8/12 vs. 2/12; P: 0.01) differed significantly between P^M and P^{WT}, respectively. Biomarker profile: In P^M group, one case (1/12) demonstrated PMS2 loss, and one (1/12) showed subclonal MLH1/PMS2 loss. Among P^{WT}, 2/12 cases showed MLH1/PMS2 loss. p53 was subclonally overexpressed in 4/10 in P^M and 1/12 in P^{WT} (P: 0.07). Mutant p53 patterns (overexpression or null) was seen in 1/10 vs. 6/12 in P^M and P^{WT}, respectively. Specificity of ambiguous histomorphology, bizarre nuclei, subclonal biomarker expression and PTL for P^M EC was 86%, 80%, 80% and 67%, respectively.

Table 1: Morphological Features of *POLE*-mutated (A) and *POLE* wild-type (B) consult cases

A	Histotype	PTL	TIL	Pattern of invasion	Bizarre nuclei	Eosinophilic cytoplasm	Squamous diff.	Atypical Hyperplasia	Heterogeneity
1	High grade carcinoma, ambiguous morphology, G3	Marked	Marked	Broad front/ pushing	Yes, with multinucleated cell	Yes	No	No	No
2	Endometrioid carcinoma, G2	Marked	Marked	Infiltrating	Yes	Yes	No	No	No
3	Endometrioid carcinoma, G2	Moderate	Mild	Infiltrating	Occasional	Yes	Yes	Yes	No
4	Endometrioid carcinoma, G3	Moderate	Moderate	Broad front/ pushing	Yes	Yes	No	No	No
5	High grade carcinoma, ambiguous morphology, G3	No	Moderate, patchy	Infiltrating	Yes	Yes	No	Yes	Yes
6	High grade carcinoma, ambiguous morphology, G3	Moderate	Moderate	Broad front/ pushing	Yes	No	No	No	Yes, mixed endometrioid and serous- like features
7	Endometrioid carcinoma, G3	Moderate	Marked	Infiltrating and broad front	Yes	Yes	No	No	Poorly Preserved

8	High grade carcinoma, favor endometroid carcinoma, G3	Mild, focally moderate	Focally mild	Infiltrating	Yes	Yes	Yes	No	Yes, areas of marked pleomorphism
9	Endometrioid carcinoma, G2	No	Moderate, patchy	Noninvasive	No	No	No	Yes	Yes
10	Intermediate-grade endometrial carcinoma, ambiguous morphology, G2	Moderate	Marked	MELF & Broad front	Occasional	Yes	Yes	No	No
11	Dedifferentiated carcinoma,with ambiguous morphology	No	Marked	Noninvasive	No	No	Yes	Yes	No, epithelial and sarcomatous area
12	Intermediate-grade endometrial carcinoma, ambiguous morphology, G2	Mild	Moderate	Infiltrating	Yes	Yes	No	No	Yes, mixed endometrioid and clear cell
B									
1	Clear cell carcinoma	Marked	Moderate	Infiltrating with desmoplasia	Occasional	Yes	No	No	No
2	Endometrioid carcinoma, G3	Mild	Mild	Noninvasive	Yes	Yes	No	No	Yes (Endometrioid, serous & clear cell carcinoma-like areas)
3	Dedifferentiated carcinoma	Moderate	Moderate	Infiltrating	No	No	Yes	No	No, Dedifferentiated & well-differentiated areas
4	Serous carcinoma	Mild	Mild	Noninvasive	No	No	No	No	No
5	Endometrioid carcinoma, G3	Mild	Moderate	Infiltrating	No	Yes	No	No	No
6	Endometrioid carcinoma, G3	NA*	Mild	NA	Occasional	Yes	No	No	Yes, areas with high and low grade cytology
7	High Grade carcinoma, favor serous carcinoma	NA*	Marked	NA	Focal	No	Yes	Yes	Yes, endometrioid and serous -like areas
8	Serous carcinoma	NA*	Moderate	NA	Yes	Yes	No	No	No
9	Endometrioid carcinoma, G3	Mild	Mild	Broad front and infiltrating	No	Yes	No	No	No
10	Endometrioid carcinoma, G2	NA*	Marked	NA	No	Yes	No	No	Yes, diverse architecture (including papillary, micropapillary and solid growth)
11	High Grade carcinoma, ambiguous morphology	Focally moderate	Focally moderate	Noninvasive	No	Yes	No	No	Yes (Serous -like, CHEC-like and tubulocystic patterns)
12	Endometrioid carcinoma, G3	Moderate	Moderate	Broad front and infiltrating	Occasional	No	Yes	Yes	No

CHEC: corded and hyalinized endometrial carcinoma, PTL: Peritumoral lymphocytes, TIL: Tumor infiltrating lymphocytes, Squamous diff: squamous differentiation. *Data not available, only biopsy available for review

Figure 1 - 719

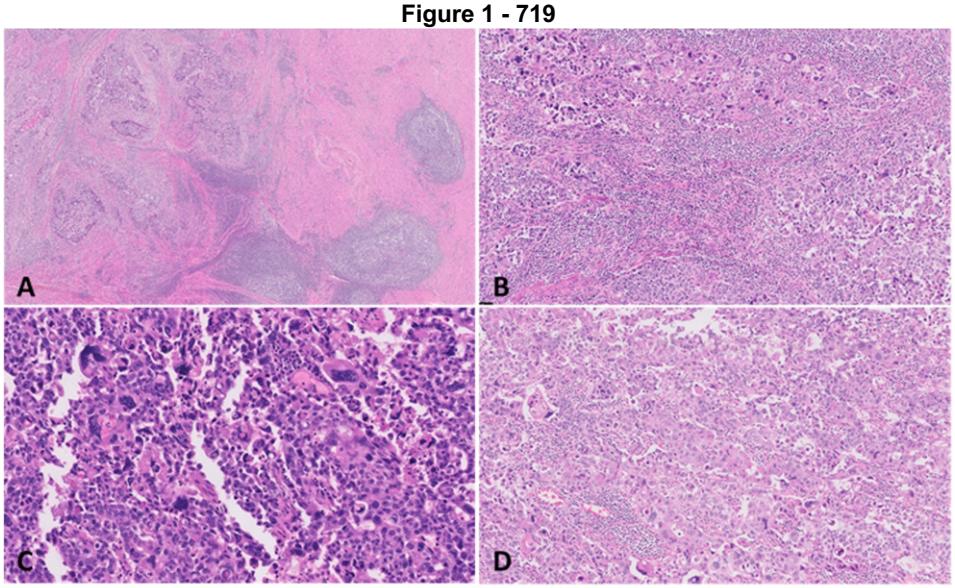

Figure 1. Histological features of POLE mutated endometrial carcinoma. A: peritumoral lymphocytes with germinal centers, B: tumor infiltrating lymphocytes, C: bizarre nuclei, D: eosinophilic cytoplasm

Conclusions: In summary, morphological screening is useful in selection of ECs for POLE testing. Certain morphological features such as ambiguous histomorphology, and presence of more than rare bizarre nuclei may help optimize testing efficiency for identification of ultramutated ECs.

720 Chemotherapy Response Score (CRS): Histologic and Molecular Correlation in High Grade Serous Ovarian Carcinoma, An Institutional Study

Mir Yousufuddin Ali Khan[1], Logan Corey[2], David Carr[1], Sudeshna Bandyopadhyay[3], Rouba Ali-Fehmi[3], Mira Kheil[3], Deepti Jain[3], Tala Tawil[3]

[1]Detroit Medical Center/Wayne State University, Detroit, MI, [2]Barbara Ann Karmanos Center and Wayne State University School of Medicine, Detroit, MI, [3]Wayne State University, Detroit, MI

Disclosures: Mir Yousufuddin Ali Khan: None; Logan Corey: None; David Carr: None; Sudeshna Bandyopadhyay: None; Rouba Ali-Fehmi: None; Mira Kheil: None; Deepti Jain: None; Tala Tawil: None

Background: Chemotherapy Response Score (CRS) is a histopathologic response to Neoadjuvant Chemotherapy (NAC) in patients with High Grade Serous Ovarian Carcinoma (HGSOC) that is known to have prognostic significance. A high percentage of HGSOC patients have Homologous Recombination Deficiency (HRD) resulting from BRCA1/2 mutation, and loss of heterozygosity (LOH). We aim to determine a correlation between HRD, CRS, and LOH score in patients with HGSOC treated with platinum-based NAC.

Design: We identified 45 patients who had received at least 3 doses of platinum-based NAC. We obtained clinical and pathological parameters including age, date of diagnosis, date, and number of cycles of NAC, date of surgery, and CRS. Their tumor molecular profiles that included the LOH score, BRCA1, BRCA2, and Tumor Mutation Burden (TMB) were analyzed. A high LOH score was defined as a score of ≥16, and a low LOH as a score of <16. TMB score was defined as low 1-5; 5-19= intermediate, and >20= high. CRS was graded on 1 to 3 based on the current standards. Fisher's exact test was used to determine the significant association between the measured variables.

Results: Of patients with a high LOH score, 43% (N= 7) showed complete response to NAC, evident by a CRS 3. Of patients with a CRS 3, 100% had a LOH score of ≥16 (p=0.0005). Of patients with a CRS 1-2, 76% (N=23) had a LOH score of <16 (p=0.0005). Of patients with a CRS 3 and LOH of ≥16, 100% were platinum-sensitive. When used independently, CRS 3 predicted platinum sensitivity in 86% of patients; LOH score of ≥16 predicted platinum sensitivity in only 66% of patients. When used together, patients with a CRS 3 and LOH score ≥16 correctly predicted 100% of the patients to be platinum-sensitive. Of patients with either BRCA 1 or BRCA 2 mutation, 100% (N=8) had a high LOH score. Of patients with LOH score ≥ 16, and either BRCA1 or BRCA2

mutation, 37% (N=3) were found to have a CRS 3. Of patients with wild-type BRCA1/2 and low LOH (N=13), no patient had a CRS 3, however, 30% (N=4) patients were found to be platinum-sensitive. 41 of 45 patients had a low TMB.

Conclusions: HGSOC with Homologous Recombination Deficiency (HRD) by high genomic Loss of Heterozygosity (LOH) (≥16) and BRCA1/2 mutation is likely to have CRS 3 to platinum-based NAC than patients with low LOH and wild type BRCA. Furthermore, CRS and LOH scores may be used in combination to predict platinum sensitivity more accurately than either alone. To further study this, larger multicenter studies are needed.

721 Uterine Mesonephric-like Adenocarcinoma: Correlations between Mismatch Repair Protein Expression and Microsatellite Instability and Responses to Lenvatinib Plus Pembrolizumab Combination Therapy

Hyunjin Kim[1], Hyun-Soo Kim[2]
[1]Samsung Medical Center, Seoul, South Korea, [2]Samsung Medical Center, Sungkyunkwan University School of Medicine, Seoul, South Korea

Disclosures: Hyunjin Kim: None; Hyun-Soo Kim: None

Background: Mesonephric-like adenocarcinoma (MLA) of the uterine corpus is a rare but distinct entity of the female genital tract due to its aggressive clinical behavior and the distinct histological, and genetic characteristics. Advanced-stage uterine MLAs are treated similarly to the common histological subtypes of endometrial carcinoma, with paclitaxel-carboplatin chemotherapy. However, the use of platinum-based regimens in the recurrent setting has shown limited efficacy. Recently, promising responses to the combination of lenvatinib plus pembrolizumab have been demonstrated in microsatellite stable (MSS)/mismatch repair (MMR)-proficient advanced endometrial carcinomas. Although the determination of MSI status is critical in setting the treatment plan, the standardized protocol has not been established. Therefore, we conducted MMR protein immunohistochemistry (IHC) and microsatellite instability (MSI)-PCR assay in uterine MLAs, and compared the results.

Design: We collected 34 cases of primary uterine MLA, and performed IHC for four MMR proteins. The percentage of nuclear expression was evaluated. Five patients whose tumors were interpreted as MMR-deficient were treated with pembrolizumab monotherapy, whereas six patients with MMR-proficient MLA received lenvatinib plus pembrolizumab combination therapy. The expression status of MMR proteins was compared with the results of MSI-PCR analysis performed using five mononucleotide repeat microsatellite targets.

Results: In all cases, MLH1 and PMS2 were expressed in >90% of the tumor cells. In contrast, MSH2 and MSH6 showed variable loss of expression with 5-20% positivity in 10 (29.4%) cases. All of these cases demonstrated at least focal (≥5%) nuclear immunoreactivity for either MSH2 or MSH6, but they were misinterpreted as loss of expression. In the meantime, we found that five patients who received pembrolizumab monotherapy experienced disease progression, whereas six patients receiving dual therapy of lenvatinib and pembrolizumab were stable or had no evidence of disease. One of the six patients with the dual therapy developed disease recurrence after halting the medication. MSI-PCR analysis revealed that all cases were MSS.

Conclusions: MMR IHC should be carefully interpreted and confirmed with PCR for MSI status. Sustained responses to lenvatinib plus pembrolizumab combination therapy in a subset of uterine MLA cases suggest that dual therapy is a promising treatment of choice for uterine MLA, which is *KRAS*-mutant and MSS/MMR-proficient.

722 Her-2 Expression in p53 and Endometrial Cancers compared to Serous Carcinomas

Marilyn Kinloch[1], Nicholas Baniak[2], Katelynn Campbell[3], Emina Torlakovic[2], C. Blake Gilks[4]
[1]University of Saskatchewan, Saskatoon, Canada, [2]University of Saskatchewan, Saskatchewan Health Authority, Saskatoon, Canada, [3]Little Rock, AR, [4]Vancouver General Hospital/University of British Columbia, Vancouver, Canada

Disclosures: Marilyn Kinloch: *Grant or Research Support*, Bayer, Astra Zeneca, Pfizer; *Advisory Board Member*, Roche; Nicholas Baniak: None; Katelynn Campbell: None; Emina Torlakovic: None; C. Blake Gilks: None

Background: A recent phase II trial with 58 patients showed those with advanced or recurrent uterine serous carcinoma and Her2 over expression treated with Trastuzumab resulted in an increased progression-free survival. This has prompted increased interest

in Trastuzumab as a precision oncology target for endometrial serous carcinoma; however, inclusion was based on serous histology alone. With the increased knowledge of molecular classification of endometrial cancer, we sought to explore the relationship of p53 abn classified endometrial cancers and Her2 over expression.

Design: Tumor samples from 2 institutions were retrieved by biopsy, hysterectomy or tissue microarray with diagnoses of serous, high-grade endometrioid, mixed histology and carcinosarcoma. p53 immunohistochemistry (IHC) was completed on all patients. Those with p53 abn staining had their mismatch repair (MMR) status confirmed as intact. Her2 (IHC) was performed and evaluated using the ASCO/CAP 2018 breast guidelines. Her2 in-situ hybridization (ISH) was performed on all specimens, regardless of Her2 IHC result. Sensitivity and specificity were calculated. A Chi-square test between histology and Her2 amplification was performed.

Results: 61 patients with high-grade endometrial cancer, p53 mutations and MMR intact were identified. The WHO histotype diagnosis breakdown was 50 serous carcinomas, 5 carcinosarcomas, 4 high-grade endometrial carcinomas, and 3 mixed serous-endometrioid carcinomas. The Her2 IHC breakdown by serous carcinoma is 0+ (33%), 1+ (27%), 2+ (20%), 3+ (20%). The non-serous Her2 IHC breakdown is 0+ (25%), 1+ (50%), 2+ (25%) and 3+ (0%). The sensitivity of the Her2 IHC is 86% and the specificity is 97%. A chi-square test of independence was performed to examine the relation between histology and Her2 amplification The relation between these variables was not significant, X^2=0.55, p=.45. 13/15 (87%) of the Her2 ISH amplified cases were serous histology, while the 2/15 (13%) of non-serous histology was mixed serous/endometrioid and HGEC p53 abn (Figure 1).

	Her 2 IHC				
WHO histotype	0+	1+	2+	3+	Total
Carcinosarcoma	2	2	1	0	5
HGEC p53 abn	1	2	1	0	4
Mixed serous/endo	0	2	1	0	3
Serous	16	13	10	10	49
Total	19	20	15	13	61
	Her 2 ISH				
Not Amplified	18	17	10	1	46
Amplified		2	4	9	15
	non-serous	serous			
Not Amplified	10	35			
Amplified	2	13			

Figure 1 - 722

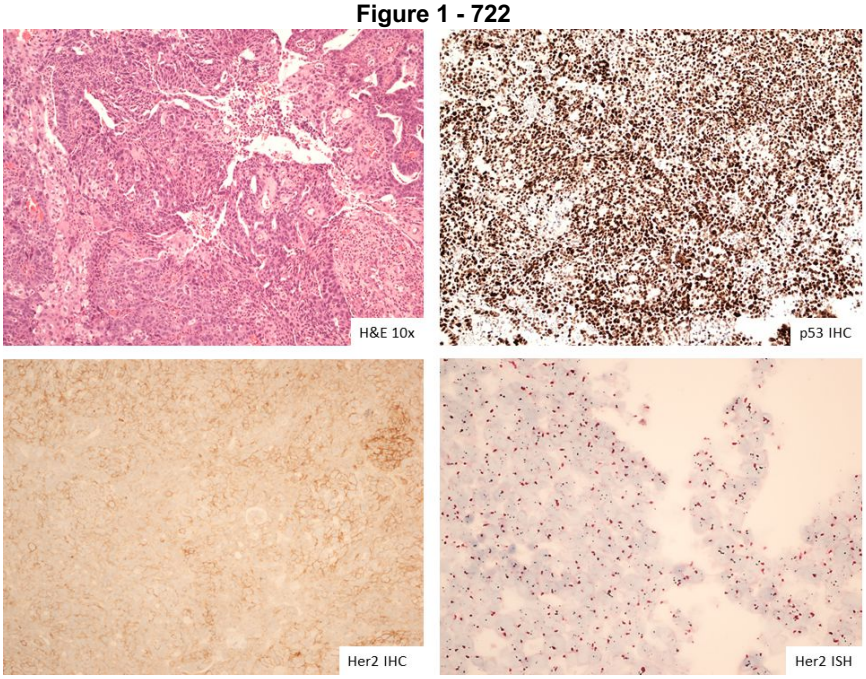

Conclusions: Using molecular classification of endometrial cancer patients with p53 abn status, regardless of histotype, do worse. As precision oncology begins for endometrial carcinoma patients, consideration of p53 IHC as an algorithmic step when testing endometrial cancers for Her2 amplification and expand inclusion criteria to include those that have a molecular classification of p53 abn and not just serous histology may be warranted.

723 Methylation Analysis Supports Classification of Endometrial Stromal Sarcomas with Variant BCOR and BCORL1 Alterations as High-Grade Endometrial Stromal Sarcomas

Felix Kommoss[1], Sarah Chiang[2], Martin Koebel[3], Christian Koelsche[1], Brendan Dickson[4], Marjan Rouzbahman[5], Golnar Rasty[6], Andreas von Deimling[7], Cheng-Han Lee[8], Gulisa Turashvili[9]

[1]University of Heidelberg, Heidelberg, Germany, [2]Memorial Sloan Kettering Cancer Center, New York, NY, [3]Alberta Precision Laboratories, University of Calgary, Calgary, Canada, [4]Mount Sinai Health System, Toronto, Canada, [5]Toronto General Hospital, University of Toronto, Toronto, Canada, [6]Markham Stouffville Hospital, Markham, Canada, [7]Heidelberg University Hospital, Heidelberg, Germany, [8]University of Alberta, Edmonton, Canada, [9]Emory University Hospital, Atlanta, GA

Disclosures: Felix Kommoss: None; Sarah Chiang: None; Martin Koebel: None; Christian Koelsche: None; Brendan Dickson: None; Marjan Rouzbahman: None; Golnar Rasty: None; Andreas von Deimling: None; Cheng-Han Lee: None; Gulisa Turashvili: None

Background: The distinction between low-grade and high-grade endometrial stromal sarcoma (LGESS, HGESS) is increasingly defined by specific genetic alterations (e.g. *JAZF1* fusions in LGESS, YWHAE or BCOR fusions in HGESS). Recently, variant genomic alterations involving *BCOR* or *BCORL1* have been reported, although it remains unclear whether these signify LGESS or HGESS. We set out to investigate the methylation profile of an ESS cohort with such alterations.

Results: A total of 13 ESS harboring *BCOR* (6 with *BCOR* internal tandem duplication, 1 with *EP300-BCOR*, 1 with *BCOR-LPP*) and *BCORL1 (*4 with *JAZF1-BCORL1*, 1 with *EPC1-BCORL1*) alterations were identified. Median patient age at primary diagnosis was 50 years (18-70). The tumors were composed of round to spindled cells with cellularity and cytologic atypia ranging from mild to marked and a median mitotic count of 20 (2-85) per 10 high-power fields. At least focally myopermeative growth was noted in 7/7 assessable cases. Of 11 patients with follow-up data (median 21 months, 11-73), recurrent/metastatic disease and cancer related death occurred in 6 and 2 patients, respectively. Unsupervised hierarchical clustering of methylation profiles showed close clustering of all variant ESS with *YWHAE-NUTM2* or *ZC3H7B-BCOR* HGSS, except for one variant case (*EPC1-BCORL1*) that co-clustered with LGESS (Fig. 1). Copy number analysis revealed *CDK4* and *MDM2* amplifications, and homozygous deletions of *CDKN2A/B* in a subset of cases.

Figure 1 - 723

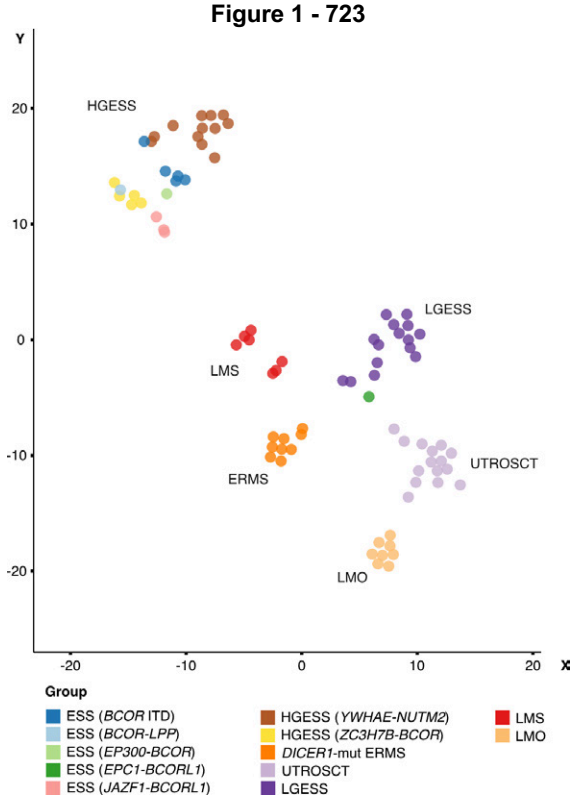

Conclusions: The great majority of ESS harboring variant *BCOR* or *BCORL1* alterations display methylation profiles similar to that of *YWHAE-NUTM2* or *ZC3H7B-BCOR* HGESS, supporting their provisional classification as HGESS.

724 SMARCA4-Deficient Uterine Sarcoma Harbor a Specific DNA Methylation Profile Distinct from Undifferentiated Endometrial Carcinoma and Other SWI/SNF-Deficient Tumors

Felix Kommoss[1], Basile Tessier-Cloutier[2], Christian Koelsche[1], Martin Koebel[3], Cheng-Han Lee[4], David Kolin[5], Andreas von Deimling[6], Brooke Howitt[7]

[1]University of Heidelberg, Heidelberg, Germany, [2]The University of British Columbia, Vancouver, Canada, [3]Alberta Precision Laboratories, University of Calgary, Calgary, Canada, [4]University of Alberta, Edmonton, Canada, [5]Brigham and Women's Hospital, Boston, MA, [6]Heidelberg University Hospital, Heidelberg, Germany, [7]Stanford Medicine/Stanford University, Stanford, CA

Disclosures: Felix Kommoss: None; Basile Tessier-Cloutier: None; Christian Koelsche: None; Martin Koebel: None; Cheng-Han Lee: None; David Kolin: None; Andreas von Deimling: None; Brooke Howitt: None

Background: *SMARCA4*-deficient uterine sarcoma (SDUS) represents an aggressive neoplasm with distinct clinicopathological features. Nevertheless, such tumors may show significant morphological overlap with other SWI/SNF-deficient tumors, such as undifferentiated endometrial carcinoma (UEC). Here we aimed to investigate whole genome DNA methylation profiles of SDUS in the context of other uterine and extrauterine SWI/SNF-deficient tumors.

Design: We collected a multicenter cohort including SDUS, UEC and small-cell carcinoma of the ovary, hypercalcemic type (SCCOHT). Whole genome DNA-methylation analysis was performed using the Illumina Infinium MethylationEPIC 850k BeadChip kit. Data were analyzed by t-distributed stochastic neighbor embedding analysis together with a previously generated methylation data set including endometrioid endometrial carcinomas (EEC), serous endometrial carcinomas (SEC) and extrauterine malignant rhabdoid tumors (MRT; *SMARCB1*-deficient).

Results: 9 SDUS, 17 UEC and 8 SCCOHT were available for methylation analyses. The previously generated methylation data set encompassed 40 EEC, 3 SEC and 17 extrauterine MRT. t-distributed stochastic neighbor embedding analysis of array-based whole genome DNA methylation data revealed two larger methylation clusters (Figure 1). Cluster one encompassed EEC, SEC, as well as UEC. Within cluster one we identified a sub clustering, setting UEC apart from EEC and SEC. Cluster two encompassed SDUS, SCCOHT and extrauterine MRT. Here, SDUS, SCCOHT and extrauterine MRT each formed distinct and entity-specific methylation subclusters, with few outliers observed in the SCCOHT group of tumors.

Figure 1 - 724

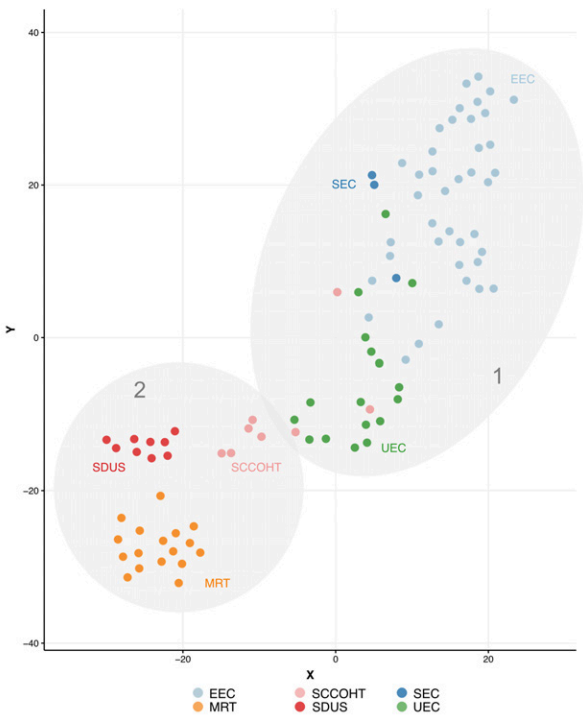

Conclusions: Our results show SDUS to harbor specific DNA methylation profiles, further substantiating its recognition as a distinct tumor entity. Furthermore, our results indicate that SDUS is more closely related to extrauterine MRT and SCCOHT than UEC or other endometrial carcinomas.

725 A Deeper Dive into Endometriosis: Improved Diagnoses with the Utilization of Widely Available Tools

Andrea Krajisnik[1], Horacio Maluf[1], Bonnie Balzer[1], Matthew Siedhoff[1], Mireille Truong[1], Kelly Wright[1], Kate Lawrenson[1], Fabiola Medeiros[1]
[1]Cedars-Sinai Medical Center, Los Angeles, CA

Disclosures: Andrea Krajisnik: None; Horacio Maluf: None; Bonnie Balzer: *Consultant*, Core Diagnostics, Castle Biosciences, PathologyWatch; Matthew Siedhoff: *Consultant*, Applied Medical; Mireille Truong: *Consultant*, Medtronic, Ethicon; Kelly Wright: None; Kate Lawrenson: None; Fabiola Medeiros: None

Background: The diagnosis of endometriosis is complicated by non-specific clinical presentations, inaccurate laparoscopic findings, and challenges in histologic interpretation. Delays in diagnosis can often be attributed to a lack of histologic evidence to support suspected endometriosis and can lead to underdiagnosis and undertreatment. Histologic confirmation of a proportion of cases is hindered by undefined diagnostic criteria and unfamiliarity in recognizing ectopic endometrial-type tissue against its mimickers. In addition, some diagnoses may be missed due to a lack of protocols for inspecting the tissue more thoroughly when endometriosis is not identified. We examine whether obtaining deeper sections or immunohistochemical stains improve the identification of endometriosis in cases where it was not originally detected.

Design: Pathology reports from 487 patients who underwent surgery for clinically suspected endometriosis from 2016 to 2019 were reviewed and categorized as either endometriosis histologically confirmed (419), or endometriosis not histologically confirmed (68). 100 peritoneal resection specimens from the 68 patients originally diagnosed as negative for endometriosis were selected and blindly reviewed by a gynecologic pathologist. Subsequently, 3 deeper sections at 50 microns were obtained and reviewed by the same pathologist. Immunohistochemical stains ordered at the time of diagnosis were also reviewed.

Results: Of the 100 specimens originally diagnosed as negative for endometriosis, 16 (16.0%) showed sufficient histologic evidence of endometriosis on re-review of the original slides. Findings in these cases included glands and stroma (8), stroma only (7), and stroma with hemosiderin (1). Additional 50-micron deeper sections yielded 7 additional diagnoses (8.3%) which showed glands and stroma (6) or stroma with hemosiderin (1). Immunostains, including CD10, were deemed not helpful in 18 of 19 cases.

Conclusions: In the absence of histologic evidence of endometriosis in initial sections, examination of deeper sections yields diagnostic findings in a relevant proportion of cases while immunohistochemistry tends to be non-contributory. Defining minimal histologic diagnostic criteria for endometriosis and promoting acquaintance with microscopic findings may further enhance our ability of reaching definitive tissue diagnoses, potentially impacting the management of a substantial subset of patients.

726 Five-Year Universal Sequencing of BRCA1/2 and Homologous Recombination-Related Genes in Epithelial Ovarian Carcinoma; Is Histotype Directed Testing Justified?

Claire Kramer[1], Nienke Solleveld[1], Giacomo Santandrea[2], Marthe de Jonge[1], Hans Marten Hazelbag[3], Marjolein Kagie[3], Elisabeth Ahsmann[4], Judith Kroep[1], Nienke van der Stoep[1], Cor de Kroon[1], Katja Gaarenstroom[1], Tom van Wezel[1], Vincent Smit[1], Christi van Asperen[1], Maaike Vreeswijk[1], Tjalling Bosse[1]
[1]Leiden University Medical Center, Leiden, Netherlands, [2]Azienda Unità Sanitaria Locale - IRCCS di Reggio Emilia, Reggio Emilia, Italy, [3]Haaglanden Medical Center, The Hague, Netherlands, [4]Groene Hart Ziekenhuis, Netherlands

Disclosures: Claire Kramer: None; Nienke Solleveld: None; Giacomo Santandrea: None; Marthe de Jonge: None; Hans Marten Hazelbag: None; Marjolein Kagie: None; Elisabeth Ahsmann: None; Judith Kroep: None; Nienke van der Stoep: None; Cor de Kroon: None; Katja Gaarenstroom: None; Tom van Wezel: None; Vincent Smit: None; Christi van Asperen: None; Maaike Vreeswijk: None; Tjalling Bosse: None

Background: Here, we report on the results of five consecutive years of prospective, universal sequencing of *BRCA1/2* and homologous recombination (HR)-related genes in epithelial ovarian cancers (EOC). We aimed to specifically look at EOC histotype

distribution with pathogenic variants (PVs), to potentially justify a shift towards histotype-directed screening for PVs in *BRCA1/2* and HR-related genes.

Design: Next Generation Sequencing (NGS) results were collected for 441 EOC sequenced between September 2017 and June 2021. For all EOC, the NGS-panel included *BRCA1/2* and for a subset of cases (*n* = 341) the panel was expanded to include additional HR-related genes: *ATM, BARD1, BRIP1, CDK12, CHEK1/2, FANCL, PALB2, RAD51B/C/D* and *RAD54L.* All cases underwent central pathology review by a gynaecologic pathologist, blinded for the molecular findings. Histotype, grade, p53 immunohistochemistry, PVs (class 4 and 5), variant allele frequencies (VAFs) and loss of heterozygosity (LOH) of the wildtype allele were evaluated. A Chi-Square test was used to test differences in frequencies in *BRCA1/2* PVs between HGSOC and non-HGSOC.

Results: Universal sequencing was performed on 441 EOC, including 320 HGSOC (73%) and 121 non-HGSOC (27%). PVs in *BRCA1/2* were identified across the entire *BRCA1* and *BRCA2* gene (Figure 1). In HGSOC, we identified *BRCA1/2* PVs in 18% of the cases (Table 1A). In contrast, in non-HGSOC, the diagnostic yield of PVs in *BRCA1/2* was significantly lower (1.7%, *p* = 0.000). The two non-HGSOC *BRCA1/2*-mutated EOC were a low-grade serous OC (LGSOC) and a GR3 endometrioid ovarian cancer (EnOC). Despite the fact that the cases were p53 wildtype (wt) and had a non-HGSOC morphology, these cases carried a PV with high VAFs and LOH of the wildtype allele, suggestive that these tumors might be HR-deficient (HRD). Interestingly, in the 341 EOC that were sequenced with a broader panel, 38% (*n* = 7) of the PVs in HR-related genes other than *BRCA1/2* identified were detected in p53 wt non-HGSOC (Table 1B).

Table 1.

A. Distribution of Pathogenic Variants (PVs) in Homologous Recombination (HR)-Related Genes, Including *BRCA1/2*, Identified in High-Grade Serous Ovarian Carcinomas (HGSOC) and non-HGSOC.					
	HGSOC (*n* = 320)	**non-HGSOC (*n* = 121)**	**All EOCs (*n* = 441)**		
Yield PVs in *BRCA1/2*	59[#] (18%)	2[±] (1.7%)	61 (14%)		
Yield PVs in HR-related genes	13[*] (4.1%)	7 (5.8%)	20 (4.5%)		
B. Yield of PVs in HR-related genes in non-HGSOCs.					
	Non-HGSOC				
	LGSOC (*n* = 32)	**EnOC (*n* = 24)**	**MC (*n* = 19)**	**CCC (*n* = 23)**	**Other [¶] (*n* = 22)**
Yield PVs in HR-related genes **HR-related gene with PV**	2 (6.3%) *CHEK, PALB2*	1 (4.2%) *ATM*	1 (5.3%) *CHEK2*	2 (8.7%) *ATM, FANCL*	1 (4.3%) *PALB2*[×]

¶ Including carcinosarcoma, malignant Brenner tumor, mixed-type histology, mesonephric-like adenocarcinoma, undifferentiated carcinoma and small cell carcinoma. # In two EOCs both a PV in *BRCA1* as well as *BRCA2* was detected: in total, n = 61 PVs in *BRCA1/2.* ± One LGSOC and one high risk grade 3 EnOC. * One EOC had a PV in *FANCL* and *CDK12*: in total, n = 14 PVs in HR-related genes in HGSOC. × Identified in a carcinosarcoma. HGSOC, high-grade serous ovarian cancer; LGSOC, low-grade serous ovarian cancer; EnOC, endometrioid ovarian carcinoma; MC, mucinous carcinoma; CCC, clear cell carcinoma; HR, homologous recombination; PV, pathogenic variant.

Figure 1 - 726

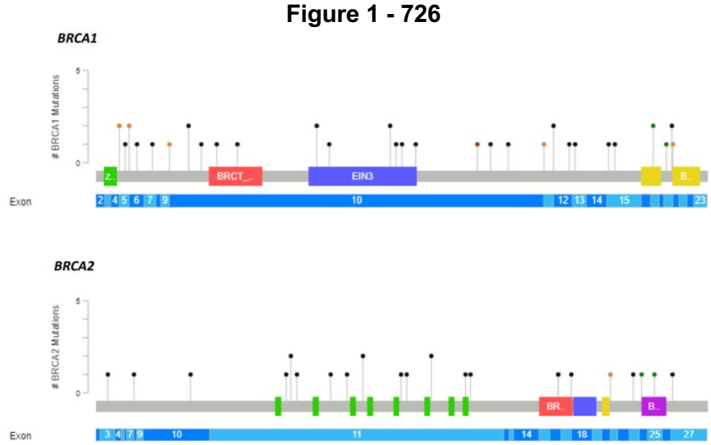

Figure 1. Spectrum of Pathogenic Variants Detected in Epithelial Ovarian Carcinomas in *BRCA1* and *BRCA2*, respectively. The colour of the circle indicates the mutation type; black = truncating, green = missense, brown = in frame, orange = splice site. The figure was prepared using the cBioPortal MutationMapper application.

Conclusions: From this large 'real-world' cohort of prospectively sequenced EOC we can confirm that *BRCA1/2* PVs are almost exclusively identified in HGSOC, which seems to justify a histotype-directed approach in *BRCA1/2* screening. Interestingly, PVs in HR-related genes other than *BRCA1/2* were identified in a significant proportion of non-HGSOC. Further germline and (functional) HRD tumor testing will help inform us about the clinical relevance of this finding in non-HGSOC.

727 High-risk Human Papilloma Virus RNA in-situ Hybridization Staining Patterns Outperform p16 Immunohistochemistry in Stratifying Cervical Squamous Dysplasia

Nicholas Ladwig[1], Karuna Garg[2]
[1]University of California, San Francisco, San Francisco, CA, [2]Cleveland Clinic, Cleveland, OH

Disclosures: Nicholas Ladwig: None; Karuna Garg: None

Background: The 2012 Lower Anogenital Squamous Terminology Standardization (LAST) project recommendations proposed that the three-tiered “-IN” system for cervical squamous dysplasia be collapsed into a two-tiered system [low-grade squamous intraepithelial lesion (LSIL) and high-grade squamous intraepithelial lesion (HSIL)]. However, clinical management for squamous dysplasia of the uterine cervix in reproductive age patients requires stratification of HSIL into CIN2 or CIN3 to decide whether an excision procedure can be deferred. LAST recommends the use of p16 immunohistochemistry (IHC) to separate LSIL from HSIL in difficult cases. However, subsequent studies demonstrate that > 50% of LSIL show aberrant p16 IHC.

High-risk HPV RNA in-situ hybridization [HR-HPV RNA (ish)] has been suggested to show distinct patterns of staining in CIN1, CIN2, and CIN3. However, HR-HPV RNA (ish) staining patterns have not been scrutinized in detail to determine the utility of this stain to stratify squamous dysplasia.

Design: Cases of CIN1, CIN2, and CIN3 in which a consensus diagnosis was reached based on morphologic findings alone were stained with p16 and HR-HPV RNA (ish). p16 was considered aberrant/positive if diffuse block-like staining was noted. HR-HPV RNA (ish) staining was classified as either the transformative pattern (single or multiple punctate dot-like signal) or productive pattern (diffuse solid nuclear staining). Digital scanned slides were used for quantifying the extent and pattern of distribution of the transformative and productive patterns.

Results: HR-HPV RNA (ish) staining was confined to areas of squamous dysplasia with no staining in adjacent benign mucosa. Both LSIL and HSIL were HR-HPV RNA (ish) positive (transformative pattern) in 100% of cases, but the productive pattern was not always present, particularly in HSIL. Some cases of HSIL show single punctate nuclear HR-HPV RNA (ish) signals and may require high-power evaluation. The transformative pattern extends from the basal layer upwards, with the thickness of this pattern being greatest in CIN3 (CIN1 < CIN2 < CIN3).<cin2<cin3).<cin2<cin3).<cin2<cin3).< span=""></cin2<cin3).<cin2<cin3).<cin2<cin3).<> The productive pattern extends from the surface downwards, with the thickness of this pattern being greatest in CIN1 (CIN1 > CIN2 > CIN3).

CIN1 (n=20)		
	Cases	%
p16 (+)	12	60%
p16 (-)	8	40%
HRHPV (+)	20	100%
HRHPV (-)	0	0%

CIN2 (n=13)		
	Cases	%
p16 (+)	13	100%
p16 (-)	0	0%
HRHPV (+)	13	100%
HRHPV (-)	0	0%

CIN3 (n=10)		
	Cases	%
p16 (+)	10	100%
p16 (-)	0	0%
HRHPV (+)	10	100%
HRHPV (-)	0	0%

Transformative Pattern Quantification	CIN1	CIN2	CIN3
Cases with transformative pattern (%)	20 (100%)	13 (100%)	10 (100%)
Average thickness transformative pattern	54%	74%	89%
Maximum thickness of transformative pattern	100%	100%	100%
Minimum thickness of transformative pattern	13%	50%	47%

Productive Pattern Quantification	CIN1	CIN2	CIN3
Cases with productive pattern (%)	17 (85%)	7 (54%)	3 (30%)
Average thickness productive pattern	51%	15%	1%
Maximum thickness of productive pattern	87%	50%	12%
Minimum thickness of productive pattern	0%	0%	0%

Figure 1 - 727

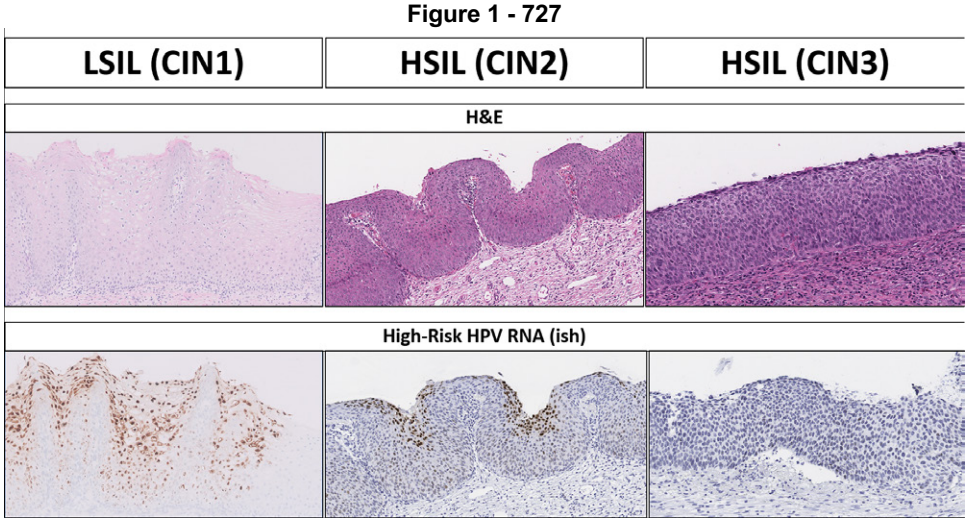

Conclusions: Aberrant p16 IHC does not distinguish LSIL from HSIL. The extent of productive pattern HR-HPV RNA (ish) staining separates LSIL and HSIL and helps in distinguishing CIN2 versus CIN3. HR-HPV RNA (ish) is more sensitive (100%) for LSIL compared to aberrant P16 IHC (60%).

728 Uterine Mesenchymal Tumors with SRF-RELA Gene Fusions

Yimin Li[1], Rui Bi[2], Dan Huang[1], Qianming Bai[3], Qianlan Yao[2], Xiaoyan Zhou[2], Wentao Yang[3]
[1]Fudan University Shanghai Cancer Center, Fudan University Shanghai Medical College, Shanghai, China, [2]Fudan University Shanghai Cancer Center, Shanghai Medical College, Fudan University, Shanghai, China, [3]Fudan University Shanghai Cancer Center, Shanghai, China

Disclosures: Yimin Li: None; Rui Bi: None; Dan Huang: None; Qianming Bai: None; Qianlan Yao: None; Xiaoyan Zhou: None; Wentao Yang: None

Background: In 2017, a subset of cellular variants of myofibroma and myopericytoma showing a smooth muscle-like immunophenotype and harboring recurrent SRF-RELA gene fusions were reported. These tumors mimic sarcomas with myogenic differentiation and might raise challenge in daily practice. Although the anatomic distribution is quite broad, no tumors in female genital system have been illustrated. Herein, we report the histological and immunophenotypical features of 3 uterine mesenchymal tumors with SRF-RELA gene fusions.

Design: Three consultation cases from Fudan University Shanghai Cancer Center with unique features were studied. Clinicopathological features were investigated and next-generation targeted RNA sequencing was performed using a 630 gene panel.

Results: All three patients experienced irregular menstruation. The age of them was 20, 22 and 39 years old respectively. Polyp or mass were found in the uterine and all of them underwent polypectomy. Grossly, the tumors were all well-circumscribed, ranged 20mm, 11mm and 35cm, respectively. Microscopically, all three tumors were composed of cellular oval to spindle cells, arranged in intersecting fascicles with variable amounts of collagen. The tumor cells were mild with either no mitotic figures in the first 2 cases and less than 2/10HPF in the third case. The most prominent feature of the tumor was clusters of rich capillary network. No necrosis was found. In the third case, entrapped endometrial glands and intraglandular stromal projections raised consideration for adenosarcoma. Immunohistochemical staining revealed strong ER and PR positivity in all three cases. Desmin and SMA were diffusely positive in all 3 cases. The first case was negative for h-caldesmon and the latter 2 cases had multifocal positivity. RNA sequencing analysis revealed SRF-RELA fusion in all three cases. In case 1, fusion of exon 4 of SRF gene with exon 9 of RELA gene and fusion of exon 5 of SRF gene with exon 8 of RELA gene were detected. In case 2, fusion of exon 5 of SRF gene with exon 8 of RELA gene was detected. In case 3, fusion of exon 5 of SRF gene with exon 9 of RELA gene was detected.

Figure 1 - 728

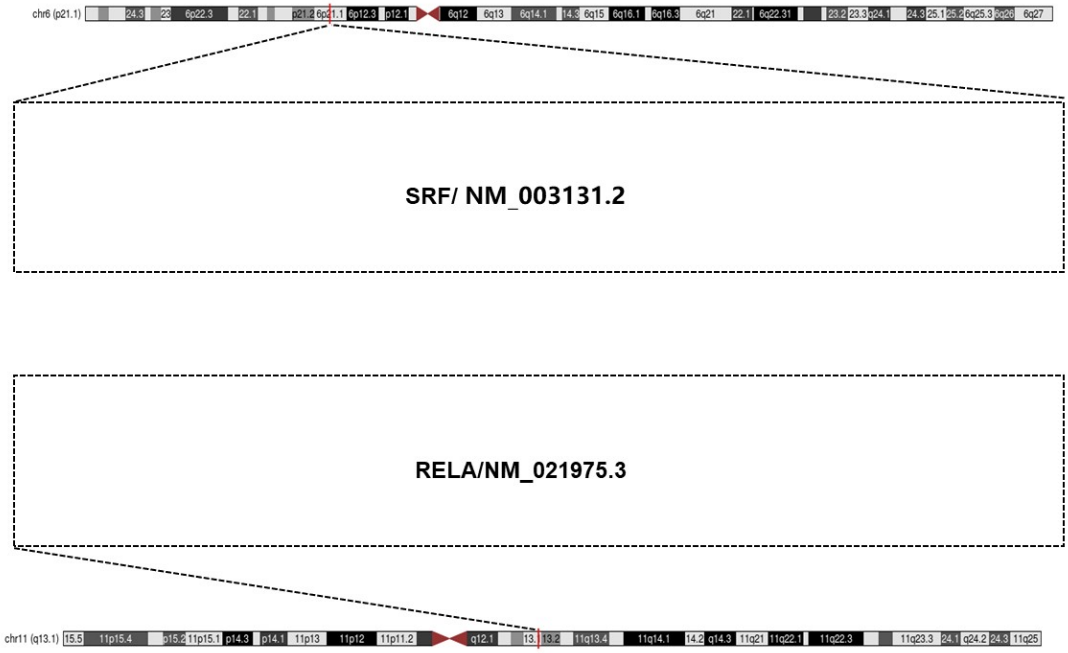

Figure 2 - 728

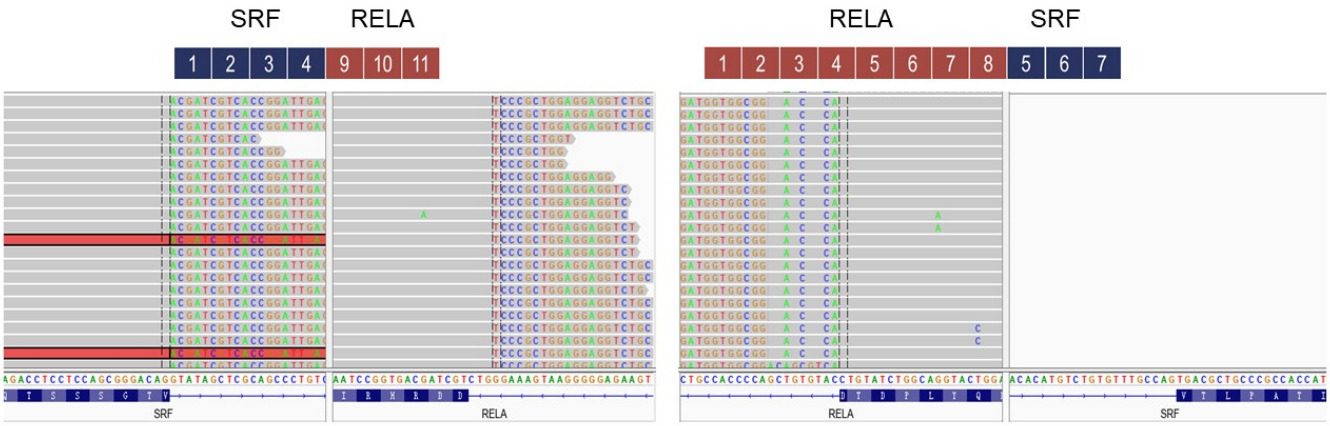

Fig 1. Schematic representation of SRF-RELA gene fusions in the first case.

Conclusions: We reported a special group of uterine tumors harbouring SRF-RELA fusion. These cellular tumors with strong positivity for myogenic markers should be differentiated from other common uterine smooth muscle tumors and adenosarcoma. Further studies with longer follow-up are needed to clarify the biological nature of this tumor.

729 Racial Disparities in Endometrial Carcinoma: An Analysis of Tumors from Black/African American Patients to Determine the Value of the TCGA Molecular Classification System in this Population

Brooke Liang[1], Peng Wang[2], Rishikesh Haridas[3], George Steinhardt[4], Katherine Kurnit[4], Nita Lee[4], David Chapel[5], Jennifer Bennett[4]

[1]Stanford Health Care, Stanford, CA, [2]University of Chicago Medical Center, Chicago, IL, [3]University of Chicago Medicine, Chicago, IL, [4]University of Chicago, Chicago, IL, [5]Michigan Medicine, University of Michigan, Ann Arbor, MI

Disclosures: Brooke Liang: None; Peng Wang: None; Rishikesh Haridas: None; George Steinhardt: None; Katherine Kurnit: None; Nita Lee: None; David Chapel: None; Jennifer Bennett: None

Background: The Cancer Genome Atlas (TCGA) study classified endometrial carcinomas (EC) into four novel, prognostically distinct molecular groups. However, only 12% (46/373) of women in that study identified as Black. It is well established that Black women tend to develop more aggressive EC histotypes, but genomic profiling of ECs in this population has received limited attention.

Design: ECs occurring over a period of 17 years were retrospectively identified. Inclusion criteria included 1) patient self-identification as Black, 2) at least 3 years of follow-up (or earlier if disease-specific death), 3) no neoadjuvant chemotherapy, and 4) no synchronous primary tumor. Slides were reviewed to provide a histotype according to current guidelines. Next-generation sequencing was performed using a 154-gene panel, and each tumor was assigned a TCGA molecular classifier (POLE, microsatellite unstable (MSI), copy-number low (CNL), copy-number high (CNH)). Data was compared to White women from the original TCGA cohort.

Results: Thus far, 102 ECs in the study cohort have been sequenced. TCGA classifier correlated strongly with EC subtype ($p<0.0001$) but not stage ($p=0.16$) (Fig 1). 5-year disease-specific survival (DSS) was significantly shorter for CNH tumors (58%) than POLE (100%; $p<0.0001$), CNL (100%; $p<0.0001$), and MSI (93%; $p=0.0002$) (Fig 2a). Similar results were observed for progression-free survival (PFS) (Fig 2b).

Distribution of TCGA classifiers differed significantly between Black and White women ($p=0.0006$), with more CNH tumors (44% vs 23%) and fewer CNL ECs (22% vs 42%) among Black women. 5-year DSS was significantly shorter in the study cohort (79% vs 90%; $p=0.01$; Fig 2c). In particular, Black women with CNH tumors had significantly decreased DSS compared to White women (58% vs 75%; $p=0.04$). There was no difference in PFS between the two groups.

Histotype distribution differed significantly between the study and TCGA cohorts ($p=0.0007$), with serous ECs more prevalent among Black women (31% vs 16%). BMI was significantly higher among Black than White women (median, 35 vs 33 kg/m^2; $p=0.02$), with no difference in age ($p=0.22$) or stage ($p=0.57$).

Disease-Specific and Progression-Free Survival between Study and TCGA Cohorts by TCGA Genomic Classification

Survival Measure	TCGA Classifier	Study Cohort (n=101*)	TCGA Cohort (n=171)	*P*-value
5-year DSS	Overall	79%	90%	0.01
5-year PFS		73%	73%	0.80
5-year DSS	CNH	58%	75%	0.04
5-year PFS		47%	52%	0.51
5-year DSS	CNL	100%	96%	0.33
5-year PFS		95%	63%	0.06
5-year DSS	MSI	93%	92%	0.76
5-year PFS		90%	83%	0.62
5-year DSS	POLE	100%	100%	N/A
5-year PFS		100%	100%	N/A

DSS=disease-specific survival; PFS=progression-free survival; CNH=copy number high; CNL=copy number low; MSI=microsatellite instability; N/A=not applicable. *1 case excluded from survival analysis as patient died due to surgery-related complications

Figure 1 - 729

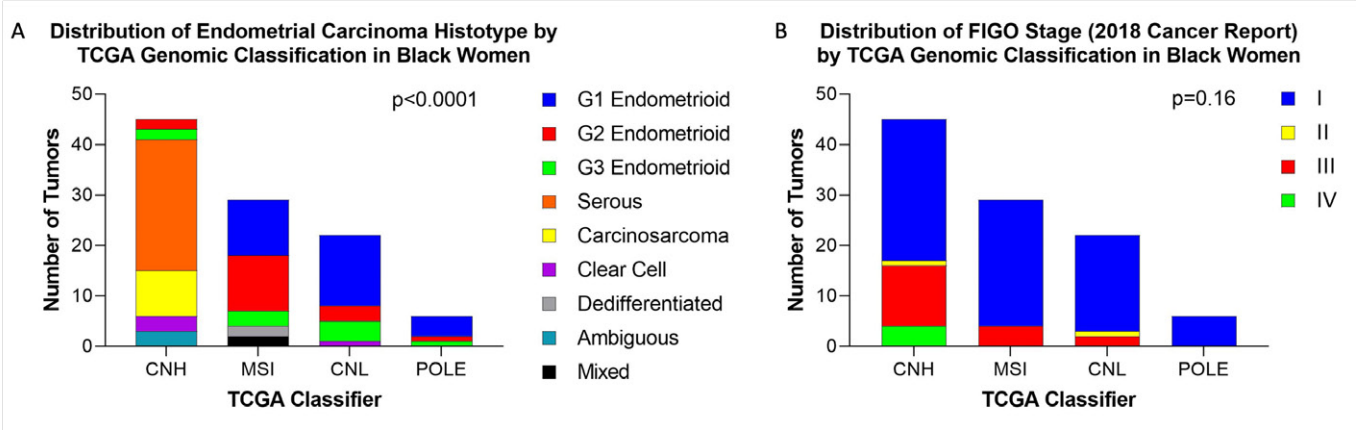

Figure 2 - 729

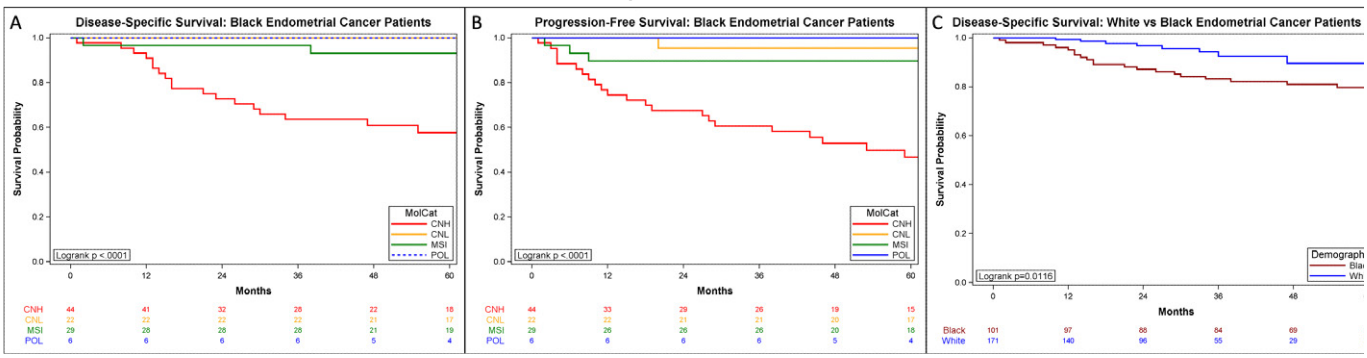

Conclusions: Black women show different distributions of EC histotype (serous enriched) and TCGA classifiers (CNH dominant), and significantly decreased DSS in contrast to White women. While further study is necessary to explore the pathobiology behind this difference, our data suggest that TCGA classifiers are prognostically relevant in Black women.

730 Epithelial-to-Mesenchymal Transition and Immune Evasion of Tubal Mucosae Play a Role for Ovarian HGSC Development in Women with Germline BRCA1 Mutation

Wanrun Lin[1], Yan Wang[1], Yiying Wang[2], Wenxin Zheng[1]
[1]UT Southwestern Medical Center, Dallas, TX, [2]Henan Provincial People's Hospital, Zhengzhou, China

Disclosures: Wanrun Lin: None; Yan Wang: None; Yiying Wang: None; Wenxin Zheng: None

Background: High-grade serous carcinoma (HGSC) is the most frequent and lethal type of ovarian cancer. Tubal secretary cells are assumed to be the origin of ovarian HGSC and *BRCA* mutations are a high-risk for HGSC. However, the molecular mechanisms remain elucidated. Single cell RNA sequencing (scRNAseq) potentially may reveal early events in this process.

Design: Three women with *BRCA1* germline mutation (*BRCA1*$^+$) and 3 age-matched normal controls (non-*BRCA1* carriers, *BRCA1*$^-$) were recruited for the study. Fresh fallopian tubal samples were obtained after IRB approval. The scRNAseq was performed by the 10x Genomic single-cell 5' VDJ library platform. Single-cell gene expression and T-cell receptor (TCR) libraries were generated according to the manufacturer's instructions. Differential gene expression analyses, characterization of epithelial-to-mesenchymal transition (EMT), cluster analysis, single cell pseudotime trajectory analysis, and RNA velocity-based cell fate tracing were performed by bioinformatics expert.

Results: Exploring the transcriptomes of 19,008 cells, predominantly from *BRCA1*$^+$ samples, we identified 5 major cell populations in the fallopian tubal mucosae. The secretory cells of *BRCA1*$^+$ samples had differentially expressed genes involved in tumor growth and regulation, chemokine signaling, and antigen presentation. A subset of tubal secretory cells from one *BRCA1* carrier exhibited an EMT phenotype, which was also present in the mucosal fibroblasts. Importantly, we identified a previously unreported

phenotypic split of the EMT secretory cells with distinct evolutionary endpoints. Furthermore, we observed increased clonal expansion among the $CD8^+$ T cell population from *BRCA1*$^+$ samples. Among those clonally expanded $CD8^+$ T cells, PD-1 was significantly increased in tubal mucosae of *BRCA1*$^+$ patients compared with that of normal controls. Immunohistochemically, representative markers of EMT and immune cells from the scRNAseq study findings were validated in the tubal sections of normal and serous tubal intraepithelial carcinoma.

Conclusions: The results indicate that EMT process and immune evasion in normal tubal mucosae may represent early events to allow tubal epithelial cells of *BRCA1*$^+$ carriers having growth advantage over those non-*BRCA1*$^+$ carriers. The findings provide a probable molecular mechanism explaining why some women with *BRCA1* germline mutation present with early development and rapid dissemination of the HGSC.

731 Loss of MHC Class I Expression in Ovarian Clear Cell Carcinoma is Associated with Fewer CD8-Positive Tumor-Infiltrating Lymphocytes and Shorter Survival in FIGO Stage I/II Patients

Shih-Yao Lin[1], Jen-Fan Hang[1], Yen-Yu Lin[1], Chiung-Ru Lai[1], Yi-Jen Chen[1]
[1]Taipei Veterans General Hospital, Taipei, Taiwan

Disclosures: Shih-Yao Lin: None; Jen-Fan Hang: None; Yen-Yu Lin: None; Chiung-Ru Lai: None; Yi-Jen Chen: None

Background: Major histocompatibility complex (MHC) class I is a key molecule in antigen presentation, which is essential for cytotoxic T cell responses. An association between the loss of MHC class I and fewer CD8-positive tumor-infiltrating lymphocytes (CD8+ TILs) has been demonstrated in several cancer types, suggesting a role in immune evasion. Recent studies also found the loss of MHC class I in some PDL1-positive cancers as a possible resistance mechanism to anti-PD1/PDL1 therapy. The above findings have not yet been evaluated in ovarian clear cell carcinoma (OCCC). This study aimed to evaluate MHC class I, CD8, and PDL1 expression in OCCC and to correlate the results with clinicopathological features.

Design: A retrospective search of OCCCs from surgical pathology archives between 2009 and 2019 was performed. Clinical data and pathologic slides were reviewed. Immunohistochemistry for MHC class I, CD8, and PDL1 (SP263) was performed on the tissue microarrays. MHC class I expression in tumor cells was classified as intact (>90% of the tumor cells), subclonal loss (10-90% of the tumor cells), or diffuse loss (<10% of the tumor cells). Cases showing subclonal or diffuse loss were grouped together for statistical analysis. The number of intraepithelial CD8+ TILs per high power field was quantified. PDL1 staining in tumor cells was scored and ≥1% was defined as positive. Progress-free survival (PFS) and overall survival (OS) were analyzed.

Results: A total of 76 cases were included. Thirty-two (42.1%) cases showed subclonal (34.2%) or diffuse (7.9%) loss of MHC class I expression. CD8+ TILs were significantly fewer in cases showing loss of MHC class I expression (P=0.015). Twenty-one (27.6%) cases were PDL1-positive, and 9 (42.9%) of them showed loss of MHC class 1 expression. Univariate analysis demonstrated that loss of MHC class I expression was significantly associated with shorter PFS in FIGO stage I/II patients (P=0.028) (Figure 1) but not in FIGO stage III/IV patients (Figure 2). The association was insignificant for OS. Multivariate analysis did not reveal survival differences in cases showing loss of MHC class I expression after adjusting for age, FIGO stage, residual disease, CD8+ TILs, and PDL1 expression.

Figure 1 - 731

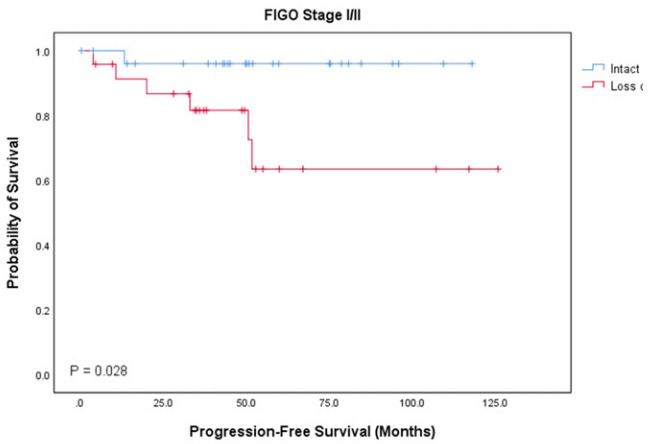

Figure 2 - 731

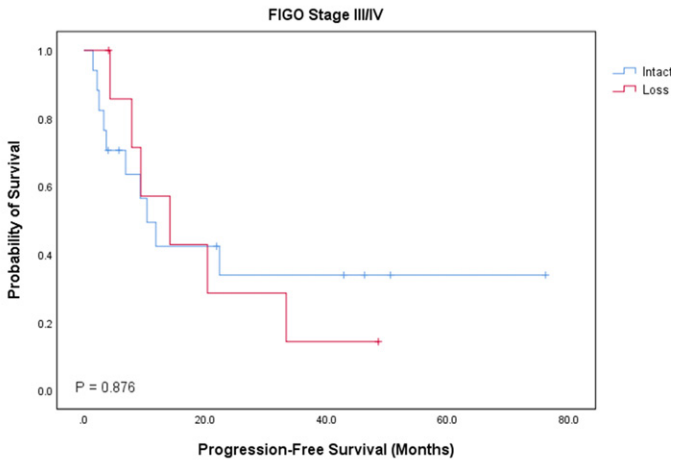

Conclusions: Loss of MHC class I expression was associated with fewer CD8+ TILs in OCCC and shorter PFS in patients with FIGO stage I/II diseases. Nearly half of the PDL1-positive OCCCs showed loss of MHC class I and might be associated with a poor response to anti-PD1/PDL1 therapy.

732 Reporting Responses to Progestin Therapy in Atypical Endometrial Hyperplasia or Well Differentiated Endometrioid Carcinoma

Wanrun Lin[1], Yan Wang[1], Ruijiao Zhao[2], Yiying Wang[2], Yue Wang[3], Yuxin Liu[4], Wenxin Zheng[5]
[1]UT Southwestern Medical Center, Dallas, TX, [2]Henan Provincial People's Hospital, Zhengzhou, China, [3]Henan Provincial People's Hospital, People's Hospital of Zhengzhou University, School of Clinical Medicine, Henan University, Zhengzhou, China, [4]Mount Sinai Health System, New York, NY, [5]UTSouthwestern Medical Center, Dallas, TX

Disclosures: Wanrun Lin: None; Yan Wang: None; Ruijiao Zhao: None; Yiying Wang: None; Yue Wang: None; Yuxin Liu: None; Wenxin Zheng: None

Background: Patients with atypical endometrial hyperplasia or endometrial endometrioid carcinoma (AEH/EEC) are commonly treated with progestin. Pathologists play a major role to properly interpret the progestin treated endometrial biopsies. However, no uniform reporting categories are available, no studies on reproducibility and no large studies correlating to histologic findings and clinical outcomes were performed. A uniform reporting system is needed.

Design: A survey including 20 progestin-treated endometrial samples was sent to 25 gynecologic pathologists. The survey was reviewed twice by each pathologist with the first time without any guidelines, while the second time survey provided quantitative and specific diagnostic categories. Pathology reporting for the first survey was mainly based on individual pathologists' experience and the way they got used to report. The second survey was not sent out until the first survey completed. Each case contained a brief history and representative H&E pictures. The diagnostic guidelines provided the responsive categories include 1) non-response or persistent/recurrent disease, partial or uncertain response, and complete response or fully decidualized/optimally treated. Each responsive component was quantified with a percentage based on the pictures viewed.

Results: A total of 1000 survey responses was received with 500 from the first round, and additional 500 from the second round. The results from the first survey were inconsistent among pathologists with various descriptive phrases/diagnoses cross the board. Presence or absence of residual disease was mentioned by 12/25 (48%) participants; Management recommendation was mentioned by 4/25 (12%) pathologists. In contrast, the second survey showed a significantly uniformed report. All (100%) pathologists quantitively reported three different responsive components for each case. Percentage variations for all three components ranged from 5-30% with the most variations for the partial or uncertain responses. For the cases with partial responses only, 21/25 (84%) made a diagnostic comment to clarify uncertainty for residual/recurrent diseases and recommended follow-up biopsies.

Conclusions: Current pathology reporting responses to progestin therapy needs to be unified. The proposed reporting system including non-, partial, and complete responses with quantitative analyses for each category may be easily applied in practice and ultimately improve patient care.

733 ARID1A Regulates Progesterone Receptor Expression in Endometrial Carcinoma and xAtypical Hyperplasia

Ying Liu[1], Shiho Asaka[2], Tian-Li Wang[1], Ie-Ming Shih[3]
[1]Johns Hopkins Medical Institutions, Baltimore, MD, [2]Shinshu University School of Medicine, Matsumoto, Japan, [3]Johns Hopkins Hospital, Baltimore, MD

Disclosures: Ying Liu: None; Shiho Asaka: None; Tian-Li Wang: None; Ie-Ming Shih: None

Background: Progesterone is a key hormone in the endometrium that prevents unopposed estrogen driven overgrowth. Loss of progesterone receptor (PR) expression is an established risk factor for endometrial atypical hyperplasia and endometrioid carcinoma. ARID1A is one of the most commonly mutated genes in endometrioid carcinomas and its loss of expression is associated with disease progression. We sought to investigate the role of ARID1A in PR expression in human and murine endometrial epithelial lesions.

Design: We performed immunohistochemistry to correlate the protein expression among ARID1A, ER, and PR in 50 endometrial atypical hyperplasia and 75 primary endometrial carcinomas obtained from endometrial curettages and hysterectomies specimen. Genome-wide chromatin immunoprecipitation sequencing (ChIp-seq) and RNA sequencing (RNA-seq) were performed on the two independent clones of human endometrial epithelial ARID1A-/- and ARID1A+/+ cells. We used Arid1a conditional knockout as well as Pten and Pten/Arid1a conditional knockout mouse models to investigate PR expression in normal endometrial epithelial cells as well in endometrial carcinoma and atypical hyperplasia. Statistical analyses were performed using GraphPad Prism software.

Results: PR expression was significantly lower in ARID1A deficient low-grade endometrial carcinomas and atypical hyperplasia ($p = 0.0002$). Genome-wide ChIp-seq and RNA-seq in isogenic ARID1A-/- and ARID1A+/+ human endometrial epithelial cells revealed that ARID1A-/- cells showed significantly less ChIP-seq signals of ARID1A, BRG1, and H3K27AC at the PR enhancer region and less PR mRNA levels. An Arid1a conditional knockout murine model revealed that epithelial PR expressions was decreased in normal endometrial epithelial cells of Arid1a-/- mice compared with those of Arid1+/+ mice. Moreover, using Pten and Pten/Arid1a conditional knockout murine models, Pten-/-/Arid1a-/- mice showed significantly decreased epithelial PR expressions in endometrial carcinoma and atypical hyperplasia compared with Pten-/-/Arid1a+/+ mice ($p = 0.003$ and $p < 0.0001$, respectively).

Conclusions: Our in vitro and in vivo results suggested in endometrioid carcinomas, inactivating ARID1A mutations downregulates PR expression by modulating its enhancer regions. This was also supported by loss of ARID1A correlated with a decreased expression of PR but not ER in low-grade endometrioid carcinomas and atypical hyperplasia based on patient specimen.

734 Gastrointestinal Stromal Tumors Mimic Gynecologic Disease: Clinicopathological Analysis of 14 Cases

Ying Liu[1], Maryam Shahi[2], Deyin Xing[3]
[1]Johns Hopkins Medical Institutions, Baltimore, MD, [2]Mayo Clinic, Rochester, MN, [3]Johns Hopkins Hospital, Baltimore, MD

Disclosures: Ying Liu: None; Maryam Shahi: None; Deyin Xing: None

Background: Gastrointestinal stromal tumors (GISTs) most often occur in the stomach, small intestine. When occasionally presented as pelvic mass, diagnosis could be challenging because of overlying features with gynecological neoplasms.

Design: 32 cases of GIST were identified our institution between 2000 and 2021 through search of “gastrointestinal stromal tumors” and “pelvic mass”. Of which, 14 cases with slide availability, including 7 cases from in-house service, and the remaining 7 cases from consultation files. Histologic and clinicopathological features, including clinical presentation, age at diagnosis, operative procedure, tumor site and size, and follow-up information were analyzed.

Results: In this series of 14 cases, the median age was 52 years (range 23-83). 11 patients presented with pelvic/omental/adnexal/uterine mass and/or abdominal pain concerning for gynecological disease. 2 patents presented with the same symptoms with history of GIST and 1 patient presented with posterior vaginal mass between vagina and rectum. On gross examination, ovary/ovaries were involved in 3 cases, uterus 2 cases, broad ligament 1 case, and vagina 1 case. Histologically, 9 cases were classified as high-grade (3 spindle type and 6 mixed epithelioid and spindle type) and 5 low-grade (3 spindle type, 1 epithelioid type, and 1 mixed epithelioid and spindle type) based on the mitotic count. All tumors were diffusely immunereactive for C-Kit. DOG-1 was also diffusely positive (tested in 8 cases) and CD34 displayed focal to diffuse positivity (tested in 9 cases). All tested tumors (10 cases) were negative for Desmin. Mutational analysis was performed in 5 cases and of which, 4 cases had C-Kit mutation and 1 with FGFR3 mutation. Interestingly, 3 tumors also harbored RB1 mutations in addition to either C-Kit or FGFR3 mutation. One tumor developed a second C-Kit mutation that conferred resistance to Gleevec treatment. Follow-up information was available for 9 cases with median time 94 months (range 18-178). 3 patients died of the disease and 1 patient died of another malignancy.

Conclusions: GIST can mimic gynecologic disease and pose a diagnostic challenging, especially in biopsy/excisional specimen. The main differential diagnosis are smooth muscle tumor, metastatic endometrial stromal tumor, and ovarian sex-cord stromal tumor (fibroma/fibrothecoma and adult granulosa cell tumor if with epithelioid morphology). A combination of clinical history, morphology as well as immunophenotype can facilitate the diagnosis.

735 Molecular Genetic Evidences Support the Benign Connotation of Struma Ovariis and Ovarian Carcinoids

Congrong Liu[1], Xiaojie Sun[2], Yan Liu[3]
[1]Peking University Third Hospital, China, [2]Peking University Health Science Center, Beijing, China, [3]School of Basic Medical Sciences, Third Hospital, Peking University Health Science Center

Disclosures: Congrong Liu: None; Xiaojie Sun: None; Yan Liu: None

Background: Although the origin from germ cells is well documented in ovarian monodermal teratomas, the molecular characteristics and pathogenesis of struma ovariis and ovarian carcinoids are less well studied.

Design: Here we performed short tandem repeat genotyping on 21 ovarian carcinoids and 52 struma ovariis, in which 42 cases were applied to Nanostring mRNA profiling based on oocyte development-specific genes. Additionally, 58 struma ovariis, 24 ovarian carcinoids, 24 papillary thyroid carcinomas and 30 nodular goiters were subjected to immunohistochemistry of CD117, whereas 24 ovarian carcinoids and 72 gastroenteropancreatic neuroendocrine neoplasms (NENs) were investigated to PAM and menin protein.

Results: We found significant higher homozygosity in struma ovariis (63.5%, 33/52) than that in ovarian carcinoids (28.6%, 6/21), especially in struma ovariis without mature teratoma. According to mRNA profiling, we clearly identified three clusters. Cluster 1 (mainly struma ovariis) highly expressed the representative genes of germline, oogenesis stage and BMP pathway. In line with high-level transcription of *KIT* gene in Cluster 1, CD117 presented strong intensity in struma ovariis, similar to the regenerative microfollicles in nodular goiters. Conversely, ovarian carcinoids, mature thyroid follicles with colloid and papillary thyroid carcinomas showed absent or weak CD117 staining. Thus, most struma ovariis are most likely derived from oogenesis-stage oocytes, which has escaped from meiotic arrest and entered thyrocyte differentiation. Cluster 2 consisted of 15 ovarian carcinoids and demonstrated upregulation of *PAM*, *RFX6* and *SYT5*, which indicated the cellular origin from oocytes in primordial to primary follicle and the differentiation toward neuroendocrine lineage. We confirmed the intensive cytoplasmic granular expression of PAM protein and nuclear staining of menin in ovarian carcinoids, which were significantly stronger than gastroenteropancreatic NENs. Cluster 3 included four ovarian carcinoids and two struma ovariis, with homozygosity in half. This cluster harbored active transcription of almost all stage-specific genes.

Table 1. Comparison of menin and PAM expression in ovarian carcinoids and gastroenteropancreatic neuroendocrine tumors

Histology	Ovarian carcinoid	NET (G1+G2)	NET (G3)+NEC
Number	24	56	16
menin			
Positive number (%)	24 (100%)	43 (76.8%)	14 (87.5%)
IHC score(X±S)	7.1 ± 4.1	4.1 ± 3.9	7.1 ± 4.8
Moderate to strong (IHC score≥4) number (%)	18 (75%)	29 (51.8%)	12 (75.0%)
P value (vs ovarian carcinoid)	—	0.002	0.948
PAM			
Positive number (%)	22 (91.7%)	55 (98.2%)	15 (93.8%)
IHC score (X±S)	3.1 ± 1.2	2.2 ± 0.9	1.5 ± 0.7
Moderate to strong (IHC score≥3) number (%)	18 (75.0%)	26 (46.4%)	1 (6.1%)
P value (vs ovarian carcinoid)	—	0.001	<0.001

Figure 1 - 735

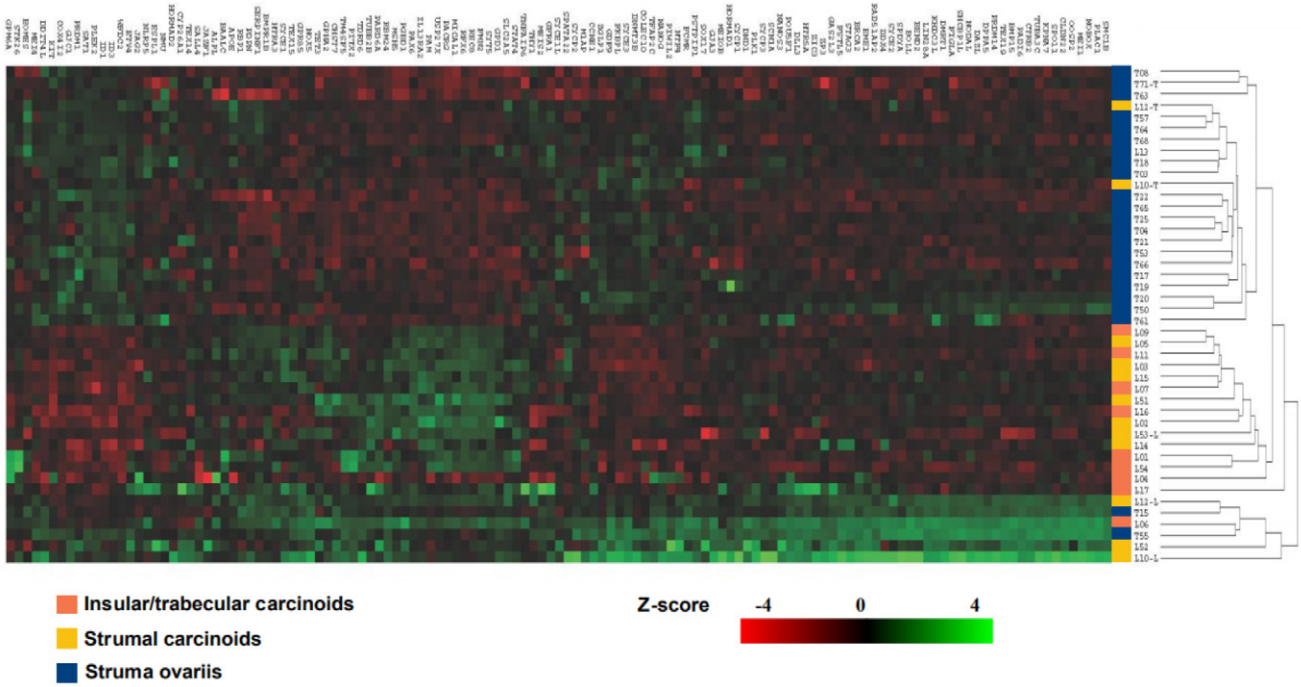

Figure 2 - 735

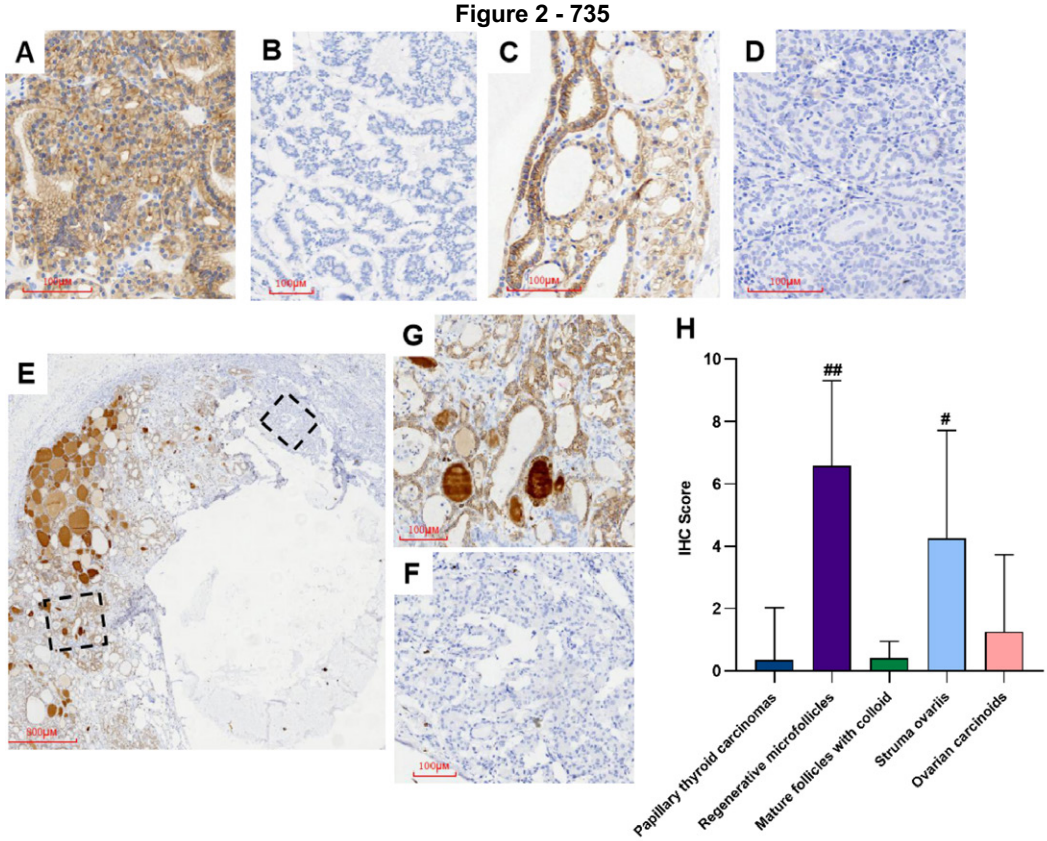

Conclusions: Overall, both ovarian carcinoids and struma ovariis arise from germ cells in different developmental stages that has fallen into meiotic failure and switched on different lineage differentiation. Our work provides key insights into developmental origin and molecular features of ovarian carcinoids and struma ovariis.

736 A Comparison Study Between Preoperative Imaging and Histological T-Staging of Endometrial Cancers

Trang Lollie[1], Yuna Kang[1], Nora Ostrzega[1], Neda Moatamed[1]
[1]David Geffen School of Medicine at UCLA, Los Angeles, CA

Disclosures: Trang Lollie: None; Yuna Kang: None; Nora Ostrzega: None; Neda Moatamed: None

Background: Endometrial cancer is the most common type of gynecological malignancy. Patients' intraoperative management depends on the type of tumor, grade and the pathological tumor (T) stage. This study was designed to compare the diagnostic performance of preoperative imaging studies to the final pathology diagnosis and T-staging.

Design: A retrospective review of 179 endometrial cancer cases from March 2016 to October 2019 was obtained through an electric medical records search (Epic/Beaker) of hysterectomy specimens with corresponding preoperative CT (with or without PET) and MRI scans that report myometrial and cervical stromal invasion or extrauterine metastasis. American Joint Committee on Cancer (AJCC) staging system was followed to determine the pathologic T-stage of the tumors. T-stage "1a" designates tumors limited to the endometrium or invading less than half (<50%) of the myometrium. T-stage "1b" designates tumors that invade ≥50% of the myometrium. T-stage "2" designates tumors invading the cervical stroma. T-stage "3" designates tumors involving serosa, adnexa, vagina, or parametrium.

Results: Thirty-two cases met our inclusion criteria. Of the 11 cases that were diagnosed as grade 1 endometrioid adenocarcinoma, 3 cases (27%) had discordant imaging findings. Of the 10 cases diagnosed as grade 2 endometrioid adenocarcinoma, 4 cases (40%) had discordant imaging findings. Two cases diagnosed as grade 3 endometrioid adenocarcinoma

(100%) were both discordant. Five cases with high grade serous cancer (HGSC) were all concordant. Two cases of clear cell carcinoma had 50% discordance. Additionally, there was one case of carcinosarcoma and one with undifferentiated carcinoma, both had concordant imaging findings. Overall, 39% of all endometrioid adenocarcinomas were discordant, while in non-endometrioid endometrial cancers, 11% were discordant.

Table 1. Summary of the histological results with T-stages and correlation with imaging findings

Histological diagnosis	n	Patients' Age	T1a stage	T1b Stage	T2 Stage	T3 Stage	Radiology concordant	Radiology discordant
Endometrioid, FIGO I	11	29-71	9	2	0	0	8	3
Endometrioid, FIGO II	10	53-75	4	3	0	3	6	4
Endometrioid, FIGO III	2	54-69	1	1	0	0	0	1
High grade serous Carcinoma	5	63-78	1	1	2	1	5	0
Clear cell carcinoma	2	37-76	2	0	0	0	1	1
Undifferentiated carcinoma	1	54	0	0	1	0	1	0
Carcinosarcoma	1	85	0	0	0	1	1	0

Conclusions: The highest rate of discordance was seen in cases with endometrioid adenocarcinoma. In addition to the increased cost of the mentioned imaging work-up, our study shows that preoperative radiology work-up is not accurate with pathologic T-stages for endometrioid endometrial adenocarcinomas.

737 MMR, PD-L1, and MHC Class I and Response to Checkpoint Inhibitor Therapy in Endometrial Carcinomas

Ngome Makia[1], Brooke Howitt[2], Elizabeth Gaughan[3], Kari Ring[1], Anne Mills[1]
[1]University of Virginia, Charlottesville, VA, [2]Stanford Medicine/Stanford University, Stanford, CA, [3]University of Virginia Health System, Charlottesville, VA

Disclosures: Ngome Makia: None; Brooke Howitt: None; Elizabeth Gaughan: None; Kari Ring: None; Anne Mills: None

Background: Loss of MHC Class I (MHC I) expression represents a putative mechanism of resistance to checkpoint inhibitors. However, its impact on therapeutic response has not been established, particularly in the context of established biomarkers such as mismatch repair (MMR) proteins and PD-L1.

Design: MHC I, PD-L1, and MMR immunohistochemistry was assessed on pre-treatment whole tissue sections of 20 endometrial cancers from patients treated with anti-PD-1/PD-L1 checkpoint inhibitor therapy either in isolation (n=9), or in combination with other therapies (n=11).

Results: Tumors consisted of 11 endometrioid, 2 dedifferentiated, 1 clear cell, and 6 serous carcinomas. Immunohistochemical staining was done on whole sections from the pre-treatment primary. 80% (16/20) were PD-L1+ with a Combined Positive Score (CPS) ≥1. 55% (11/20) had subclonal MHC I loss; no cases had complete loss. 45% (9/20) were MMR-deficient. 14 cases had available response data, and 57% (8/14) showed either complete/partial response or disease stabilization. One dedifferentiated carcinoma demonstrated complete response, while 5 cases (4 endometrioid, 1 clear cell carcinoma) showed partial response. Two endometrioid carcinomas showed disease stabilization. The remaining 6 cases—including all 4 serous cancers with available data—had progressive disease. Of the 8 cases with either response or stable disease, 7 (87%) were MMR-deficient; the MMR-intact responder was the clear cell carcinoma. Notably, this case also lacked *POLE* mutations. All cases with response/stable disease (100%, 8/8) were PD-L1+, however PD-L1 expression was also seen in 67% (4/6) of progressive cases. Although MHC class I subclonal loss was overall more common in progressive cases than in response/stable disease (67%, 4/6 vs 37%, 3/8), two MMR-deficient endometrioid carcinomas with partial response and the MMR-deficient dedifferentiated carcinoma with complete response had subclonal loss of MHC I expression.

Figure 1 - 737

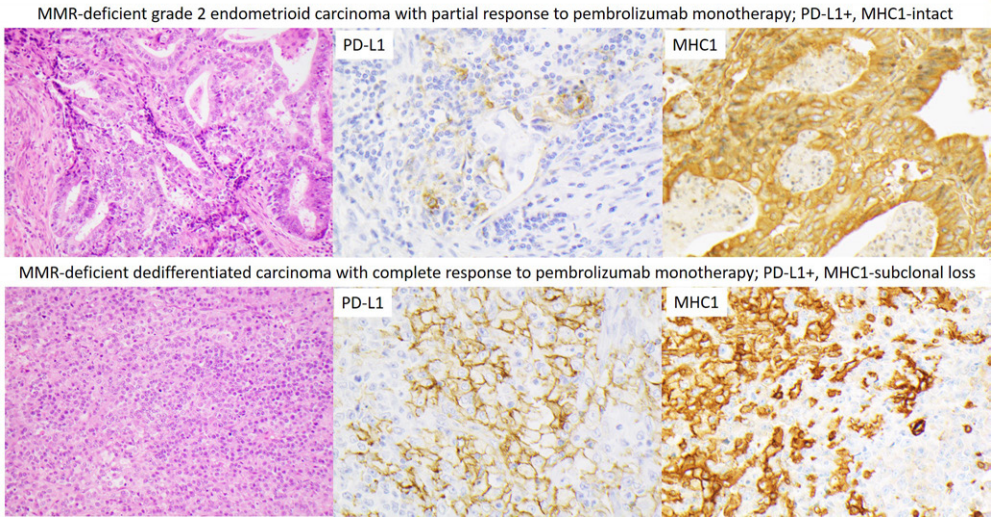

Conclusions: Anti-PD-1/PD-L1 response was more common in MMR-deficient endometrioid, clear cell, and dedifferentiated carcinomas than in tumors with intact MMR and serous histology. A positive PD-L1 CPS (≥1) captured all responders, but also identified many cases that failed to benefit. While there was a trend towards improved response in MHC I-intact tumors, subclonal loss of MHC I expression did not preclude successful disease stabilization and response to anti-PD-1/PD-L1 therapy, particularly in the context of deficient MMR.

738 Characterization of Lymphoid Landscape in Mesonephric-Like Carcinoma (MLCa) of the Ovary

Mario Marques-Piubelli[1], Cibelle Lima[1], Edwin Parra[1], Luisa Solis Soto[1], Auriole Tamegnon[1], Saxon Rodriguez[1], Renganayaki Pandurengan[1], Ignacio Wistuba[1], Anais Malpica[1], Preetha Ramalingam[1], Elizabeth Euscher[1]
[1]*The University of Texas MD Anderson Cancer Center, Houston, TX*

Disclosures: Mario Marques-Piubelli: None; Cibelle Lima: None; Edwin Parra: None; Luisa Solis Soto: None; Auriole Tamegnon: None; Saxon Rodriguez: None; Renganayaki Pandurengan: None; Ignacio Wistuba: *Advisory Board Member*, Genentech/Roche, Bayer, Bristol-Myers Squibb, Astra Zeneca, Pfizer, HTG Molecular, Merck, GlaxoSmithKline, Novartis, Sanofi, Daiichi Sankyo, Amgen, Oncocyte; *Consultant*, Flame; *Speaker*, Platform Health, AstraZeneca, Genentech/Roche; *Grant or Research Support*, Genentech, HTG Molecular, Merk, Bristol-Myers Squibb, Medimmune/Astra Zeneca, Adaptimmune, Adaptive, EMD Serono, Pfizer, Takeda, Amgen, Karus, Johnson & Johnson, Bayer, Iovance, 4D, Novartis, Akoya; Anais Malpica: None; Preetha Ramalingam: None; Elizabeth Euscher: None

Background: Extra-uterine mesonephric-like carcinoma (eMLCa) is rare. Although eMLCa has histologic and mutational overlap with low grade endometrioid Ca, it is associated with advanced stage disease and distant recurrences in some studies. Underlying mechanisms for this are not apparent by conventional microscopy. This study characterizes the tumor immune microenvironment of eMLCA utilizing an immune microenvironment panel of multiplex immunofluorescence (mIF).

Design: 15 eMLCa (2002-2021) were included in the study. Clinical information (age, primary site, FIGO stage, recurrence site, follow up) and genomic test results were obtained from the medical record. Formalin-fixed paraffin-embedded tissue was used to apply an immune microenvironment panel of mIF, including Pancytokeratin, εCD3, CD4, CD8, CD20, CD56, Foxp3, and Ki67 was validated and applied to the samples (Figure 1). Five intratumoral areas were selected from scanned images and analyzed using Inform software (v2.4.8). Cell densities of areas were correlated with clinicopathologic characteristics and outcome. ANOVA and Wilcoxon signed-rank test were performed using GraphPad Prism version 9.0.0 for Windows (GraphPad Software, San Diego, CA, USA, www.graphpad.com). A P value < 0.05 was considered significant.

Results: Table 1 summarizes clinicopathologic features. Mismatch repair protein (MMR) immunohistochemistry was performed on 6 cases; all showing intact expression. All cases had T-cells (CD3+) with a median cell density of 13.39 cells/mm^2 (range: 0.62 – 84.48). Among the T-cell subpopulations, CD4+ cells had a slightly higher median cell density compared to cytotoxic (CD3+CD8+)

(2.68 vs 2.49 cells/mm^2). B-cells (CD20+) were detected in 12/15 (80%) cases with a median of 1.47 cells/mm^2 (range: 0 – 13.85) and had a lower cell density compared with the T-cell population (p= 0.0004). T-regulatory cells (εCD3+ CD4+ Foxp3+) were detected in 12/15 (80%) cases and had a median cell density of 1.24 cells/mm^2 (range: 0 – 13.8) (Figure 2).

Clinicopathologic Features of eMLCa Cases

Case	Age	Primary Site	FIGO stage	Recurrence site	Patient outcome	Mutation detected
1	37	Ovary	I	Liver	AWD 37 mo	Not done
2	50	Ovary	I	None	Recent case	Not done
3	52	Ovary	I	None	Recent case	KRAS G12D, SPOP
4	60	Ovary	I	None	Recent case	Not done
5	64	Ovary	I	None	NED 8 mo	Not done
6	53	Ovary	II	None	LTF	Not done
7	48	Ovary	III	Pelvic Peritoneum	AWD 74 mo	NRAS exon 3
8	68	Ovary	I	Abdominal Peritoneum	AWD 18 mo	KRAS G12V
9	74	Ovary	II	Liver	AWD 36 mo	KRAS exon 3, PTEN
10	66	Ovary	III	Lung	AWD 31 mo	KRAS G12V, PIK3CA, TP53
11	61	Ovary	III	Lung	AWD 34 mo	NRAS exon 3
12	66	Peritoneum	IV	Lung	AWD 77 mo	TP53
13	69	Peritoneum	IV	Lung	DOD 45 mo	KRAS G12D
14	61	Ovary	I	None	LTF	Not done
15	51	Peritoneum	III	Lung	AWD 220 mo	KRAS G12C, PTEN

Figure 1 - 738

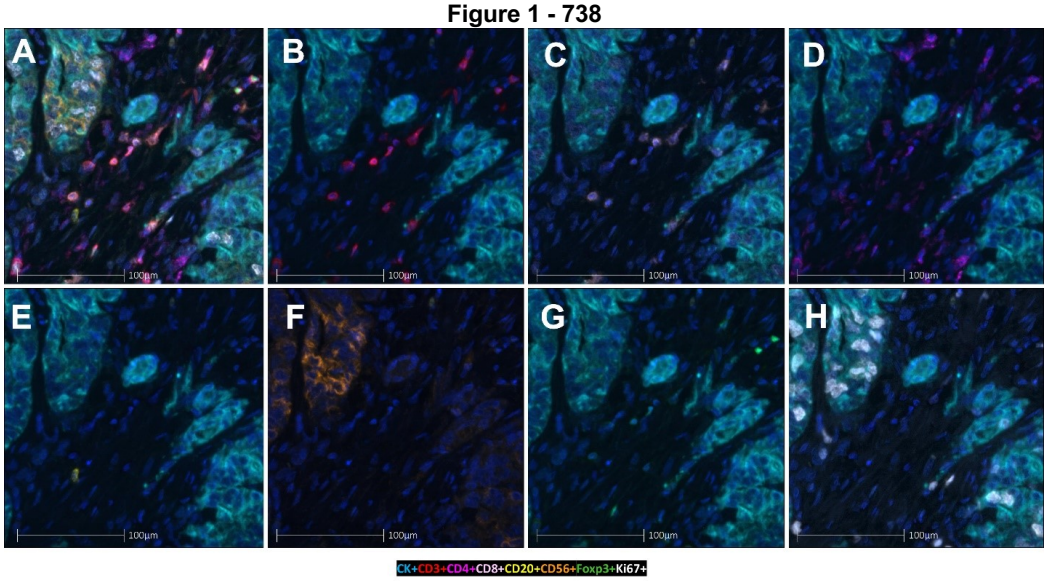

Figure 2 - 738

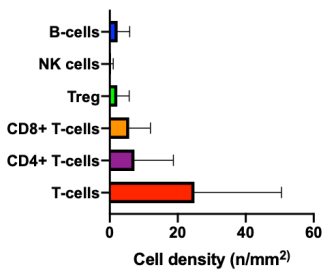

Conclusions: EMLCa has a unique lymphoid microenvironment characterized by overall low cell densities of lymphocytes and a predominant T-cell population. Microsatellite stability in all tested cases may correlate with this finding. The low density lymphocyte microenvironment offers potential insight into the reported aggressive of eMLCa. Further studies using larger cohorts are necessary to better characterize the diversity of immune landscape in eMLCa.

739 Uterine Leiomyosarcoma Associated with Leiomyoma with Bizarre Nuclei: Clinical, Histology and Molecular Analysis of Four Cases

Melissa Mejia Bautista[1], Victoria Fischer[2], Xinyan Lu[3], Jian-Jun Wei[4]
[1]McGaw Medical Center of Northwestern University, Chicago, IL, [2]The University of North Carolina at Chapel Hill, Chapel Hill, NC, [3]Northwestern University Feinberg School of Medicine, Chicago, IL, [4]Northwestern University, Chicago, IL

Disclosures: Melissa Mejia Bautista: None; Victoria Fischer: None; Xinyan Lu: None; Jian-Jun Wei: None

Background: Uterine leiomyosarcomas (LMS) are a rare group of aggressive malignancies with a high risk of recurrence, limited treatment options available, and poor prognosis. Leiomyoma with bizarre nuclei (LM-BN) is a rare variant of leiomyoma with remarkable atypia and overall benign clinical course. The diagnosis is challenging due to a wide range of overlapping histologic and molecular features between LM-BN and LMS. The potential association of these two tumor types has not been clearly established.

Design: To characterize the histologic and molecular relationship between existing LM-BN with LMS in four cases. Immunohistochemistry and whole-genome copy number alteration (Oncoscan) analysis were performed in both tumor components.

Results: We collected four cases of hysterectomy for LMS coexisting with LM-BN. The diagnosis was confirmed with the consensus of at least 3 gynecologic pathologists. The major clinical, histologic, and molecular findings were summarized in Table 1. Patient 1 had a tumor containing LMS and LM-BN with a clear transition between two components. Molecular analyses showed both areas shared segmental chromosomal losses at 1q, 11q, 14q, and 15q, LOHs at Xq, 3q, 9p, 10q, 11p and 13q, and Copy Neutral-Loss Of Heterozygosity (CN)-LOH at 1p, 2q, 4p, 4q, 5q, 19q and 22q. Patient 2 had a myomectomy with LM-BN. She presented with lung metastatic LMS 4-years later. Both LM-BN and LMS showed copy number losses at 4q, 5q, 7p, 7q, 13q, 14q, 16p, 16q, 17p and 19q, and same LOH pattern, including 2p, 4q, 5q, 7p, 7q, 15q, and 20q. Patient 3 had LMS immediately adjacent to LM-BN. Both components shared segmental losses at 13q, Xq, 16q, and 17q. One year later, she presented with a recurrence of LMS. Patient 4 had a hysterectomy with LM-BN and an iliac soft tissue mass consistent with LMS. LMS showed complex chromosomal aberrations, mostly independent from LM-BN. Further immunostaining demonstrated a non-Mullerian origin of LMS (negative for ER, PR, and WT-1). The histologic and molecular findings support a shared origin and connection between the LM-BN and LMS in three of four cases. One case shows a different tumor origin based on their IHC and genomic patterns.

Table 1. Summary of pathology and molecular characteristics of coexisting LM-BN and LMS

			Case 1	Case 2	Case 3	Case 4
Age			43	42	42	53
LM-BN	**Location**		Uterus	Uterus	Uterus	Uterus
	Size (cm)		6.0	5.0	7.8	1.6
	IHC	**Mitoses (HPF)**	2-3 /10	1-6 /10	Rare	Rare
		Ki67	<5%	10-20%	<5%	<5%
		P16	-	++	+++	+++
		P53	Mutant	WT	Mutant	Mutant
	CNA		**Loss:** 1q,11q, 14q, 15q **LOH:** Xq, 3q, 9p, 10q, 11p, 13q	**Loss:** 4q, 5q, 7p, 7q, 13q, 14q, 16p, 16q, 17p, 19q **LOH:** 2p, 4q, 5q, 7p, 7q, 15q, and 20q	**Loss:** 13q14.2, Xq, 16q, 17p	**Loss:** Xq, 1q,7p,13q
LMS	**Location**		Uterus	Lung Mets	Uterus	Iliac
	Size (cm)		7.5	Up to 3.4	7.8	8.1
	IHC	**Mitoses (HPF)**	24 /10	>50/10	12 /10	26 /10
		Ki67	50%	30%	30-40%	50%
		P16	-	+++	+++	+++
		P53	Mutant	WT	Mutant	WT
	CNA		**Loss:** 1p, 1q,11q, 2q, 4p, 4q, 5q, 14q, 15q, 19q, 22q **LOH**:Xq, 3q, 9p, 10q, 11p, 13q	**Loss:** 4q, 5q, 7p, 7q, 13q, 14q, 16p, 16q, 17p, 19q **LOH:** 2p, 4q, 5q, 7p, 7q, 15q, and 20q	**Loss:** 13q14.2, Xq, 16q, 17p	**Loss:** 1p,7, 8q, 9p, 10q, 11, 12p, 13q, 16q, 18q, and complex **LOH**: 17p.
Clonal origin: LMS from LM-BN			Yes	Yes	Yes	No

Conclusions: Coexisting of LM-BN and LMS is extremely rare. We demonstrated that LMS were clonal or shared molecular origin from existing LM-BN in three of four cases. Our findings suggest these two tumor types may share a common pathogenic pathway or represent different stages of tumor progression in certain cases.

740 Molecular Profiling of Endometrial Carcinomas with Heterogeneous Mismatch Repair Protein Expression

Rachelle Mendoza[1], Peng Wang[2], Jefree Schulte[3], Melissa Tjota[2], Ina Jani[1], Anna C Martinez[1], George Steinhardt[1], Elizabeth Kertowidjojo[2], S Diane Yamada[1], Jennifer Bennett[1]
[1]University of Chicago, Chicago, IL, [2]University of Chicago Medical Center, Chicago, IL, [3]University of Wisconsin-Madison, Madison, WI

Disclosures: Rachelle Mendoza: None; Peng Wang: None; Jefree Schulte: None; Melissa Tjota: None; Ina Jani: None; Anna C Martinez: None; George Steinhardt: None; Elizabeth A: None; S Diane Yamada: None; Jennifer Bennett: None

Background: Immunohistochemistry for mismatch repair proteins (MMR) in endometrial carcinoma (EC) is essential for Lynch syndrome screening, prognosis, and response to immunotherapy. On occasion, weak or patchy staining, usually due to poor fixation or technical failure, may be seen. While true heterogeneous expression (HE) (i.e. abrupt loss of staining adjacent to strong and diffuse staining) has been described, the clinical significance and molecular profile have not been well characterized.

Design: We retrospectively reviewed 310 ECs with available MMR stains for HE. In tumors with HE, each component was macrodissected and underwent next-generation sequencing on a 155-gene panel.

Results: MMR deficiency was present in 84 (27%) ECs, with most showing MLH1/PMS2 loss (73; 87%). HE was identified in 6 (2%) tumors (Figure 1, Table). Cases 1, 2, and 6 had HE of MLH1/PMS2 with retained MSH2/6. A recurrence in case 2 showed retained MMR. Case 3 had MLH1/PMS2 loss with *MLH1* hypermethylation and MSH2/6 HE. Case 4 showed PMS2, MSH2, and MSH6 loss with MLH1 HE. Case 5 had PMS2 HE with retained MLH1 and MSH2/6.

For cases 1 and 2, MMR-deficient foci were unstable by microsatellite analysis (MSI-H) with high tumor mutational burden (TMB) while MMR-retained areas were stable (MSS) with low TMB. Both components of cases 3 and 4 were MSI-H with high TMB. No MMR alterations were detected in cases 1 and 2, aside from a *MLH3* mutation in case 1; hence, HE is presumed secondary to subclonal *MLH1* hypermethylation. Identical *PMS2* and *MSH6* aberrations and *MLH1* hypermethylation were noted in case 3. As the MSH2/6-retained focus was ~1mm, contamination from the MSH2/6-deficient component likely occurred. Case 4 showed identical *MLH1* and *PMS2* mutations, with a *MSH6* mutations in the MLH1-retained focus. As this cannot be conceptually explained, further analysis is in process. Figure 2 depicts non-MMR gene alterations.

Case #	Age (years)	BMI (kg/m²)	Size (cm)	Tumor Type	FIGO Grade	TNM Stage (AJCC 8th edition)	FIGO Stage (2018)	MLH1	PMS2	MSH2	MSH6	MLH1 Hyper-methylation	Recurrence	Status (duration of follow up)
1	60	35	2.2	Endometrioid	1	pT1a N0	IA	H	H	R	R	Not performed	None	NED (150 months)
2*	61	37.2	5	Endometrioid	1	pT2 N2a	IIIC2	H	H	R	R	Not performed	Lung (22 months)	AWD (66 months)
3	57	22.1	4.5	Undifferentiated	N/A	pT2 N0	II	L	L	H	H	Present	None	NED (58 months)
4	57	48.7	4.3	Endometrioid	3	pT1b N0	IB	H	L	L	L	Not performed	None	NED (66 months)
5	62	48.7	2.1	Endometrioid	3	pT1a N0	IA	R	H	R	R	Not performed	None	NED (11 months)
6	64	38	3.8	Endometrioid	1	pT1a N0	IA	H	H	R	R	Pending (recent case)	N/A (recent)	N/A (recent)

H - heterogeneous; R - retained; NED - no evidence of disease; AWD - alive with disease ; N/A - not applicable; L- loss
*previously reported

Figure 1 - 740

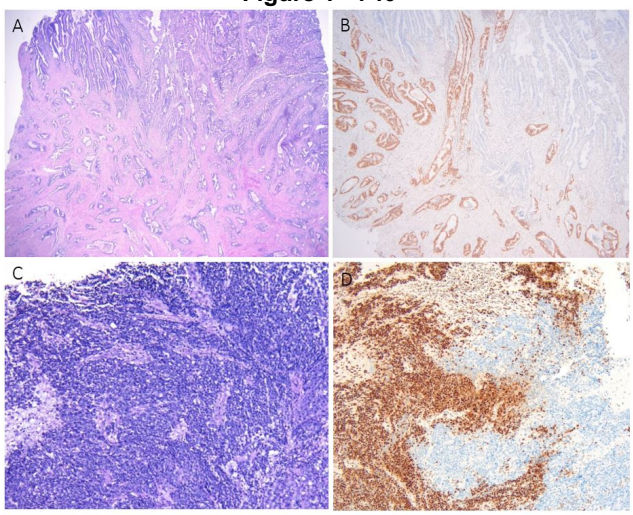

Figure 1. Case 2: Endometrial endometrioid carcinoma (A) with heterogeneous MLH1 expression (B). Case 3: Undifferentiated carcinoma (C) with heterogeneous MSH6 expression (D).

Figure 2 - 740

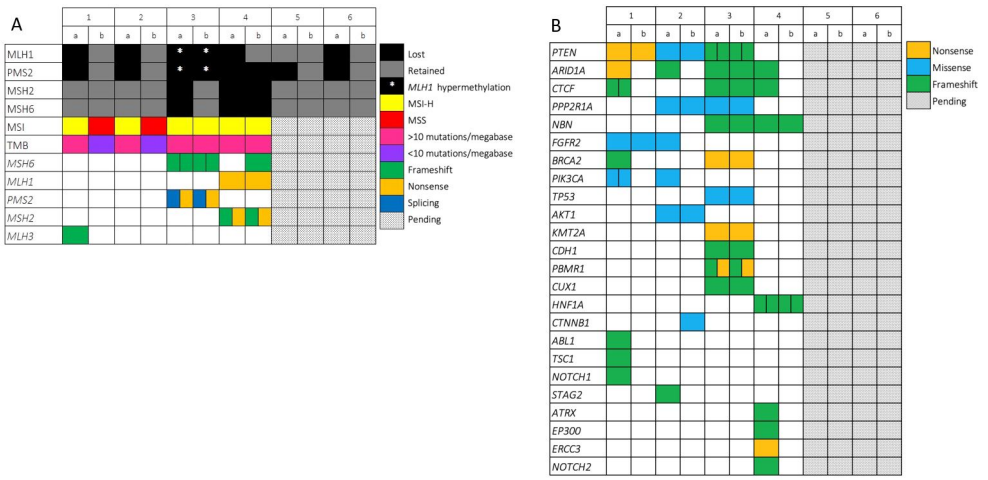

Figure 2. Immunohistochemical analysis, microsatellite instability results, and mismatch repair protein gene alterations in tumors with heterogeneous expression (A). Additional genomic alterations in tumors with heterogenous expression (B).

Conclusions: HE is rare in EC with two tumors showing heterogeneous MLH1/PMS2, favored to be due to subclonal *MLH1* hypermethylation. Both components of the other ECs had essentially identical MMR gene alterations, possibly secondary to technical failure. As only one patient recurred, HE requires further investigation in a larger cohort to assess its clinical significance. Currently, a tumor is considered MMR-retained if any nuclear staining is present, but our findings suggest HE should be recognized as a distinct pattern of MMR expression and any recurrences should be tested for MMR.

741 Uterine Malignancies in African American Women Show More Frequent Targetable Molecular Mutations

Rachelle Mendoza[1], Absia Jabbar[2], Elmer Gabutan[2], Tahmineh Haidary[3], Steve Xie[4]
[1]University of Chicago, Chicago, IL, [2]SUNY Downstate Medical Center, Brooklyn, NY, [3]UCI Medical Center, Irvine, CA, [4]Savannah, GA

Disclosures: Rachelle Mendoza: None; Absia Jabbar: None; Elmer Gabutan: None; Tahmineh Haidary: None; Steve Xie: None

Background: Uterine malignancies have consistently been reported to have higher frequency and poorer prognosis in African American women, yet investigations on the molecular basis of this disparity is limited. The objective of this study is to analyze the molecular profiles of uterine cancers in African American patients and compare the results with published data.

Design: Eighteen cases of uterine malignancy from African American patient population were retrospectively evaluated, and the cohort included 5 serous carcinomas, 5 endometrioid carcinomas, 2 sarcomas (rhabdomyosarcoma, undifferentiated sarcoma) and 6 carcinosarcomas (MMMT). Next-generation sequencing was performed on a representative tumor section. Clinical follow up data was obtained from electronic medical records.

Results: The most common mutated gene was *TP53* (15/18), which was observed even in low grade endometrioid carcinomas (2/5) and well differentiated sarcomas (2/2). *ERBB2* amplification was seen in most serous carcinomas (3/5), while *ERBB2* mutation was observed in carcinosarcoma (1/5). MMMT cases showed *PIK3CA* and *PTEN* mutations in addition to *TP53*, suggesting a background of endometrioid carcinoma. As expected, endometrioid carcinomas had mutations in *PIK3CA*, *PTEN* and mismatch protein genes (*PMS2* and *MSH6*). Six serous, endometrioid and MMMT cases harbored mutations in *ATM*, 4 of which were variants of unknown significance. Other than *TP53*, sarcoma cases had mutations in *PIK3CA*, *PTEN*, *FGFR1* and *POLE*. Interestingly, *KRAS* mutations were seen on endometrioid and carcinosarcoma, and not in serous.

The median follow up was 21.8 months. Three patients died of the disease (2 MMMT, 1 sarcoma), and two were alive with disease (1 MMMT, 1 endometrioid).

Case No.	Age (years)	BMI (kg/m²)	Tumor Size (cm)	Type	FIGO Grade	Pathologic Stage	FIGO Stage	Recurrences	Status at last follow up (months)
1	82	31.3	5	MMMT	High	pT1bN2a	IIIC2	None	Deceased (6.5)
2	67	43.27	5	MMMT	High	pT3a	IIIA	None	Alive, ND (26.7)
3	75	25.97	3.5	MMMT	High	pT1a	IA	Peritoneum, lung	Alive, WD (14.8)
4	74	27	18	MMMT	High	pT3aN2a	IIIC2	Peritoneum	Deceased (12.5)
5	73	36.56	15	MMMT	High	pT1a	IA	None	Alive, ND (20.7)
6	73	35.35	7	MMMT	High	pT3a	IIIA	None	Alive, ND (20.2)
7	74	39.06	6	Endometrioid	2	pT1aN0	IA	None	Alive, ND (32.4)
8	74	29.18	4.5	Endometrioid	2	pT1b	IB	None	Alive, ND (24.0)
9	67	29.7	8.5	Endometrioid	2	pT1aN0	IA	None	Alive, ND (23.7)
10	52	36.79	9	Endometrioid	2	pT1aN1	IA	None	Alive, ND (21.8)
11	69	24.5	5	Endometrioid	3	pT1bN0	IB	None	Alive, WD (0.7)
12	69	27.8	13	Rhabdomyosarcoma	High	pT1bN0	IB	None	Alive, ND (4.9)
13	50	42.09	12	Undifferentiated Sarcoma	High	pT1bN0	IB	None	Deceased (0.0)
14	66	35.28	3	Serous	High	pT1aN0	IA	None	Alive, ND (49.5)
15	60	34.4	2.5	Serous	High	pT1aN1	IA	None	Alive, ND (31.9)
16	69	29.29	2.4	Serous	High	pT1aN2	IA	None	Alive, ND (42.4)
17	77	34.85	3	Serous	High	pT1aN3	IA	None	Alive, ND (40.1)
18	64	24.89	0.9	Serous	High	pT1aN0M1	IVB	None	Alive, ND (16.8)

MMMT - carcinosarcoma; ND - no disease; WD - with disease.

Figure 1 - 741

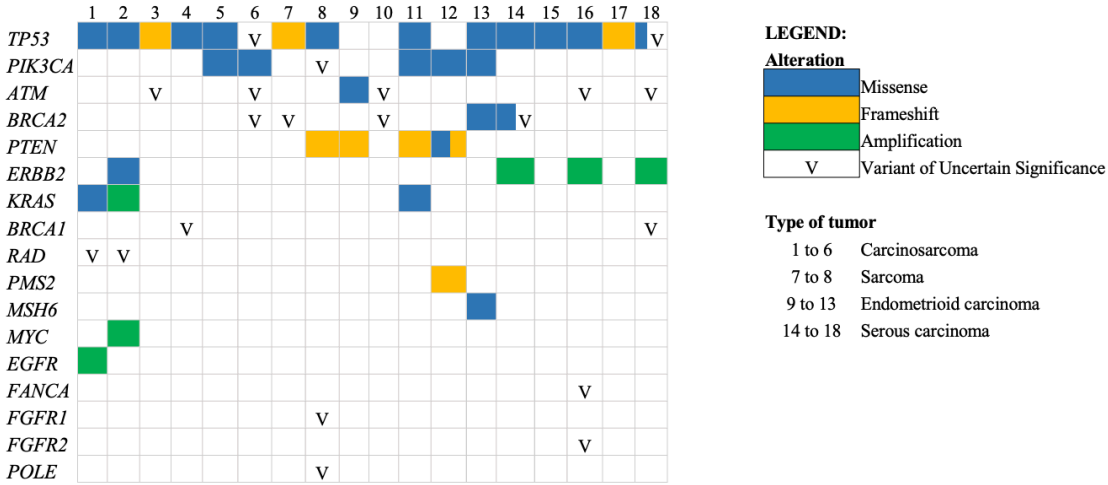

Conclusions: The molecular profile of uterine malignancies in African American women have important alterations that may have prognostic and treatment implications. They harbor more frequent *ERBB2* amplifications and *PIK3CA* mutations, which are now targetable genetic alterations. *ATM* variants of unknown significance were observed in considerable cases, warranting further investigation on its clinical implications. Alterations in *TP53* were frequently observed even in low grade tumors, which may be an important biomarker of aggressive clinical behavior. The unique molecular profile of uterine malignancies in this patient population must be investigated further for the purpose of establishing guidelines to improve and customize management strategies for African American patients.

742 Universal p53 Staining of Endometrial Carcinomas: Experience from a Large Academic Institution

Michael Mertz[1], Amy Joehlin-Price[2], Karuna Garg[2]
[1]Cleveland Clinic Pathology and Laboratory Medicine Institute, Cleveland, OH, [2]Cleveland Clinic, Cleveland, OH

Disclosures: Michael Mertz: None; Amy Joehlin-Price: None; Karuna Garg: None

Background: Traditionally, the main utility of p53 staining in endometrial carcinoma (EC) has been to differentiate between endometrioid (EEC) and serous carcinoma (USC). More recently, the prognostic significance of aberrant p53 staining in EEC has been documented by the TCGA and other studies. Clinicians are beginning to utilize this as a parameter in clinical and therapeutic decisions and to determine the need for adjuvant therapy. To that end, we have been performing p53 IHC in all newly diagnosed EC at our institution for 13 months, irrespective of grade and subtype. Here, we aim to report our experience with universal p53 staining in EC, specifically evaluating the incidence of aberrant p53 staining in different tumor subtypes and grades.

Design: After obtaining IRB approval, the pathology database was searched to identify all cases of endometrial carcinoma diagnosed since September 2020 in which p53 IHC was performed. The p53 and MMR staining pattern was noted. Clinical information was obtained from electronic medical records.

Results: A total of 191 total cases of EC with p53 IHC were identified. Aberrant p53 staining was noted in 1.9% FIGO grade 1 EEC (2/105), 24% FIGO 2 EEC (7/ 29 - 3 with subclonal ab-p53), 61% of FIGO 3 EEC (8/13 - 1 with subclonal ab-p53), 96% USC (25/ 26), 100% of carcinosarcomas (9 of 9), 50% of clear cell carcinoma (2/4) and 50% of undifferentiated/dedifferentiated carcinomas (2 of 4 - 1 subclonal) (see table). Of these, 3 FIGO 2 EEC, 1 FIGO 3 EEC, and 1 undifferentiated carcinoma showed a subclonal aberrant p53 pattern, such that a portion of the tumor was aberrant while the remaining tumor was wild type. MMR loss was seen in 18%, 51% and 36% of FIGO grade 1, 2 and 3 EEC respectively. Synchronous MMR loss and aberrant p53 was noted in 2 FIGO 3 EEC, 1 carcinosarcoma and 1 dedifferentiated carcinoma.

Although anecdotal comments from gynecologic oncologists suggest that preoperative imaging and adjuvant therapy practices are occasionally being altered with aberrant p53 results, it is difficult to draw any systematic clinical or therapeutic associations given our limited follow up period.

Subtype and Grade	Aberrant p53 IHC	MMR Loss	MMR Loss with Aberrant p53
FIGO 1 EEC (n = 106)	1.9% (2/105*)	18% (29/106)	0
FIGO 2 EEC (n = 29)	24% (7/29) (3 subclonal)	51% (15/29)	0
FIGO 3 EEC (n = 13)	61% (8/13) (1 subclonal)	38% (5/13)	2 (1 with MLH1/PMS2 Loss and 1 with PMS2 Loss)
USC (n = 26)	96% (25/26)	0	0
Carcinosarcoma (n = 9)	100% (9/9)	11% (1/9)	1 (MLH1/PMS2 Loss)
Clear Cell Carcinoma (n = 4)	50% (2/4)	0	0
Undifferentiated/Dedifferentiated (n = 4)	50% (2/4) (1 subclonal)	3/4 (75%)	1 (MLH1/PMS2 Loss)
Total = 191	**Total = 55 (28%)**	**Total = 53 (27%)**	**Total = 4 (2%)**

* one showed equivocal p53

Conclusions: Of unselected 191 unselected endometrial carcinomas, 28% showed aberrant p53 staining, including almost all USC and carcinosarcoma. Aberrant p53 staining was noted in 11% of all EEC with the vast majority representing FIGO grade 3 EEC.

743 Immunohistochemical Screening for Mesonephric-like Endometrial Carcinoma: Morphologic and Molecular Features of Screen-Positive Cases

Anne Mills[1], Taylor Jenkins[2], Brooke Howitt[3], Jinbo Fan[2], Kari Ring[1], Ian Cook[1]
[1]University of Virginia, Charlottesville, VA, [2]University of Virginia Health System, Charlottesville, VA, [3]Stanford Medicine/Stanford University, Stanford, CA

Disclosures: Anne Mills: None; Taylor Jenkins: None; Brooke Howitt: None; Jinbo Fan: None; Kari Ring: None; Ian Cook: None

Background: Mesonephric-like endometrial carcinoma is a rare but frequently misclassified and aggressive malignancy. It can show variable morphology including tubular, papillary, corded, and spindled growth and nuclei which can be bland and cuboidal, open and vesicular, or atypical and hobnailed. *KRAS* mutations, lack of or limited ER expression, and immunopositivity for TTF-1, GATA3, and luminal CD10 are described in these tumors, but an IHC-based screening approach has not been well-studied.

Design: We assessed 300 consecutive endometrial carcinomas/carcinosarcomas (ECAs) on tissue microarray for TTF-1, GATA3, CD10, and ER expression to ascertain the specificity of TTF1/GATA3/luminal CD10 expression with or without ER staining for this diagnosis. Next generation sequencing (Trusight 170 and *POLE* mutation testing) and morphologic review were performed on all screen-positive cases.

Results: 3% (9/300) of ECAs were TTF1+; two co-expressed GATA3. No cases expressed luminal CD10 or GATA3 in isolation. Two TTF1+ cases, one of which was also GATA3+, were reclassified as mesonephric-like based on morphology, IHC, and molecular results (ER-, *KRAS* mutations without MMR deficiency, *TP53* mutations, or *PTEN* mutations): these represented 0.7% of all ECAs (2/300). The reclassified cases were originally diagnosed as grade 1 and grade 2 endometrioid carcinoma, and the latter had pulmonary metastases and pelvic recurrences on 2-year follow-up (Fig 1). Six TTF1+ cases retained their original serous (3) and endometrioid (3) diagnoses on morphologic and molecular review; one case was reclassified as dedifferentiated. *KRAS* mutations were identified in four TTF1+ non-mesonephric-like cases, including one serous carcinoma and one grade 3 endometrioid carcinoma with concomitant p53 abnormalities, one MMR-deficient endometrioid carcinoma with a complex molecular profile, and one endometrioid carcinoma with extensive mucinous differentiation (Fig 2).

Figure 1 - 743

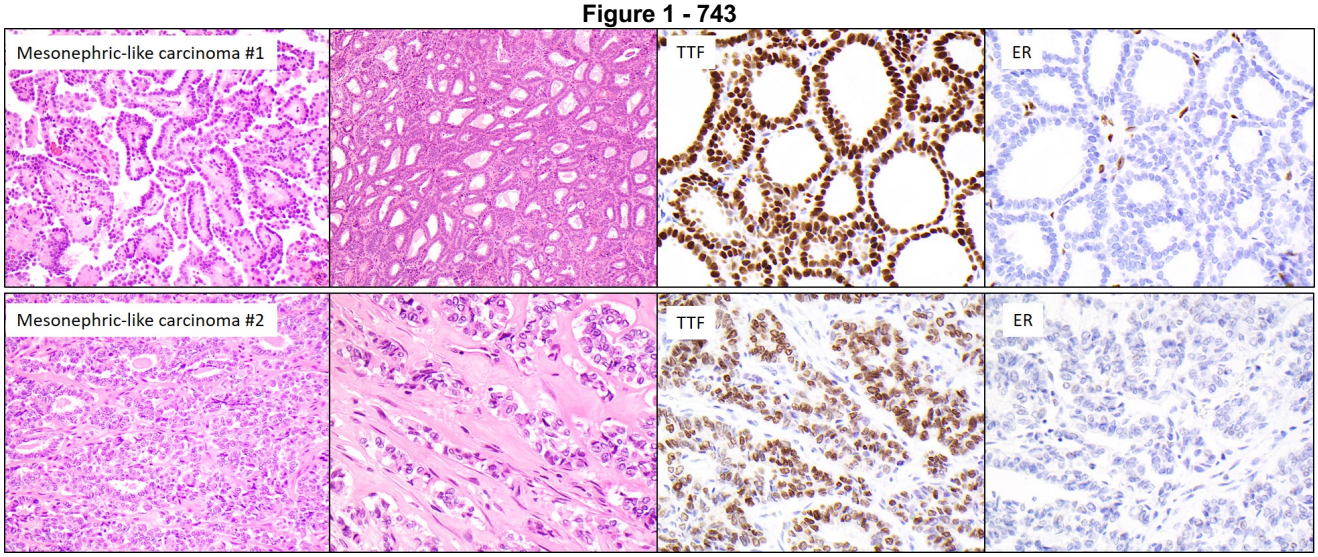

Figure 2 - 743

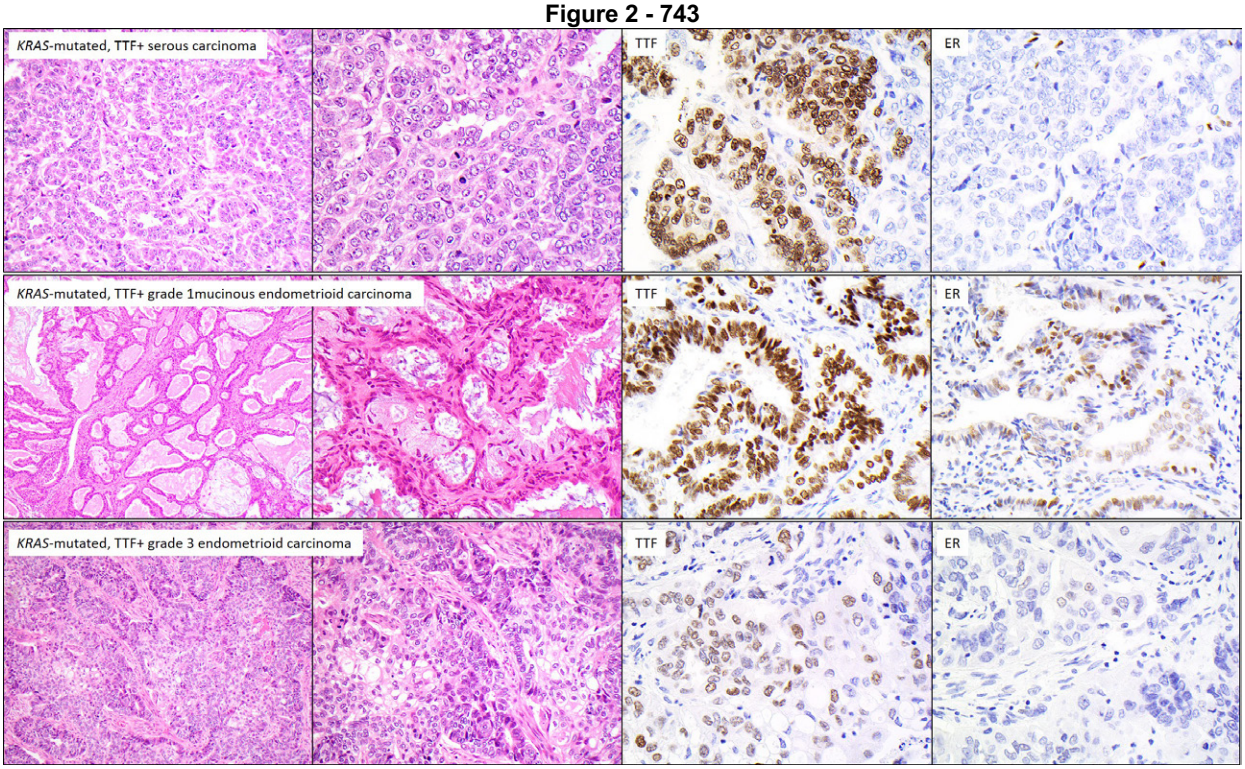

Conclusions: Although mesonephric-like carcinomas comprise <1% of ECAs, their aggressive behavior and frequent misclassification as lower grade endometrioid tumors makes their detection critical. These findings suggest that TTF1 and ER are good first-line screens for a diagnosis mesonephric-like carcinoma, but caution that a TTF1+/ER- immunoprofile is not specific for this diagnosis, even in the setting of *KRAS* mutations. Thus, a final diagnosis of mesonephric-like endometrial carcinoma first and foremost requires the appropriate morphology, with confirmation through appropriate immunohistochemical staining and, when relevant, additional molecular support.

744 Comparison of Microsatellite Instability Detection by Immunohistochemistry and Molecular Techniques in Endometrioid Adenocarcinomas

Conrad Moher[1], Cheryl Mather[1], Remegio Maglantay[1], Soufiane El Hallani[2]
[1]Alberta Precision Laboratories, University of Alberta, Edmonton, Canada, [2]University of Alberta, Edmonton, Canada

Disclosures: Conrad Moher: None; Cheryl Mather: None; Remegio Maglantay: None; Soufiane El Hallani: *Consultant*, MarocPath Technologies

Background: Microsatellite instability (MSI) is being used as an important biomarker to guide the molecular classification, genetic predisposition screening and immunotherapy treatment for women with endometrial and ovarian endometrioid adenocarcinomas. Immunohistochemistry (IHC) is the gold standard for efficient evaluation of the mismatch repair (MMR) genes and MSI-polymerase chain reaction (MSI-PCR) is alternatively used for equivocal IHC results. Next generation sequencing (NGS) can offers additional advantages to conventional PCR methods. The objective of this study is to determine the real-world performance of MSI-PCR in gynecologic endometrioid adenocarcinomas and evaluate the added value of NGS to overcome the MSI-PCR limitations.

Design: A study set of 57 endometrioid adenocarcinoma FFPE specimens with known MMR immunohistochemistry status (47 from the endometrium and 10 from the ovary) was selected. We evaluated a commercial 7-marker MSI-PCR detection system and a custom next-generation sequencing panel (including 76 MSI markers), and compared the performance of each method to the widely used immunohistochemistry for mismatch repair genes.

Results: By immunohistochemistry, 40 out of 57 endometrioid adenocarcinomas had an abnormal MMR profile including MLH1/PMS2 deficiency (n=29), MSH2/MSH6 deficiency (n=3), MSH6 deficiency (n=7) and PMS2 deficiency (n=1). Although 100% specific, the MSI-PCR method had an overall sensitivity of 75% with accurate MSI-High calls in 3/3 (100%) of MSH2/MSH6 loss, 26/29 (90%) for MLH1/PMS2 loss, 1/7 (15%) for MSH6 loss and 0/1 (0%) for PMS2 loss. In all IHC/MSI-PCR discordant cases, NGS accurately detected the presence of genetic mutations in the corresponding MMR genes. NGS yielded an improved MSI call sensitivity (95%) using a dedicated NGS bioinformatics algorithm.

Conclusions: We found that conventional MSI-PCR testing has inferior sensitivity to NGS when applied to the endometrial/ovarian endometrioid adenocarcinomas with isolated MSH6 or PMS2 gene deficiency, and that NGS testing with an expanded panel of markers performs well. In addition, NGS offer advantages over MSI-PCR methods, including no requirement of matched normal tissue, the integration of MSI calling into a more comprehensive list of evaluated genes (i.e POLE, TP53, copy number alterations), direct sequencing of the MMR genes and determination of the variant allele fraction which can guide to the somatic versus germline origin of the MMR gene mutations.

745 Ovary as Initial Presenting Site of Lymphoma: A Rare Diagnosis with Potential Diagnostic Challenges and Therapy Implications

Aysha Mubeen[1], Jacob Havens[2], Vishnu Reddy[3], Deepti Dhall[2]
[1]Brigham and Women's Hospital, Boston, MA, [2]The University of Alabama at Birmingham, Birmingham, AL, [3]UAB Hospital, Birmingham, AL

Disclosures: Aysha Mubeen: None; Jacob Havens: None; Vishnu Reddy: None; Deepti Dhall: None

Background: Lymphomas very rarely (less than 1%) initially present as ovarian masses. More commonly, ovaries can be secondarily involved by systemic lymphoma. The initial presentation of lymphoma as an ovarian or pelvic mass can pose significant diagnostic challenges. These are rare tumors not readily on the differential of surgical pathologists. We are presenting single institution assessment of clinicopathologic features of ovarian lymphomas and highlight potential diagnostic issues.

Design: A total of fifteen cases of ovarian involvement by lymphoma were found in our institutional files. Detailed review of the clinicopathologic features was performed.

Results: Mean patient's age was 49 years (Range 26-82). A known history of lymphoma was present in only three cases. In twelve cases, ovary was the initial site of presentation without a known history of lymphoma.7 patients had unilateral and 8 had bilateral ovarian masses. All cases were of Non-Hodgkin Lymphoma and majority (14/15, 93.3%) were B-cell lymphomas. Histologic subtypes were diffuse large B cell lymphoma (DLBCL) (n= 10), Burkitt lymphoma (n=2), anaplastic large cell lymphoma (ALCL) (n=1) and B-Acute lymphoblastic lymphoma (B-ALL) (n=1). One or more ancillary studies (immunohistochemistry, flow

cytometry and Fluorescence in situ hybridization (FISH)) were performed to confirm the diagnoses. Intraoperative frozen section was performed in 7 cases. One case was misinterpreted as dysgerminoma on frozen section. Most patients were treated with adjuvant chemotherapy; 2 patients also received stem cell transplant. The average follow up was 21.3months.Only three patients achieved remission. Two patients died of the disease and treatment complications; one patient died from an unknown cause. The clinico-pathologic findings are summarized in the Table. Morphology and IHC of one case (DLBCL, non-germinal center type) are shown in Figure 1.

Case No.	Age (yrs)	Clinical Presentation	Laterality	Size (cm)	Frozen section results	Diagnosis	Treatment	Outcome
1	43	Abdominal pain	BL	6, 22	Neoplasm, defer to permanent	DLBCL	Adjuvant chemotherapy	AWD
2	31	Complex ovarian cyst discovered in pregnancy	UL	4.9	Dysgerminoma	DLBCL	Adjuvant chemotherapy	AWD
3	82	Ascites and weight loss	UL	NA	ND	DLBCL	Adjuvant chemotherapy	Lost to follow up
4	50	History of NHL status post chemotherapy with ovarian mass	BL	NA	ND	DLBCL	Adjuvant chemotherapy	AWD
5	79	Abdominal pain	BL	2.5, 9	Atypical lymphoid infiltrate	DLBCL	NA	Transferred care
6	43	NA	UL	NA	ND	DLBCL	NA	Insufficient follow up
7	35	Abdominal pain and uterine mass	UL	21	ND	Burkitt Lymphoma	Adjuvant chemotherapy and SCT	Remission
8	35	Ovarian cyst	BL	3.8, 5	Poorly differentiated malignant tumor	ALCL	Adjuvant chemotherapy	Insufficient follow up
9	42	History of DLBCL status post chemotherapy with ovarian mass	UL	1	Lymphoma	DLBCL	Adjuvant chemotherapy	Dead (unknown cause)
10	61	Abdominal pain and weight loss	BL	3.5, 9	ND	DLBCL	Adjuvant chemotherapy	DOD
11	49	Adnexal mass discovered in work up of back pain	BL	1, 2.2	ND	Burkitt Lymphoma	Adjuvant chemotherapy	DOD
12	65	Pelvic mass	BL	2.3, 2.5	ND	DLBCL	Adjuvant chemotherapy	AWD
13	60	Postmenopausal bleeding	UL	6	Atypical lymphoid infiltrate	DLBCL	Adjuvant chemoradiation	Remission
14	35	Abdominal pain and weight loss	BL	5.5, 12	Malignant neoplasm	DLBCL	Adjuvant chemotherapy	Remission
15	26	History of B-ALL with ovarian mass	UL	14.5, 18	ND	B-ALL	Adjuvant chemotherapy and SCT	AWD

UL: Unilateral, BL: Bilateral, ND: Not done, NA: Not available, SCT: Stem Cell Transplant, AWD: Alive with disease, DOD: Dead of disease

Figure 1 - 745

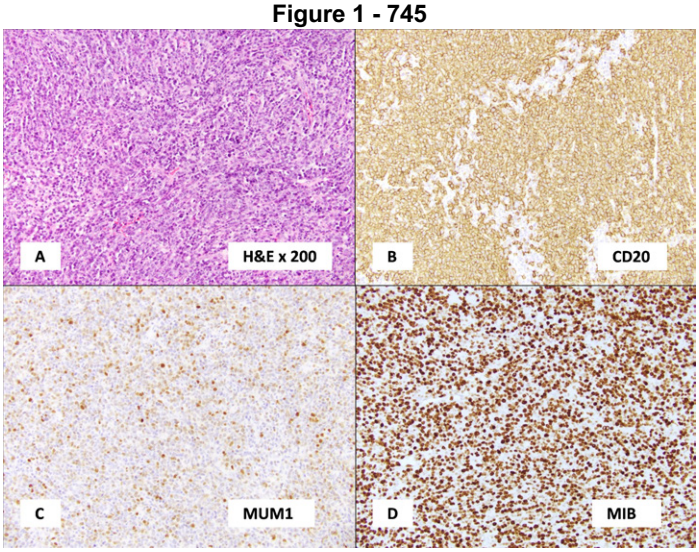

Conclusions: Ovary can be the initial site of presentation of hematolymphoid neoplasms. An awareness of this differential is critical in making the right diagnosis especially in small biopsies or at the time of frozen section evaluation. Distinguishing lymphoma from the more common epithelial and germ cell tumors of the ovary can have significant implications for therapy. A correct pre/intraoperative diagnosis may save the patient for unnecessary surgery and potentially change the course of management.

746 Endometrioid Endometrial Carcinoma with Gastrointestinal Metastases: Clinicopathological and Molecular Correlation Shows Enrichment in Mismatch Repair Deficiency Due to MLH1/PMS2 Loss

Ilke Nalbantoglu[1], Pei Hui[2], Natalia Buza[1]
[1]Yale School of Medicine, New Haven, CT, [2]Yale University School of Medicine, New Haven, CT

Disclosures: Ilke Nalbantoglu: None; Pei Hui: None; Natalia Buza: None

Background: Luminal gastrointestinal (GI) tract metastases from endometrioid endometrial carcinomas (EEC) are rare and may pose a diagnostic challenge clinically and pathologically, especially when transmural bowel involvement is present. Aggressive clinical behavior in EEC has been recently linked to specific molecular alterations, including sporadic mismatch repair (MMR) deficiency. Our study aimed to evaluate the morphological, immunophenotypical, and molecular characteristics of EEC with GI tract involvement.

Design: Luminal GI metastases from EEC were retrospectively identified over a 22-year period in our departmental archives. All available H&E and immunohistochemical (IHC) slides were reviewed and included MLH1, PMS2, MSH2, and MSH6. The results of molecular studies and clinical follow-up information have been retrieved from pathology reports and electronic medical records.

Results: A total of 31 metastatic tumors met the study criteria from 18 patients ranging between 47-93 years of age (mean: 65) at the time of initial presentation. The most common site was rectosigmoid colon (18/31, 58%) and mucosal involvement was present in 19 cases (61%) with surface ulceration in 16 tumors (53%). Most patients originally presented with low stage disease (14/18, 78%): stage 1 in 10 and stage 2 in 4 patients. The tumor FIGO grade at the metastatic site was most frequently grade 2 (48%), followed by grade 3 (39%), grade 1 (6%), and undifferentiated carcinoma (6%). MMR deficiency was identified in 78% of tumors (14/18), most of them due to sporadic MLH1/PMS2 loss (12/14), while loss of MSH2/MSH6 and loss of PMS2 were seen in 1 case each. None of the patients had known Lynch syndrome.

Conclusions: Luminal GI tract metastases by EEC often show transmural involvement with mucosal ulceration. Over 75% of tumors in our series were MMR-deficient, most often due to sporadic MLH1/PMS2 loss – a significantly higher proportion compared with unselected cohorts of EEC in the literature (~35%). Sporadic MMR-deficiency in EEC is an adverse prognostic marker with propensity for luminal GI metastases even in patients presenting with low stage disease, indicating a need for closer clinical follow up and a high index of suspicion in these cases.

747 Utility of a Comprehensive NGS 523-Gene Panel for the Simultaneous Analysis of Homologous Recombination Deficiency Score and Percent Genomic Loss of Heterozygosity Using a Cytogenetic Software Applied to the Evaluation of Epithelial Ovarian Tumors

Janira Navarro Sanchez[1], Zan Halford[2], Jason K.S. Pon[2], Amy Woron[1], Christopher Lum[1]
[1]University of Hawaii, John A. Burns School of Medicine, Honolulu, HI, [2]University of Hawaii, Honolulu, HI

Disclosures: Janira Navarro Sanchez: None; Zan Halford: None; Jason K.S. Pon: None; Amy Woron: None; Christopher Lum: None

Background: Homologous recombination repair (HRR) is a key pathway that repairs DNA double strands breaks. Cells with defects in HRR are susceptible to cell death induced by Poly (ADP-ribose) polymerase inhibitors (PARPi). Other mechanisms of HRR impairment beyond BRCA1/2 mutations can confer PARPi sensitivity. Quantitative measures of homologous recombination deficiency (HRD) associated chromosomal abnormalities were developed based on studies of patients with BRCA1/2 deficiency and assessed three types of genomics scarring patterns: Loss of heterozygosity (LOH), Large scale state transitions (LST), and

Telomeric allelic imbalance (TAI). Our study explores the performance of the NGS 523 gene panel and NxClinical Software in evaluating genomic scars in epithelial ovarian tumors.

Design: Sixteen ovarian neoplasms were selected for the study. They were sequenced using TSO500 Illumina NGS and interpreted with NxClinical software. Two parameters were evaluated, HRD score and percent genomic LOH (LOH%). A score of ≥42 was determined to be HR-deficient and a score <42 was considered HR-proficient. The cutoff for identifying HRD tumors was set at ≥ 16 for LOH%. Chemotherapy response scores (CRS) were available in 8 of 16 cases. We correlated the CRS with HRD scores and LOH%. Additionally, we aimed to identify the optimal tumor content rate needed for detection of HRD or LOH alterations.

Results: In this study, visualization of a 523-gene cancer exome panel was shown to be 66.7% sensitive and 100% specific at detecting genomic scars (HRD score). 68.75% of cases showed low HRD score and 31.25% of cases showed a high HRD score. An LOH%<16 was observed in 75% of the cases and a LOH% ≥16 was seen is 25% of the cases. All cases with a high HRD score had a high LOH%. CRS1 cases were HR-proficient and LOH% low. With a tumor content rate of 70%, NGS results can be adequate for most specimens.

Conclusions: Assessment of HRD in the clinical setting is an important tool that can help in select patients for PARPi in ovarian cancer. Defects in the genomic maintenance machinery that can be used therapeutically and leave a genetic imprint detectable by current technologies are ready for the development of genomic scar biomarkers to predict drug response. HRD was found to be sensitive to tumor heterogeneity and tumor content. We propose a new alternative for routine diagnostics that uses targeted panels and bioinformatics algorithms in lieu of commercial tests used in clinical trials.

748 Pattern-A Endocervical Adenocarcinomas with Ovarian Metastasis are Indolent and Molecularly Distinct from Destructively Invasive Adenocarcinomas

Alexander Neil[1], Yvonne Li[2], Ardeshir Hakam[3], Marisa Nucci[4], Carlos Parra-Herran[4]
[1]Brigham and Women's Hospital, Boston, MA, [2]Dana-Farber Cancer Institute, Boston, MA, [3]H. Lee Moffitt Cancer Center & Research Institute, University of South Florida, Tampa, FL, [4]Brigham and Women's Hospital, Harvard Medical School, Boston, MA

Disclosures: Alexander Neil: None; Yvonne Li: None; Ardeshir Hakam: None; Marisa Nucci: None; Carlos Parra-Herran: None

Background: The invasive pattern in HPV-associated endocervical adenocarcinoma (HPVA) has prognostic value. Non-destructive (pattern A) HPVA has excellent prognosis mirroring adenocarcinoma in situ (AIS). However, the rare occurrence of ovarian spread has been portended as a sign of aggressiveness in these otherwise indolent lesions. We hypothesize that AIS/pattern-A HPVA with ovarian metastases are biologically different than metastatic destructively invasive HPVA.

Design: We identified 11 patients with HPVA and synchronous or metachronous metastases. Material was reviewed to determine the Silva pattern in the primary lesion and to confirm the presence of metastases (ovarian, nodal, other). For each case, normal tissue, cervical tumor and at least one metastasis underwent comprehensive sequencing using a 447-gene panel. Pathogenic alterations, molecular signatures, single-nucleotide variants (SNV), tumor mutational burden (TMB), and segmental copy number alterations (CNA) were evaluated and compared between primary and metastases, and among invasive pattern categories.

Results: Three patients had AIS/Pattern-A primaries, while 8 had pattern-B/C tumors. All AIS/pattern-A lesions had metastasis only to the ovary. Sequencing confirmed the genetic relationship between primary and metastatic tumors in each case. All AIS/Pattern-A HPVAs harbored PIK3CA variants, compared to 3 of 8 pattern-B/C tumors with distant metastases. While TMB was similar between the two groups, pattern-B/C tumors showed a notably higher number of segmental CNA in both primary tumor and matched metastases. Metastatic AIS/pattern-A HPVA lacked novel pathogenic variants compared to the primary. Conversely, 3 of 6 pattern-B/C tumors with sequenced metastases developed novel pathogenic variants in the metastasis not seen in the primary. All 3 AIS/Pattern-A patients were alive and free of disease at 31, 47 and 212 months after initial diagnosis. Conversely, cancer-related death was documented in 3 of 6 pattern-B/C patients with follow-up, at 7, 20 and 87 months.

Case	Age at dx	Invasive pattern	Met sites (* designates sequenced)	TMB (per mb)	CNA #	Pathogenic Molecular alterations in primary	New pathogenic molecular alterations in metastases
1	55	A	Ovary*	0.76	12	PIK3CA, PTEN, TERC amp	none
2	33	A	Ovary*	4.562	4	PIK3CA, ARID1A	none
3	42	A	Ovary*	3.041	13	PIK3CA, KRAS	none
4	50	C	Ovary*, omentum*, pleura*, brain	3.011	24	ATR, ERBB2 amp	none
5	35	B	Breast, abd wall*	0.761	27	None identified	FANCA
6	61	C	Ovary, tube, endometrium, omentum*	5.323	17	KRAS, TP53, MYC amp	CREBBP, TERT
7	46	C	Sigmoid*	4.562	17	PIK3CA	none
8	40	C	Iliac node*, ureter	2.282	7	TP53	FAN1
9	33	C	Pelvic node	3.042	8	PIK3CA, CASP8	n/a
10	39	C	Pelvic node	6.844	12	PIK3CA, PTEN	n/a
11	52	C	Ovary*, supraclavicular node	3.802	21	ATM, ERBB3, U2AF1	none

Conclusions: From a genomic perspective, AIS/Pattern-A HPVA is distinct from frankly invasive tumors, even in the setting of secondary ovarian involvement. This difference may explain the indolent outcome observed in patients with AIS/Pattern-A HPVA and ovarian metastasis. Our study acknowledges the infrequent phenomenon of ovarian spread but underscores the potential for conservative management approaches to Pattern-A HPVA, different from overtly invasive (pattern-B/C) forms.

749 Somatic Malignancies Arising in Ovarian Mature Cystic Teratomas: A Multi-Institutional Study Examining Novel Malignancies and Outcomes

Grace Neville[1], Kyle Devins[2], Marisa Nucci[1], Jaclyn Watkins[3]
[1]Brigham and Women's Hospital, Harvard Medical School, Boston, MA, [2]Massachusetts General Hospital, Boston, MA, [3]Massachusetts General Hospital, Harvard Medical School, Boston, MA

Disclosures: Grace Neville: None; Kyle Devins: None; Marisa Nucci: None; Jaclyn Watkins: None

Background: Somatic malignancy arising in an ovarian mature cystic teratoma (MCT) is a well described but rare phenomenon. We aimed to document the incidence and outcomes of patients with such a diagnosis in a contemporary, multi-institutional study. We also report occurrences of novel malignancies arising in MCT.

Design: The pathology archives and consultation files of the participating institutions were searched for all cases of MCT arising between 2005 and 2021. The pathology reports were reviewed for the presence of somatic malignancy arising from an MCT. Carcinoid tumors, Mullerian neoplasms, collision tumors, and neoplasms suspected to arise from MCT but without microscopic proof of MCT were excluded. Histomorphologic and sociodemographic variables, including follow-up, were obtained when available.

Results: 39 patients ranging in age from 16-75 (mean-49.9) years harbored a somatic malignancy arising in MCT. The incidence ranged between institutions from 0.4 - 0.65%. Histologic types included squamous cell carcinoma (SCC) (n=21), papillary thyroid carcinoma (PTC) (n=6), sebaceous carcinoma (n=2), neuroendocrine carcinoma (n=2) and single incidences of other neoplasms including Wilm's tumor, glioblastoma, adenocarcinoma ex goblet cell carcinoid (AexGCC), malignant melanoma, adenosquamous carcinoma, anaplastic carcinoma, an adnexal carcinoma and poorly differentiated oncocytic thyroid carcinoma. In most cases, the associated MCT components were prominent; however, in 3 the residual MCT component was only focally present. Follow up was available in 18 cases (range: 4 months to 16 years, mean: 6.4 years). Of these, 12 were initially stage 1A or 1B; the remaining 6 were 1C or higher. Of the low stage patients, one with PTC and one with malignant melanoma subsequently developed distant metastases. All other cases with recurrence/metastasis(4 SCC, 1 neuroendocrine carcinoma, and 1 AexGCC) occurred in cases of higher initial stage. 2 patients with SCC died of their disease.

Conclusions: Although SCC was the most common somatic malignancy identified, other rare or novel subtypes also occurred. Poor outcomes occurred across multiple histologies and were often associated with higher initial stage at diagnosis. Long-term follow up is recommended for all patients, with more aggressive management to be determined on a case-by-case basis. The

focality of the residual MCT in some cases highlights the need for thorough sampling in somatic tumors that are detected in the ovary without a known primary site.

750 Mullerian Adenosarcoma: A Clinico-pathologic Study with Histologic Reclassification of 66 Cases and CGH-array Analysis

Carine Ngo[1], Sophie Cotteret[1], Maria Kfoury[1], Jean-Yves Scoazec[1], Patricia Pautier[1], Catherine Genestie[2]
[1]Gustave Roussy, Cancer Campus, Grand Paris, Villejuif, France, [2]Gustave Roussy, Villejuif, France

Disclosures: Carine Ngo: None; Sophie Cotteret: None; Maria Kfoury: None; Jean-Yves Scoazec: None; Patricia Pautier: None; Catherine Genestie: None

Background: Mullerian adenosarcoma (AS) is a rare biphasic tumor occurring most commonly in the uterus. Despite an indolent clinical course in early-stage tumors, 5-year survival for stage III AS was reported lower than 50%. Sarcomatous overgrowth (SO) defined as pure stromal component ≥ 25% of the tumor and high-grade AS defined by severe atypia were found to be the histological features associated with worse prognosis.

We aimed to re-classify uterine AS as low-grade, high-grade, low-grade with SO and high-grade with SO according to histologic criteria and to evaluate whether these histological patterns are associated with different clinical outcomes and/or molecular profile.

Design: We reviewed all AS diagnosed in our center between 2010 and 2019. Histopathological features including degree of atypia (mild, moderate, severe), mitotic activity (/10HPF), presence of SO and heterologous differentiation have been re-assessed by a sarcoma pathologist (CN) and a gynecologic pathologist (CG). We subsequently investigated genome-wide copy number alterations (CNA) with the Affymetrix OncoScan™ CNV Assay.

Results: We reviewed 66 uterine AS with histological material: 16(24%) were low-grade, 6 (9%) low-grade with SO, 9 (14%) high-grade and 35(53%) high-grade with SO. The median mitotic count in 10 HPF was respectively 5 vs 11 vs 20 vs 22 mitoses. Rhabdomyosarcomatous heterologous elements were only seen in high-grade AS: 4/9 (44%) in purely high-grade group and 18/35 (51%) in SO group. Up to now, clinical information was recorded for 28 patients. Recurrence occurs in 1/3 (33.3%) low-grade AS with SO, 1/5 (20%) high-grade AS and 8/17 (47%) high-grade AS with SO. At time of last follow-up, only patients with high-grade AS with SO died of her disease (5/17, 29%). Preliminary results of CNA analysis in 11 cases (3 low-grade AS, 4 low-grade AS with SO and 4 high-grade AS with SO) showed a simple genome profile in low-grade AS compared to low-grade AS with SO which displayed numerous CNA. *MDM2* amplification was noted in 1/3 low-grade AS and 2/4 low-grade AS with SO. Low-grade and high-grade AS with SO showed frequent losses in chromosome 11q , 13q and 19q. Loss of chromosome 17q was more frequent in high-grade AS (4/4) than in low-grade AS with SO (1/4).

Conclusions: Despite the small number of patients, low-grade AS with SO might recur compared to purely low-grade AS and show similar chromosomal losses as high-grade AS which are associated with worse prognosis.

751 Primary and Secondary Involvement of the Female Genital Tract by Lymphoma: An Updated Institutional Experience

Meredith Nichols[1], Amy Joehlin-Price[1], Sarah Ondrejka[1], Karuna Garg[1]
[1]Cleveland Clinic, Cleveland, OH

Disclosures: Meredith Nichols: None; Amy Joehlin-Price: None; Sarah Ondrejka: None; Karuna Garg: None

Background: Lymphoma of the female genital tract is rare and can occur as a primary or in the form of secondary involvement. By a systemic lymphoma. It can be a challenging diagnosis with many non-lymphoid malignancies in the differential diagnosis. There have been no recent studies examining gynecologic tract lymphomas using the updated 2017 WHO classification system that relies on a more robust molecular workup for final diagnosis of many entities.

Design: Institutional archives were searched from 1995 to 2021. Demographic, clinical, flow cytometric, and molecular data were reviewed. All cases underwent histologic review by a hematopathologist and were reclassified according to the 2016 WHO

Classification of Tumours of Hematopoietic and Lymphoid Tissues. Cases were classified as primary gynecologic lymphoma if the involved sites were restricted to the gynecologic tract only or the gynecologic tract accompanied by regional lymph nodes.

Results: Forty-three cases of lymphoma of the gynecologic tract were identified. Slides were available for review in 26 cases. The average patient age was 62 years (range 25-93). Most patients presented with abdominal symptoms or vaginal bleeding, and lymphoma was an incidental findings in four patients undergoing surgery for prolapse. Ten cases were classified as primary gynecologic lymphoma and 14 were classified as gynecologic involvement by systemic lymphoma. Two cases are pending additional clinical testing required for staging. The specific gynecologic site of involvement included ovary (10 cases), uterus (1 case), cervix (5 cases), vagina (5 cases), vulva (3 cases). Ten cases involved multiple gynecologic sites. Twenty-five of 26 cases were B cell lymphoma (the final diagnoses are summarized in Table 1). Most staged patients received chemotherapy and/or radiation with mixed clinical outcomes. Ten patients are in complete remission, 4 are alive with disease, 4 are dead of disease, and 6 are dead from unrelated causes.

Diagnosis	Number of Cases
Follicular lymphoma	7
DLBCL, GC phenotype	8
DLBCL, non-GC phenotype	4
DLBCL with MYC translocation	1
High-grade B cell lymphoma with MYC and BCL6 rearrangements	1
CLL	2
Favor large cell lymphoma	1
B cell lymphoma of follicle center origin	1
Mycosis fungoides	1

DLBCL: diffuse large B cell lymphoma; GC: germinal center; CLL: chronic lymphocytic leukemia

Conclusions: Lymphomas can rarely involve the gynecologic tract, either exclusively or as part of systemic involvement. Almost all are B cell lymphomas and diffuse large B cell lymphoma is the most common subtype. Given the changes in the most recent classification system and reliance on FISH testing to definitively classify large B cell lymphomas, the largest change in pathology workflow is the importance of tissue triage to ensure adequate material for molecular analysis.

752 Mesonephric Marker Expression in Non-Mesonephric-Like Endometrial Carcinoma

Kelly Olson[1], Yang Hu[2], Mary Kao[1], Dandi Huang[1], Nhu Vu[2], Bradly Stelter[2], Ahmed Al-Niaimi[2], Paul Weisman[2], Stephanie McGregor[2]
[1]University of Wisconsin Hospital and Clinics, Madison, WI, [2]University of Wisconsin-Madison, Madison, WI

Disclosures: Kelly Olson: None; Yang Hu: None; Mary Kao: None; Dandi Huang: None; Nhu Vu: None; Bradly Stelter: None; Ahmed Al-Niaimi: None; Paul Weisman: None; Stephanie McGregor: None

Background: Mesonephric-like adenocarcinomas (MLAs) occurring in the endometrium can have a variety of morphologic patterns that overlap with multiple other types of carcinoma. Given the subjectivity of morphologic assessment, immunohistochemical (IHC) stains can be used as an adjunct to diagnosis but may be focal and are associated with lack of specificity. We sought to characterize the extent to which lack of specificity may confound differential diagnoses that include MLA.

Design: A previously published tissue microarray generated at our institution was stained for mesonephric markers (CD10, GATA3, calretinin, TTF-1), ER, PMS2, MSH6, and p53; 216 cases had satisfactory tissue represented for all markers (131 endometrioid, 23 clear cell, and 62 serous). Cases were assessed for the percent of cells and staining intensity for mesonephric markers, the number of mesonephric markers that were positive, and expression of other features of a mesonephric-like phenotype (ER-/low, p53 wild type, and MMR intact).

Results: 50/216 EC had significant expression: 21 expressed at least two markers in >1% of cells (CD10: n=8, TTF-1: n=4, calretinin: n=16, and GATA3: n=17) and 42 demonstrated >25% staining and/or moderate to strong intensity of at least one marker; 13 cases had both. Significant expression was more common in cases diagnosed as clear cell carcinoma (CCC, 8/23, 35%) than in endometrioid (EEC, 26/131, 20%) or serous (16/62, 26%). Four EEC cases that had staining in >25% of cells were also ER-/low (<10%), mismatch repair intact, and p53 wild-type, and two CCC with these same features had expression of two mesonephric markers; none of these six cases had unequivocal mesonephric morphology. Among these 6, 3 EEC were FIGO stage IA, whereas 1 EEC and the 2 CCC were FIGO stage III. The stage III EEC was the only case to recur.

Conclusions: Endometrial cancers without unequivocal mesonephric morphology can express multiple markers of mesonephric differentiation, including staining in >25% of cells. In this series, there is no clear association of this expression pattern with a poor prognosis. Additional study is necessary to determine the clinical significance of mesonephric marker expression in the absence of unequivocal mesonephric morphology.

753 Molecular Profiling of Vulvovaginal Melanomas

Zehra Ordulu[1], Kristine Cornejo[2], Thomas Krausz[3], Jennifer Bennett[4]
[1]University of Florida, Gainesville, FL, [2]Massachusetts General Hospital, Boston, MA, [3]University of Chicago Medicine, Chicago, IL, [4]University of Chicago, Chicago, IL

Disclosures: Zehra Ordulu: None; Kristine Cornejo: None; Thomas Krausz: None; Jennifer Bennett: None

Background: Melanomas of the female genital tract represent an uncommon subset of mucosal melanomas (18%), with vulva being the most common site. Thus, the literature is limited regarding their comprehensive genomic profile, with the most frequent alterations involving *NRAS*, *KIT,* and *BRAF*. Recently, *NRAS* mutations were found to be associated with decreased survival in a large series of mucosal melanomas, while in another study, *SF3B1* mutations showed a trend toward decreased overall and progression-free survival.

Design: Seven vulvovaginal melanomas (vulvar: n=4; vaginal: n=3) underwent next-generation sequencing (NGS) on a 154-gene panel. NGS was performed on 4 primary tumors, 2 recurrences, and 1 metastasis.

Results: Patient's age ranged from 57 to 80 (mean: 65; median: 64) years and follow-up interval (available in 6) from 15 to 104 (mean: 36; median: 29) months. All received immunotherapy, along with radiation in 4 and chemotherapy in 1. At last follow-up, 3 died of disease, 2 were alive and well, and 1 died from treatment-related issues. Patients presented with clinical stage group: I (n=1), II (n=4), III (n=1) and IV (n=1). Tumors averaged 9 (range: 4 to 15) cm in size and thickness ranged from 0.98 to 11 (mean: 5.72) mm. Ulceration was present in 6 tumors (1 unknown).

Recurrent alterations included *NRAS* (n=4), *NF1* (n=2), and *TERT* (n=2) mutations, segmental amplification of 4q12 including *PDGFRA*, *KIT,* and *KDR* (n=2, 1 with concurrent *KIT* mutation), deletion of *CDNK2A* (n=2), and alterations in *PTEN* (n=2, 1 mutation, 1 deletion). All tumors had at least one nucleotide level change, except for a vaginal melanoma with only *CCND1* amplification. No alterations in *BRAF* or *SF3B1* were detected.

Although our series is small, those with *NRAS* mutations had variable outcomes. Two were alive and well, 1 died from therapy-related issues, and 1 was lost to follow-up. *NRAS* mutations were mutually exclusive from *KIT* alterations. Both patients with segmental amplification of 4q12 died from disease, but concurrent *TERT* or *ATRX/TP53* mutations likely affected the prognosis. *CCND1* amplification is not a recurrent finding in vulvovaginal melanomas but has been described in cutaneous melanomas.

Clinicopathologic Features of Vulvovaginal Melanomas

Case	Age (years)	Primary Site	Size (cm)	Thickness (mm)	Ulceration	AJCC pStage	AJCC cStage Group	Treatment	Follow-Up (months)
1	59	Vagina	Biopsy	6	Yes	pT4b	IIC	Multiple courses of IT, palliative RT	DOD (18)
2	80	Vulva	2.9	7	Yes	pT4b	IIC	IT, Imatinib, RT	DOD (15)
3	57	Vagina	9	1.6	Yes	pT2b N1 M1	IV	IT	NED (36)
4	64	Vulva	4.4	0.95	Yes	pT1b	IB	Multiple courses of IT, RT, CT	DOD (104)
5	68	Vagina	Biopsy	7	Yes	pT4b	IIC	N/A	LTFU
6	59	Vulva	2.3	6.5	Yes	pT4b N0	IIC	Multiple courses of IT, RT	DOT (24)
7	70	Vulva	N/A	At least 11	Unknown	pT4 N1a	III	IT	NED (29)

IT=immunotherapy; RT=radiation therapy; DOD=dead of disease; NED=no evidence of disease; CT=chemotherapy; NA=not available; LTFU=lost to follow-up; DOT=died of treatment-related issues

Figure 1 - 753

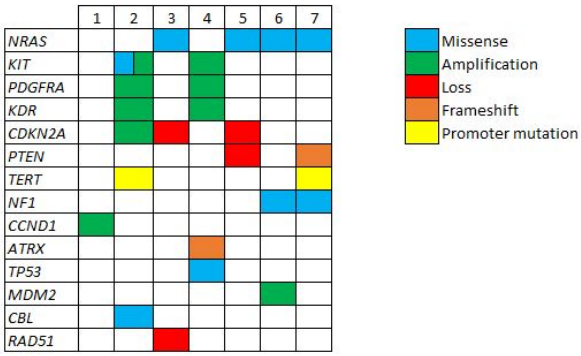

Conclusions: This small cohort provides further insight into molecular pathogenesis of vulvovaginal melanomas. Larger studies using comprehensive genomic panels are warranted to fully assess the relationship between specific molecular alterations and prognosis.

754 Implantation of Ultrastaging Methods for Endometrial Cancer Sentinel Lymph Nodes: Impacts and Recommendations

Florence Perrault[1], Roselyne Choiniere[1], Perrine Granger[2]
[1]Sherbrooke University, Sherbrooke, Canada, [2]Hôpital Fleurimont, Sherbrooke, Canada

Disclosures: Florence Perrault: None; Roselyne Choiniere: None; Perrine Granger: None

Background: Ultrastaging methods are recommended to increase detection rates of metastasis in endometrial cancer sentinel lymph nodes (SLN) as it has been hypothesized that pelvic recurrences occurring despite favorable prognostic features may be caused by "occult" metastases, undetected by routine H&E. The aim of the study was to evaluate the impacts of the implantation of ultrastaging protocols in our pathology department.

Design: Our prospective cohort included patients with endometrial cancer and SLN mapping from 2018 to 2020. After the initial H&E, our ultrastaging method included an unstained slide followed by two consecutive H&E levels and two immunohistochemistry at 50 µm intervals. Later, the method evolved with the addition of three unstained slides; following the initial H&E and the first and second immunohistochemistry slides to better differentiate isolated cells with keratin staining of uncertain origin. Detection rates were compared to the initial H&E, without ultrastaging.

Results: Ultrastaging was performed on 372 SLN from 117 patients with a mean age of 66.7 years (range 28-88). The detection rate was significantly superior with ultrastaging methods (16.2% vs 9.4%, p=0,008). Positive SLN identified by ultrastaging consisted of isolated tumor cells (12/13 SLN) and a single micrometastasis (1/13 SLN). Of these, 23% were first identified on the first level, 69% on the first IHC and 8% on the second IHC. For one patient, ultrastaging increased the FIGO stage to IIIC1 (N0 to N1mi). The first and second versions of the protocol cost 95.94$/SLN and 108.96$/SLN, respectively. The difference of 13.02$/SLN is explained by the addition of three unstained slides for the second protocol. The cost of the addition of ultrastaging was 19,543.95$/year, representing a increase of 18,331.23$/year.

Table 1. Detection Rates of SLN

		Without Ultrastaging (%)	With Ultrastaging (%)	p
Per Patient	V1 (n=37)	2.7	5.4	1.000
	V2 (n=80)	12.5	21.3	0.016
	Total (n=117)	**9.4**	**16.2**	**0.008**
Per SLN	V1 (n=111)	1.8	4.6	1.000
	V2 (n=261)	2.7	9.1	<0.0005
	Total (n=372)	**3.8**	**7.3**	**<0.0005**

SLN - Sentinel Lymph Node, V1 and V2 - versions 1 and 2 of ultrastaging protocols

Figure 1 - 754

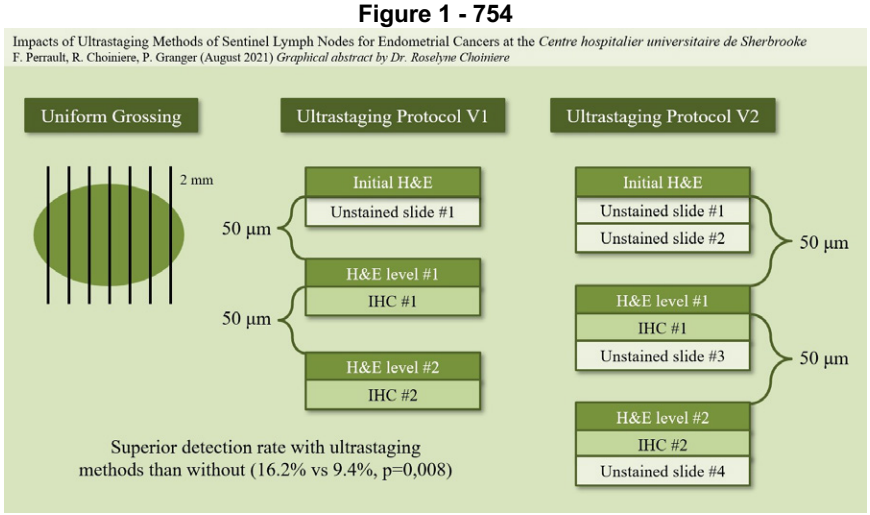

Figure 2 - 754

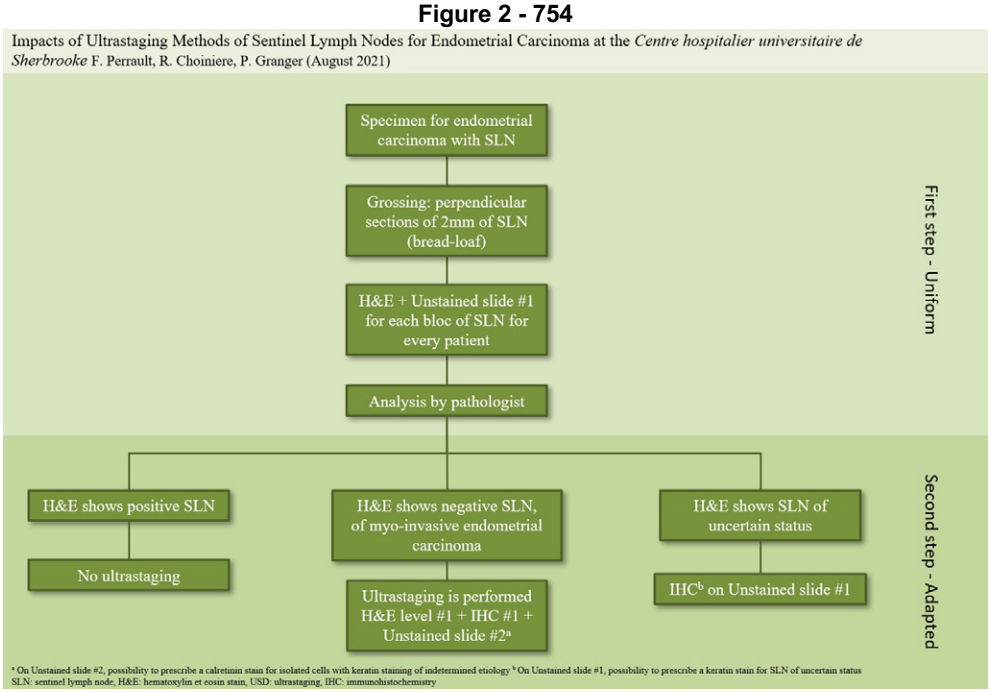

Conclusions: The implantation of ultrastaging methods in our institution significantly increased the detection rate of positive SLN in endometrial carcinoma and upgraded the FIGO stage of one patient. Nevertheless, the pertinence of ultrastaging remain limited since the overwhelming majority of detected positive SLN consisted of isolated tumor cells which have an uncertain clinical significance. From our experimentation, we suggest a revised and alleviated protocol which considers three possible situations following the analysis of the initial H&E to limit the use of ultrastaging for selected and more pertinent cases.

755 Implementation of Endometrial Cancer TCGA Classification Using ProMisE: Experience at a Tertiary Care Center

Devon Pino[1], Lynelle Smith[1], Kurtis Davies[1], Amber Berning[1], Miriam Post[1], Bradley Corr[1], Saketh Guntupalli[1], Christine Fisher[1], Dara Aisner[3], Rebecca Wolsky[3]
[1]University of Colorado Anschutz Medical Campus, Aurora, CO, [2]University of Colorado, Denver, [3]University of Colorado, Denver, CO

Disclosures: Devon Pino: None; Lynelle Smith: None; Kurtis Davies: *Advisory Board Member*, Novartis; Amber Berning: None; Miriam Post: None; Bradley Corr: *Advisory Board Member*, Merck, AstraZeneca, Novocure; *Primary Investigator*, Clovis; Saketh Guntupalli: None; Christine Fisher: *Consultant*, Axio biostatistics; Dara Aisner: *Consultant*, Blueprint Medicines, Loxo Oncology, Sanofi Genzyme; *Grant or Research Support*, Genentech; Rebecca Wolsky: None

Background: In 2013, the TCGA identified 4 prognostic groups for endometrial carcinomas (EMCA) . The ProMisE algorithm employs IHC where possible, rendering the TCGA classification more accessible, which has been endorsed by the WHO. Other recent consensus guidelines also encourage molecular testing in EMCA (European Society of Gynaecological Oncology, NCCN). Here we describe the *de novo* implementation of EMCA testing at one tertiary care center and the related results utilizing the EPIS framework (Exploration, Preparation, Implementation, Sustainment).

Design: Following a request from the gynecologic oncology group, we assembled a multi-disciplinary task force to identify need for testing and barriers, as well as potential solutions (Exploration and Preparation phases). These phases took approximately 6 weeks, with launch of testing in 11/2020. As of 7/2021, 121 EMCA have undergone this new testing protocol (Implementation phase, Fig 1).

Results: The Sustainment phase includes tracking the distribution of molecular subtypes and histotypes (Table 1). There were 9 dual classifiers: 2 *POLE*-p53 (1 endometrioid (emoid) and 1 carcinosarcoma), and 7 MMRd-p53 (6 emoid and 1 poorly differentiated). Notably, 13 cases (11%) harbored *TP53* mutations but were p53 IHC wild-type (wt); all were emoid. Of the p53 discordant cases, 7 (54%) were dual classifiers: 6 MMRd-p53 and 1 *POLE*-p53. The remaining 6 p53 discordant were grade 1 emoid. 13% of all emoid were p53 discordant, an unexpected result calling into question whether these cases, in particular emoid grade 1, stage I, should truly be classified in the TCGA p53 group. Further investigation of the *TP53* mutations (mut) suggests approximately 2/3 of discordances may be attributable to subclonality, indicating that the *TP53* mut may be a consequence of underlying pathobiology rather than a truncal event.

Histotype	POLE n (% of POLE)	MMRd n (% of MMRd)	NSMP n (% of NSMP)	P53 n (% of p53)	Dual classifier n (% of dual)
Emoid	5 (100)	29 (96)	50 (98)	7 (27)	7 (8)
Serous	0 (0)	0	0	8 (31)	0 (0)
Carcinosarcoma	0 (0)	0	1 (2)	9 (35)	1 (1)
Undiff/dediff	0 (0)	1 (3)	0	1 (4)	0 (0)
Total (% of all cases)	**5 (4)**	**30 (25)**	**51 (42)**	**26 (22)**	**9 (7)**

Figure 1 - 755

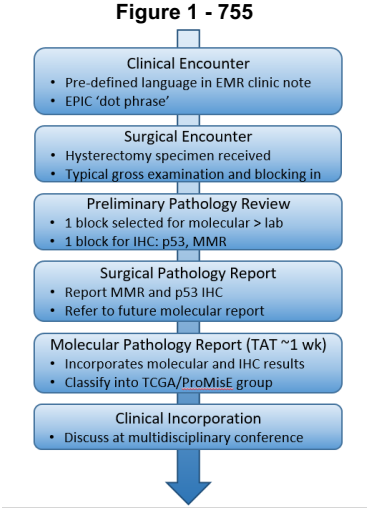

Conclusions: The highly anticipated results from the ongoing PORTEC 4a trial of molecular profile-based adjuvant therapy will inform standardized, specific, practical recommendations for EMCA testing and reporting. This study describes in detail the implementation process at one tertiary care center using the EPIS framework and the results thus far, including a subset of low-stage, low-grade emoid carcinomas that are *TP53* mut, yet p53 wt, an unexpected result.

756 Histopathological and Clinical Analysis of 19 Placentas in Patients Diagnosed with COVID-19 Infection

Joaquin Ponce-Zepeda[1], Beverly Wang[2], Delia Tifrea[1], Kirk Sheplay[3], Robert Edwards[4]
[1]University of California, Irvine, Orange, CA, [2]UCI Medical Center, Orange, CA, [3]Irvine, CA, [4]UC Irvine Health, Orange, CA

Disclosures: Joaquin Ponce-Zepeda: None; Beverly Wang: None; Delia Tifrea: None; Kirk Sheplay: None; Robert Edwards: None

Background: Although there are many studies examining the clinical outcomes of women and their infants diagnosed with severe acute respiratory syndrome coronavirus 2 (SARS-CoV-2) infection, during pregnancy, the reasons causing the possible adverse outcomes remain unclear[1]. This study examines placental pathology from women who contracted COVID-19 during pregnancy at this university hospital institution.

Design: This study was centered around all 19 placenta specimens from patients infected with COVID-19 at this university hospital. The American College of Obstetricians and Gynecologists (ACOG) allow for the judgement of the Obstetrics physician to be the predominant factor in the decision of sending the placenta specimen for pathology evaluation. Therefore ACOG and CRICO (a risk retention group for medical practitioners) work in conjunction to recommend that placentas be sent for pathology evaluation when clinically indicated. All 19 placenta specimens that were submitted in this study met at least one of these recommendations and therefore 19 age matched controls without COVID-19 infection were reviewed in order to outline any significant clinical trends. The age matched controls were selected within the same time frame as the COVID-19 specimens, which was June 2020 to August 2021.

Results: The interval of initial COVID-19 diagnosis and time of placenta evaluation was documented in each case, with the median time interval being 2 days (minimum 1day to maximum 91 days). The gestational age for each patient was calculated, and the average gestational age was a full term pregnancy of 37.2 weeks. 90% of the patients were identified to be of Hispanic ethnicity and heritage, while the other two patients were of Caucasian descent. 63% of the placental weights from the COVID specimens were 25th percentile or lower, whereas only 21% of the age matched controls were 25th percentile or lower. 63% of the cases were recognized to contain histopathological abnormalities, 10.5% in aged matched controls. 4 cases were found to have intra-placental infarction (figure 1), 2 cases were identified to have chorangiosis, 1 case of villous ischemic change, 1 case of decidual laminar necrosis, 1 case of meconium, and 2 cases of acute chorioamnionitis.

19 Placentas in Patients diagnosed with COVID 19.

Cases	Type of delivery	Weeks of gestation	Age years/ethnicity	Clinical findings	Weight of fetus (grams)	Weight of placenta (grams)	Interval from COVID-19 Dx (days)	Placenta weight percentile
1	N-Vaginal	39	25/Hispanic	GDM, BMI 43	3890	593	2	>75th%
2	N-Vaginal	39	23/Hispanic	Chlamydia, BMI 34	3690	579	2	>75th%
3	C-section	37	33/Hispanic	Cholestasis	3110	393	14	10th%
4	N-Vaginal	38	37/Hispanic	IDA, HIV +	2140	292	3	<10th%
5	N-Vaginal	36	19/Hispanic	Cholestasis, BMI 33	2550	366	2	<10th%
6	N-Vaginal	39	39/Hispanic	Oligohydramnios	2820	485	4	<25%
7	N-Vaginal	40	21/Caucasian	Unremarkable	3540	460	1	25th%
8	N-Vaginal	37	40/Hispanic	Pre-eclampsia	3600	596	8	>90th%
9	C-section	29	39/Hispanic	PPROM	1320	199	4	<10th%
10	N-Vaginal	39	15/Caucasian	Unremarkable	3500	605	2	>90th%
11	Vacuum assisted	40	38/Hispanic	HSIL	3000	548	2	>50th%
12	Induction	31	31/Hispanic	IUFD	N/A	402	1	>75th%
13	N-Vaginal	38	35/Hispanic	Preeclampsia, BMI 37	3300	413	1	<25th%
14	N-Vaginal	38	19/Hispanic	Methamphetamine	3600	457	1	25th%
15	N-Vaginal	39	23/Hispanic	IDA	3620	440	12	<25th%
16	N-Vaginal	37	30/Hispanic	GDM	3430	373	1	<10th%
17	Induction	39	33/Hispanic	GHTN, BMI 29, HPV	3410	501	5	>50th%
18	N-Vaginal	39	26/Hispanic	Late Decels, BMI 31	3310	393	1	25th%
19	C-section		29/Hispanic	BMI 44	2115	305	3	<10%

Figure 1 - 756

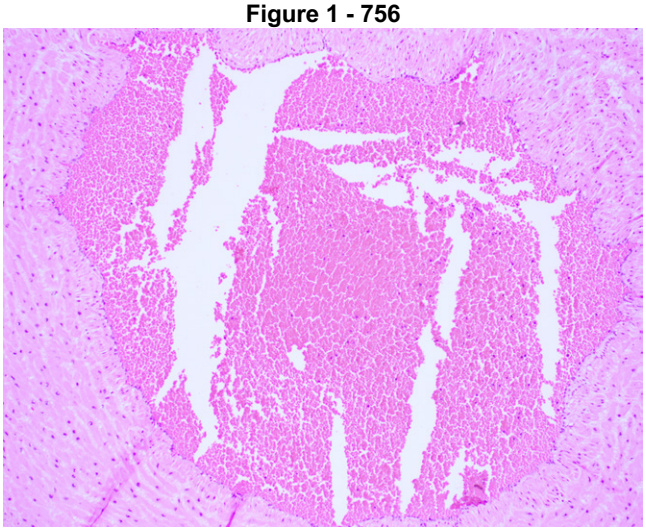

Figure 2 - 756

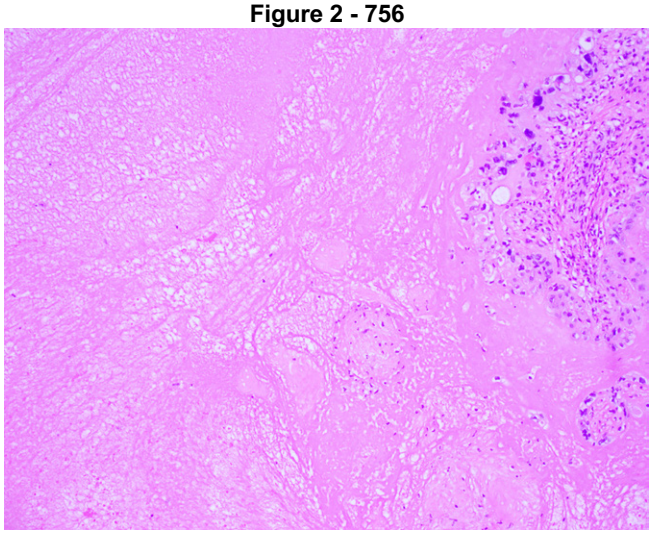

Conclusions: In this study on average the placenta weight was identified to be lower than age matched controls and placental abnormalities were identified more often in patients infected with COVID 19 (63% vs. 10.5%).

757 p53 Status Correlates with the Differential Expression of Mismatch Repair Protein in Vulvar Squamous Cell Carcinoma

Jiani Qu[1], Wei Dong[1], Bin Du[1]
[1]Shanghai First Maternity and Infant Hospital, Shanghai, China

Disclosures: Jiani Qu: None; Wei Dong: None; Bin Du: None

Background: Vulvar squamous cell carcinoma (VSCC) represents approximately 5% of all female genital cancers. Immune checkpoint inhibitor treatment has been approved for DNA mismatch repair (MMR) deficient patients in head and neck cutaneous squamous cell carcinomas. However, there was no data on the frequency of MSI and altered MMR protein expression in vulvar squamous cell carcinoma (VSCC) are available to date. Some studies show that aberrations involving MMR genes and p53 are frequent in cervical carcinoma with a significant correlation between them. This study examines the expression of 4 MMR proteins (hMLH1, hMSH2, hMSH6, and hPMS2) in VSCC and correlates with the status of p53 expression and clinicopathologic factors.

Design: The cohort included 43 vulvar squamous cell carcinoma cases between 2013 and 2021. Immunohistochemistry for MMR proteins and p53 was performed. If the tumor showed complete absence or nuclear expression in < 5% of the tumor cells of at least 1 MMR protein (and showing regular MMR expression in the associated normal tissue), the case was scored as negative (Figure1). The p53 IHC stains were scored as wild-type (weak, variable nuclear staining). Two patterns of staining were defined as "p53 abnormal (p53abn)" (i) diffuse (75-100% nuclear staining) (ii)null-phenotype (no nuclear or cytoplasmic staining). Clinicopathological data was recorded.

Results: Deficient MMR protein expression was observed in 8 cases (18.6%). Seven cases showed loss of two MMR protein. Of these, five cases showed loss of hMLH1 in combination with hPMS2, two patients demonstrated both hMSH6 and hMSH2 expression loss. Loss of hMSH2 expression only occurred in hMSH6 deficient tumors. Only one case demonstrated deficient expression pattern for all four MMR proteins. Deficient mismatch repair (dMMR) was correlated with aberrant p53 expression (Table 1). Six of 8 (75.0%) deficient mismatch repair (dMMR) carcinomas were aberrant p53 expression, and only 8 of 35 (22.9%) proficient mismatch repair (pMMR) tumors were also aberrant p53 expression ($P<0.01$). The median age (68 years and 63 years) was similar between the MMR deficient and MMR proficient patients ($P=0.83$). The primary tumor characteristics were similar in both groups, with no significant difference in family history, FIGO-stage, morphologic subtype, N-category, HPV status or treatment patterns.

Table 1. p53 immunophenotype and cohort clinicopathological features association with MMR status

	pMMR	dMMR	P-value
Number of patients	35	8	
Age			
Median (range)	68(29-82)	63(55-78)	0.83
Family history (n [%])			
positive	10（28.6）	3（37.5）	0.31
negative	25（71.4）	5（62.5）	
Stage (n [%])			
Stage I	20(57.1.)	4(50.0)	0.17
Stage II	10(28.6)	2(25.0)	
Stage III	4(11.4)	1(12.5)	
Stage IV	1(2.9)	1(12.5)	
Morphologic subtype (n [%])			
Basaloid	7(20.0)	1(12.5)	0.14
Warty	7(20.0	0	
Keratinizing	21(60.0)	7(87.5)	
N-stage (n [%])			
N0	28(80.0)	6(75.0)	0.28
N1-2	4(11.4)	1(12.5)	
N＞2	3(8.6)	1(12.5)	
HPV status (n [%])			
positive	14(40.0)	2(25.0)	0.42
negative	21(60.0)	6(75.0)	
Treatment (n [%])			
Surgery	9(25.7)	3(37.5)	0.36
Adjuvant treatment	26(74.3)	5(62.5)	
p53 immunophenotype (n [%])			
wild-type	27(77.1)	2(25.0)	＜0.01
mutant-type	8(22.9)	6(75.0)	

Figure 1 - 757

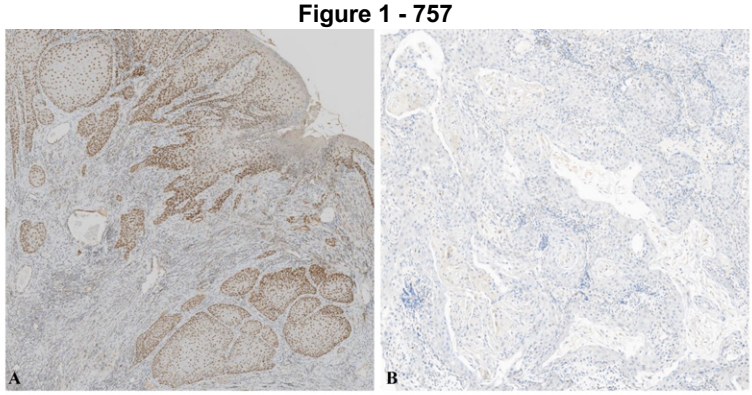

A Mismatch repair（MMR) protein proficient expression B Mismatch repair（MMR) protein deficient expression

Conclusions: We found that MMR deficiency is uncommon in VSCC, most likely sporadic, and not associated with any clinicopathologic parameters. However, MMR deficiency has a positive association with aberrant p53 expression in VSCC. Our data demonstrate that using MMR in conjunction with p53 immunohistochemistry may provide additional information in the treatment of VSCC.

758 P53 Expression in Mucinous Borderline Tumors with Intraepithelial Carcinoma

Charles Quick[1], Azin Mashayekhi[1]
[1]*University of Arkansas for Medical Sciences, Little Rock, AR*

Disclosures: Charles Quick: None; Azin Mashayekhi: None

Background: Recent studies have implicated *TP53* as a possible driver of progression from mucinous borderline tumor (MBOT) to mucinous ovarian carcinoma (MOC) and another recent study validated immunohistochemistry for p53 as a surrogate

for *TP53* mutation. The focus of these studies has centered on borderline tumors and carcinomas; however, little is known about p53 expression in borderline tumors containing intraepithelial carcinoma (IEC). We evaluated p53 expression in MBOT, with and without IEC, by p53 IHC.

Design: Our archive was searched for MBOT/IEC and MBOT (controls) over the past 18 years. MOC was excluded. Slides were pulled and reviewed noting MBOT and IEC. IEC was defined as areas of severe nuclear atypia, cribriform growth or both. Representative, separate slides containing MBOT and IEC were submitted for p53 staining for each case. P53 expression was scored as wild type (WT) or abnormal (mutant [>70% nuclear or cytoplasmic staining] and null [complete absence]). Tumor stage and clinical follow up were recorded from patient charts.

Results: 16 cases with MBOT/IEC were identified and adequate for staining. Twenty-three MBOT were included as controls. Ages ranged from 20-80 years (median: 40). P53 was abnormal in 63% (10/16) of MBOT/IEC, and 2/23 (9%) MBOT. 8/10 (80%) p53 abnormal MBOT/IEC cases showed abnormal p53 in adjacent histologically borderline areas. The two cases of MBOT (2/23, 9%) with abnormal p53 staining were stage 1c due to capsular rupture. Seven cases contained micro-invasion, 6 of which contained IEC (86%) [4/10 p53 abnormal MBOT/IEC, 2/10 p53 WT MBOT/IEC] and 1/23 (4%) MBOT. 10/39 cases were stage 1c (the rest were 1a), of these 6 (38% of all cases) contained IEC (4 p53 abnormal), whereas only 4/23 (17% of all cases) MBOT were stage 1c. No patients died of disease.

Conclusions: P53 mutation is much more common in MBOT/IEC (63%) compared to MBOT (9%). Interestingly, background borderline tumor (i.e. areas lacking IEC) was p53 abnormal in 80% of MBOT/IEC cases, suggesting that p53 mutation occurs before the development of atypia, a finding further hinted at by the identification of abnormal p53 staining in 9% of MBOT without IEC. Tumors with IEC have an increased incidence of micro-invasion and higher stage (1c vs. 1a) disease when compared to borderline tumors lacking IEC.

759 Risk Reducing Salpingectomy With Delayed Oophorectomy In Women with BRCA Germline Mutation Seeking Temporary Fertility Preservation: Pathologic Findings And Outcome In A Pilot Series

Joseph Rabban[1], Amanda Borgen[1]
[1]*University of California, San Francisco, San Francisco, CA*

Disclosures: Joseph Rabban: None; Amanda Borgen: None

Background: Risk reducing salpingectomy with delayed oophorectomy (RRS-DO) for women with a *BRCA1/2* germline mutation has recently received attention as an alternative to risk reducing salpingo-oophorectomy (RRSO) in order to temporarily preserve fertility or delay surgical menopause. In this strategy, completion bilateral oophorectomy is delayed until after completion of fertility plans. The pathologic findings and outcome of RRS-DO are not well studied.

Design: Women with *BRCA1/2* germline mutation who underwent RRS without concurrent oophorectomy were identified from our pathology archives. Our departmental protocol for managing RRS specimens is to use the same SEE-Fim protocol as used for fallopian tubes in RRSO. RRS cases from other institutions submitted for secondary review were also included. Standard morphologic and immunohistochemical (p53, Ki67) criteria were used to diagnose serous tubal intraepithelial carcinoma (STIC) and high grade serous carcinoma (HGSC). Clinical data and follow up was collected from electronic medical records. Results of pelvic washing cytology, when performed, was also evaluated.

Results: STIC occurred in 4.5% (1/22) of RRS cases (median age 37 years for all 22 patients). The patient with STIC had bilateral microscopic foci of HGSC (FIGO stage IIC) on subsequent oophorectomy staging surgery (alive without disease at 71 m). Post-RRS ovarian HGSC (FIGO stage I) developed in 4.7% (1/21) benign RRS cases; this occurred 89 months following RRS at another institution, in which the full SEE-Fim protocol was not performed; the patient is alive without disease. Post-RRS metastatic breast cancer to ovaries developed in 4.7% (1/21) benign RRS; this occurred 18 months after RRS. Pelvic washing cytology at the time of RRS was benign in all cases for which it was performed. In the remaining 19 benign RRS cases, 9 underwent completion oophorectomy at a median interval of 37 months following RRS. All 9 showed benign pathology and pelvic cytology. One patient achieved post-RRS pregnancy via assisted reproductive technology. All patients are alive at last follow up.

Conclusions: The prevalence of occult STIC and of post-prophylaxis pelvic HGSC in women with *BRCA1/2* who undergo RRS with delayed oophorectomy is similar to that for women who undergo conventional RRSO. Post RRS surveillance for pelvic HGSC remains important, especially in the interim until completion oophorectomy is performed.

760 Differential Etiopathogenic and Clinic-pathologic Characteristics of Vulvar Squamous Cell Carcinomas in Sub-Saharan Africa and Europe

Natalia Rakislova[1], Nuria Carreras Dieguez[1], María Teresa Rodrigo[1], Sherley Diaz-Mercedes[2], Carla Carrilho[3], Marta del Pino[1], Inmaculada Ribera[1], Lucília Trindade Lovane Matias[3], Cesaltina Lorenzoni[3], Lorena Marimon[4], Ofélia Neves Saúde[3], Fabiola Fernandes[3], Ricardina Rangeiro[3], Jaume Ordi[5], Naiara Vega[1]
[1]Hospital Clinic, Barcelona, Spain, [2]Hospital Clinic, University of Barcelona, Barcelona, Spain, [3]Maputo Central Hospital, Maputo, Mozambique, [4]Institute for Global Health (ISGloblal), Spain, [5]University of Barcelona, Barcelona, Spain

Disclosures: Natalia Rakislova: None; Nuria Carreras Dieguez: None; María Teresa Rodrigo: None; Sherley Diaz-Mercedes: None; Carla Carrilho: None; Marta del Pino: None; Inmaculada Ribera: None; Lucília Trindade Lovane Matias: None; Cesaltina Lorenzoni: None; Lorena Marimon: None; Ofélia Neves Saúde: None; Fabiola Fernandes: None; Ricardina Rangeiro: None; Jaume Ordi: None; Naiara Vega: None

Background: Mozambique is a sub-Saharan country in South-East Africa with high prevalence of human papillomavirus (HPV) and HIV co-infection. We aimed to compare the features of the vulvar squamous cell carcinomas (VSCC) from Mozambique with those from Spain, a European country with relatively low prevalence of HPV and a low proportion of people living with HIV.

Design: We included all VSCC diagnosed at two tertiary, public institutions from sub-Saharan Africa and Europe: the Maputo Central Hospital (MCH), in Mozambique, and the Hospital Clinic of Barcelona (HCB), in Spain, from January 2018 to December 2020 (n=35 and n=41, respectively). In all tumors, HPV DNA detection and genotyping using a PCR-based technique (SPF10/DEIA/LiPA25), and immunohistochemistry for p16 and p53 were performed. VSCCs showing diffuse p16 positive staining and/or HPV DNA positivity were considered HPV-associated lesions, whereas lesions negative for p16 and HPV DNA were considered HPV-independent VSCC. p53 staining was evaluated as suggestive of wild-type protein (scattered or mid-epithelial patterns) and suggestive of mutation (basal or diffuse overexpression, cytoplasmic positivity or null patterns).

Results: Thirty-four out of the 35 tumors (97%) from Mozambique and only 8/41 (20%) from Spain were HPV-associated ($p<0.001$). Mean age of the patients from Mozambique and Spain was 45 ± 12 and 72 ± 14, respectively ($p<0.001$). No significant differences were found either in terms of HPV genotypes (HPV16 43%, HPV33 29%, HPV58 24%, HPV18 14% in Mozambique, and HPV16 50%, HPV33 25%, HPV53 7%, HPV56 7% in Spain), nor in terms of multiple infection (33% in Mozambique, 25% in Spain). One out of 35 tumors (3%) from Mozambique and 29/41 (70%) from Spain showed abnormal pattern of p53 immunostaining ($p<0.001$). Histologically, 37% of the tumors from Mozambique were keratinizing and 63% were basaloid, warty or non-keratinizing, whereas in Spain, 73% of the tumors were keratinizing, and 27% were basaloid, warty or non-keratinizing ($p=0.002$).

Conclusions: In contrast with the predominance of HPV-independent VSCC affecting old women observed in Europe, the vast majority of VSCC in sub-Saharan Africa are HPV-associated tumors arising in young women. This data may have an important impact in primary prevention policies of VSCC worldwide.

761 Mucinous Ovarian Neoplasms Associated with Teratomas Usually Present with Low Stage Disease and Overall Favorable Outcome

Preetha Ramalingam[1], Mario Marques-Piubelli[1], Isabel Alvarado-Cabrero[2], Maria Delia Perez Montiel[3], Nidhi Tandon[4], Elizabeth Euscher[1], Anais Malpica[1]
[1]The University of Texas MD Anderson Cancer Center, Houston, TX, [2]Mexican Oncology Hospital SXXI, IMSS, Mexico City, Mexico, [3]Instituto Nacional de Cancerologia, Mexico City, Mexico, [4]The University of Texas Health Science Center at Houston

Disclosures: Preetha Ramalingam: None; Mario Marques-Piubelli: None; Isabel Alvarado-Cabrero: None; Maria Delia Perez Montiel: None; Nidhi Tandon: None; Elizabeth Euscher: None; Anais Malpica: None

Background: Mucinous ovarian neoplasms associated with teratomas (MOvNTs) are uncommon tumors with only a few large series published thus far. The spectrum of clinical, histologic, and immunohistochemical findings are evaluated in this multi-institutional study.

Design: 50 MOvNTs were retrieved from the files of four institutions over a 15-year (yr) period. The following parameters were recorded: patient age, CEA and CA-125 levels, family history (FHx) of neoplasms, laterality, tumor size, ovarian (Ov) surface

involvement, type of mucinous tumor, immunohistochemical (IHC) profile , FIGO stage, presence or absence of pseudomyxoma ovarii (PO) and peritonei (PP), follow up (f/u) in months (mos), and outcome. All pathology reports and available hematoxylin and eosin–stained slides were reviewed (median 10). Uni and multivariate (Cox regression) were performed using SPSS (Statistics for Windows, Version 24.0. Armonk, NY: IBM Corp.).

Results: Table 1 summarizes selected findings. 22% of pts had a FHx of carcinoma (Ca) with >50% breast Ca. Histotypes included: 16 mucinous cystadenomas, 17 mucinous borderline tumors (MBT), 1 MBT with intraepithelial Ca, 1 MBT with microinvasive Ca, and 14 mucinous Cas (MCas). Of the MCas, 8 were grade 1, 4 were grade 2, and 2 were grade 3. Increased Ca-125 levels correlated with MCa histotype (p=.0108) while CEA levels were not significant. 26/50 cases had IHC performed: 8 were CK20/CDX2/SATB2 positive (+), while CK7 negative (-) or focal (+). 18/26 cases were CK7 (+) >CK20 and SATB2 (-). 15/22 (68%) cases were PAX8 (+), usually focal. Almost all pts presented with FIGO stage I disease; except one each with FIGO II and IIIc disease. At last f/u (range 2-180 mos, median 53.5 mos): 64% of pts had no evidence of disease, 4% died of disease, 8% alive with disease, 4% died of other causes, and 22% were lost to f/u.

Characteristics	Results
Age [range; median (years)]	17 to 74; 42
Tumor size [range; median (cm)]	6 - 34; 18
CA125 level [range; median (units/ml)]	6.2 - 154; 44.75
Clinical presentation (n=41)	
Abdominal/pelvic pain	21
Bloating	4
Abdominal/pelvic mass	9
Vaginal bleeding	6
Incidental during staging for breast cancer	1
Laterality	
Left	28 (56%)
Right	22 (44%)
Histologic subtype	
Mucinous cystadenoma	16/50 (32%)
Mucinous borderline tumor	17/50 (34%)
Mucinous borderline tumor with intraepithelial carcinoma	1/50 (2%)
Mucinous borderline tumor with microinvasive carcinoma	2/50 (4%)
Mucinous carcinoma	14/50 (28%)
Pseudomyxoma ovarii	15/50 (30%)
Pseudomyxoma peritonei (p=.943)	12/50 (24%)
FIGO stage (p=.651)	
FIGO IA	32/44 (72%)
FIGO IC	10/44 (23%)
FIGO II	1/44 (2%)
FIGO III	1/44 (2%)
FIGO IV	0/44 (0%)
Treatment	
Surgery without staging	30/47 (64%)
Surgery with staging	17/47 (36%)
Chemotherapy	9/43 (21%)
Radiation	0/43 (0%)
Outcome (Follow-up 2 - 180 months, median 53.5)	
Alive no evidence of disease	32/50 (64%)
Alive with disease	4/50 (8%)
Died of disease	1/50 (2%)
Died of other causes	2/50 (4%)
Lost follow-up	11/50 (22%)

Conclusions: In this study the majority of MOvNTs presented with FIGO stage 1 disease. FIGO stage and PP were not associated with worse outcome. Family history of Ca, particularly of breast ca, was present in 22% of pts. All pts with FIGO stage I MCa, regardless of tumor grade, were ANED. The one patient who presented with advanced stage MCa, with intestinal phenotype, had an overall survival of 10yrs. This differs from pts with non-teratoma associated MCa who typically have a much shorter survival in the presence of extraovarian disease. The latter findings should be further investigated.

762 Exophytic Endocervical Adenocarcinoma is Rare and Typically Accompanied by Conventional Stromal Invasion: A Single Institutional Experience, Emphasizing Implications for Tumor Staging and Outcome

Lara Richer, Joseph Rabban[2]
[1]Eastern Ontario Regional Laboratory Association, University of Ottawa, Ottawa, Canada, [2]University of California, San Francisco, San Francisco, CA

Disclosures: Lara Richer: None; Joseph Rabban: None

Background: Exophytic growth by endocervical adenocarcinoma (EC) is uncommon compared to the typical pattern of endophytic infiltration of the cervical wall stroma. The outcome of pure or predominantly exophytic EC is poorly studied and therefore an evidence-based approach to tumor staging is lacking. Thus, we report a single-institutional experience on the prevalence, clinicopathological features and outcome of exophytic EC.

Design: Pathology reports of EC from a single academic tertiary care cancer center diagnosed between 1990 and 2020 were reviewed. Those described as having a component of exophytic growth, defined as papillary, glandular, solid or cribriform architecture without invasion of the cervical wall stroma, were included. Slides of each case and all subsequent cervical specimens were reviewed where available to determine if the exophytic pattern was pure or admixed with a component of conventional stromal invasion. Cases were assigned a 2018 FIGO stage (with the ISGyP recommended modification that EC with an exophytic component and tumor thickness >0.5cm be assigned FIGO IB1). Follow up data was reviewed.

Results: Among 323 EC patients, 2.5% (8/323) had pure exophytic EC and 9% (30/323) had both exophytic and conventional stromal invasive EC components, though 60% (18/30) of the latter had an initial specimen suggesting pure EC but a subsequent specimen containing typical invasive EC. Among the 8 pure exophytic EC, the median age was 40.5 years, all showed HPV associated morphology and/or positive p16 immunohistochemistry, 3/8 showed villoglandular architecture, the median tumor size was 4.5 mm, the stage was IA1 (2), IA2 (4), IB1 (1) and unknown (1). Follow up of 6/8 pure exophytic EC showed 1/6 had recurrence (FIGO stage IA1) but no deaths. For patients with exophytic and invasive EC, the median age was 39 years and 14/30 had villoglandular architecture. The FIGO stage distribution was IA1 (7), IA2(6), IB1 (8), IB2(4), IIIC1(2) and unknown (3) and 3/28 with follow up data available had a recurrence and 2/28 died of their disease, of which 4/5 were IB1 or higher stage and 4/5 had a component of villoglandular architecture.

Conclusions: Pure exophytic EC is rare and most cases will show stromal invasion in a subsequent specimen, resulting in a final stage >IB1 in half of such cases as well as a small risk for recurrence and death. Exclusively exophytic EC may also rarely be associated with recurrence. Similarly, villoglandular architecture can be associated with adverse outcomes.

763 Histologic Features of Uterine Leiomyosarcomas Clinically Profiled by Targeted DNA-Based Next Generation Sequencing

Stephanie Riviere[1], Amir Momeni Boroujeni[2], Martee Hensley[1], Marc Ladanyi[1], Lora Ellenson[1], Sarah Chiang[1]
[1]Memorial Sloan Kettering Cancer Center, New York, NY, [2]Brigham and Women's Hospital, Harvard Medical School, Boston, MA

Disclosures: Stephanie Riviere: None; Amir Momeni Boroujeni: None; Martee Hensley: *Consultant*, Sanofi, Lilly; *Advisory Board Member*, GSK; *Consultant*, Thrive; *Speaker*, Research To Practice; Marc Ladanyi: None; Lora Ellenson: None; Sarah Chiang: None

Background: Uterine leiomyosarcomas (LMS) can exhibit spindle, myxoid and/or epithelioid features. Diagnostic criteria exist for conventional and variant LMS but remain controversial for epithelioid LMS and lacking in tumors demonstrating a mixture of cell types. The amount of myxoid change required to diagnose myxoid LMS is also not known. Detailed histologic analysis of conventional and variant uterine LMS and correlation with mutation profiles have not been previously explored. We evaluated histologic features of all conventional and variant LMS that were clinically profiled by targeted DNA-based next generation sequencing (NGS) to determine whether diagnostic criteria for malignant uterine smooth muscle tumors can be refined.

Design: All conventional and variant uterine LMS that were clinically profiled by targeted DNA-based NGS from 2004 – 2019 were retrieved. Only cases in which all H&E slides of the primary or recurrent tumor were included. Pathology reports and complete sets of H&E slides of 64 LMS (17 primary, 47 recurrent) with NGS data were reviewed. Percentage of spindle, myxoid, and epithelioid

morphology, mitotic index (MI), tumor necrosis (TN), and atypia were evaluated blinded to mutational profiles. Histologic features were then compared to mutational profiles to determine trends in genotype-phenotype correlation.

Results: LMS showed the following cell types: conventional (spindle with/without <50% epithelioid) (n=39, 61%), myxoid (any amount) (n=19, 30%), and epithelioid (>50%) (n=6, 9%). For conventional LMS, median MI was 33 (range, 6-97), 15/39 (38%) had TN and 34/39 (56%) had moderate-severe atypia. For myxoid LMS, median MI was 35 (range, 11-100), 10/19 (53%) had TN and 17/19 (89%) had moderate-severe atypia. For epithelioid LMS, median MI was 49 (range, 17-81), 3/6 (50%) had TN and 6/6 (100%) had moderate to severe atypia. For conventional LMS, the mutation frequency for *TP53*, *RB*, *ATRX*, *PTEN*, *MED12*, *DAXX* and *MDM2* was 67%, 62%, 33%, 33%, 15%, 5% and 5%, respectively. For myxoid LMS, the mutation frequency for *TP53, RB, ATRX, PTEN, DAXX* and *CDKN2A* was 68%, 63%, 32%, 26%, 11% and 5%, respectively. For epithelioid LMS, the mutation frequency for *TP53, RB, ATRX, PTEN, MED12 and CDKN2A* was 67%, 9%, 33%, 33%, 17% and 17%, respectively.

Conclusions: Conventional and variant LMS frequently harbor *TP53, ATRX, RB, PTEN, DAXX, MED12, CDKN2A* and *MDM2* abnormalities. Most genetically profiled LMS including epithelioid and myxoid types have ≥2 features: moderate-severe atypia, TN and MI ≥10.

764 Adenocarcinomas of the Gynecologic Tract Involving the Urinary Bladder: A Series of 16 Cases Mimicking Primary Bladder Malignancy

Daniel Russell[1], Jonathan Epstein[2], Oleksandr Kryvenko[3], Matthew Schlumbrecht[3], Merce Jorda[3], Andre Pinto[4]
[1]Jackson Memorial Hospital/University of Miami Hospital, Miami, FL, [2]Johns Hopkins Medical Institutions, Baltimore, MD, [3]University of Miami Miller School of Medicine, Miami, FL, [4]University of Miami Health System, Miami Beach, FL

Disclosures: Daniel Russell: None; Jonathan Epstein: None; Oleksandr Kryvenko: None; Matthew Schlumbrecht: None; Merce Jorda: None; Andre Pinto: None

Background: Urothelial carcinoma with glandular differentiation and secondary involvement of the bladder by colorectal, prostatic, or uterine squamous cancer are well-recognized. There is limited data describing gynecologic (GYN) adenocarcinomas involving the bladder.

Design: Cases of GYN adenocarcinomas involving the urinary bladder from two academic institutions were retrospectively evaluated during a 10-year period, including from consultation files. Cases with only serosal or muscularis propria involvement were excluded. Slides were reviewed and on those with material available, immunohistochemistry (IHC) for PAX8, GATA-3, ER, PR, p16, p63, CK7, and CK20 was performed, and clinical information was obtained.

Results: 16 cases (15 patients) were identified (42-82 yrs, 61 median). Most (13/15) had a prior history of GYN malignancy (9 endometrial, 2 tubo-ovarian, 1 endocervical, and 1 not specified). 19% (3/16) of cases were initially misdiagnosed as invasive high-grade urothelial carcinoma with (2/3) or without (1/3) squamous differentiation. Revised diagnoses consisted of endometrial endometrioid carcinoma (9/16) (2 low grade, 7 high grade), endometrial serous carcinoma (4/16), tubo-ovarian high grade serous carcinoma (2/16), and cervical adenosquamous carcinoma (1/16). Cases were diagnosed on TUR (10), biopsy (4), and cystectomy (2). Clinical follow-up was available on 13/15, and in patients with prior history of GYN malignancy the time to bladder relapse was 3 weeks-120 mos (median 22 mos). Imaging favored a non-bladder primary in 8, bladder primary in 5, and was equivocal in 2 cases. By cystoscopy, 10/13 were favored extra-vesical and 3/13 intra-vesical (2 flat, 1 papillary). Prominent morphologic findings included uniform glandular histology without heterogeneity (9/13), tumor overrunning bladder mucosa without discernable normal epithelium (9/13), and squamous differentiation (4/13). Tumors were diffusely positive for PAX8 (10/12), ER (12/15), p16 (10/15), and CK7 (12/12), and focally positive for GATA-3 (5/13), PR (7/14), and p63 (3/12), and were negative for CK20 (0/14).

Conclusions: Gynecologic adenocarcinomas rarely involve the urinary bladder. Key features to the correct diagnosis include awareness of prior GYN malignancy, morphological tumoral homogeneity, absence of a urothelial precursor, and expression of ER/PR/PAX8 with negative CK20. Pitfalls include misleading radiologic and cystoscopy findings, squamous differentiation, focal GATA-3/p63 positivity, and lack of PAX8 staining.

765 Clinical Utility of Endometrial Carcinoma Genomic Classification Using TruSight Tumor 500 Next Generation Sequencing

Azhar Saeed[1], Jordan Mattson[1], Shannon Welter[2], Guang Yang[3], Maria Fernanda Rodriguez[1], Sarah Munro[1], Christine Henzler[1], Colleen Forster[1], Molly Klein[1], Sally Mullany[1], Mahmoud Khalifa[1], Boris Winterhoff[2], Andrew Nelson[1]
[1]University of Minnesota, Minneapolis, MN, [2]University of Minnesota Medical Center, Minneapolis, MN, [3]Perelman School of Medicine, Hospital of the University of Pennsylvania, Philadelphia, PA

Disclosures: Azhar Saeed: None; Jordan Mattson: None; Shannon Welter: None; Guang Yang: None; Maria Fernanda Rodriguez: None; Sarah Munro: None; Christine Henzler: None; Colleen Forster: None; Molly Klein: None; Sally Mullany: None; Mahmoud Khalifa: None; Boris Winterhoff: *Stock Ownership*, Verastem, Exact Science; Andrew Nelson: None

Background: Current clinical approaches for molecular classification of endometrial carcinomas (ECs) rely on limited sequential assessment of single biomarkers. This may insufficiently assess ECs' molecular profile. Here, we study the clinical utility of the comprehensive genomic profiling (CGP) assay Trusight Tumor Oncology (TSO) 500 for characterizing EC.

Design: 36 unique patient samples with EC from a retrospective patient cohort were selected to include clinical recurrence, high, and low risk cases. DNA was extracted, sequenced, and analyzed on Illumina's TSO500 platform. Interim analysis for 24 unique patients completed include: endometrioid FIGO 1 (n=3), FIGO 2 (n=11), FIGO 3(n=7), Clear Cell (n=1), Mixed (n=1), and serous (n=1) histologies. Immunohistochemistry (IHC) for p53 and L1CAM was compared to mutation status. Patient replicates and synthetic controls were sequenced to assess precision and accuracy, respectively.

Results: We classified cases into 5 molecular subgroups (Table) using the detected signature mutations, tumor mutational burden (TMB), and Microsatellite Instability (MSI) status. TMB and MSI results were essential in classifying hypermutated tumors: high TMB with Microsatellite Stable (MSS) status established the best classification (*POL*mut) of 2 cases with variants of uncertain significance (VUS) in the *POLE/POLD1* genes. Also, secondary variants in signature genes can arise in other subgroups (*POLE* and *TP53* variants found in 2 MSI-H cases). Of interest, we identified potentially targetable mutations in other genes across several subtypes, including: *IDH1* (NSMP), *BRCA2* (*POL*mut), and *PALB2* (*TP53*mut), thus highlighting the importance of CGP in characterization of EC for personalized therapy. Copy number alterations (CNA) in *TP53* mutated (n=5/9) and *TP53* wild type (n=4/7) groups were similar and thus not helpful in separating these groups. Overall IHC interobserver interpretive agreement for p53 IHC was 68%, although it was 100% for dominant negative missense *TP53* mutants. L1CAM staining was heterogeneous across molecular groups. Assay precision was 100% (inter and intra run comparison); analytic sensitivity was 95%.

Molecular groups	Number of Cases	Additional Genomic Characteristics	TMB range	MSI Status (20% cutoff)	Histopathologic Category and L1CAM Status
***POL*mut** (*POLE* or *POLD1* variants with elevated TMB and MS-stable)	3	*a) POLE*: Pathogenic Mutation (n=1); Variant of Unknown Significance (VUS) (n=1) *b) POLD1*: VUS (n=1) *c) BRCA2* mutation (n=1)	32-80	MSS	FIGO 2 (n=3) L1CAM+ (n=1) L1CAM neg (n=2)
MSI-H Microsatellite Instability High (>20% markers unstable)	4	*a) POLE* VUS (n=2) *b)* Multiple *TP53* mutations (n=1)	15-48	MSI high range: 29-43%	FIGO 2 (n=2) FIGO 3 (n=1) Mixed (75% FIGO 3, 20% clear cell, 5% serous) (n=1) L1CAM+ (n=2) L1CAM neg (n=2)
TP53mut (*TP53 Pathogenic* Mutation on NGS)	9	*a) TP53* missense mutation (n=7) *b) TP53* Loss of function (LOF) mutations (n=2) *c) POLD1* VUS (n=1) *d) PALB2* mutation (n=1)	0.8-10.3	MSS	FIGO 1 (n=1) FIGO 2 (n=2) FIGO 3 (n=4) Clear cell (n=1) Serous (n=1) L1CAM+ (n=2) L1CAM neg (n=6) *1 stain failed
***TP53* Wild Type / *CTNNB1* Mutated**	1	*a) CTNNB1* G34E	17.5	Borderline MSI, 20%	FIGO 3 (n=1) L1CAM neg (n=1)
NSMP (No specific Molecular Profile)	7	*a) IDH1* Pathogenic Mutation: R132C (n=1)	0.8-25.2	MSS	FIGO 1 (n=2) FIGO 2 (n=4) FIGO 3 (n=1) L1CAM+ (n=2) L1CAM neg (n=5)

Conclusions: Findings from this Interim analysis supports the clinical utility of CGP using TSO500 for complete molecular classification of EC and highlights complexity in EC genomics. In addition to prognostication, CGP offers wider avenues for personalized therapy in the context of EC heterogeneity.

766 Endometrioid Squamous Proliferations of the Endometrium Express Alpha-Methylacyl-CoA Racemase (AMACR)

Shabnam Samankan[1], Maryam Tahir[2], Marilyn Huang[3], Andre Pinto[4]
[1]George Washington University, Washington DC, DC, [2]University of Miami Miller School of Medicine, Miami, FL, [3]University of Miami, Miami, FL, [4]University of Miami Health System, Miami Beach, FL

Disclosures: Shabnam Samankan: None; Maryam Tahir: None; Marilyn Huang: None; Andre Pinto: None

Background: Squamous morular metaplasia (SMM) is closely associated with endometrioid proliferative lesions such as endometrial intraepithelial neoplasia (EIN), while endometrioid adenocarcinomas (EMCA) also may demonstrate squamous differentiation (morular or non-morular). Alpha-Methylacyl-CoA Racemase (AMACR; P504s) is an immunohistochemistry (IHC) marker commonly expressed in many tumors, including prostate adenocarcinoma, renal cell carcinoma, and a subset of gynecologic tumors, predominantly of clear cell histology. In small biopsy samples, the distinction between cervical high-grade squamous intraepithelial lesions (HSIL) involving endocervical glands from endometrioid squamous proliferation can be challenging, given the anatomical vicinity and some degree of morphological overlap. Moreover, p16 immunostain tends to be positive in both lesions, which precludes its utilization in this differential diagnosis.

Design: Following the observation of AMACR positivity by IHC within squamous morules in an index case, 30 endometrial samples (biopsies, curettages and resections) containing SMM (15) and non-morular (15) squamous metaplasia (NMSM), and 32 cases of cervical HSIL involving endocervical glands were stained with AMACR. The endometrial cohort consisted of 1 benign anovulatory endometrium, 6 endometrial polyps, 8 EINs, and 15 EMCAs. Positive cases were scored as diffuse (≥50%) or focal (<50%). Controls were appropriately used.

Results: AMACR staining was seen in 96.7 % of endometrial squamous lesions, including 14 (93.3%) of endometrioid carcinomas and in all cases of EINs, EMPs, and anovulatory endometrium with SMM or NMSM. Most positive cases (69%) showed diffuse IHC labeling, while in 31% it was focal. Only 2 cases (5.8%) of endocervical glands involved by HSIL demonstrated positivity with AMACR.

Conclusions: AMACR is frequently expressed in squamous metaplasias of the endometrium, of both morular and non-morular types. This novel immunohistochemical finding needs to be considered to avoid pitfalls in other differential diagnoses, including carcinomas of clear cell histology. Additionally, AMACR can reliably differentiate the origin (endocervical vs. endometrial) of squamous lesions in instances where the diagnostic material is limited and correct interpretation may define patient management.

767 Evaluating HER2 status using HER2 Gene Protein Assay in Endometrial Cancer

Saba Shafi[1], Anil Parwani[2], Zaibo Li[1], Hiro Nitta[3]
[1]The Ohio State University Wexner Medical Center, Columbus, OH, [2]The Ohio State University, Columbus, OH, [3]Roche Tissue Diagnostics, Tucson, AZ

Disclosures: Saba Shafi: None; Anil Parwani: None; Zaibo Li: None; Hiro Nitta: None

Background: HER2 gene amplification/protein expression occurs in up to 40% of endometrial serous carcinoma, an aggressive subtype of endometrial carcinoma. Patients with HER2 positive serous carcinoma may benefit from anti-HER2 therapies. HER2 status is usually determined by immunohistochemistry (IHC) for protein expression or in-situ hybridization (ISH) for gene amplification. In current study, we employed a novel HER2 gene protein assay (GPA), which simultaneously assesses HER2 gene copy number (Dual ISH) and protein expression (IHC) on a single slide, to determine HER2 status in endometrial cancers.

Design: This study included 117 endometrial cancers (66 serous carcinomas, 11 malignant Müllerian mixed tumors (MMMT), 40 mixed epithelial carcinomas. GPA assay was performed on whole tissue sections and GPA slides were interpreted for both HER2 IHC and HER2 ISH. HER2 intratumoral heterogeneity (ITH) was evaluated and categorized into genetic ITH (a mixture of HER2 positive tumor cells (gene amplification and protein expression) and HER2 negative tumor cells (no HER2 gene amplification, no HER2 protein overexpression)] and non-genetic ITH (a mixture of HER2 gene amplified tumor cells with or without HER2 protein overexpression).

Results: Out of the 66 serous carcinomas analyzed, HER2 IHC was positive (3+) in 17 (25.8%), equivocal (2+) in 13 (19.7%) and negative in 36 (54.5%) cases. (Table 1) HER2 ISH results showed gene amplification in 8 of 13 HER2 equivocal cases, while no

amplification in the other 5 cases. The overall HER2 positive rate was 38% in serous carcinoma, significantly greater than that in MMMTs (0%, *p*= 0.018) or mixed epithelial carcinomas (12.5%, *p*= 0.0075). HER2 ITH was better appreciated on GPA slides (Figure 1). Up to 32% of serous carcinomas showed ITH, significantly more than MMMT (0%) and mixed epithelial carcinomas (7.5%).

Table 1. HER2/neu status of endometrial cancer evaluated by GPA assay

Characteristics	Serous carcinoma (*N=66*)	Malignant mixed Müllerian tumor (*N=11*)		Mixed epithelial carcinoma (*N=40*)	
HER2 IHC			*p value*		*p value*
0	19 (28.8%)	4 (36.4%)		19 (47.5%)	
1+	17 (25.8%)	3 (27.3%)		12 (30.0%)	
2+	13 (19.7%)	4 (36.4%)		4 (10.0%)	
3+	17 (25.8%)	0 (0.0%)		5 (12.5%)	
HER2 2+ ISH					
Negative	5 (38.5%)	4 (100.0%)		4 (100.0%)	
Positive	8 (61.5%)	0 (0.0%)		0 (0.0%)	
Overall HER2 status					
Negative	41 (62.1%)	11 (100.0%)	0.018	35 (87.5%)	0.0075
Positive	25 (37.9%)	0 (0.0%)		5 (12.5%)	
HER2 ITH					
GH	11 (16.7%)	0 (0.0%)	0.59	1 (2.5%)	0.016
NGH	10 (15.2%)	0 (0.0%)		2 (5.0%)	
Total ITH	21 (31.8%)	0 (0.0%)		3 (7.5%)	

Figure 1. Representative images of HER2 gene protein assay (GPA) in endometrial serous carcinoma. (A, B) HER2 negative staining; (C, D) HER2 homogenous positive staining; (E, F) HER2 positive staining with genetic intratumoral heterogeneity; and (G, H) HER2 positive staining with non-genetic heterogeneity. Brown circles represent HER2 protein expression while black dots and red dots represent HER2 gene and chromosome 17 centromere, respectively. A, C, E, G: 100x; B, D, F, H: 600 ×.

Figure 1 - 767

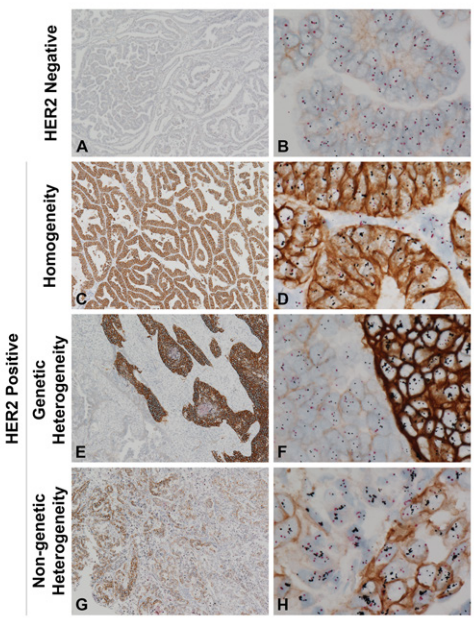

Conclusions: GPA assay accurately determines HER2 status not only for unequivocally positive and negative endometrial cancer cases, but also for the most challenging (IHC 2+) cases. Additionally, we found a significantly greater expression of HER2 in serous carcinomas than in MMMTs or mixed epithelial carcinomas.

768 Molecular Correlates of Invasion Pattern in HPV-Associated Endocervical Adenocarcinoma: Emergence of Two Distinct Risk-Stratified Tiers

Aarti Sharma[1], Anjelica Hodgson[2], Brooke Howitt[3], Bojana Djordjevic[4], Kay Park[5], Marisa Nucci[6], Carlos Parra-Herran[6]
[1]Brigham and Women's Hospital, Boston, MA, [2]Toronto General Hospital, University Health Network, Toronto, Canada, [3]Stanford Medicine/Stanford University, Stanford, CA, [4]University of Toronto, Sunnybrook Health Sciences Centre, Toronto, Canada, [5]Memorial Sloan Kettering Cancer Center, New York, NY, [6]Brigham and Women's Hospital, Harvard Medical School, Boston, MA

Disclosures: Aarti Sharma: None; Anjelica Hodgson: None; Brooke Howitt: None; Bojana Djordjevic: None; Kay Park: None; Marisa Nucci: None; Carlos Parra-Herran: None

Background: The pattern-based (Silva) classification of invasive HPV-associated endocervical adenocarcinomas (HPVA) is an established and reproducible method to predict outcomes for this otherwise stage-dependent group of tumors. Previous studies utilizing targeted sequencing have shown a correlation between mutational profiles and invasive pattern. However, such correlation has not been explored using comprehensive molecular testing.

Design: Clinicopathologic data including invasive pattern (Silva groups A, B, and C) was collected for a cohort of invasive HPVA which underwent massive parallel sequencing using a panel covering 447 genes. Pathogenic alterations, molecular signatures, single-nucleotide polymorphisms, tumor mutational burden (TMB), and copy number alterations (CNA) were correlated with pattern of invasion.

Results: 45 HPVA (11 pattern A, 17 pattern B and 17 pattern C tumors, Table 1) were included. Patients with pattern A presented at stage I with no involved lymph nodes or evidence of recurrence (in those with > 2 months of follow-up). Patterns B and C patients also mostly presented at stage I with negative lymph nodes but had greater frequency of recurrence. 3/17 pattern B and 1/17 pattern C HPVAs harbored lymphovascular space invasion (LVI), respectively. APOBEC mutational signature was detected only in Silva pattern C tumors (5/17), and pathogenic PIK3CA alterations were detected only in destructively invasive HPVA (patterns B and C, Figure 1). When cases were grouped as low-risk (pattern A and pattern B without LVI) and high-risk (pattern B with LVI and pattern C), high-risk tumors were enriched in single-nucleotide variations in PIK3CA and ATRX, as well as ERBB2 amplification. There was a statistically significant difference in TMB between low-risk and high-risk pattern tumors (p=0.006), as well as between Pattern C tumors with and without an APOBEC signature (p=0.002). Volume of CNA increased along the progression from pattern A to C (Figure 2).

	n	Age	Stage IA	Stage IB	Stage 2	Neoadjuvant Chemoradiation	LVI	Lymph Node Metastasis	Recurrence
Silva A	11 (24%)	43 ± 17	3/11 (27%)	7/11 (64%)	1/11 (1%)	2	0	0	0
Silva B	17 (38%)	41 ± 10	4/17 (24%)	11/17 (65%	2/17 (12%)	2	3	0	5
Silva C	17 (38%)	45 ± 16	5/17 (30%)	7/17 (41%)	2/17 (12%)	5	1	0	2

Figure 1 - 768

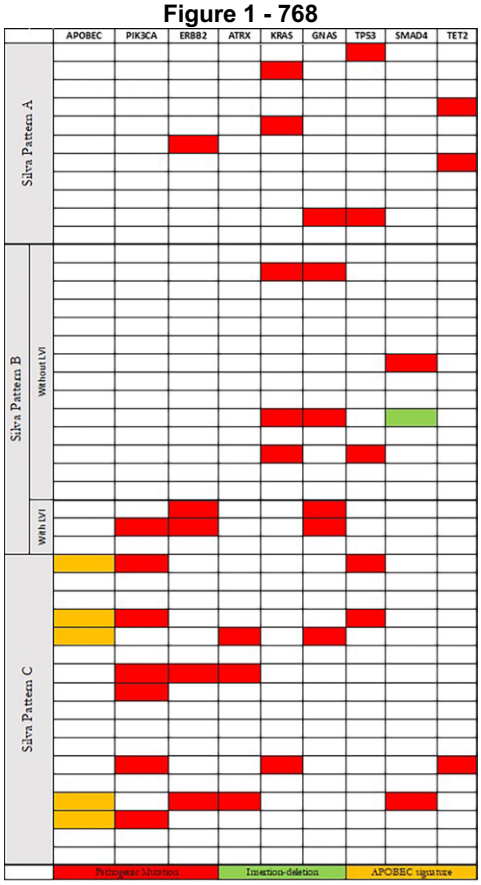

Figure 2 - 768

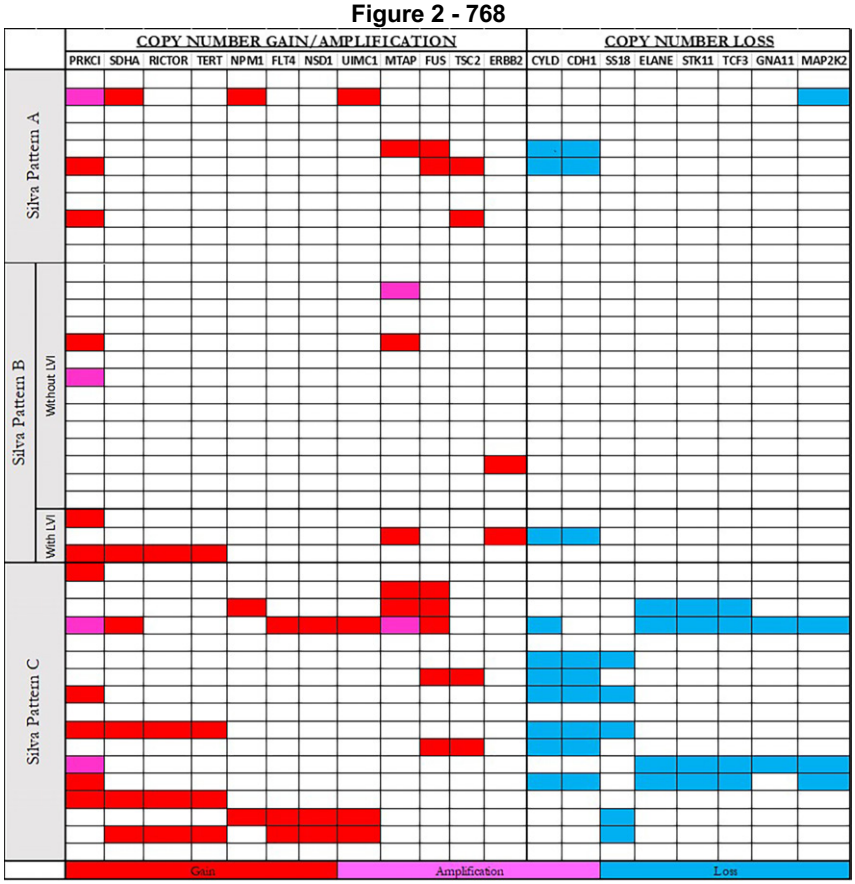

Conclusions: Our findings corroborate the hypothesis that key molecular events in HPVA correlate with the morphologic invasive properties of the tumor and their aggressiveness. Pattern B tumors with LVI clustered with pattern C tumors, whereas pattern B tumors without LVI approached pattern A genotypically. Our study provides a biologic basis for consolidating the Silva system into low-risk (pattern A + B without LVI) and high-risk (pattern B with LVI and pattern C) categories.

769 SMARCB1/INI1-Deficient Vulvar Soft Tissue Neoplasms Encompass a Broad Spectrum of Tumors: A Clinicopathologic Analysis of 55 Cases

Aarti Sharma[1], Marisa Nucci[2], Jason Hornick[2], Christopher Fletcher[1], David Kolin[1]
[1]Brigham and Women's Hospital, Boston, MA, [2]Brigham and Women's Hospital, Harvard Medical School, Boston, MA

Disclosures: Aarti Sharma: None; Marisa Nucci: None; Jason Hornick: None; Christopher Fletcher: None; David Kolin: None

Background: Vulvar tumors with SWI/SNF-complex abnormalities are uncommon and often aggressive. Tumors defined by SWI/SNF inactivation may also be sensitive to targeted EZH2 inhibition and immunotherapy. However, their diagnosis is challenging due to their rarity and histologic overlap. We sought to better characterize this group of tumors by examining the clinicopathologic features of a cohort of SMARCB1 (INI1)-deficient vulvar neoplasms.

Design: Vulvar SMARCB1-deficient neoplasms were identified retrospectively from institutional and consultation archives at a single institution. Clinical, morphologic, and immunohistochemical data were obtained.

Results: Fifty-five cases of SMARCB1-deficient vulvar tumors were collected, including epithelioid sarcoma (ES, n=45, 39 proximal-type), myoepithelial carcinoma (MC, n=7), yolk sac tumor (YST, n=2), and epithelioid schwannoma (n=1). Mean patient age was 44 (range 14-89) years, and median tumor size was 3.7 (range 0.6-30) cm.

Both proximal-type ES and MC were composed of epithelioid cells with vesicular chromatin and prominent nucleoli, and frequently rhabdoid cells. While ES displayed a sheetlike pattern, MC invariably had architectural heterogeneity and focally spindled morphology (Table 1, Figures 1+2). Tumors with yolk sac differentiation demonstrated architecture reminiscent of their gonadal counterpart, without significant histologic overlap with other tumors. All tumors showed loss of SMARCB1 staining by IHC.

ES were all positive for EMA (100%, 38/38), occasionally CD34 positive (30%, 12/41), and variably for keratins. ER was inconsistently positive by IHC (4/9). While MC were also all positive for EMA (100%, 6/6), all showed at least focal IHC evidence of myoepithelial differentiation with S100 or GFAP. Tumors with yolk sac differentiation were positive for SALL4 and glypican-3. Follow-up was available for 12 patients (range 2 -216 months): 2 with ES had metastases at presentation, 8 recurred locally (6 ES and 2 MC), and 2 died of disease (both YST).

	Epithelioid Sarcoma	Myoepithelial Carcinoma	Yolk Sac Tumor	Epithelioid Schwannoma
Total n	45	7	2	1
Age (years)	45 (14-72)	40 (28-67)	34 (both)	60
Tumor size (cm)	5.3 (1.5 - 14)	5 (1.2-12)	3.7 and 4.5	0.6
Subtype	Proximal 87% (39/45)	NA		
Grade	NA	Low (4/6) High (2/6)		
Superficial vs. Deep-seated	Superficial 75% (12/16) Deep 25% (4/16)	Superficial 50% (1/2) Deep 50% (1/2)		
Atypical mitoses	36% (16/45)	29% (2/7)		
Myxoid stroma (focal or prominent)	24% (11/45)	100% (7/7)		
Fascicular/nested/ trabecular areas	28% (17/45)	100% (7/7)		
Vesicular chromatin	87% (39/45)	100% (7/7)		
Prominent nucleoli	73% (33/45)	86% (6/7)		
Rhabdoid Cells	73% (29/40)	60% (3/5)		
EMA (+)	100% (38 /38)	100% (6/6)		
AE1/AE3 (+)	45% (9/ 20)	Not performed		
CAM5.2 (+)	29% (4/14)	Not performed		
panCK (+)	36% (12/33)	60% (3/5)		
CD34 (+)	30% (12/41)	0% (0/5)		
SMA (+)	36% (5/ 14)	25% (1/4)		
S100 (+)	0% (0/ 31)	17% (1/6)		
GFAP (+)	0% (0/ 20)	17% (1/6)		
Desmin (+)	0% (0/21)	0% (0/3)		

Figure 1 - 769

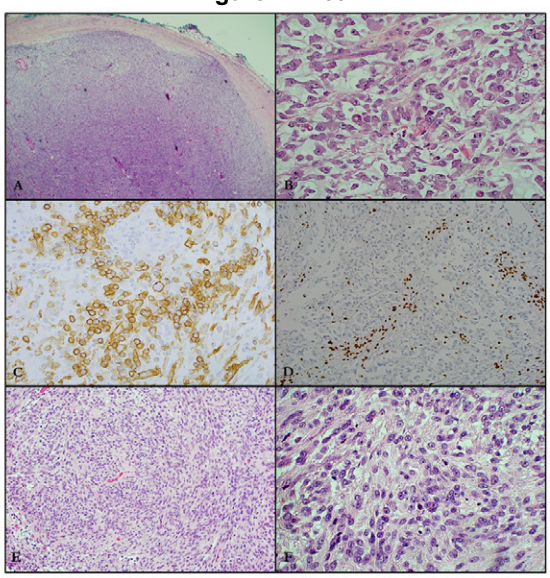

Figure 1. **A-D.** *Vulvar Proximal-type Epithelioid Sarcoma.* **A.** ES with well-circumscribed border. **B.** Sheets of rhabdoid cells with vesicular chromatin and prominent large nucleoli. **C.** Multifocal, strong positivity for EMA. **D.** Loss of INI1/SMARCB1 staining in tumor cells. **E-F.** *Vulvar Epithelioid Schwannoma.* **E.** Fascicular to streaming architecture. **F.** Epithelioid cells with pale eosinophilic cytoplasm and prominent nucleoli.

Figure 2 - 769

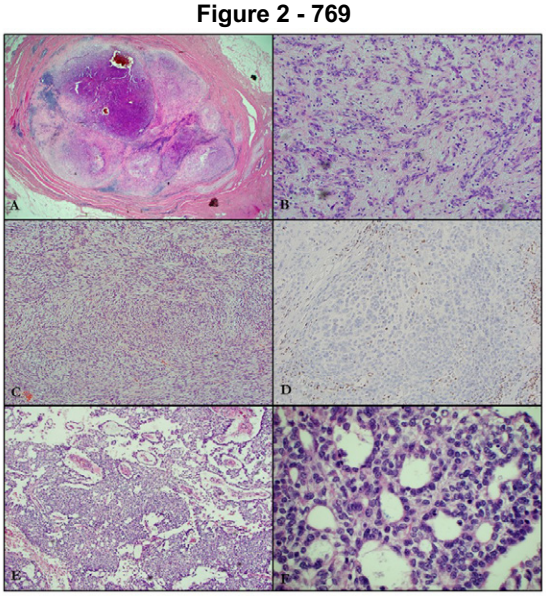

Figure 2. **A-D.** *Vulvar Myoepithelial Carcinoma.* **A.** Well-circumscribed, lobulated mass. **B.** Epithelioid to spindled cells arranged in nests and trabeculae. **C.** Fascicular architecture. **D.** Loss of INI1/SMARCB1 in tumor cells. **E-F.** *Vulvar Yolk Sac Tumor.* **E.** Microcystic and reticular architecture. **F.** Primitive, angulated cells forming microcysts.

Conclusions: This series of 55 tumors is the largest (to date) characterizing SMARCB1-deficient vulvar tumors, and highlights their distinctive morphologies. These tumors should be considered in the differential diagnosis of a vulvar soft tissue mass displaying epithelioid/rhabdoid morphology, myxoid stroma, spindle cells and/or yolk sac features. SMARCB1 IHC can be invaluable in these settings, and accurate diagnosis of these tumors is critical for appropriate prognostication and treatment.

770 Clinical-Pathological Characteristics of HER2 Expression in Mucinous Ovarian Tumors

Marie Smithgall[1], Anna Yemelyanova[1], Bing He[2], Brian Robinson[3], Jiangling Tu[4]
[1]New York-Presbyterian/Weill Cornell Medical Center, New York, NY, [2]Cornell University Medical College, New York, NY, [3]Weill Cornell Medicine, New York, NY, [4]Weill Cornell Medical College, New York, NY

Disclosures: Marie Smithgall: None; Anna Yemelyanova: None; Bing He: None; Brian Robinson: None; Jiangling Tu: None

Background: Primary ovarian mucinous carcinoma (MOC) is a rare subtype of ovarian epithelial cancer which is often refractory to chemotherapy. HER2-targeting therapy has been increasingly considered in gynecologic malignancies. To date, there have been limited studies examining the HER2 status of MOCs with overexpression of HER2 reportedly ranging from 18 to 37%. However, the criteria for scoring HER2 expression have not been standardized for MOC as it has been for carcinomas of other sites. This study aimed to survey immunohistochemical HER2 expression patterns in MOC and its precursor, mucinous borderline tumor (MBT) in correlation with fluorescence in situ hybridization (FISH).

Design: The pathology database was searched for MOC and MBT. 12 cases of MOC and 15 MBT, including 7 cases of MBT with intraepithelial carcinoma (ICA), were included. Immunohistochemical staining for HER2 (SP3; 1:100 dilution) was performed. The slides were reviewed by two gynecologic pathologists. A modified HER2 scoring system was utilized. Cases were considered 3+ if the tumor cells displayed strong complete or basolateral membranous staining in >10% of tumor cells. 2+ cases had weak to moderate staining in >10% of tumor cells. 1+ cases had faint staining in >10% of tumor cells. Cases considered 0 had no staining or faint staining in <10% of tumor cells.

Results: Patients' age ranged from 24-86 years, mean 52.7 years for MOC and 14-68 years, mean 40.5 years for MBT. Of the 12 MOC cases 6 were stage pT1a, 4 stage pT1c and 2 stage pT3. 25% of MOC cases were 3+ and 1 MBT with ICA had 3+ staining. All three 3+ MOC cases were stage pT1a. The 2 stage pT3 MOC cases had 0 HER2 IHC staining. Immunohistochemical findings are summarized in Table 1.

Table 1. HER2 IHC Score in Ovarian Mucinous Tumors

Tumor Type	HER2 IHC				
	0	1+	2+	3+	Total
MOC	6	2	1	3	12
ICA	0	4	2	1	7
MBT	2	5	1	0	8

Conclusions: Primary MOC showed HER2 overexpression (3+) in up to 25% of cases, all stage pT1a. An additional 25% of primary MOC in this study had weak to equivocal staining raising the possibility of underlying gene amplification. Correlation with fluorescence in situ hybridization is in progress. Presence of HER2 overexpression in MOC and ICA and not in MBT may reflect a mechanism of tumor progression. Additional studies are needed to determine clinical significance and potential therapeutic implications of HER2 overexpression in ovarian mucinous neoplasms.

771 Mismatch Repair Protein Status of Endometrial Hyperplasia in Cases with Concomitant MMR Deficient Endometrial Carcinoma

Marie Smithgall[1], Jiangling Tu[2], Anna Yemelyanova[1]
[1]New York-Presbyterian/Weill Cornell Medical Center, New York, NY, [2]Weill Cornell Medical College, New York, NY

Disclosures: Marie Smithgall: None; Jiangling Tu: None; Anna Yemelyanova: None

Background: Immunohistochemical analysis (IHC) of mismatch repair proteins (MMR) in endometrial carcinoma is routinely used for germline (Lynch syndrome) screening and detection of somatic alterations. Staining is often performed on endometrial biopsy/curettage specimens, which demonstrate superior tissue preservation and immunogenicity compared to hysterectomies. The diagnosis of endometrial carcinoma in fragmented biopsy specimens can be challenging. Occasionally, the diagnosis of atypical hyperplasia bordering on endometrioid carcinoma is rendered. Expression of MMR in endometrial hyperplasia is less well studied. The goal of this study is to evaluate MMR expression in endometrial hyperplasia and its predictive value for detecting MMR deficiency/MSI-high status.

Design: Cases of endometrial carcinoma with loss of at least one MMR protein by IHC and concurrent endometrial hyperplasia were selected. IHC stains for MLH1, PMS2, MSH2, MSH6 performed as routine clinical care were reviewed in conjunction with H&E to evaluate MMR expression in atypical (AH) and non-atypical hyperplasia (NAH).

Results: 18 cases (7 biopsies and 11 hysterectomies) for 17 unique patients were included in the study. The patient age ranged from 41-76 years, mean 57 years. Eleven cases (11) were FIGO grade 1, 2- FIGO grade 2, and 3- FIGO grade 3 endometrioid carcinoma. One case was mixed clear cell carcinoma and FIGO 2 endometrioid carcinoma. Of the 15 carcinoma cases with loss of MLH1/PMS2 (8 confirmed sporadic), 9 (60%) showed complete loss of MLH1/PMS2 in AH, 3 (20%) showed partial loss in AH. Three (20%) cases showed retained MMR proteins in AH (1 case) and NAH (2 cases). In two cases MSH6 loss was seen in carcinoma and AH (both confirmed Lynch Syndrome by germline testing). The mixed carcinoma case had MLH1/PMS2 loss in clear cell carcinoma component and retained staining in AH and endometrioid carcinoma FIGO 2. One case showed heterogeneous staining for MSH2, predominantly lost with focal weak staining in carcinoma and AH (MSH2 VUS by germline testing).

Conclusions: MMR expression in atypical endometrial hyperplasia mirrors the expression in carcinoma in 65% of cases including cases with both germline and somatic alterations. However, at least partial retention of staining in some cases of AH and NAH (35%) makes it a less reliable predictor of MMR deficiency. Therefore, careful evaluation of MMR immunohistochemistry in conjunction with an H&E is important, particularly in fragmented biopsy specimens.

772 Prognostic Significance of Immune Biomarkers in Ovarian Low-Grade Serous Carcinoma (LGSC) and Serous Borderline Tumor (SBT): A Clinicopathologic Study with Gene Expression Correlation

Thing Rinda Soong[1], Yusi Fang[1], Lauren Skvarca[2], Alyssa Wield[2], Douglas Hartman[2], Esther Elishaev[3], Chengquan Zhao[4], Mirka Jones[1], George Tseng[1], Rohit Bhargava[3], Sarah Taylor[2]
[1]University of Pittsburgh, Pittsburgh, PA, [2]University of Pittsburgh Medical Center, Pittsburgh, PA, [3]UPMC Magee-Womens Hospital, Pittsburgh, PA, [4]Magee-Womens Hospital, University of Pittsburgh Medical Center, Pittsburgh, PA

Disclosures: Thing Rinda Soong: None; Yusi Fang: None; Lauren Skvarca: None; Alyssa Wield: None; Douglas Hartman: *Speaker*, Philips; *Consultant*, Iqvia; Esther Elishaev: None; Chengquan Zhao: None; Mirka Jones: None; George Tseng: None; Rohit Bhargava: None; Sarah Taylor: *Speaker*, AstraZeneca

Background: LGSC and SBT are rare ovarian tumors that are resistant to conventional chemotherapy. Little is known on the role of tumor immune environment in their prognosis. We examined the association of intratumoral T cell and macrophage levels with their clinicopathologic and gene expression profiles.

Design: We compared intratumoral densities of CD3+/CD8+ T cells, CD68+/CD163+ macrophages and FOXP3+ Treg cells in 23 LGSCs and 139 SBTs via immunohistochemistry and digital quantification. Overall survival (OS), disease-specific survival (DSS) and recurrence-free survival (RFS) analyses were done using logrank tests and Cox regression models with adjusted hazard ratios (aHRs) and 95% confidence intervals (CIs). NanoString platform was used to study the expression of 364 genes associated with

immune response, tumor–stromal interactions and hormonal resistance. Differentially expressed genes were identified and evaluated using Ingenuity pathway analysis (IPA).

Results: Median age was 52 years. More than half (68%) were of FIGO 1. All were ER+. LGSC had higher densities of CD3+ or CD8+ T cells, CD68+ or CD163+ macrophages, and FOXP3+ Treg cells than SBT (Table 1). FIGO 2 or above was associated with higher CD3+/CD8+ T cell densities (p<0.01). Median follow-up time was 96 months (range: 2-589), with a total of 32 deaths, 11 disease-specific deaths and 24 recurrences. Compared with SBT, LGSC portended worse OS (Fig. 1A)(aHR: 4.1; CI: 1.7-9) and RFS (aHR: 7.0; CI: 2.6-18.7). High CD68+ macrophage density was an independent predictor of poor OS (Fig. 1B)(aHR: 3.0; CI: 1.1-7.8) after controlling for tumor type, age, FIGO stage and ER percent positivity. High CD68+ cell density predicted shorter DSS (P: 0.005) and RFS (P: 0.006), and high CD163+ cell density correlated with worse DSS (P: 0.005) but they were not independent predictors after confounding adjustment. CD3+, CD8+ or FOXP3+ cell densities did not show significant independent associations with clinical outcomes. IPA highlighted gene expression pathways related to immune regulation when comparing differentially expressed genes between LGSC and SBT, and between tumors with and without recurrence in this cohort (Fig. 1C).

Table 1. Comparison of immune cell subset densities between LGSC and SBT (Total N=162)

		SBT (n=139) Column %	LGSC (n=23) Column %	P*
CD3+ T cell density (cells/mm^2)	Median (IQR)	81 (91)	112 (131)	**0.05**
	Low (≤150)	77	57	**0.04**
	High (>150)	23	43	
CD8+ T cell density (cells/mm^2)	Median (IQR)	54 (55)	134 (161)	**<0.0001**
	Low (≤100)	80	39	**<0.001**
	High (>100)	20	61	
CD68+ macrophage density (cells/mm^2)	Median (IQR)	60 (64)	145 (141)	**<0.0001**
	Low (≤110)	83	39	**<0.001**
	High (>110)	17	61	
CD163+ macrophage density (cells/mm^2)	Median (IQR)	263 (178)	375 (218)	**0.02**
	Low (≤400)	87	61	**0.003**
	High (>400)	13	39	
FOXP3+ Treg cell density (cells/mm^2)	Median (IQR)	8 (14)	29 (55)	**0.001**
	Low (≤20)	78	48	**0.003**
	High (>20)	22	52	

IQR: Interquartile range

*Comparisons were tested by Wilcoxon rank-sum tests (for continuous variables) and Fisher's exact or Chi-square tests (for categorical variables).

Figure 1 - 772

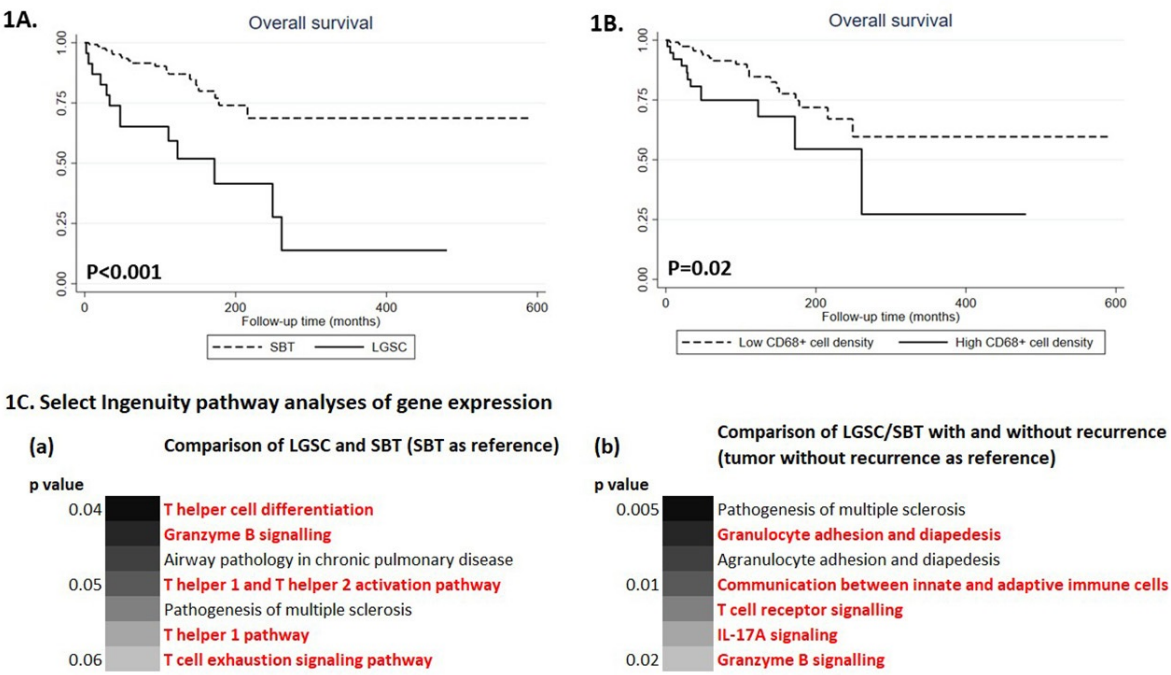

Conclusions: Our study showed that high intratumoral CD68+ macrophage density is an independent poor OS prognostic indicator of LGSC and SBT with upregulation of immune-related pathways. The findings suggest the immune environment as a potential venue for identifying new therapeutic targets and prognostic biomarkers in these tumors.

773 Classification of Uterine Mesenchymal Neoplasms by Deep Learning Algorithms

Tanner Storozuk[1], Annie Zhu[2], Sara Kochanny[2], James Dolezal[1], David Chapel[3], Brooke Howitt[4], David Kolin[5], Grace Neville[6], Marisa Nucci[6], Esther Oliva[7], Zehra Ordulu[8], Andre Pinto[9], Joseph Rabban[10], Alexander Pearson[11], Jennifer Bennett[2]

[1]University of Chicago Medical Center, Chicago, IL, [2]University of Chicago, Chicago, IL, [3]Michigan Medicine, University of Michigan, Ann Arbor, MI, [4]Stanford Medicine/Stanford University, Stanford, CA, [5]Brigham and Women's Hospital, Boston, MA, [6]Brigham and Women's Hospital, Harvard Medical School, Boston, MA, [7]Massachusetts General Hospital, Harvard Medical School, Boston, MA, [8]University of Florida, Gainesville, FL, [9]University of Miami Health System, Miami Beach, FL, [10]University of California, San Francisco, San Francisco, CA, [11]University of Chicago Medicine, Chicago, IL

Disclosures: Tanner Storozuk: None; Annie Zhu: None; Sara Kochanny: None; James Dolezal: None; David Chapel: None; Brooke Howitt: None; David Kolin: None; Grace Neville: None; Marisa Nucci: None; Esther Oliva: None; Zehra Ordulu: None; Andre Pinto: None; Joseph Rabban: None; Alexander Pearson: None; Jennifer Bennett: None

Background: Uterine mesenchymal neoplasms (UMN) are diagnostically challenging as many subtypes show extensive morphological and immunohistochemical overlap. The number of targeted therapies is rapidly evolving for these tumors; however, determining which genomic alteration a neoplasm harbors typically requires ancillary molecular testing, which can be expensive and not easily accessible. Deep learning algorithms have been found to assist pathologists in tumor classification and prediction of biomarker status based on H&E slides alone. Herein we evaluate a series of UMNs using deep learning to assess whether this modality can accurately separate molecularly classified tumors based only on H&E.

Design: 135 primary uterine UMNs with a confirmed molecular diagnosis (Table) were retrieved and digitized from 7 institutions. The tumor region from each whole slide image (WSI) was manually annotated. Individual 604 um image tiles were extracted from these regions and saved at 598 px (~1 um/px resolution). Pixel data was normalized and tiles were used as input to a single multicategorical deep convolutional neural network (Xception architecture pretrained on Imagenet, implemented with Tensorflow/Keras) trained to predict histologic diagnosis. Performance results were reported as the average of threefold cross-validation, averaged at the patient level. Learned image features were then mapped with the dimensionality reduction technique UMAP and a mosaic map was created.

Results: Diagnosis of UMNs could be predicted from WSIs with a high degree of accuracy. The averaged area under the receiver operator curve for all outcomes was 0.929 (mean range per diagnosis, 0.829-0.978). UMAP evaluation revealed distinct clusters for IMT, PEComa, UTROSCT, LGESS, and NTRK (Figure 1). ERMS often clustered near IMTs and review of the mosaic map showed these tiles were rich in myxomatous stroma. HGESS with *BCOR/BCORL1* alterations clustered near IMT, whereas HGESS with *YWHAE* fusions clustered near LGESS and UTROSCT. LMS distribution was highly variable. Figure 2 highlights representative tiles of discrete clusters, which exhibit characteristic morphologic features of these entities.

Diagnosis	Number of Cases	Molecular Alteration	Patient-Level AUROC
Low-grade endometrial stromal sarcoma (LGESS)	35	*JAZF1* fusions (n=25) *PHF1* fusions (n=10)	0.950
Inflammatory myofibroblastic tumor (IMT)	26	*ALK* fusions (n=25) *ROS1* fusions (n=1)	0.939
PEComa	17	*TSC1* alterations(n=8) *TSC2* alterations (n=8) *TFE3* fusion (n=1)	0.978
High-grade endometrial stromal sarcoma (HGESS)	16	*BCOR* fusions (n=9) *YWHAE* fusions (n=5) *BCORL1* fusion (n=1) *BCOR* internal tandem duplication (n=1)	0.874
Embryonal rhabdomyosarcoma (ERMS)	16	*DICER1* (n=16)	0.974

Leiomyosarcoma (LMS)	10	1. Morphologically and immunohistochemically compatible, AND 2. Negative for alterations characteristic of other entities, AND 3. *ATRX* (n=6), *TP53* (n=5), *RB1* (n=4), and/or *MED12* (n=2) alterations or *PGR* fusion (n=1)	0.921
Uterine tumor resembling ovarian sex cord tumor (UTROSCT)	9	*ESR1* fusions (n=5) *GREB1* fusions (n=4)	0.963
NTRK spindle cell sarcoma (NTRK)	6	*NTRK* fusions (n=6)	0.829

AUROC=area under receiver operator curve

Figure 1 - 773

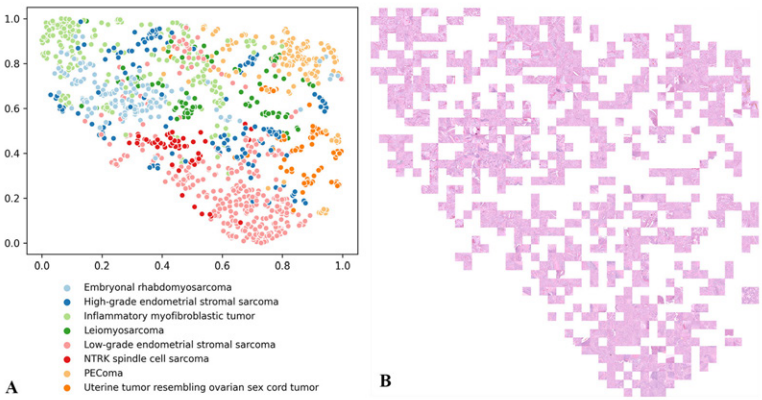

Figure 1. UMAP distribution of uterine mesenchymal neoplasms by diagnosis. Each data point represents a single tile from the whole slide image, with 10 tiles shown per individual slide (A). Mosaic map created from the UMAP by replacing plotted tiles with the corresponding H&E images (B).

Figure 2 - 773

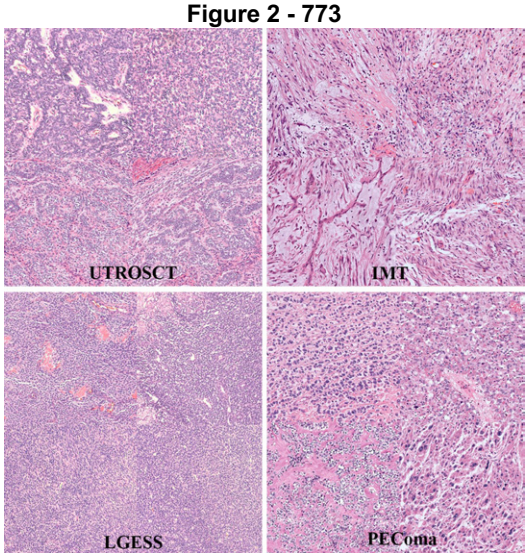

Conclusions: Pilot data revealed the UMN deep learning model successfully classified molecularly-confirmed tumors based only on H&E evaluation. A validation cohort is currently being procured for additional analysis. This study represents the first step in identifying a more cost-effective method to correctly diagnose these tumors.

774 Placentas from Mothers with Positive SARS-CoV-2 (COVID-19) Test Results at Labor Showed Neither Specific Histopathological Changes Nor Evidence of COVID-19 Infection

Tong Sun[1], Mingkui Chen[2], Natalia Buza[1], Pei Hui[3]
[1]Yale School of Medicine, New Haven, CT, [2]Yale New Haven Hospital, Yale School of Medicine, New Haven, CT, [3]Yale University School of Medicine, New Haven, CT

Disclosures: Tong Sun: None; Mingkui Chen: None; Natalia Buza: None; Pei Hui: None

Background: Evidence has shown that pregnancy is a risk factor for severe illness in women with SARS-CoV-2 (COVID-19). Yet their newborns are mostly doing well. The placenta is a complex, highly specialized, but poorly understood organ. The COVID-19 infection related specific pathological changes in placenta and prevalence of transplacental transmission of COVID-19 has not been fully explored and validated.

Design: Universal screening for COVID-19 among all pregnant women on admission to labor and delivery unit was initiated in April 2020 at our institute. With IRB approval, 54 term pregnant women with positive COVID-19 nasopharyngeal swap results at admission during April 2020 to Jun 2021 were recruited. Patients' demographic characteristics and clinical presentation were summarized in Table 1. Histopathology of all placentas was independently reviewed by two board certified pathologists. RNA was extracted from Formalin-Fixed Paraffin-Embedded (FFPE) blocks of 15 randomly selected placentas. ThermoFisher TaqPath™ SARS-CoV-2/COVID-19 RT-PCR assays were performed to detect the presence of the virus with proper controls.

Results: Hispanic or Latino pregnant women represented 39% of the study cohort tested positive for COVID-19 at admission, followed by American Africa (26%) and Caucasian (17%). Most patient were overweight before pregnancy and 1/3 patients had at least one comorbidity. Majority patients (72%) were completely asymptomatic. The rest of patients had somewhat mild symptoms including sore throat, cough, low-grade fever, and/or loss of taste/smell. All deliveries were term. All neonates were in healthy status at birth. No suspected vertical transmission was observed. Histopathological inspection of placentas showed nonspecific features of maternal or fetal vascular malfunction and inflammation (Table 2). Among 15 placental samples tested, no SARS-CoV-2 virus was detected.

Table 1. Cohort Demographic Characteristics and Clinical Information

Characteristics		N	%
	Total	54	(100 %)
Maternal age, median (range)		27 (19 - 43) years	
Self-reported ethnicity			
	Caucasian	9	(17 %)
	African American	14	(26 %)
	Hispanic or Latino	21	(39 %)
	Asian	6	(11 %)
	Refused	4	(7 %)
Pregravid BMI, median (range)		27.6 (22.8 - 46.3)	
Maternal comorbidities			
	Hypertension or preeclampsia	2	(4 %)
	Diabetes or gestational diabetes	9	(17 %)
	Preexisting pulmonary condition	3	(6 %)
	HIV	1	(2 %)
Gestational age at delivery, median (range)		39.2 (37.1 - 41.8) weeks	
Mode of delivery			
	Vaginal delivery	37	(68 %)
	Caseation section	17	(32 %)
Infant birth weight, median (range)		3120 (2360 - 4400) grams	
Neonate sex			
	Male	23	(42 %)
	Female	31	(58 %)
Apgar scores (at 1 and 5 minutes)			
	9 and 9	50	(93 %)
	8 and 9	4	(7 %)
	Below 8 and 9	0	(0 %)
COVID-19 positive result date before the labor		1.5 (0 - 4) days	
COVID-19 symptoms			
	Asymptomatic	39	(72 %)
	Mild symptoms (including sore throat, cough, mild fever, loss of taste/smell etc.)	15	(28 %)
	Severe symptoms	0	(0 %)

Figure 1 - 774

Table 2. Histopathological Changes in Placentas from Mothers with Positive SARS-CoV-2 (COVID-19) Test Results at Labor

Histopathological features	N	%
Maternal vascular malperfusion		
Increased fibrin deposition	28	(52 %)
Infarction	17	(31 %)
Decidual vasculopathy	7	(13 %)
Intervillous/subchorionic thrombosis	3	(5 %)
Distal villous hypoplasia	1	(2 %)
Retroplacental hemorrhage	1	(2 %)
Inflammation		
Chorioamnionitis/subchrorionitis	21	(39 %)
Intervillositis	11	(20 %)
Villitis	7	(13 %)
Deciduitis	12	(22 %)
Fetal vascular malperfusion		
Chorangiosis	7	(13 %)
Delayed villous maturation	3	(5 %)
Avascular villi	6	(11 %)
Other findings		
Meconium	34	(63 %)
Architecture structure abnormality	4	(7 %)
Total	54	(100 %)

Conclusions: Multiple studies indicated that only a very small proportion of neonates delivered to mothers with COVID-19 infection were also tested positive for COVID-19. Our data suggested that COVID-19 infected mothers who were asymptomatic or only with mild symptoms at labor unlikely vertically transmit the virus through the placenta. This finding may ease the anxiety of asymptomatic mothers caused by positive COVID-19 test result at delivery admission.

775 DICER1 and FOXL2 Mutation Status of Ovarian Sertoli-Leydig Cell Tumours in Patients 50 Years of Age and Older

Nairi Tchrakian[1], Anne-Sophie Chong[2], Anne-Laure Chong[2], Ciara Murray[3], Anjelica Hodgson[4], Gulisa Turashvili[5], Ju-Yoon Yoon[6], Marisa Nucci[7], Barbara Rivera[8], Colin Stewart[9], W. Glenn McCluggage[10], William Foulkes[2], Blaise Clarke[11]
[1]Barts and The London NHS Trust, London, United Kingdom, [2]McGill University, Montreal, Canada, [3]Laboratory Medicine Program, Departments of Anatomical Pathology, University Health Network and University of Toronto, Toronto, Canada, [4]Toronto General Hospital, University Health Network, Toronto, Canada, [5]Emory University Hospital, Atlanta, GA, [6]Unity Health Toronto, Toronto, Canada, [7]Brigham and Women's Hospital, Harvard Medical School, Boston, MA, [8]University Hospital of Bellvitge-IDIBELL, Barcelona, Spain, [9]King Edward Memorial Hospital, Subiaco, Australia, [10]The Royal Hospitals/Queen's University of Belfast, Birmingham, United Kingdom, [11]University of Toronto, Toronto, Canada

Disclosures: Nairi Tchrakian: None; Anne-Sophie Chong: None; Anne-Laure Chong: None; Ciara Murray: None; Anjelica Hodgson: None; Gulisa Turashvili: None; Ju-Yoon Yoon: None; Marisa Nucci: None; Barbara Rivera: None; Colin Stewart: None; W. Glenn McCluggage: None; William Foulkes: *Grant or Research Support*, Astra Zeneca; Blaise Clarke: None

Background: Recent studies have shown that Sertoli-Leydig cell tumours (SLCTs) of the ovary segregate into three molecular subtypes (DICER1-mutant, FOXL2-mutant and DICER1/FOXL2 wild type) and that these three groups also differ according to their clinicopathologic features. Previous studies have shown that SLCTs, grades 2 and 3, in patients younger than 50 years of age have a DICER1 mutation in up to 90% of cases, depending on the study. Here, we aimed to genomically interrogate moderately and poorly differentiated SLCTs from woman age 50 years and older, with the goal of establishing the proportion of each molecular subtype in this specific clinical group.

Design: A total of 17 cases originally diagnosed at SLCT, grades 2 and 3, were included and all available slides underwent central review to confirm the diagnosis and tumour grade. Each case was subjected to molecular analysis in order to evaluate for mutations in DICER1 (specifically RNase IIIb domain) and FOXL2.

Results: 47% of cases (9/17) were wild type for FOXL2 and DICER1 while 18% (3/17) harbored DICER1 mutations and the remaining 5 (29%) harbored FOXL2 mutations. As previously reported, the mutations were always exclusive. One of the cases found to have a FOXL2 mutation was also noted to have a focal area of adult granulosa cell tumor upon re-review (i.e. gynandroblastoma). Molecular testing of additional cases (n=16) and correlation with clinical parameters is pending.

Conclusions: These data reinforce the notion that FOXL2 mutations are more prevalent than DICER1 mutations in SLCTs in women over 50 years of age. In cases of SLCT with FOXL2 mutation, careful review to exclude gynandroblastoma is warranted.

776 Ovarian Seromucinous Tumors: A Reappraisal of Classification, Including the Existence of Seromucinous Carcinoma

Abebe Teklu[1], Dandi Huang[1], Mariza De Peralta-Venturina[1], Horacio Maluf[1], Bonnie Balzer[1], Kenneth Kim[1], Fabiola Medeiros[1]
[1]Cedars-Sinai Medical Center, Los Angeles, CA

Disclosures: Abebe Teklu: None; Dandi Huang: None; Mariza De Peralta-Venturina: None; Horacio Maluf: None; Bonnie Balzer: *Consultant*, Core Diagnostics, Castle Biosciences, PathologyWatch; Kenneth Kim: *Consultant*, Ethicon; *Grant or Research Support*, Intuitive Surgical; Fabiola Medeiros: None

Background: Diagnosis of seromucinous ovarian tumors (SMOT) has been historically challenging, particularly versus serous (SOT) and gastrointestinal mucinous tumors (MOT). The proportion of ciliated and mucinous cells in SMOT is highly variable and often endometrioid, clear and squamous cells are also present. Reproducible histologic criteria are lacking, and the latest WHO

classification excluded the category 'seromucinous carcinoma' (SMCA) on this basis, particularly the overlap with endometrioid carcinoma (EC). We have encountered prototypical SMCAs in clinical practice and propose that SMOT can be recognized histologically, including SMCA.

Design: The pathology database was searched for ovarian tumors containing the terms 'seromucinous', 'endocervical type' and 'müllerian type' from 2005 to 2020 from a single institution to include diagnoses from eleven staff pathologists. A total of 63 cases were retrieved: 48 borderline (BT), 5 borderline with microinvasion (BTmi), 7 carcinoma (CA) and 3 with epithelial proliferation (EP). Archival H&E slides re-reviewed blindly by a gynecologist pathologist. Immunohistochemistry was subsequently performed in all cases for CK7, CK20, PAX8, CDX2, WT1 and ER.

Results: On H&E review of 63 cases, 38 remained classified as SMOT, 13 were reclassified as SOT, 6 as MOT, 1 as EC and 5 as prominent metaplastic changes in endometrioma. All 7 original diagnosis of CA and 5 of BTmi were maintained of which 9 (of 12, 75%) represented SMOT on secondary review; two were reclassified as SOT and 1 as EC. 35 (of 48, 73%) BT remained as such; 13 (of 48, 27%) were deemed benign. 22 (of 35, 69%) BT were categorized as SMOT while 8 were regarded SOT and 5 as MOT. All 38 SMOT were positive for CK7 and ER, and negative for CK20 and CDX2. The majority of SMOT were positive for PAX 8 (35 of 38, 92%) and negative for WT1 (35 of 38, 92%). Endometriosis/endometrioma was present in 35 (of 38, 92%) SMOT and 8 (of 18, 44%) SOT/MOT on re-review.

Conclusions: In our study, contrary to the common current perception, the diagnosis of carcinoma and microinvasion in SMOT was quite consistent (75% agreement) over a wide range of time and by a number of pathologists. For seromucinous BT it was lower at 69%. EC did not represent a major confounding factor, being identified in only one case. Endometriosis was more commonly seen in association with SMOT (60%), as previously shown, but is also found in a considerable proportion of SOT and MOT and therefore it aids little in the differential diagnosis.

777 Large Scale Genomic and Clinicopathologic Analysis of SWI/SNF-deficient Undifferentiated Malignancies of the Gynecologic Tract

Basile Tessier-Cloutier[1], Marc Ladanyi[2], Robert Soslow[3]
[1]The University of British Columbia, Vancouver, Canada, [2]Memorial Sloan Kettering Cancer Center, New York, NY, [3]Memorial Sloan Kettering Cancer Center/Weill Medical College of Cornell University, New York, NY

Disclosures: Basile Tessier-Cloutier: None; Marc Ladanyi: None; Robert Soslow: None

Background: Core SWI/SNF protein inactivation has been strongly associated with undifferentiated malignancies across many sites including the gynecologic tract. These lesions are morphologically distinct and have an aggressive clinical course. There is a need for a large scale genomic and clinicopathologic analysis to identify the relevant mutations associated with the undifferentiated phenotype and poor clinical outcome.

Design: We searched a clinically annotated cohort for uterine, ovarian, cervical, vaginal and vulvar malignancies previously characterized by a targeted sequencing panel. We included any lesion with at least one core SWI/SNF gene alteration, defined as nonsynonymous somatic mutation in *SMARCA4*, *SMARCB1*, or *ARID1B*. The morphology of each case was reviewed for features of undifferentiation including discohesion, monomorphism, mitotic activity, and lack of glandular or papillary structures.

Results: We included 565 gynecologic malignancies with genomic alterations in one of the core SWI/SNF genes, 526 with one or more somatic mutations and 41 with structural variants. Of these, 418 were uterine, 118 ovarian, 24 cervical, and 5 vaginal. Pathology review identified 41 (7.3%) bona fide undifferentiated tumors which included 29 DDEC/UEC, 8 SCCOHT, 2 DDOC/UOC, and 1 UCC. Among cases showing undifferentiation, deleterious alterations for SMARCA4 was seen in 20/41 cases, SMARCB1 in 1/41 case, and ARID1B in 20/41 cases. Almost all mutations associated with undifferentiation were nonsense, frameshift, or splice site mutations (36/40), but we report two undifferentiated malignancies associated with structural variants in *SMARCA4*. Finally, two cases were associated with deleterious missense mutations. The overall survival was significantly worse in uterine tumors with molecular and morphologic evidence of core SWI/SNF inactivation compared to those without ($p<0.0001$).

Conclusions: Core SWI/SNF alterations are very common among gynecologic malignancies, however most are not sufficient to trigger morphologic dedifferentiation/undifferentiation. We report for the first time that structural variants represent an alternate pathway for the development of SWI/SNF-deficient undifferentiated malignancies. Correlation with morphologic features and immunohistochemistry expression for SMARCA4, SMARCB1, and ARID1B are key to reliably make the diagnosis of SWI/SNF-deficient undifferentiated malignancies and clinically stratify the patients accordingly.

778 Molecular Characterization of a Series of HPV-associated Undifferentiated Carcinomas of the Cervix and Vagina

Basile Tessier-Cloutier[1], Kay Park[2]
[1]The University of British Columbia, Vancouver, Canada, [2]Memorial Sloan Kettering Cancer Center, New York, NY

Disclosures: Basile Tessier-Cloutier: None; Kay Park: None

Background: Undifferentiated and dedifferentiated carcinomas are well described tumors that can occur in the gynecologic tract. They are characterized by a proliferation of discohesive, monomorphic cells which lack architectural differentiation and have decreased expression of tissue specific markers. In the gynecologic tract, these tumors most commonly involve the endometrium, and less commonly the ovary and vulva. Here we report a series of undifferentiated carcinomas of the cervix and vagina and describe their morphologic, immunohistochemical, and genomic characteristics.

Design: We included 3 cases of undifferentiated carcinomas (2 cervical, 1 vaginal), each case was reviewed for salient morphologic features, and ancillary tests results. The MSKCC-IMPACT sequencing panel was performed on all cases.

Results: The patients were 27, 51, and 66 years-old. All three samples showed diffuse growth of monomorphic cells with brisk mitotic activity and at least focal discohesion, and all were positive for high-risk HPV in situ hybridization with diffuse p16 expression (see Table 1 and Figure 1). All showed expression of at least one epithelial marker by immunohistochemistry. One case showed focal PD-L1 expression (CPS=20)(ID1). One case (ID2) had loss of expression for SMARCA4 and SMARCA2 (Figure 2) with focal weak expression for synaptophysin and CD56. p53 IHC had a wild-type pattern in the two cases that were stained (ID2,3). Sequencing analysis was notable for a relatively low tumor mutational burden across all three cases. One case (ID1) had a complex genome, and another (ID2) had broad deletion of 19p including the SMARCA4 gene.

Cases	Positive/retained	Focal/weak positive	Negative/loss
ID1	HR-HPV ISH, p16, CK18, PMS2, MLH1, MSH6, MSH2, SMARCA4, SMARCA2, SMARCB1, PD-L1(CPS:20)	HER2 2+ (not amplified by FISH)	EMA, p63
ID2	HR-HPV ISH, p16, AE1/3, EMA, p53(WT)	CAM 5.2, synaptophysin, CD56	Chromogranin, SOX10, SMARCA4, SMARCA2
ID3	HR-HPV ISH, p16, AE1/3, CAM 5.2, PMS2, MLH1, MSH6, MSH2, SMARCA4, SMARCA2, SMARCB1, ARID1B, PTEN, p53(WT)	PAX8, WT-1, CK20, GATA-3	CK7, p40, ER, PR, PAX-2, CDX-2, TTF-1, chromogranin, INSM1, synaptophysin, S100, melan-A

Figure 1 - 778

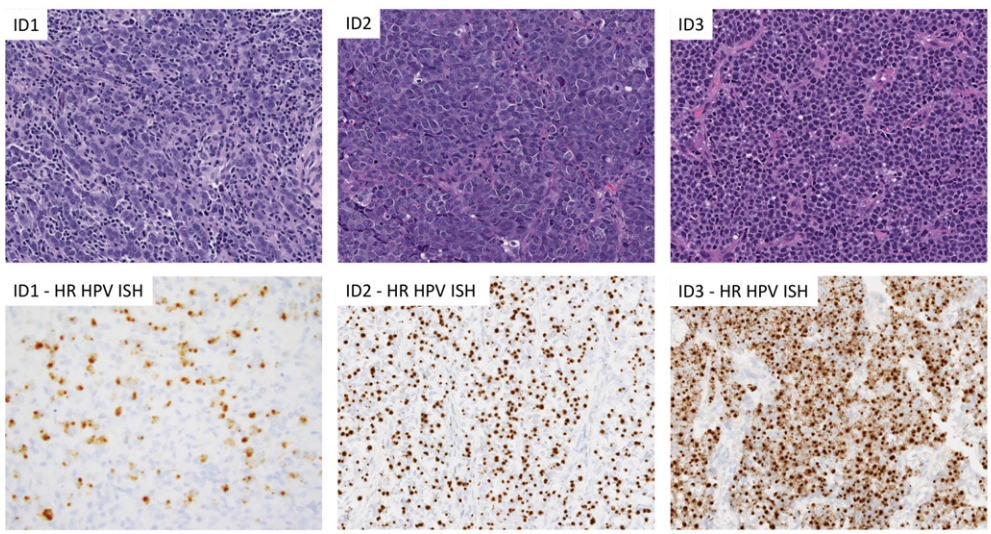

Figure 2 - 778

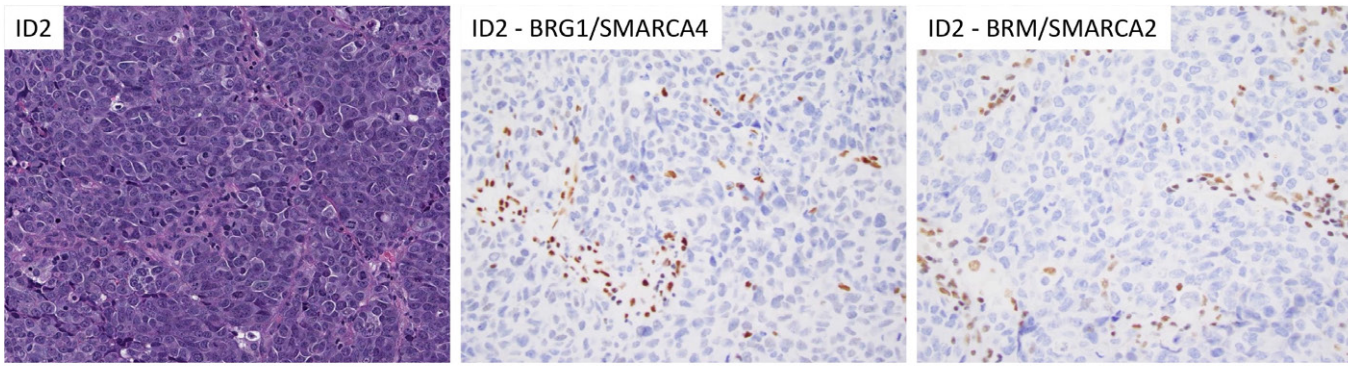

Conclusions: To our knowledge this is the first report of molecularly characterized, HPV-associated undifferentiated carcinoma of the cervix and vagina. These lesions have similar morphologic features to other undifferentiated tumors of the gynecologic tract. The rate of mutations was low across all cases and one was associated with inactivation of the SWI/SNF complex. This series is evidence that undifferentiated carcinomas associated with HPV can arise in the cervix and the vagina. The importance of recognizing undifferentiated tumors has become increasingly important for management and identification of targetable alterations.

779 Detection of a Novel GLI1 Gene Fusion in Low Grade Endometrial Stromal Sarcoma

Jiangling Tu[1], Majd Al Assaad[2], Samantha McNulty[3], Hussein Alnajar[4], David Wilkes[5], Sarah Kudman[5], Feng He[5], Jenny Xiang[5], Olivier Elemento[5], Melissa Frey[2], Juan Miguel Mosquera[5]
[1]Weill Cornell Medical College, New York, NY, [2]New York-Presbyterian/Weill Cornell Medicine, New York City, NY, [3]ArcherDX, Inc., Boulder, CO, [4]NorthShore University HealthSystem, Evanston, IL, [5]Weill Cornell Medicine, New York, NY

Disclosures: Jiangling Tu: None; Majd Al Assaad: None; Samantha McNulty: *Employee*, Invitae Corporation; Hussein Alnajar: None; David Wilkes: None; Sarah Kudman: None; Feng He: None; Jenny Xiang: None; Olivier Elemento: *Stock Ownership*, Volastra Therapeutics, OneThree Biotech; Melissa Frey: None; Juan Miguel Mosquera: None

Background: Gene fusions are increasingly recognized as important oncogenic events that define molecular and prognostic subgroups of all endometrial stromal sarcomas (ESS). Half of all ESS are known to harbor an oncogenic *JAZF1-SUZ12* or *YWHAE-NUTM2* fusion, respectively. A minority of cases harbor other, less-frequent fusions while approximately one third of cases lack genetic lesions that are readily detectable using standard laboratory methods.

Design: We used an anchored multiplex PCR-based transcriptome profiling method (Archer® FusionPlex® Sarcoma Kit) to identify novel gene fusions in a heterogenous group of 64 tumors and controls (Table 1). Among these cases were two distinct low-grade ESS of a 42 and 54 year-old patients, one with aggressive course but no known fusions (Case 1) and one with *JAZF1* fusion (Case 2), respectively. We searched published RNA-seq data to facilitate annotation and developed FISH break-apart assays to validate novel events.

Results: Diagnostic oncogenic fusions were detected in 28 of the 64 cases we profiled in this study. Additional 3 novel events were nominated including a *LRRN2:GLI1* fusion in Case 1 (Table 1). The breakpoint between *LRRN2* and *GLI1* occurred in exon 1 of both genes and was predicted to preserve the open reading frame. A *GLI1* break-apart FISH assay confirmed the gene rearrangement in the primary tumor and metastases (Figure 1). The fusion is correlated with increased expression of GLI1. Additional 5 low-grade ESS without canonical fusions have been screened by FISH; none demonstrate *GLI1* break-apart signals.

Table 1. Diagnosis and anatomic site of 31 of 64 tumors with fusions detected by custom Archer® FusionPlex Sarcoma

Diagnosis	n	Anatomic site(s)	Fusion (or gene partner)
Low-grade ESS #1	1	Uterus	LRRN2-GLI1*
Plexiform fibromyxoma	1	Gastric antrum	GLI1*
Low-grade ESS #2	1	Uterus	JAZF1
Inflammatory myofibroblastic tumor	2	Uterus	ALK1
Dermatofibrosarcoma protuberans	2	Breast, chest	COL1A1-PDGFβ
Desmoplastic small round cell tumor	2	Peritoneum	EWSR1-WT1
Ewing sarcoma	3	Soft tissue	EWSR1- FLI1
Myoepithelioma	1	Parotid	EWSR1
Spindle cell rhabdomyosarcoma	1	Bone	EWSR1-TFCP2
Giant cell tumor of bone	1	Bone	FN1-TEK*
Embryonal rhabdomyosarcoma	1	Sinonasal	PAX3-FOXO1
Low grade fibromyxoid sarcoma	1	Soft tissue	FUS-CREB3L2
Solitary fibrous tumor	1	Nasal	NAB2-STAT6
Mammary analog secretory carcinoma	1	Salivary gland	NTRK3-ETV6
Astrocytoma	1	Brain	PHIP-ROS1*
Pleomorphic adenoma	3	Parotid gland	CTNNB1-PLAG1
Synovial Sarcoma	2	Chest, soft tissue	SS18-SSX2
Adenocarcinoma	1	Colon	TPM3-NTRK1*
Nodular fasciitis	3	Chest, soft tissue	MYH9-USP6
Epithelioid hemangioendothelioma	2	Liver	WWTR1-CAMTA1

**FISH break-apart assays were developed and support the presence of known and novel gene fusions or gene partners. Additional orthogonal experiments are ongoing. Table summarizes 31 of the total 64 cases in the study cohort. 28 tumor types with known driver fusions were included (controls), and 3 novel events were identified in low-grade endometrial stromal sarcoma, giant cell tumor of bone, and astrocytoma.*

Figure 1 - 779

Figure 1. Novel *LRRN2:GLI1* fusion in an aggressive low-grade endometrial stromal sarcoma. A. Representative histopathology of uterine low-grade ESS is shown (H&E slide; 4x and 20x original magnification). **B.** Schematic diagram of the novel *LRRN2:GLI1* in-frame fusion that basically puts all GLI1 under the control of LLRN2 promoter. **C.** Representative Heatmap comparing GLI1 expression with other genes. Low-grade ESS with novel *LRRN2:GLI1* fusion has highest GLI1 RNA expression (Case 59 LGESS_1).

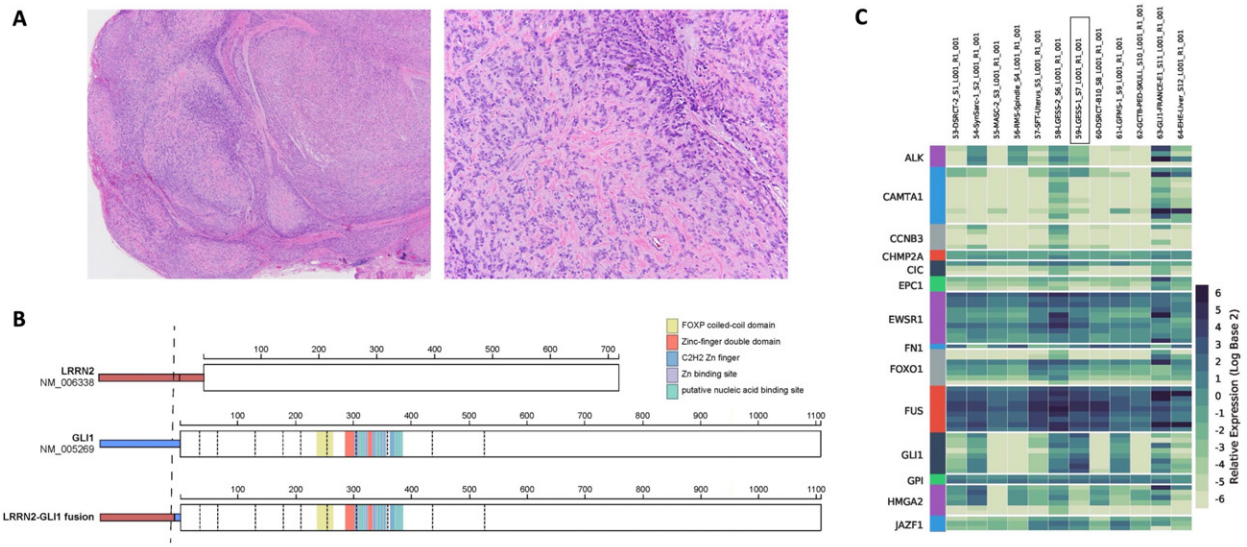

Conclusions: In this study, we identified a novel *GLI1* fusion in a low-grade ESS that metastasized. *ACTB:GLI1* and *PTCH1:GLI1* fusions were previously described in a series of ESS (Brahmi *et al., Cancers* 2020), but authors related them to other soft tissue tumors. Further studies will determine if *GLI1* fusions represent a prognostic biomarker and potential target in low-grade ESS.

780 Integrative Analysis of Ovarian Clear Cell Carcinoma Tumor Immunophenotype and Microenvironment

David Twa[1], Cheng-Han Lee[2], Martin Koebel[3]
[1]University of Calgary, Calgary, Canada, [2]University of Alberta, Edmonton, Canada, [3]Alberta Precision Laboratories, University of Calgary, Calgary, Canada

Disclosures: David Twa: None; Cheng-Han Lee: None; Martin Koebel: None

Background: Ovarian clear cell carcinoma (OCCC) is an epithelial neoplasm that carries a dismal prognosis in high stage disease. To date, mutation and expression profiling has facilitated characterization of OCCC with the potential to improve risk stratification and identify candidates for targeted therapies. Here, we integrated intrinsic tumor alterations with constituents of the tumor microenvironment (TME).

Design: We assessed 164 pre-treatment OCCCs for tumor cell ARIDA1 expression and utilized previously published data for tumor expression of: CDKN2A, ERBB2, HNF1B, IGF2BP3, NAPSA, PTEN, and TP53, in addition to TME markers: CD8, CD20, CD68, FOXP3, IDO1, PD1, PDL1, and arithmetically derived CD4. We first investigated the association between intrinsic tumor alterations and the microenvironment, adjusting for multiple hypotheses. Next, we performed unsupervised hierarchical clustering on both tumor phenotype and TME constituents to generate case clusters, which were evaluated against progression-free survival (PFS) and disease-specific survival (DSS). Finally, subset analysis among patients with progressive disease was also performed using chemotherapy relapse time (CRT; date of chemotherapy start to relapse).

Results: We found there was enrichment for lymphocytic infiltrate (CD4, CD8) among tumors with CDKN2A, IGF2BP3, and TP53 alterations (P<0.01). Further, absence of NAPSINA and HNF1B were associated with regulatory constituents FOXP3 (P=5.0e-4) and PD1 (P=3.6e-4), respectively, and loss of PTEN expression was associated with CD68 macrophages (P=8.4e-4). We did not observe an association with TME and ARIDA1 alterations. Unsupervised clustering using tumor markers revealed three distinct clusters that were independent of stage at diagnosis, specifically: (a) concurrent CDKN2A, IGF2BP3, and TP53 alterations, (b) ARIDA1 with a secondary alteration, and (c) cases with few or no specific alterations. The clusters were able to prognosticate clinical outcome for CRT (P=0.04), PFS (P=0.01), and DSS (P=0.03). There was also an increased risk of peritoneal relapse among patients with HNF1B and/or PTEN alterations. Hierarchical clustering on TME constituents revealed three distinct clusters: (a) CD68, (b) IDO1, and (c) PDL1 enriched cases, however, these clusters did not prognosticate outcome.

Conclusions: Conclusion: Integrative analysis of the tumor cell phenotype and TME is critical to understanding OCCC pathogenesis particularly in light of forthcoming immunotherapies.

781 Dystrophin as a Novel Biomarker for Leiomyosarcoma Classification and Prognosis

Brian Vadasz[1], Jian-Jun Wei[2]
[1]Feinberg School of Medicine/Northwestern University, Chicago, IL, [2]Northwestern University, Chicago, IL

Disclosures: Brian Vadasz: None; Jian-Jun Wei: None

Background: Uterine Leiomyosarcoma (LMS) is a deadly disease with high rates of recurrence, and poor prognosis. It is histologically heterogeneous with varied degrees of differentiation, and complex genetic abnormalities. Currently, no reliable biomarkers can be used for differentiating LMS from other mimics including leiomyoma with bizarre nuclei (LM-BN). Genomic studies have shown a loss of dystrophin gene to be associated with dedifferentiated LMS of gynecologic origin and worse outcome. This prompted us to examine dystrophin expression in various types of benign and malignant uterine smooth muscle tumors.

Design: Cases included usual type leiomyoma (ULM, n=35), fumarate hydratase-deficient leiomyoma (FH-LM, n=31), LM-BN (n=20), spindle cell LMS (n=34) and myometrium (n=48) for this study. Tissue microarray was prepared and immunohistochemical analysis for dystrophin was performed. Immunostaining results were determined by either presence (positive) or absence (negative) of dystrophin expression. A correlation of dystrophin to clinical course was assessed. The study was approved by our Institutional Review Board

Results: Dystrophin expression can be detected in 94% (45/48) of myometrium. Dystrophin expression was detected in most benign leiomyoma variants: including 97% of ULM (34/35), 84% of FH-LM (26/31), 70% of LM-BN (14/20), and 18% of LMS (6/34) (Table 1, Figure 1). Dystrophin expression was significantly different between benign and malignant tumors (p<0.01). 4/6 LMS

positive for dystrophin showed low grade and well differentiated histology and the remaining 2 cases showed changes reminiscent to LM-BN. Among 6 LMS with dystrophin expression, 4 are currently alive, 1 died from other disease and 1 survival status is unknown. Among 28 LMS with loss of dystrophin expression, 16 died for LMS within 5 years (5 year death rate of 57%), 4 died from other diseases.

	Positive	Negative
ULM	34/35 (97%)	1/35 (3%)
FH-LM	26/31 (84%)	5/31 (16%)
LM-BN	14/20 (70%)	6/20 (30%)
LMS	6/34 (18%)	28/34 (82%)
Myometrium	45/48 (94%)	3/48 (6%)

Table 1. Summary of immunoreactivity for dystrophin in three benign and one malignant uterine smooth muscle tumors.

Figure 1 - 781

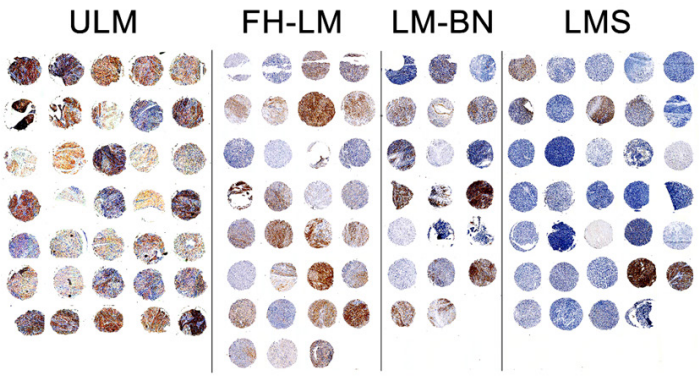

Figure 1. Immunostaining pattern of dystrophin in usual type leiomyoma (ULM), fumarate hydratase-deficient leiomyoma (FH-LM), leiomyoma with bizarre nuclei (LM-BN) and leiomyosarcoma (LMS).

Conclusions: Dystrophin is a novel biomarker for LMS, and loss of dystrophin is common and associated with worse outcome of LMS. Most benign variants of leiomyoma retain expression of dystrophin. A loss of dystrophin expression in small portion of LM-BN deserves further investigation as these cases may represent potential unfavorable molecular features. Dystrophin may be a novel and useful surrogate biomarker in LMS.

782 Is It Time to Test All Endometrial Carcinomas for p53 Mutation?

Elmira Vaziri Fard[1], Sara Imboden[2], Tilman Rau[3], Elisabeth Epstein[4], Saloni Walia[5], Joseph Carlson[5]
[1]LAC+USC Medical Center/Keck Medicine of USC, Los Angeles, CA, [2]Insel University Hospital, University of Bern, Bern, Switzerland, [3]University Bern, Bern, Switzerland, [4]Karolinska Institutet, Stockholm, Sweden, [5]Keck School of Medicine of USC, Los Angeles, CA

Disclosures: Elmira Vaziri Fard: None; Sara Imboden: None; Tilman Rau: None; Elisabeth Epstein: None; Saloni Walia: None; Joseph Carlson: None

Background: Historically, p53 mutation has been considered a diagnostic marker for serous endometrial carcinoma. Of the recently adopted molecular subtypes, p53 mutated is the most aggressive. The aim of this study was to explore the histologic and clinical characteristics of p53 mutated endometrial carcinoma regardless of their histologic subtype or grade.

Design: A total of 146 p53 mutated endometrial carcinoma cases were included (44 cases from the Karolinska Institute, 37 cases from Bern University Hospital and 65 cases from the TCGA database). Based on availability, 1-2 representative digital slides from each case were reviewed. Morphologic, clinical and follow up data were recorded if available. Survival analysis was performed using Kaplan Meier curves and log-rank test.

Results: After review, 64 cases (43.8%) were endometrioid, 58 (39.7%) serous, 9 (6.2%) clear cell, 8 (5.5%) mixed, 6 (4.1%) carcinosarcoma, and 1 (0.7%) dedifferentiated/undifferentiated subtype. Of the endometrioid, 13 cases (20.3%) were FIGO grade 1, 27 cases (42.1%) were grade 2 and 24 cases (37.5%) were grade 3. Thus, a total of 40 cases (27%) were endometrioid FIGO grade 1-2. The dominant architecture in 104 cases (71.2%) was glandular, in 13 cases (8.9%) papillary, in 2 cases (1.4%) tubulocystic, and in 27 cases (18.5%) solid. Nine cases (6.2%) showed nuclear atypia grade 1, 45 cases (37.2%) grade 2 and 91 cases (62.3%) grade 3. In addition, 26 cases (17.9%) showed squamous differentiation, 35 cases (24%) had at least moderate tumor infiltrating lymphocytes (TILs) and 59 cases (43.7%) showed peritumoral lymphocytes (PTL).

Tumors with moderate to high tumor infiltrating lymphocytes had notably better survival than mild TILs, but this finding was not significant (*p* value= 0.18). Additionally, there was lower overall survival for tumors with necrosis (*p* value=0.003).

Figure 1 - 782

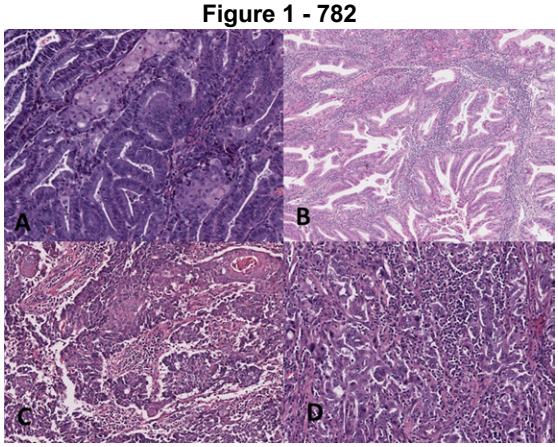

Conclusions: The findings of our study indicate that a substantial number of p53 mutated tumors are endometrioid and do not show high-grade morphologic features, and thus may go unrecognized. Given that therapy is increasingly guided by molecular subtype, these results indicate that routine testing for p53 may be necessary. The presence of at least moderate TILs in 24% of p53 mutated endometrial carcinomas indicates that these patients may potentially benefit from immunotherapy. The survival trend in tumors with high TILs and/or PTLs speaks to the role of the immune system in eliminating cancer cells.

783 Prognostic Relevance of FIGO Grading is Limited to NSMP Endometrial Carcinomas

Lisa Vermij[1], Jan Jobsen[2], Mariel Brinkhuis[3], Suzan Roothaan[3], Alicia León del Castillo[4], Naveena Singh[5], Linda Mileshkin[6], Melanie Powell[7], Prafull Ghatage[8], C. Meg Mclachlin[9], Alexandra Leary[10], Catherine Genestie[10], Hans Nijman[11], Harry Hollema[12], Ina Jürgenliemk-Schulz[13], Remi Nout[14], Vincent Smit[1], Stephanie de Boer[1], Carien Creutzberg[1], Nanda Horeweg[1], Tjalling Bosse[1]

[1]Leiden University Medical Center, Leiden, Netherlands, [2]Medisch Spectrum Twente, Enschede, Netherlands, [3]LabPON, Hengelo, Netherlands, [4]Antoni van Leeuwenhoek Hospital, Amsterdam, Netherlands, [5]Vancouver General Hospital, Vancouver, Canada, [6]Peter MacCallum Cancer Centre, Mt Stuart, Australia, [7]Barts Health NHS Trust, London, United Kingdom, [8]Tom Baker Cancer Centre, University of Calgary, Calgary, Canada, [9]London Health Sciences Centre, London, Canada, [10]Gustave Roussy, Villejuif, France, [11]University Medical Center Groningen, University of Groningen, Groningen, Netherlands, [12]University Medical Center Groningen, Groningen, Netherlands, [13]University Medical Center Utrecht, Utrecht, Netherlands, [14]Erasmus University Medical Center, Rotterdam, Netherlands

Disclosures: Lisa Vermij: None; Jan Jobsen: None; Mariel Brinkhuis: None; Suzan Roothaan: None; Alicia León del Castillo: None; Naveena Singh: None; Linda Mileshkin: None; Melanie Powell: None; Prafull Ghatage: None; C. Meg Mclachlin: None; Alexandra Leary: None; Catherine Genestie: None; Hans Nijman: None; Harry Hollema: None; Ina Jürgenliemk-Schulz: None; Remi Nout: None; Vincent Smit: None; Stephanie de Boer: None; Carien Creutzberg: None; Nanda Horeweg: None; Tjalling Bosse: None

Background: FIGO grading of endometrioid-type endometrial cancers (EEC) is considered standard clinical practice. However, with the incorporation of the EC molecular classification in the risk-assessment of EC patients, the role of FIGO grading is increasingly debated. In this study we assessed the prognostic value of FIGO grading in molecularly classified high-risk EC (HREC).

Design: A total of 680 HREC of consenting patients from the PORTEC-3 clinical trial (n=424), and a prospective clinical cohort from Medisch Spectrum Twente in the Netherlands (n=256), were used for this study. Targeted DNA-sequencing for pathogenic *POLE*-exonuclease domain mutations and immunohistochemistry for p53 and mismatch repair (MMR) proteins were used to molecularly classify EC following the 2020 WHO diagnostic algorithm (*POLE*-mutated [*POLE*mut], mismatch repair deficient [MMRd], no specific molecular profile [NSMP] and p53-abnormal [p53abn] EC). Central review of histologic subtype and binary FIGO grading was performed, and non-endometrioid EC were excluded from further analyses. The Kaplan-Meier method, log-rank test and prespecified multivariable Cox proportional-hazard models were used for the assessment of time to overall recurrence by molecular subgroup and FIGO grade.

Results: In total, 442 EEC were identified, including 261 (59.0%) low-grade (grade 1-2) and 181 (41.0%) high-grade (grade 3) EEC. *POLE*mut and p53abn EEC were predominantly high-grade (n=40/46, 87.0% and n=38/45, 84.4%, respectively), while NSMP EC were mostly low-grade (n=157/186, 84.4%). Within MMRd EEC there was an equal distribution between low- and high-grade (n=91/165, 55.2% and n=74/165, 44.8%, respectively). 5-year overall recurrence rate was significantly lower for patients with high-grade NSMP EEC (82.4% versus 55.2%; p = 0.007; figure 1). Both low- and high-grade *POLE*mut EEC were associated with an excellent prognosis, and p53abn EEC had a poor prognosis regardless of grade. High-grade MMRd EEC had a slightly lower risk of recurrence than low-grade MMRd EEC, but this did not reach statistical significance (figure 2). Multivariable analysis confirmed independent unfavorable prognostic impact of high grade within NSMP EEC, but not in MMRd EEC (table 1).

Table 1. Risk factors for recurrence in NSMP and MMRd HR-EEC

	Overall recurrence							
	NSMP EEC 50 events				MMRd EEC 50 events			
	Total n	HR	95% CI	p-value	Total n	HR	95% CI	p-value
Age	185	1.016	0.986-1.047	0.31	164	1.035	1.002-1.068	0.037
FIGO grade								
Grade 1-2	155	1			90	1		
Grade 3	29	2.450	1.254-4.785	0.009	74	0.831	0.456-1.514	0.54
Stage								
I-II	90	1			89	1		
III	95	1.736	0.926-3.256	0.09	75	2.380	1.286-4.407	0.006
LVSI								
Absent	116	1			79	1		
Present	69	1.800	0.972-3.333	0.06	85	0.839	0.466-1.510	0.56
Treatment								
RT*	123	1			111	1		
CTRT	62	0.473	0.240-0.931	0.03	53	1.189	0.642-2.201	0.58

** Including external beam radiotherapy (NSMP n = 119, MMRd n=111) and vaginal brachytherapy (NSMP n = 3, MMRd = 0)*
Abbreviations: NSMP, no specific molecular profile; EEC, endometrioid endometrial cancer; MMRd, mismatch repair deficient; CI, confidence interval; LVSI, lymphovascular space invasion; RT, radiotherapy; CTRT, combined chemotherapy and radiotherapy.

Figure 1 - 783

Figure 1. Time to recurrence of low-grade versus high-grade NSMP HR-EEC

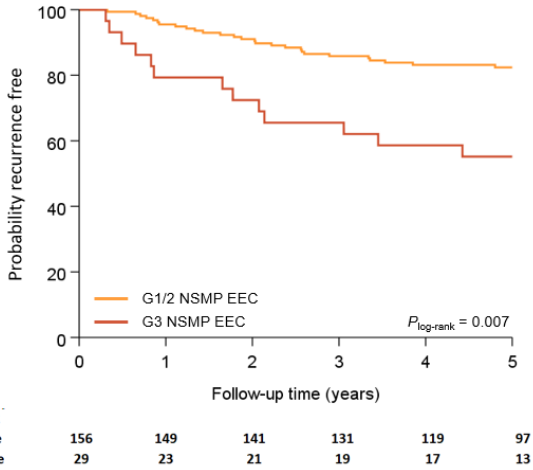

No. at risk						
Low-grade	156	149	141	131	119	97
High-grade	29	23	21	19	17	13

Kaplan-Meier survival analysis demonstrating the time to recurrence for FIGO grading in endometrioid endometrial cancers (EC) without a specific molecular profile (NSMP).

Figure 2 - 783

Figure 2. Time to recurrence of low-grade versus high-grade MMRd HR-EEC

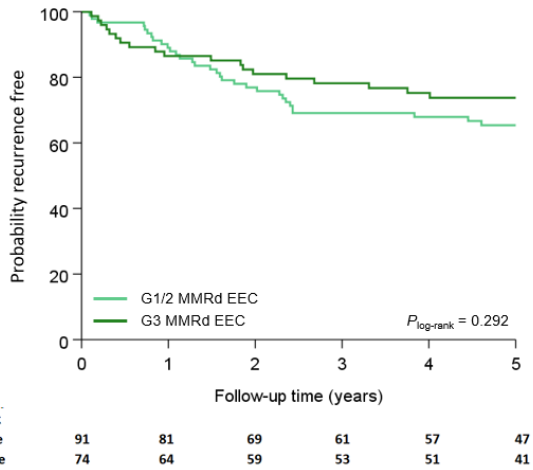

No. at risk						
Low-grade	91	81	69	61	57	47
High-grade	74	64	59	53	51	41

Kaplan-Meier survival analysis demonstrating the time to recurrence for FIGO grading in mismatch repair deficient (MMRd) endometrioid endometrial cancers (EC).

Conclusions: FIGO grading showed independent prognostic value in high-risk NSMP EEC, but not in *POLE*mut, MMRd or p53abn EEC. Future studies should clarify whether this holds up in (low-)intermediate-risk EEC. Our findings further support the use of the molecular classification.

784 Does HPV Type Matter in Cervical Squamous Cell Carcinoma: Transcriptomic Immune Profiling

John Wallbillich[1], Sharon Wu[2], Sudeshna Bandyopadhyay[3], Logan Corey[4], Evi Abada[3], Mira Kheil[3], Tala Tawil[3], Deepti Jain[3], Marilyn Huang[5], Premal Thaker[6], Nathaniel Jones[7], W. Michael Korn[2], Matthew Oberley[2], David Spetzler[2], Robert Morris[8], Rouba Ali-Fehmi[3]

[1]Wayne State University School of Medicine, Detroit, [2]Caris Life Sciences, Phoenix, AZ, [3]Wayne State University, Detroit, MI, [4]Barbara Ann Karmanos Center and Wayne State University School of Medicine, Detroit, MI, [5]University of Miami, Miami, FL, [6]Washington University School of Medicine, St. Louis, MO, [7]University of South Alabama College of Medicine, Mobile, AL, [8]Karmanos Cancer Institute, Detroit, MI

Disclosures: John Wallbillich: *Advisory Board Member*, Seagen; Sharon Wu: *Employee*, Caris Life Sciences; Sudeshna Bandyopadhyay: None; Logan Corey: None; Evi Abada: None; Mira Kheil: None; Tala Tawil: None; Deepti Jain: None; Marilyn Huang: None; Premal Thaker: *Advisory Board Member*, Agenus, Seagen, Eisai; *Consultant*, Celsion, GlaxoSmithKline, AstraZeneca; *Stock Ownership*, Celsion; *Grant or Research Support*, Merck, GlaxoSmithKline; Nathaniel Jones: None; W. Michael Korn: *Employee*, Caris Life Sciences; *Stock Ownership*, Caris Life Sciences; Matthew Oberley: *Employee*, Caris Life Sciences; David Spetzler: *Employee*, Caris Life Sciences; *Speaker*, Caris Life Sciences; Robert Morris: None; Rouba Ali-Fehmi: None

Background: Immunotherapy (IO) has shown promise in treating metastatic or recurrent cervical cancer. Transcriptomic immune profiling (TIP) in cervical cancer suggests that squamous cell carcinoma (SCC) has increased immunogenecity than adenocarcinoma. Given the near-universal HPV+ status of cervical SCC, we sought to explore whether TIP signals vary with respect to HPV variants.

Design: For tumor analysis, we used next-generation sequencing and whole exome sequencing (NGS: NextSeq, 45 or 592 Genes and NovaSEQ, WES) and WTS (NovaSeq) (Caris Life Sciences, Phoenix, AZ). PD-L1 by IHC (positive: CPS >1). Microsatellite instability (MSI) by FA, IHC and NGS. Tumor mutational burden (TMB) measured by totaling all somatic mutations per tumor (TMB-h: >10). Immune cell infiltration calculated by QuantiSeq. HPV16/18 status determined using WES. Appropriate statistical analysis was performed.

Results: 89 cervical SCC tumors with available HPV16/18 status were included: 63 (71%) were HPV16+ or 18+ while 26 (29%) were non-HPV16/18. HPV16/18+ had significantly fewer *TP53* alterations compared to non-HPV16/18 tumors (1.7% vs 33%, q=0.01). There was a trend toward increased regulatory T cell infiltration in HPV16/18+ tumors (2.2% vs 1.9%) (p=0.02; q=0.2)

accompanied with a trend towards increased immune checkpoint (IC) gene expression: CD86 (1.4-fold, p=0.05/q=0.5), IFNG (2.2-fold, p=0.03; q=0.3) and IDO1 (2.5-fold, p=0.03; q=0.3). Additionally, there was a trend towards increased T-cell inflammation (32% vs 19%, p=0.16) in HPV16/18+ tumors (Table 1). Among prevalent mutations/pathways in this dataset, there were no significant differences in PI3K (42% vs 42%), Telomerase Maintenance (12% vs 15%) or RTK RAS (22% vs 27%) pathway alterations (q=1). There were no significant differences in IO-related biomarkers: PD-L1 (92% vs 82%), dMMR/MSI-H (4.8% vs 3.7%) or TMB (25% vs 19%) (q=1). No significant genomic, transcriptomic or immune differences were seen between HPV16+ and HPV18+ tumors.

Immune Microenvironment		HPV16/18+	Non-HPV16/18	P-value	Q-value
IO Therapy Biomarkers	PD-L1 (22c3)	91.80%	81.48%	0.272	1
	dMMR/MSI-H	4.84%	3.70%	1	1
	TMB-H	25.00%	18.52%	0.506	1
Immune Cell Infiltrates (%)	B cell	4.11%	3.37%	0.0883	1
	M M.1	3.48%	2.81%	0.6204	1
	M M.2	3.00%	3.10%	0.3842	1
	Monocyte	0.00%	0.00%	0.1297	1
	Neutrophil	5.63%	6.53%	0.4508	1
	NK cell	2.31%	2.31%	0.6394	1
	CD4+ T Cells	0.00%	0.00%	0.6108	1
	T cell CD8+	0.73%	0.24%	0.1712	1
	Tregs	**2.24%**	**1.94%**	**0.0196**	**0.2156**
	MDCs	1.20%	0.70%	0.1002	1
Immune Checkpoint Genes (TPM, normalized to HPV16/18-)	CD80	1.376	1	0.077	0.772
	CD86	**1.362**	**1**	**0.050**	**0.496**
	CD274	1.834	1	0.082	0.818
	CTLA4	1.490	1	0.071	0.714
	HAVCR	1.372	1	0.146	1
	IFNG	**2.149**	**1**	**0.030**	**0.301**
	IDO1	**2.530**	**1**	**0.032**	**0.315**
	LAG3	0.964	1	0.586	1
	PDCD1	1.506	1	0.432	1
	PDCD1LG	1.463	1	0.074	0.743

Conclusions: Individual TIP markers were not significantly different with respect to high-risk HPV types for cervical SCC. Besides *TP53* alterations, major cancer-relevant mutations/pathways were not significantly different. There were simultaneous trends of increased T-cell activation and increased regulatory T-cell infiltration and IC gene expression in the HPV16/18+ group. These data are hypothesis-generating for the concept that HPV16/18+ cervical SCC might have different immunogenecity compared to non-HPV16/18 cervical SCC.

785 Exploring the Genomic Landscape of Vulvovaginal Squamous Cell Carcinoma: A Large Dataset

John Wallbillich[1], Sharon Wu[2], Logan Corey[3], Alex Farrell[2], Kurt Hodges[2], Mira Kheil[4], Sudeshna Bandyopadhyay[4], Tala Tawil[4], Deepti Jain[4], Mir Yousufuddin Ali Khan[5], Anthony Guastella[2], Marilyn Huang[6], Anthony Karnezis[7], Chadi Nabhan[2], Premal Thaker[8], W. Michael Korn[2], Matthew Oberley[2], Robert Morris[9], Rouba Ali-Fehmi[4]
[1]Wayne State University School of Medicine, Detroit, [2]Caris Life Sciences, Phoenix, AZ, [3]Barbara Ann Karmanos Center and Wayne State University School of Medicine, Detroit, MI, [4]Wayne State University, Detroit, MI, [5]Detroit Medical Center/Wayne State University, Detroit, MI, [6]University of Miami, Miami, FL, [7]UC Davis Medical Center, Sacramento, CA, [8]Washington University School of Medicine, St. Louis, MO, [9]Karmanos Cancer Institute, Detroit, MI

Disclosures: John Wallbillich: *Advisory Board Member*, Seagen; Sharon Wu: *Employee*, Caris Life Sciences; Logan Corey: None; Alex Farrell: *Employee*, Caris Life Sciences; Kurt Hodges: None; Mira Kheil: None; Sudeshna Bandyopadhyay: None; Tala Tawil: None; Deepti Jain: None; Mir Yousufuddin Ali Khan: None; Anthony Guastella: *Employee*, Caris Life Sciences; Marilyn Huang: None; Anthony Karnezis: None; Chadi Nabhan: *Employee*, Caris; Premal Thaker: *Advisory Board Member*, Agenus, Seagen, Eisai; *Consultant*, Celsion, GlaxoSmithKline, AstraZeneca; *Stock Ownership*, Celsion; *Grant or Research Support*, Merck, GlaxoSmithKline; W. Michael Korn: *Employee*, Caris Life Sciences; *Stock Ownership*, Caris Life Sciences; Matthew Oberley: *Employee*, Caris Life Sciences; Robert Morris: None; Rouba Ali-Fehmi: None

Background: Relatively little is known about the genomic landscape of vulvovaginal squamous cell carcinoma (VSC). We sought to explore this landscape and the possibility of molecularly driven outcomes in a large database of VSC.

Design: VSC tumor samples were analyzed using next-generation sequencing of DNA (TruSeq, 45 genes; NextSeq, 592 genes and NovaSeq, whole exome sequencing (WES)) and RNA (NovaSeq). PD-L1 expression was tested by IHC using SP142. Microsatellite instability (MSI) was tested by fragment analysis, IHC and NGS. Tumor mutational burden (TMB) was measured by counting all somatic mutations per tumor (TMB-high: > 10 mutations/MB). HPV16/18 status was determined using WES. Real world overall survival (OS) was obtained from insurance claims data and Kaplan-Meier estimates were calculated for molecularly defined patient cohorts as the time of first treatment of Pembrolizumab and Nivolumab (IO) to last day of contact.

Results: 651 VSC tumors were included, 67% of which were primary tumors. The top 5 most mutated genes were: *TP53* (45.8%), *CDKN2A* (23.7%), *PIK3CA* (22.6%), *TERT* (19.8%) and *KMT2D* (12.9%). The top 5 most active pathways were: TP53 (45.2%), Chromatin Remodeling (27%), PI3K (27%), Cell Cycle (26.3%), and RTK-Ras (25.7%). 78.9% of tumors were PD-L1+ and 1.8% of tumors were MSI-H.

We compared HPV 16/18+ VSC tumors (n=62) with VSC tumors that were both HPV16/18- and *TP53*-mutant (n=59). *CDKN2A* mutations were exclusive to HPV16/18-/*TP53*mut VSC tumors (49.2%, q<0.001). HPV16/18+ tumors had significantly increased alterations in the PI3K pathway (45.2% vs 11.9%) but lower alterations in the Telomerase Maintenance (9.7% vs 61%) and Cell Cycle (8.1% vs 54.2%) pathways (q<0.001).

CDKN2A (HR: 3.26, 95% CI: 0.94-11.2, p=0.049) and *TP53* (HR: 3.62, 95% CI: 1.07-12.2, p=0.028) mutations each were significantly associated with worse OS after IO. Combined survival analysis of VSC patients with *CDKN2A* or *TP53* mutations showed a trend toward worse survival after IO compared to *CDKN2A* and *TP53* WT VSC patients (HR: 3.12, 95% CI: 0.92-10.6, p=0.054) (Figure 1). Interestingly, *CDKN2A* and *TP53* WT VSC patients had improved OS with IO treatment compared to non-IO treatments (HR: 0.37, 95% CI: 0.14-1.03, p=0.047) but there was no difference in combined *CDKN2A* or *TP53* mutant VSC patients (p=0.985).

Figure 1 - 785

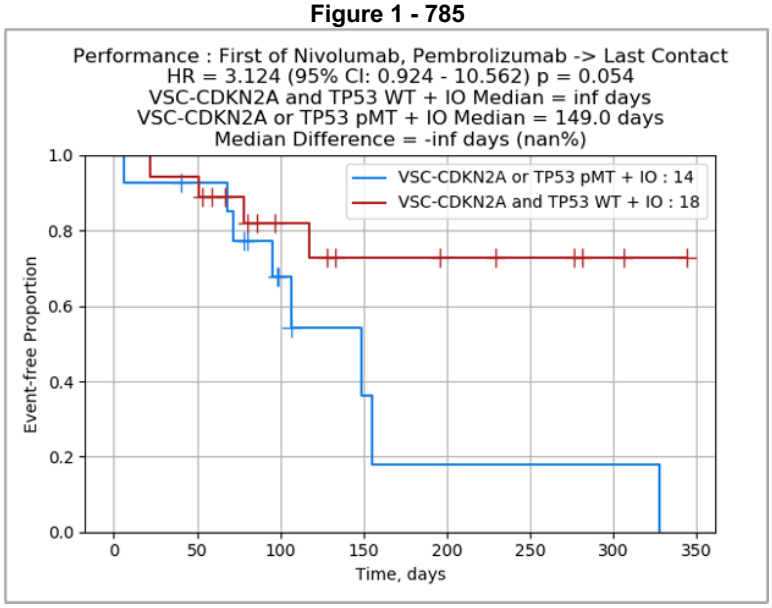

Conclusions: HPV 16/18-/*TP53*mut VSC has significantly higher activity of Telomerase Maintenance and Cell Cycle pathways, while HPV 16/18+ VSC has significantly higher PI3K pathway activity, suggesting the potential of targeted therapy. *TP53* and *CDKN2A* mutations in VSC appear limited to HPV16/18- tumors and might signal lack of benefit from IO treatment.

786 Evidence for Continuity of the Interstitium Through the Gynecologic Tract

Lucy Wang[1], Rita Astur[2], Luis Chiriboga[3], Briana Zeck[2], Rami Imam[4], Rebecca Wells[5], Neil Theise[6], Esther Adler[2]
[1]NYU Langone Medical Center, New York, NY, [2]NYU Langone Health, New York, NY, [3]New York University, New York, NY, [4]New York University Langone Health, New York, NY, [5]Perelman School of Medicine at the University of Pennsylvania, Philadelphia, PA, [6]NYU Grossman School of Medicine, New York, NY

Disclosures: Lucy Wang: None; Rita Astur: None; Luis Chiriboga: None; Briana Zeck: None; Rami Imam: None; Rebecca Wells: None; Neil Theise: None; Esther Adler: None

Background: The human interstitium, the "pre-lymphatic space", is comprised of visible sinuses within fibroconnective tissue, lined by CD34 and vimentin positive cells, through which interstitial fluid flows (Cenaj et al, Comm Bio 2021). The interstitial spaces (IS) have been demonstrated in the colon and skin using hyaluronic acid-binding protein (HABP; a protein binding assay), highlighting spatial continuity of IS of all layers of colon (lamina propria to mesenteric fascia) and skin (papillary dermis to the subcutaneous fascia). These spaces, in turn, are in continuity with a potentially body-wide network through perivascular adventitial and perineurial IS.

In the gynecologic tract, lymphatics flow from each organ, conducting fluid from the interstitial "pre-lymphatic space", and drain to retroperitoneal and pelvic lymph nodes. This "pre-lymphatic space" has not been previously well defined in the gynecologic tract and is likely to play an important role in maintaining tissue fluid balance and immune surveillance, and may play a role in cell migration.

Design: Normal or near-normal tissues were obtained from non-neoplastic hysterectomy specimens for benign and risk reduction indications. To investigate continuity of the IS between anatomic compartments in the normal gynecologic tract (fallopian tube, ovary, mesovarium, uterus, cervix and vagina), sections were stained with HABP. Chromogenic multiplex immunohistochemistry was used to show the spatial relationship of the interstitial HA (brown) with CD34+ (teal) /vimentin+ (magenta) (overlap: blue) interstitial lining cells.

Results: HABP staining was seen in all connective tissue IS of ovary, fallopian tube, uterus, cervix, adventitia and perineurium and their continuity was evident at these junctions: fallopian tube to ovary, endomyometrium to fallopian tube at the uterine cornu, endomyometrium to peritoneal reflections, and cervix to lower uterine segment (figure 1). With HABP used as a surrogate marker for IS, the interstitium was present within and between each organ. Continuity within the IS of these tissues with those of the perivascular and perineurial connective tissue was also noted.

Figure 1 - 786

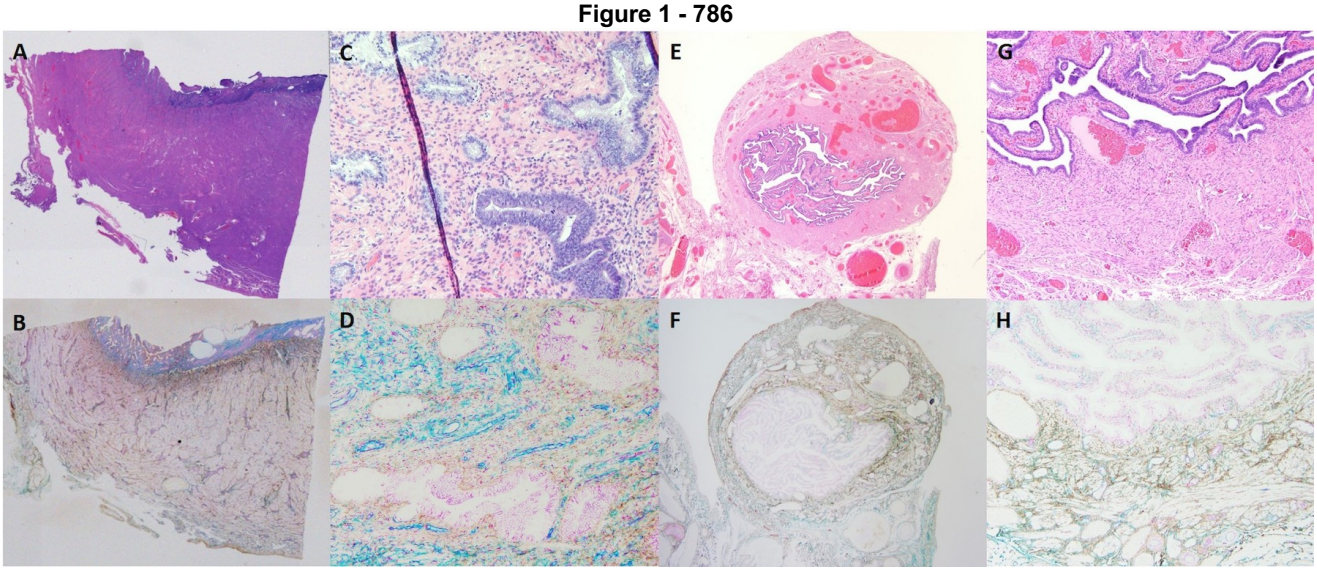

Conclusions: Connective tissue junctions in the gynecologic tract contain IS that are an inter-compartmental continuous space. Such spaces may provide previously unexplored pathways of tumor cell spread in gynecologic cancers and the migration of tissue in endometriosis and endosalpingiosis.

787 Fallopian Tube Pathology in Salpingectomies from Women with Clinically Diagnosed Tubal Factor Infertility and Hydrosalpinx: Practical Implications for Specimen Evaluation

Linyuan Wang[1], Maren Shapiro[2], Joseph Rabban[1]
[1]University of California, San Francisco, San Francisco, CA, [2]UCSF School of Medicine, San Francisco, CA

Disclosures: Linyuan Wang: None; Maren Shapiro: None; Joseph Rabban: None

Background: Hydrosalpinx is often seen in women with clinically diagnosed tubal factor infertility (TFI) and salpingectomy has been shown to improve the success rates of assisted reproductive technology (ART). Correlation of the pathologic features in these salpingectomy specimens has received scant attention and thus the spectrum of morphological alterations, including those that may be clinically unsuspected, remains to be elucidated. This study defined the macroscopic and microscopic pathology in salpingectomy specimens from women with TFI, emphasizing concordance with the clinical diagnosis of hydrosalpinx and prevalence of clinically occult diseases.

Design: The study included 48 women with TFI and suspicion of hydrosalpinx who underwent salpingectomy in a single institution (1997-2021). Clinical data and reproductive outcomes were collected from electronic medical records. Macroscopic pathology was collected from pathology reports while microscopic pathologic findings were recorded by glass slides review.

Results: Intra-operative diagnosis of hydrosalpinx by the surgeon was documented in 93% (43/48 cases), of which only 58% (25/43) had gross evidence of hydrosalpinx (median tube diameter 1.1 cm); 56% (24/43) had microscopic features of tube dilation, 51% (22/43) had loss of plicae, 51% (22/43) had plicae fibrosis, 39% (17/43) had luminal scaring. Among 18/48 cases without pathologic evidence of hydrosalpinx, 5/18 had gross cysts, 7/18 had serosal adhesions, and 7/18 were grossly normal. Microscopic findings in the grossly normal tubes included endometriosis (1/7), loss of plica (2/7), placental site nodule (1/7), or no pathology (4/7). Complete tissue submission for microscopy was performed in 54% (26/48) of cases. Pathologic lesions among all 48 cases included serosal adhesions (52%), paratubal cysts (29%), salpingitis isthmica nodosa (SIN) (21%), endometriosis (19%), mucosal adenofibroma (2%), and placental site nodule (2%). None had adenomatoid tumor, STIC, or carcinoma. Post-salpingectomy pregnancy was achieved in 65% (26/40) who underwent ART and 92% (24/26) resulted in live-birth or ongoing pregnancy. Two others had live birth after natural pregnancy.

Conclusions: Contrary to clinical expectation, hydrosalpinx was pathologically confirmed in only half of salpingectomies performed for TFI. Complete tissue submission of grossly normal specimens may identify diagnoses that permit correlation with the clinical setting of TFI such as endometriosis, SIN, paratubal cysts, and adhesions.

788 p53/CK17 Staining Patterns in Lichen Sclerosus: Value for Prediction of Progression to dVIN

Maxwell Wang[1], Steven Hrycaj[2], May Chan[2], Aaron Udager[3], Stephanie Skala[2]
[1]University of Michigan Hospitals, Ann Arbor, MI, [2]University of Michigan, Ann Arbor, MI, [3]University of Michigan Medical School, Ann Arbor, MI

Disclosures: Maxwell Wang: None; Steven Hrycaj: None; May Chan: None; Aaron Udager: None; Stephanie Skala: None

Background: Differentiated vulvar intraepithelial neoplasia (dVIN) is a human papillomavirus-independent precursor for vulvar squamous cell carcinoma (SCC) most commonly seen in postmenopausal patients with longstanding chronic inflammation of the vulva. Accurate diagnosis of dVIN is challenging partly due to subtle cytologic and/or architectural atypia. Recognition of dVIN is important due to its potential for rapid progression to SCC. Distinguishing lichen sclerosus (LS) with a higher propensity for progression to dVIN and SCC would prove beneficial as closer follow-up could be arranged for at-risk patients.

The most common immunohistochemical (IHC) stain used to support a diagnosis of dVIN is p53. However, there have been documented instances of LS with *TP53* mutation and corresponding aberrant p53 staining. CK17 has also been positive (moderate to strong intensity) in all documented stained dVIN cases and up to two-thirds of LS lesions. Here, we investigate the utility of p53/CK17 dual stain IHC staining patterns for risk stratification among patients with LS.

Design: We included 55 biopsies of LS from patients being followed for dVIN and/or vulvar SCC and 55 biopsies of LS from patients with at least two years of benign follow-up. Each case was stained with p53/CK17 dual stain. CK17 expression was evaluated as completely negative, focal/mosaic, or positive and p53 expression was evaluated as non-aberrant, equivocal, or aberrant. Expression was then documented and compared between specimens with benign follow-up and dVIN/SCC on follow-up.

Results: CK17 positivity with equivocal/aberrant p53 staining was associated with a higher frequency of dVIN/SCC on follow-up (31%) vs benign (18%), although this finding did not reach statistical significance (p = 0.17). In biopsies with negative CK17 expression, equivocal/aberrant p53 expression was not predictive of progression to dVIN (51%) vs benign follow-up (53%).

Table 1. p53/CK17 dual stain results

Diagnosis	Positive CK17			Negative CK17		
	Aberrant p53	Equivocal p53	Non-aberrant p53	Aberrant p53	Equivocal p53	Non-aberrant p53
dVIN follow-up (n=55)	5 (9%)	12 (22%)	4 (7%)	2 (4%)	26 (47%)	6 (11%)
Benign follow-up (n=55)	3 (5%)	7 (13%)	5 (9%)	2 (4%)	27 (49%)	11 (20%)

Conclusions: p53/CK17 expression alone is inadequate to predict progression of LS to dVIN/SCC. However, the combination of CK17 positivity and equivocal/aberrant p53 expression was more often seen in LS with dVIN/SCC on follow-up. Further investigation of morphologic and molecular data is underway and may be helpful to further characterize high risk LS lesions.

789 Patients with Stage III-IV ARID1A Mutated Gynecologic Carcinomas Have Better Overall Survival when Treated with Immune Checkpoint Blockade Therapy

Guoliang Wang[1], Barrett Lawson[1], Elizabeth Euscher[1], Preetha Ramalingam[1], Anais Malpica[1], Richard Yang[1]
[1]The University of Texas MD Anderson Cancer Center, Houston, TX

Disclosures: Guoliang Wang: None; Barrett Lawson: None; Elizabeth Euscher: None; Preetha Ramalingam: None; Anais Malpica: None; Richard Yang: None

Background: Mutations (mts) in the *ARID1A* gene have been associated with decreased mismatch repair protein activity. Tumors with *ARID1A* mts show higher numbers of mts than their wild-type counterparts. Therefore, *ARID1A* mutation status may represent a viable molecular biomarker for response to immune checkpoint blockade (ICB). In this study, we sought to interrogate whether mutations in *ARID1A* can be used as a molecular biomarker for response to immune checkpoint blockade in a cohort of advanced stage gynecologic carcinoma patients (pts), especially those with clear cell carcinoma (CCC).

Design: Retrospective review of institutional molecular diagnostics database for gynecologic surgical pathology cases with *ARID1A* mts. Clinicopathologic data was recorded, including: age, histologic subtype, AJCC stage, primary tumor site, if treated with immune checkpoint blockade therapy, and overall survival (OS). Descriptive statistics, Kaplan Meier curves, and survival analysis were performed in GraphPad Prism v.8.4.3 (La Jolla, CA).

Results: We identified 121 gynecologic cancer pts with *ARID1A* mutations, of which 58 (47.9%) were stage III or IV according to FIGO criteria. See Table 1 for clinicopathologic details. We found a significant overall survival advantage in advanced stage (III-IV) pts with *ARID1A* mts when treated with ICB versus non-ICB treatment (p=0.0024, Figure 1). OS of ICB treated (n=19) pts was significantly longer compared to non-ICB treated (n=39) pts (Median OS not yet reached vs 15.5 months, Hazard Ratio (HR) 0.309 [95% Confidence [CI] 0.145-0.660). Twelve of nineteen (63.2%) ICB treated pts had CCC histologic subtype. Therefore, we further interrogated whether cases with *ARID1A* mutation and presence of any CCC component were responsive to ICB. In *ARID1A* mutated clear cell carcinoma patients, overall survival of ICB treated (n=12) patients showed a trend (p=0.0635) towards longer OS compared to non-ICB treated (n=8) patients (Median OS not yet reached vs 14.3 months, HR 0.275 [95% CI 0.0701-1.076], Figure 2).

All Stage III-IV *ARID1A* mutated Gyn Cancer Patients	No ICB (n=39)	ICB (n=19)	p-value
Age range (years)			**0.3998**
20-40	1 (2.6%)	3 (15.8%)	
40-50	8 (20.5%)	2 (10.5%)	
50-60	15 (38.5%)	7 (36.8%)	
60-70	10 (25.6%)	5 (26.3%)	
>70	5 (12.8%)	2 (10.5%)	
Histologic Subtype			**0.0085**
Squamous cell carcinoma	0 (0%)	2 (10.5%)	
High grade serous carcinoma	9 (23.1%)	1 (5.3%)	
Mixed high-grade carcinoma (excluding Clear Cell Carcinoma)	3 (7.7%)	2 (10.5%)	
Carcinosarcoma	2 (5.1%)	0 (0%)	

Mixed high-grade carcinoma	2 (5.1%)	0 (0%)	
Undifferentiated and dedifferentiated endometrial carcinoma	3 (7.7%)	0 (0%)	
Endometrial endometroid adenocarcinoma	12 (30.8%)	2 (10.5%)	
Any Clear cell Carcinoma	8 (20.5%)	12 (63.2%)	
FIGO Stage			**0.1529**
III (n=27)	16 (41.0%)	11 (57.9%)	
IV (n=31)	23 (59.0%)	8 (42.1%)	
Primary Site			**0.0478**
Ovary	13 (33.3%)	9 (47.4%)	
Endometrium	26 (66.7%)	8 (42.1%)	
Cervix	0 (0.0%)	2 (10.5%)	
Stage III-IV *ARID1A* mutated Clear Cell Carcinoma Patients	**No ICB (n=8)**	**ICB (n=12)**	**P-value**
Age range (years)			**0.1567**
20-40	0 (0%)	3 (25%)	
40-50	1 (12.5%)	2 (16.7%)	
50-60	5 (62.5%)	3 (25%)	
60-70	0 (0%)	3 (25%)	
>70	2 (25%)	1 (8.3%)	
FIGO Stage			**0.0353**
III (n=13)	3 (37.5%)	10 (83.3%)	
IV (n=7)	5 (62.5%)	2 (16.7%)	
Primary Site			**0.5501**
Ovary	5 (62.5%)	9 (75%)	
Endometrium	3 (37.5%)	3 (25%)	

Figure 1 - 789

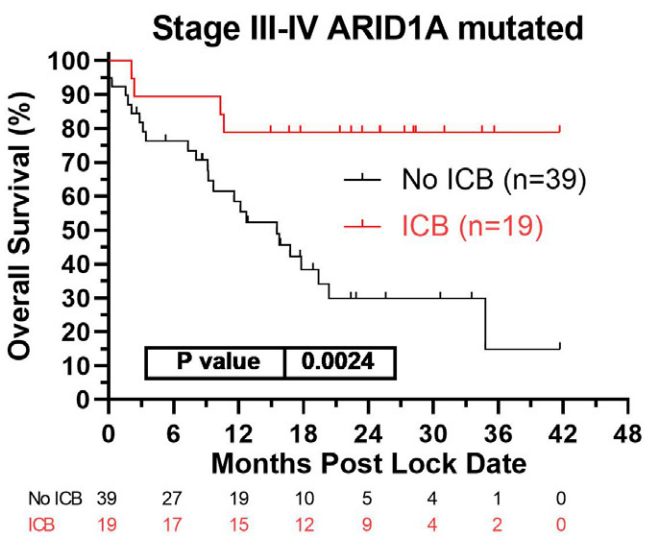

Figure 2 - 789

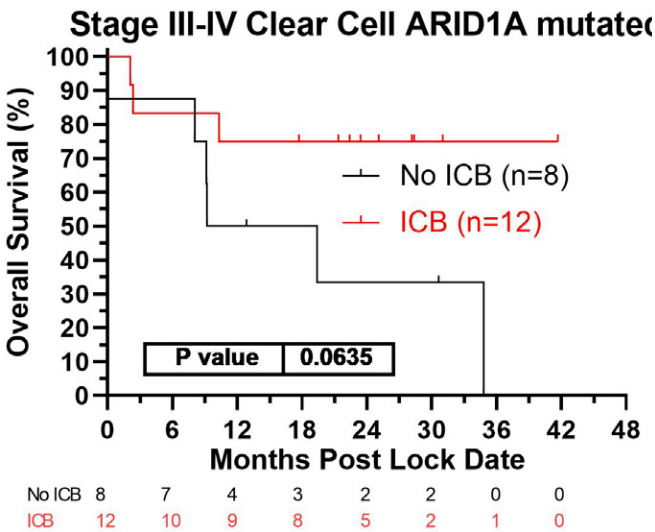

Conclusions: Advanced stage gynecologic carcinoma patients with mutated *ARID1A*, especially those with clear cell carcinomas, may be benefitting from ICB therapy. Prospective clinical studies using *ARID1A* mutations as a selective biomarker for treatment with ICB in gynecologic carcinomas, especially with clear cell histologic subtype, may be warranted.

790 Reliable Identification of Residual AEH/EIN from Progestin-Treated Endometrial Samples by Using a Panel of PTEN, PAX2, and β-Catenin Biomarkers

Yan Wang[1], Wanrun Lin[1], Ruijiao Zhao[2], Yiying Wang[2], Yue Wang[3], Wenxin Zheng[1]
[1]UT Southwestern Medical Center, Dallas, TX, [2]Henan Provincial People's Hospital, Zhengzhou, China, [3]Henan Provincial People's Hospital, People's Hospital of Zhengzhou University, School of Clinical Medicine, Henan University, Zhengzhou, China,

Disclosures: Yan Wang: None; Wanrun Lin: None; Ruijiao Zhao: None; Yiying Wang: None; Yue Wang: None; Wenxin Zheng: None

Background: Patients with atypical endometrial hyperplasia or endometrioid intraepithelial neoplasia (AEH/EIN) are commonly treated with progestin. It is challenging for surgical pathologists to evaluate those post progestin-treated follow-up endometrial samples due to progestin markedly masking the histologic features of AEH/EIN and lack of standard diagnostic criteria for residual/recurrent diseases (RRD) in such setting. This is particularly difficult when AEH/EIN lesions show partial response to the treatment. We have recently found that the expression pattern of PTEN/PAX2 in RRD is identical to that of pre-progestin treated AEH/EIN. Considering that the biomarker status is mostly unavailable from those pre-treated AEH/EIN cases, we investigated if the biomarkers PTEN/PAX2 and β-catenin can help to identify RRD in post-treatment endometrial samples.

Design: Immunohistochemical (IHC) staining using antibody against PTEN, PAX2, and β-catenin was performed on 126 post-progestin treated specimens which morphologically showed partial responses (neither obvious RRD, nor completely decidualized endometria). Among the 126 samples, 80 with at least 1 follow-up endometrial samples were similarly stained. Aberrant expression of either of the 3 biomarkers in two follow-up samples are considered as RRD. Results of the stain were analyzed by using Fisher exact test.

Results: Among 126 partial response cases, aberrant expression was found in 98 (78%) PTEN, 107 (85%) PAX2, and 28 (22%) β-catenin, respectively. Aberrant expression in 1 of the 3 markers was seen in 120 (95.2%) cases. Among 80 cases with follow-up biopsy samples, concordant aberrant expression in both specimens was found in 60/62 (97%) PTEN, 63/66 (95%) PAX2, and 20/23 (87%) β-catenin, respectively. Interesting to note that aberrant β-catenin was associated with 75% RRD with squamous morular differentiation and 25% with non-squamous RRD.

Conclusions: A focused panel of 3 biomarkers (PTEN, PAX2, and β-catenin) is useful to help identify RRD in progestin treated endometrial samples. Use of this panel can help identify a high percentage of cases with RRD (95.2%), making it useful in practice. Therefore, there should be a considerable benefit to the routine use of the 3-biomarker panel for progestin treated endometrial biopsy samples.

791 Isolation and Characterisation of Circulating Tumour Cells from Ovarian Cancer Patients

Mark Ward[1], Mark Bates[2], Bashir Mohamed[2], Tanya Kelly[2], Roisin O'Connor[2], Robert Brooks[3], Doug Brooks[3], Stavros Selemidis[4], Celine Ovaere[5], Jane Tully[5], Patrick Maguire[5], Catherine O'Gorman[5], Waseem Kamran[6], James Beirne[6], Feras Saadeh[6], Noreen Gleeson[6], Lucy Norris[2], Cara Martin[5], Sharon O'Toole[5], John O'Leary[2]
[1]Coombe Women & Infants University Hospital, Dublin, Ireland, [2]Trinity College Dublin, Dublin, Ireland, [3]University of South Australia, Adelaide, Australia, [4]RMIT, Mellbourne, Australia, [5]Trinity St. James's Cancer Institute, Dublin, Ireland, [6]St. James's Hospital, Dublin, Ireland

Disclosures: Mark Ward: None; Mark Bates: None; Bashir Mohamed: None; Tanya Kelly: None; Roisin O'Connor: None; Robert Brooks: None; Doug Brooks: None; Stavros Selemidis: None; Celine Ovaere: None; Jane Tully: None; Patrick Maguire: None; Catherine O'Gorman: None; Waseem Kamran: None; James Beirne: *Stock Ownership*, GenoME Diagnostics Ltd; Feras Saadeh: None; Noreen Gleeson: None; Lucy Norris: None; Cara Martin: None; Sharon O'Toole: None; John O'Leary: None

Background: Cancer cells that transit from primary tumours into the circulatory system are known as circulating tumour cells (CTCs). Classical CTC detection relies on EpCAM affinity-based technologies; however, CTCs are highly heterogeneous and often undergo EMT. Research has highlighted the difficultly with detection and characterisation of CTCs from ovarian cancer patients using EpCAM based techniques, with classical EpCAM CTC enumeration alone having limited prognostic significance. This study aims to isolate ovarian cancer CTCs using Parsortix technology (ANGLE Plc), and enumerate using an expanded immunofluorescence CTC-ID panel of antibody markers.

Design: Peripheral blood specimens were prospectively collected from ovarian cancer patients (high grade serous (HGSOC), clear cell, endometrioid) attending St James's Hospital for their treatment and processed for CTC isolation within 4 h of blood draw. Secondly, central ovarian vein sampling was done for a subset of patients undergoing primary debulking surgery. Ovarian cancer cell lines (SKOV3 and OVCAR3) were used as antibody controls and cell recovery. CTCs were isolated using Parsortix microfluidic device and immunophenotyped (CTC-ID; DAPI, CD45, CK7/panCK/EpCAM and platelet marker CD42b) by immunofluorescence microscopy.

Results: Spike-in of ovarian cancer cell lines to normal blood reported a 77% cell recovery using Parsortix. 70% of ovarian patients (n=10) [HGSOC, clear cell, endometroid] recruited had >1 CTC present (CTC range of 1 – 19 cells per 7.5 ml of blood). CTC doublets or CTC-clusters were detected in 28% of CTC+ samples. CTCs were detected in 60% of ovarian vein (n=5) samples isolated during surgery (CTC range of 4 – 118 cells per 7.5 ml of blood) with 100% of ovarian vein CTC+ samples positive for CTC-clusters. CD42b+ CTCs were detected in both peripheral and ovarian vein samples. Follow up of treatment response is ongoing to establish the clinical significance of findings.

Conclusions: We report that the use of expanded CTC-ID markers and Parsortix CTC enrichment, single CTC and clusters of CTCs can be isolated from ovarian cancer patients. CTCs isolated from the ovarian vein during surgery are abundant for CTC-clusters, and may provide a source of alternative indicators for monitoring of treatment response and prognosis. Characterisation of platelet cloaked CTCs too, may provide valuable clinical and biological information about haematogenous metastasis in ovarian cancer.

792 Vulvar Erythrasma: An Easily Diagnosed yet Likely Overlooked Explanation for Chronic Vulvar Itching

Jaclyn Watkins[1], Alvaro Laga Canales[2]
[1]Massachusetts General Hospital, Harvard Medical School, Boston, MA, [2]Brigham and Women's Hospital, Harvard Medical School, Boston, MA

Disclosures: Jaclyn Watkins: None; Alvaro Laga Canales: None

Background: Erythrasma, an infection of the stratum corneum by the filamentous gram-positive bacteria *Corynebacterium minutissimum*, most commonly affects intertriginous areas or skin flaps. The clinical dermatologic literature also readily identifies the process's potential to involve the vulva and suggests it be excluded in patients presenting with chronic vulvar itching. However, due to low awareness amongst both gynecologists and general/gynecologic pathologists, erythrasma is likely underdiagnosed in the vulva, and the pathology literature is extremely scant on this topic.

Design: Cases diagnosed as diagnostic of or suspicious for vulvar erythrasma were retrieved from the pathology files of both Brigham and Women's Hospital and the Massachusetts General Hospital. The results of Brown-Hopps, GMS, or PAS staining were recorded, as applicable. Patient characteristics, including age, comorbidities, presenting symptoms, and gross appearance were pulled from the medical record.

Results: Twelve cases were identified (mean age 57.2, range 39-77 yo). Of note, 9 of the 12 cases were diagnosed by a dermatopathologist and only three by a gynecological pathologist. The clinical differential diagnoses offered at the time of biopsy included squamous intraepithelial lesions, intertrigo, psoriasis, eczema, and lichenoid dermatitis. Erythrasma was not included in the clinical diagnoses for any of the cases. When performed, filamentous bacteria were readily identifiable on PAS (12/12 cases) and were gram positive on Brown-Hopps stains (6/6 cases). The underlying epithelium frequently demonstrated compact orthokeratosis (11/12 cases), acanthosis (6/12 cases), pigment incontinence (4/12 cases), minimal to moderate perivascular chronic inflammation (11/12 cases), and occasional spongiosis (2/12 cases). Seven cases involved the labia majora, one case involved the labia minora, and four involved the perineum. One case was associated with underlying lichen sclerosus, with the patient's symptoms incompletely resolving with steroidal therapy. When follow-up data was available, the patient's symptoms were noted to be entirely resolved following a course of topical antibiotics.

Conclusions: Erythrasma may be readily diagnosed by histopathology, but it is not frequently considered by clinicians and pathologists and thus likely underrecognized. Clinicians and pathologist should consider erythrasma in the differential diagnosis of unexplained vulvar erythema, pigmentation and/or itch.

793 Atypical Endometriosis: Comprehensive Characterization of Clinicopathologic and Immunohistochemical Features and Their Role as Predictors of Neoplasia

Cindy Wepy[1], Marisa Nucci[2], Carlos Parra-Herran[2]
[1]Brigham and Women's Hospital, Boston, MA, [2]Brigham and Women's Hospital, Harvard Medical School, Boston, MA

Disclosures: Cindy Wepy: None; Marisa Nucci: None; Carlos Parra-Herran: None

Background: Atypical endometriosis (A-EMS) is defined by the World Health Organization classification as EMS with a localized proliferation of crowded glands lined by atypical epithelium resembling endometrial intraepithelial neoplasia, or alteration in endometriotic cyst lining with stratification, disorganization, and cytologic atypia. While an association between A-EMS and malignant progression has been made, this phenomenon is still poorly understood. We aimed to refine the morphologic and immunohistochemical spectrum of A-EMS in a modern institutional series.

Design: Cases diagnosed as "A-EMS" or "EMS with atypical features" were identified through a structured search and reviewed by two pathologists. Clinical and pathologic features were recorded. Immunohistochemistry was performed when material was available. Cases with synchronous and/or subsequent EMS-related neoplasia were compared to those without.

Results: Of 4,598 EMS cases over an 11-year period, 36 A-EMS with archival material available for review were included. Mean age at presentation was 46 (range 26-68) years. Locations included ovary (24, 66%), tubo-ovary (6, 17%), fallopian tube (3, 8%), and peritoneum (3, 8%). Mean size was 6.5 (range 0.5-40) mm. Atypical cells represented on average 79% of the focus (range 5-100%). Cytologic atypia was 1+ in 4 (11%), 2+ in 21 (58%) and 3+ in 11 (31%). Most lesions showed hobnail nuclei (66%) and were purely flat (42%). Crowded glandular, micropapillary, and papillary architecture were seen in 31%, 42% and 6% of cases, respectively. Immunohistochemistry was performed in 33 A-EMS: 100% showed normal p53 and retained PMS2 and MSH6. 97% were positive for ER (mean 65% cells), and 76% were positive for PR (mean 30% cells). Napsin-A was positive in 13 cases (39%). Ki67 labelling was <1-10% (median 5%). Seven of 36 A-EMS presented with concurrent or subsequent ipsilateral endometrioid, seromucinous, or clear cell neoplasia (4 borderline tumors and 3 carcinomas). The only A-EMS feature statistically more frequent in this subset was gland crowding (5/7 with neoplasia versus 6/29 patients without, Chi-square 6.84, p=0.008).

Conclusions: A-EMS is a rare phenomenon (<1% of all EMS in our series) characterized by cytologic atypia and variable crowded or micropapillary architecture but low proliferation index, positive ER and normal p53 & MMR, which can be helpful in the distinction from malignancy. The prevalence of synchronous/subsequent neoplasia in our series was 19%, significantly higher than the reported 0.5-1% in conventional EMS. Therefore, it is important to report A-EMS as currently defined and describe its architectural features, especially gland crowding as this appears to increase the risk of EMS-related epithelial neoplasia. Napsin-A is often positive in A-EMS and should be interpreted with caution.

794 Localized Endometrial Proliferations of Pregnancy are Characterized by PTEN Loss and Likely Represent Clonal Outgrowths in Gestational Endometrium

Cindy Wepy[1], David Chapel[2], George Mutter[3], Marisa Nucci[3], Carlos Parra-Herran[3]
[1]Brigham and Women's Hospital, Boston, MA, [2]Michigan Medicine, University of Michigan, Ann Arbor, MI, [3]Brigham and Women's Hospital, Harvard Medical School, Boston, MA

Disclosures: Cindy Wepy: None; David Chapel: None; George Mutter: *Consultant*, Mithra Pharmaceuticals, Bayer; Marisa Nucci: None; Carlos Parra-Herran: None

Background: Gestational endometrium can demonstrate a spectrum of atypical but benign changes. One such lesion is the rare Localized Endometrial Proliferation of Pregnancy (LEPP), which is thought to represent a benign proliferation induced by pregnancy. Literature, however, is scant and limited to morphology. We therefore aimed to describe the pathologic and immunophenotypic features of this entity.

Design: Cases of LEPP were identified from 2005-2021 in departmental archives. Cases were reviewed for clinical and pathologic features. Immunohistochemistry was performed when material was available.

Results: Eight cases were included. Mean patient age was 36 (range 29-41) years. All were incidentally found in endometrial curettage after suspected or confirmed recent early gestation. Mean lesion size was 0.64 (range 0.2-1.2) cm. Architectural patterns included cribriform (n=6), solid (n=5), villoglandular (n=2), micropapillary (n=1), and papillary (n=1). Cytologic atypia was mild in 7

cases and moderate in one case. Mitotic activity was low (mean 1 per 10 high power fields, range 0-3). All lesional glands were associated with neutrophils; a subset had calcifications (3/8) or mucin (2/8). Arias-Stella reaction was present in other areas of the endometrium in 4/8 cases. Immunohistochemistry was performed in 6 LEPP (Table 1), all of which demonstrated wildtype p53, membranous beta-catenin, and positivity for ER (mean 70% of cells) and PR (mean 72% of cells). All were negative for p40 except one case (focal basal positivity). 2/6 cases showed focal Napsin A, and 5/6 cases showed patchy p16. PTEN expression was markedly reduced in background secretory glands, but completely negative in LEPP areas in 5/6 cases; one case showed staining comparable to background. Ki67 ranged from 10-40% (mean 28%), 4/8 LEPP had a basal-only staining pattern. In 5 cases with available follow-up (mean length = 49 months, range 5-153), no subsequent neoplasia was identified.

Table 1. Immunohistochemical features of localized endometrial proliferations of pregnancy.

Case	p40	p53	Napsin A	p16	ER	PR	B-catenin	PTEN	Ki67
1	Negative	Wildtype	Negative	Patchy	70%	80%	Membranous	Lost	40%
2	Negative	Wildtype	Negative	Patchy	70%	40%	Membranous	Lost	20%
3	Negative	Wildtype	Focal	Patchy	90%	80%	Membranous	Lost	30%, basal
4	Focal, basal	Wildtype	Focal	Patchy	80%	80%	Membranous	Retained	10%
5	Negative	Wildtype	Negative	Negative	20%	70%	Membranous	Lost	30%, basal
6	Negative	Wildtype	Negative	Patchy	90%	80%	Membranous	Lost	40%, basal

Figure 1 - 794

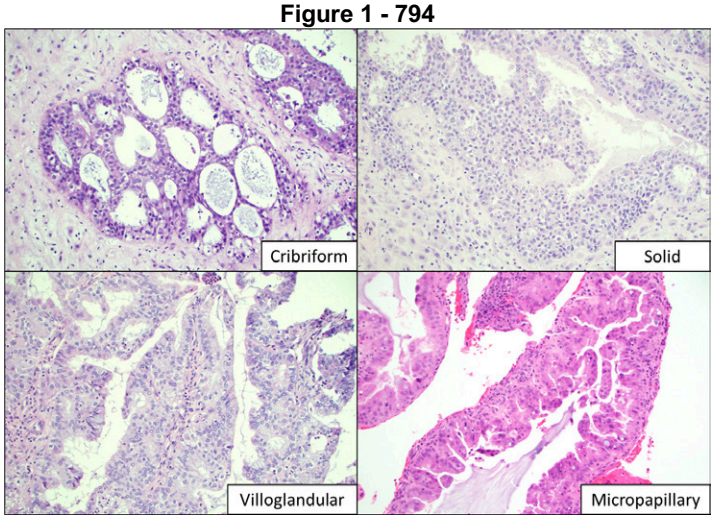

Figure 2 - 794

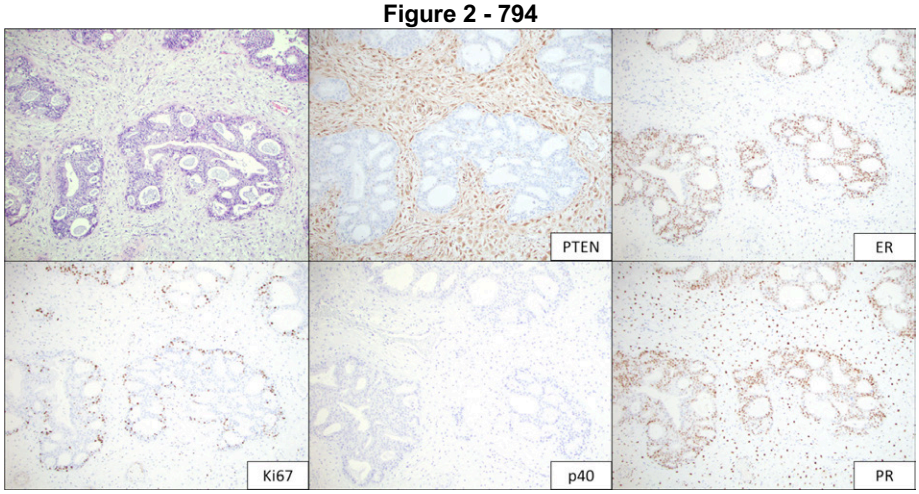

Conclusions: LEPP is a rare epithelial proliferation characterized by cribriform/solid architecture, positive ER/PR, negative p40, PTEN loss, and elevated Ki67, often in a basal distribution. Basal Ki67 can help distinguish this lesion from carcinoma which is important as LEPP is not associated with subsequent neoplasia. LEPP differs from EIN in that the proliferation is complex but entirely intraglandular. Negative p40 staining also distinguishes this lesion from microglandular hyperplasia. Complete loss of PTEN suggests a clonal etiology for this lesion.

795 Lack of Identifiable Driver Mutations is Associated with Worse Disease-Specific Survival in Patients with Low-Grade Serous Carcinoma of the Ovary

Ju-Yoon Yoon[1], Thing Rinda Soong[2], Lynette Sholl[3], Ursula Matulonis[4], Michelle Hirsch[5], Marisa Nucci[6], David Kolin[5]
[1]Unity Health Toronto, Toronto, Canada, [2]University of Pittsburgh, Pittsburgh, PA, [3]Harvard Medical School, Boston, MA, [4]Dana-Farber Cancer Institute, Boston, MA, [5]Brigham and Women's Hospital, Boston, MA, [6]Brigham and Women's Hospital, Harvard Medical School, Boston, MA

Disclosures: Ju-Yoon Yoon: None; Thing Rinda Soong: None; Lynette Sholl: *Consultant*, Genentech, Lilly; *Grant or Research Support*, Genentech; Ursula Matulonis: *Consultant*, Novartis, AstraZeneca, Merck, NextCure; *Advisory Board Member*, Trillium; Michelle Hirsch: *Consultant*, Janssen Pharmaceuticals; Marisa Nucci: None; David Kolin: None

Background: Although driver mutations have been relatively well characterized in low-grade serous carcinomas (LGSCs) of the ovary, their clinical significance and the larger mutational spectra of LGSC are poorly characterized. We present data that represents the largest genetically characterized LGSC cohort to date.

Design: LGSC of the female genital tract which had undergone targeted tumor-only molecular profiling at a single institution were retrospectively identified. The NGS assay used hybrid capture to target 275+ tumor suppressor and oncogenes for point mutations and copy number changes. Kaplan-Meier and multivariate survival analyses were performed using the survfit and survival R packages.

Results: The genetic landscape of LGSC (n=96) was characterized by low tumor-mutational burden (TMB; median = 3.6 mutations/Mb), with driver mutations identified in 54/96 (56%) cases. *KRAS* driver mutations were the most common (31/96), with none harboring the targetable p.G12C variant. This was followed by *BRAF* (9/96; all p.V600E) and *NRAS* (9/96; all p.Q61R). *ERBB2* driver mutations were identified in 3/96, along with single cases each with *NF1* and *NF2* putative driver mutations. *TP53* mutations were absent. In total, 54/96 cases are genetically identified to be driven by alterations in the RAS/MAPK pathway, and 12/96 cases (12.5%) harbored potentially targetable mutations (i.e. *BRAF* and *ERBB2*). Followup was available for 65 cases (median followup 4.4 years, range 0.5-27.6 years). The absence of an identifiable driver mutation was associated with worse disease-specific survival (DSS, log-rank $p = 0.0008$), but not progression-free survival. There were no significant differences in ages at diagnosis, FIGO stage at presentation, TMB, or CNV burden, with respect to the driver mutation status (presence/absence). By multivariate analysis, in a model factoring in age at diagnosis, and FIGO stage, driver mutation status was the only significant predictor of survival (hazard ratio = 8.9, 95% confidence interval = 1.8-42.6).

Figure 1 - 795

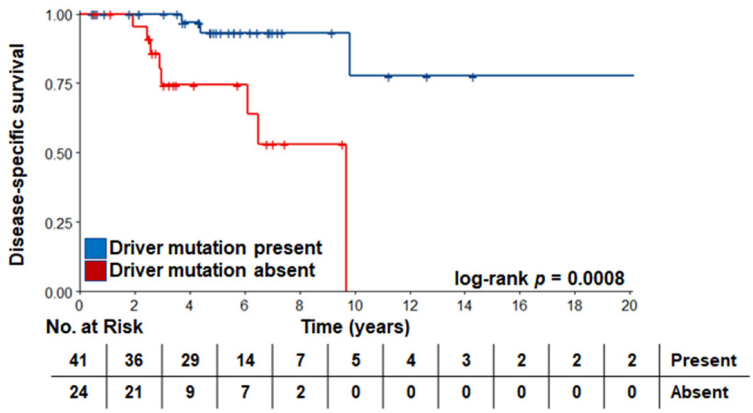

Figure 1. Disease-specific survival in 65 patients with LGSC, grouped by driver mutation status (present/absent), as identified by large, targeted panel-based molecular profiling results.

Conclusions: Our analysis of genomic panel data study on a large cohort of LGSC is the first to demonstrate that tumors without driver mutation were associated with worse DSS, independent of patient age and tumor stage. Further work is necessary to identify genomic or transcriptomic alterations which correlate with aggressive behavior.

796 PTEN Loss in High-Grade Serous Carcinomas is Associated with Reduced Expression of Hormonal Receptors and Poor Progression-Free Survival, and Mutually Exclusive with CCNE1 Amplification

Xiaoming Zhang[1], Lucy Han[2], Brooke Liang[3], Aihui Wang[1], Brooke Howitt[4]
[1]Stanford University School of Medicine, Stanford, CA, [2]Stanford Pathology, Stanford, CA, [3]Stanford Health Care, Stanford, CA, [4]Stanford Medicine/Stanford University, Stanford, CA

Disclosures: Xiaoming Zhang: None; Lucy Han: None; Brooke Liang: None; Aihui Wang: None; Brooke Howitt: None

Background: As a critical tumor suppressor, PTEN has gained much attention in cancer research. Emerging evidence showed that PTEN loss has been associated with resistance of immune checkpoint inhibitors (ICIs) in melanomas while PTEN-deficient prostate cancer may be more sensitive to PARP inhibitors. However, the significance of PTEN loss in high-grade serous carcinomas (HGSC) is still poorly understood. We aim to evaluate PTEN expression in HGSCs and its clinical relevance.

Design: A cohort of 38 HGSC specimens was profiled using tissue microarray. Immunohistochemical analysis of PTEN, ER, PR, AR, CD8, FOXP3, and PD-L1 was carried out. Digital image analysis and automated cell count (QuPath software) were utilized to calculate the densities of CD8+ or FOXP3+ T cells. Targeted gene panel testing by massively parallel sequencing was performed in 28 cases. Clinical history, treatment, and follow-up were reviewed. Statistical analysis was performed with SPSS software.

Results: The clinicopathological findings of 38 HGSCs are summarized in Table 1. 9 of 38 cases (24%) demonstrated either negative or focally negative (heterogeneous) staining for PTEN. Loss of PTEN was significantly correlated with reduced expression of ER, PR, and AR ($P<0.05$), but not with PD-L1 expression or the densities of CD8+ tumor-infiltrating lymphocytes (TILs) and FOXP3+ regulatory T cells (Fig 1). Besides *TP53* and *BRCA1*, the *CCNE1* amplification was the most common gene alteration (18%) in our cohort, and it occurred exclusively in PTEN+ HGSCs (Fig 2A). Almost all patients received platinum-based adjuvant therapy and 31 had PARP inhibitors as maintenance therapy; no correlation was found between treatment response and PTEN expression. Since only 2 cases were treated with ICIs (both were PTEN positive and ICI-resistant), a definitive conclusion regarding the impact of PTEN status on ICIs response cannot be drawn. Importantly, we found loss of PTEN expression was associated with poor progression-free survival (PFS) but not overall survival in HGSCs (Fig 2B).

Characteristic, units		All (N=38)	PTEN negative or heterogeneous loss*	PTEN positive*	*P*-value
Mean age at diagnosis, years (range)		61 (32-77)	63 (56-73)	61 (32-77)	0.575
FIGO stage, n (%)					
	I-II	2 (5)	0 (0)	2 (7)	0.588
	III	25 (66)	7 (78)	18 (62)	
	IV	11 (29)	2 (22)	9 (31)	
Surgery modality, n (%)					
	PDS	16 (42)	3 (33)	13 (45)	NA
	NACT/IDS	22 (58)	6 (67)	16 (55)	
BRCA mutation, n (%)					
	BRCA1	5 (13)	1 (11)	4 (14)	0.638
	BRCA2	1 (3)	0 (0)	1 (3)	
	No mutation	23 (61)	5 (56)	18 (62)	
	Unknown	9 (24)	3 (33)	6 (21)	
Adjuvant chemotherapy regimen, n (%)					
	Platinum/taxane	34 (89)	9 (100)	25 (86)	NA
	Platinum/topoisomerase inhibitor	1 (3)	0 (0)	1 (3)	
	Platinum/taxane/bevacizumab	2 (5)	0 (0)	2 (7)	
	Other (non-platinum-based)	1 (3)	0 (0)	1 (3)	
Response to platinum-based chemotherapy, n (%)					
	Sensitive	34 (92)	7 (78)	27 (96)	0.141
	Resistant	3 (8)	2 (22)	1 (4)	
PARP inhibitor as maintenance therapy, n (%)					
	Used, sensitive	6 (16)	0 (0)	6 (21)	0.342
	Used, resistant	15 (39)	3 (30)	12 (41)	
	Not used	16 (42)	5 (60)	11 (38)	
	Unknown	1 (3)	1 (10)	0 (0)	
Immune checkpoint inhibitors, n (%)					
	Used, sensitive	0 (0)	0 (0)	0 (0)	NA
	Used, resistant	2 (5)	0 (0)	2 (7)	
	Not used	36 (95)	9 (100)	27 (93)	
Mean follow-up time, months (range)		34 (7-80)	33 (13-80)	35 (7-79)	NA
Status at last follow-up, n (%)					

	Alive	25 (66)	6 (67)	19 (66)	NA
	Deceased	13 (34)	3 (33)	10 (34)	
Median PFS, months (95% CI)		16 (11 -21)	14 (8-20)	19 (15-23)	**0.011**
Median OS, months (95% CI)		53 (41-65)	48 (16-80)	56 (45-67)	0.664
PTEN expression*					
	Negative or heterogenous loss	9 (24)	NA	NA	NA
	Positive	29 (76)	NA	NA	

* Negative: <10% of tumor cells with any immunoreactivity; heterogeneous loss: tumor contained discrete positive (at least 10%) and negative staining cell (at least 20%) populations; Positive: >= 80% of tumor cells with any immunoreactivity.
Abbreviations: PDS, primary debulking surgery; NACT/IDS, neoadjuvant chemotherapy/interval debulking surgery; NA, not applicable; PFS, progression-free survival; OS, overall survival.

Figure 1 - 796

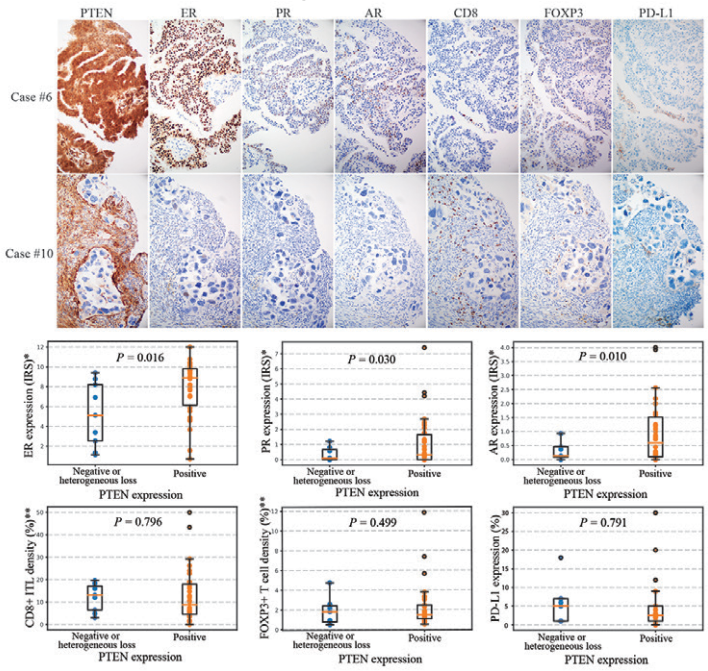

* Immunoreactivity scoring system (IRS) was used for IHC evalution of ER, PR, and AR expression as described in *Fedchenko et al., Diagn Pathol, 2014; 9:221.*
** Digital image analysis and automated cell count (QuPath software) were used to calculate the densities of immunostained cells.

Figure 2 - 796

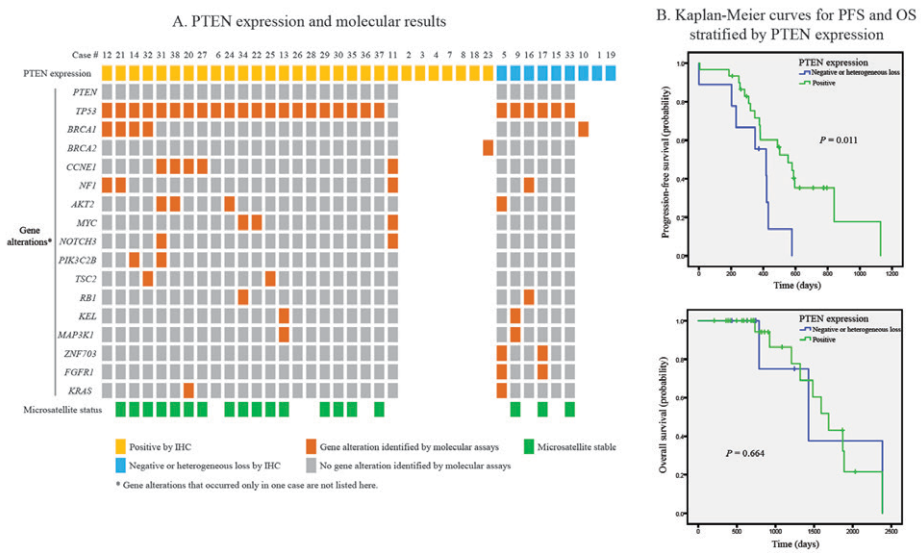

Conclusions: PTEN expression is significantly associated with ER/PR/AR status and loss of PTEN predicts poor PFS in HGSCs. TIL densities and PD-L1 expression are not affected by PTEN status. *CCNE1* amplification, proposed as a marker for platinum

resistance, is mutually exclusive with PTEN loss. These results indicate that PTEN expression plays a non-negligible role in the progression and treatment response of HGSC and deserves further investigation.

797 Specific Expression of SOX17 in Tumors of Mullerian Origin

Xudong Zhang[1], Na Niu[1], Anil Sood[1], Qingqing Ding[1], Jinsong Liu[1]
[1]The University of Texas MD Anderson Cancer Center, Houston, TX

Disclosures: Xudong Zhang: None; Na Niu: None; Anil Sood: *Grant or Research Support*, M-Trap; *Consultant*, Merck, Kiyatec; *Stock Ownership*, Biopath; Qingqing Ding: None; Jinsong Liu: None

Background: SOX17 (SRY-BOX containing gene 17) plays a critical role in regulating embryonic development and acts as a suppressor in several malignant tumors. Although RNA-seq data for the tissue-specificity of SOX17 in different tissues are available in the public database, protein expression in different tumors is unknown. Here we report the distribution and expression of SOX17 in carcinomas of bladder, liver, colon, kidney, ovary and uterine, by immunohistochemical staining.

Design: Tissue microarray slides were prepared from archived tumors in the Department of Pathology in MDACC and US Biomax. Slides were stained with SOX17 antibody (1:2000 dilution, ab224637, Abcam) in bladder cancer (80 cases), colon carcinoma (75 cases), hepatocellular carcinoma (75 cases), kidney carcinoma (75 cases), endometrial carcinoma (48 cases), and ovarian tumors including 93 high grade serous, 3 serous borderline tumor/low grade serous carcinoma, 3 malignant mixed Mullerian tumors, and 4 clear carcinoma, 3 endometrioid adenocarcinoma, and one mucinous carcinoma, a total of 107 cases. The positive signals were defined as the tumor cells stained with a brown precipitate in the nucleus. The intensity of the staining was scored no staining, weak, and strong. All statistical analyses were performed with SPSS 27.0 software (SPSS Inc). Data are presented as mean ± SD. Statistical differences between the two groups were determined by Chi-Square Test or a Mann-Whitney test. $P \leq 0.05$ was considered statistically significant.

Results: SOX17 was diffusely positive in ovarian tumors (97/107, 90.7%) and endometrial adenocarcinoma and normal endometrium (34/48, 70.8%). In contrast, carcinomas of bladder (0/80), colon (0/75), and liver (0/75) are all negative for SOX17 (Figure 1). Only one case has weak nuclear staining in kidney carcinoma (1/75). The representative images of immunohistochemical staining are shown in Figure 1, and summary of data is shown in Figure 2.

Figure 1. Expression and distribution of SOX17 in multiple carcinoma. Bars, 50 μm.

Figure 2. Frequency of positive SOX17 in different types of tumors.

Figure 1 - 797

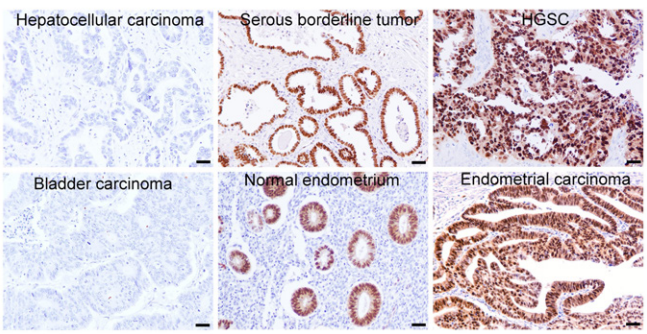

Figure 2 - 797

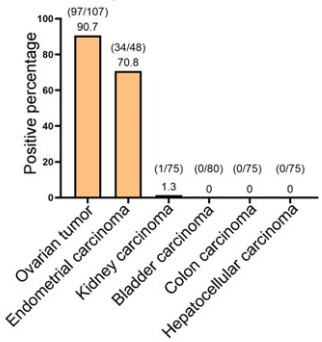

Conclusions: SOX17 is uniquely expressed in Mullerian tumor including ovarian and endometrial cancer. SOX17 may represent a novel diagnostic marker for tumors of Mullerian origin. Immunohistochemical staining of additional tumor cases from different organs is in progress to further test the specificity of this marker.

798 Molecular Findings of 16 Cases of Endometrial Stromal Sarcomas

Longmei Zhao[1], Yu-Wei Cheng[2], Maria Luisa Policarpio-Nicolas[1]
[1]Cleveland Clinic Foundation, Cleveland, OH, [2]Cleveland Clinic Pathology and Laboratory Medicine, Cleveland, OH

Disclosures: Longmei Zhao: None; Yu-Wei Cheng: None; Maria Luisa Policarpio-Nicolas: None

Background: Currently, endometrial stromal tumors (ESSs) are classified as endometrial stromal nodule/low-grade endometrial stromal sarcoma (ESN/LG-ESS), high-grade endometrial stromal sarcoma (HG-ESS) and undifferentiated uterine sarcoma (UUS) based on morphology and immunohistochemical stain results. Likewise, genetic aberrations have been identified in ESN/LG-ESS (*JAZF1* and *SUZ12* fusion) and in HG-ESS (*YWHAE-FAM22* fusion and *ZC3H7B-BCOR*). In contrast, USS have complex chromosomal changes and specific molecular signatures have not yet been identified.

Design: Electronic medical record search was performed for key words "endometrium, stroma, low-grade, high-grade, undifferentiated uterine sarcomas". To minimize sampling error, we limited our selection to TAHBSO and resection specimens with prior immunohistochemical stain results supportive of the diagnoses. Next-generation sequencing (NGS) sarcoma panel was performed to identify any genetic abnormality in these tumors.

Results: A total of 17 cases were identified (16 TAHBSO and 1 rectal resection). Based on morphology and immunohistochemical results, tumors were classified LG-ESS (9), HG-ESS (3) and USS (5). NGS was not performed in 1 USS. A novel *CRTC1-MKL2* gene fusion was present in 1 UUS. The morphology showed sheets of uniform round cells with brisk mitotic figures (Figure 1). Two UUS showed no genetic abnormality and 1 UUS failed NGS test due to poor mRNA extraction. One HG-ESS harbored *YWHAE- NUTM2B* gene fusion and 2 failed NGS testing. Six LG-ESS showed no genetic abnormality and one had *JAZF1-SUZ12* gene fusion. One LG-ESS had *ZC3H7B- BCOR* gene fusion which on slide re-review, this showed a 2.2 cm intramural nodule with typical LG-ESS morphology juxtaposed to fibromyxoid spindle cells with minimal atypia. (Figure 2). One LG-ESS was found to have *ESR1- NCOA2* gene fusion, which have been reported in uterine tumors resembling ovarian sex-cord tumor (UTROSCT).

Figure 1 - 798

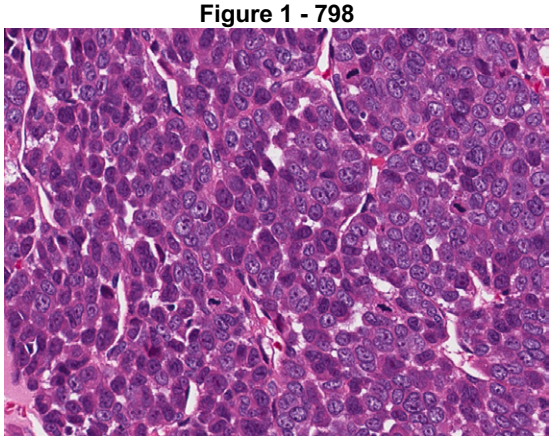

Figure 2 - 798

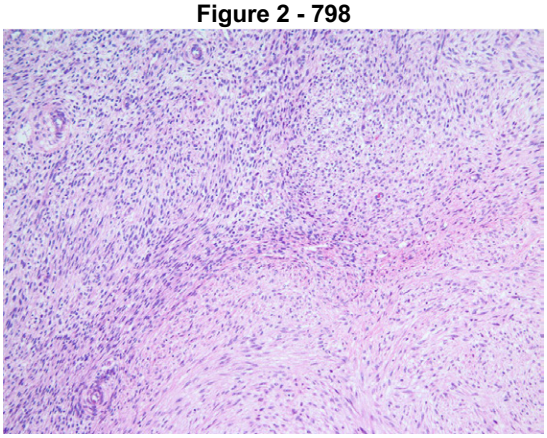

Conclusions: Half of our cases showed the presence of gene fusion, two of which were concordant with the histologic diagnosis. A novel *CRTC1- MKL2* gene fusion was seen in USS. *ZC3H7B- BCOR* and *ESR1- NCOA2* gene fusion were present in 2 cases initially diagnosed as LG-ESS. While the current classification of endometrial stromal tumors is often based on gross and histologic findings, given that immunophenotype can have overlapping results and difference in prognosis and management, confirmatory molecular testing is helpful in optimally classifying these tumors.

799 Validation of HER2 Testing in Endometrial Serous Carcinoma

Roman Zyla[1], Anthony Wing[2], Jenny Jimenez[2], John White[2], Neha Seebocus[2], Gulisa Turashvili[3]
[1]University of Toronto, Toronto, Canada, [2]Mount Sinai Hospital, University of Toronto, Toronto, Canada, [3]Emory University Hospital, Atlanta, GA

Disclosures: Roman Zyla: None; Anthony Wing: None; Jenny Jimenez: None; John White: None; Neha Seebocus: None; Gulisa Turashvili: None

Background: Recent clinical trial data has shown that treatment with trastuzumab, an anti-human epidermal growth factor receptor 2 (HER2) monoclonal antibody, is associated with improved survival in patients with HER2-positive endometrial serous carcinoma (ESC). However, there are no standardized guidelines for HER2 testing in ESC, which makes HER2 validation for this indication challenging for pathology laboratories. We sought to perform a validation study for determining HER2 status by immunohistochemistry (IHC) and fluorescence *in situ* hybridization (FISH) in ESC.

Design: Archival cases of ESC were reviewed retrospectively. Representative tissue sections were stained with the anti-HER2 (4B5) rabbit monoclonal antibody and assessed by a single, subspecialty-trained consultant in gynecologic and breast pathology, using a scoring system in which 0 is defined as no staining, 1+ as weak/incomplete membrane staining or complete membrane staining in <10% of tumor cells, 2+ as complete membrane staining in 10-30% or weak but complete membrane staining in >10%, and 3+ as strong, complete membranous staining in >30%. FISH is being performed on 20 negative (0/1+), 20 positive (3+) and 20 equivocal (2+) cases, as well as tumors with biphasic IHC pattern, using a dual-probe assay, with classification into 5 groups based on the mean HER2 copy number and HER2/chromosome enumeration probe 17 (CEP 17) ratio.

Results: A total of 83 archival ESCs underwent HER2 IHC, including 41 (49%) biopsies and 42 (51%) hysterectomies. Of these, HER2 was negative in 45 (54%) tumors (22 [26%] with a score of 0, 23 [28%] with 1+), 2+ in 29 (35%) and 3+ in 5 (6%), while 4 (5%) showed a biphasic staining pattern. To date, 23 tumors have undergone FISH analysis, of which 9 (39%) were HER2 amplified and 11 (48%) were non-amplified. One (4%) tumor was borderline by FISH classified as non-amplified after 2 reads, while 2 (9%) tumors were biphasic by both IHC and FISH. Of 10 HER2 IHC negative cases, 9 (90%) were non-amplified by FISH. Two of 2 (100%) HER2 IHC positive tumors were amplified by FISH. Of 9 HER2 IHC equivocal tumors, 6 (67%) were amplified, 2 (22%) were non-amplified and 1 (11%) was borderline, classified as negative after 2 reads.

Conclusions: In light of recent clinical trials data showing positive clinical outcomes for HER2-positive ESCs, there will be increasing demands on pathology laboratories to reliably determine and report the HER2 status of these tumors. Our preliminary results show strong concordance between IHC and FISH for determining HER2 status and could serve as a validation model for HER2 testing in ESC.